Recueil des contributions de la 27e Rencontre du Non-Linéaire (Paris 2024)

Éric Falcon, Marc Lefranc, François Pétrélis, Chi-tuong Pham

Université Paris Cité

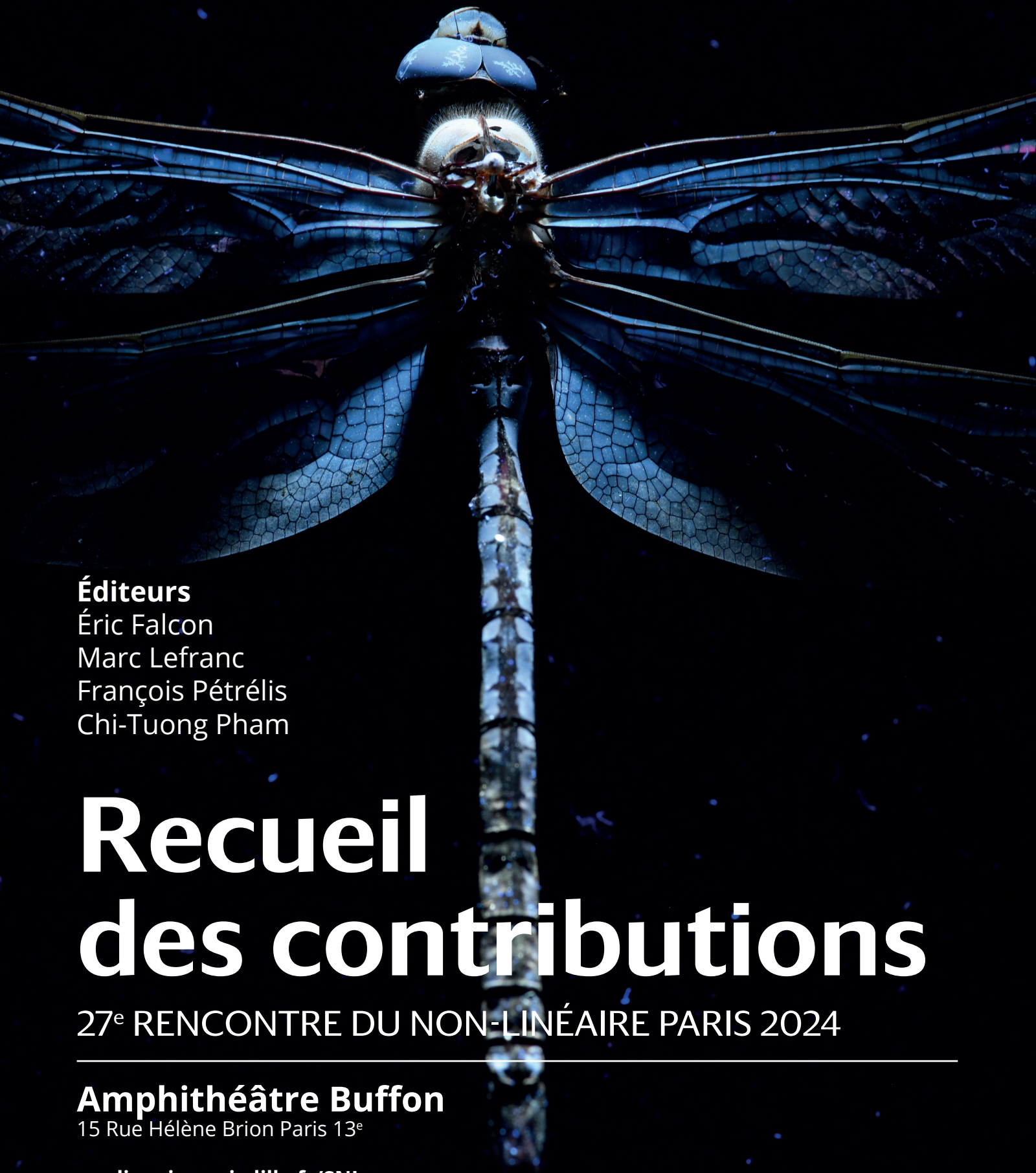

Éditeurs
Éric Falcon
Marc Lefranc
François Pétrélis
Chi-Tuong Pham

Recueil des contributions

27e RENCONTRE DU NON-LINÉAIRE PARIS 2024

Amphithéâtre Buffon
15 Rue Hélène Brion Paris 13e

nonlineaire.univ-lille.fr/SNL

u-paris.fr

É. Falcon, M. Lefranc
F. Pétrélis, C.-T. Pham
Éditeurs

Résumés de la 27e Rencontre du Non-Linéaire Paris 2024

Université Paris Cité

Non-Linéaire Publications

27e Rencontre du Non-Linéaire

Université de Paris

18–20 Mars 2024

Nous remercions vivement pour leur soutien matériel et financier l'université Paris Cité, le CNRS, le laboratoire MSC de l'université Paris Cité, le LISN de l'université Paris-Saclay, le Laboratoire de Physique de l'École normale supérieure, le Laboratoire de Physique de l'École normale supérieure de Lyon, le laboratoire PhLAM de l'université de Lille, le laboratoire PMMH de l'ESPCI, le LIPhy de l'université de Grenoble, le CPT de l'université Aix–Marseille, l'Institut Jean Le Rond d'Alembert de Sorbonne Université, la Société Française de Physique.

Le comité scientifique est composé de :

Serge Bielawski	PhLAM — Lille
Éric Falcon	MSC — Université Paris Cité
Isabelle Gallagher	DMA – ENS Paris
Xavier Leoncini	CPT — Aix–Marseille
François Pétrélis	LP — ENS Paris
Chi-Tuong Pham	LISN — Paris-Saclay
Juliette Pierre	IJLRDA — Sorbonne Université
Catherine Quilliet	LIPhy — Grenoble
Christophe Raufaste	INPhyNI — Côte d'Azur
Étienne Reyssat	PMMH — ESPCI, PSL
Emmanuelle Rio	LPS — Paris-Saclay
Stéphane Santucci	LP — ENS Lyon

Les Rencontres du Non-Linéaire sont organisées par :

Éric Falcon	MSC – Paris Diderot
Marc Lefranc	PhLAM – Lille
François Pétrélis	Laboratoire de Physique – ENS Paris
Chi-Tuong Pham	LISN – Paris-Saclay

Le mini-colloque « *Nonlinear soft interfaces: Wetting, adhesion, flow, and fracture* » est organisé par :

Étienne Reyssat	PMMH – ESPCI, PSL
Stéphane Santucci	LP – ENS Lyon

Les comptes-rendus des années précédentes sont disponibles auprès de :

Non-Linéaire Publications,
Bâtiment 508
Rue John von Neumann
91400 Orsay

Toutes les informations concernant les Rencontres sont publiées sur le serveur :

`http://nonlineaire.univ-lille1.fr/`

Renseignements :

`rnl@univ-lille1.fr`

Sommaire

Exposés longs de la 27e Rencontre du Non-Linéaire

Exposés courts de la 27e Rencontre du Non-Linéaire

Focus Point on Nonlinear Physics Advances in EPJ Plus

To increase their impact, RNL proceedings is now published as articles in
The European Physical Journal Plus (EPJ Plus)

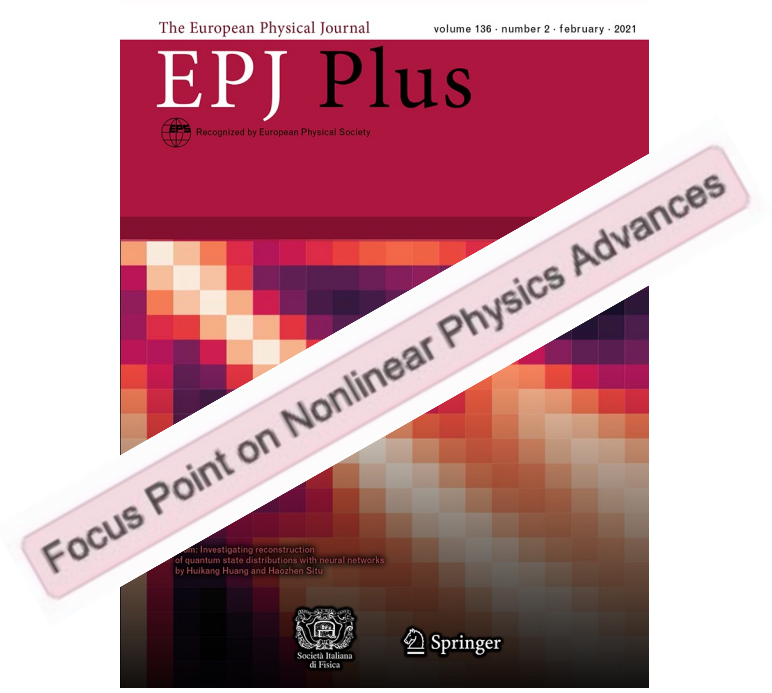

You are invited to submit an article in
EPJ Plus **Focus Point on Nonlinear Physics Advances**

Deadline for submissions: as they arise and each year mid-November
http://nonlineaire.univ-lille.fr/SNL/instructions_articles/
or
https://epjplus.epj.org/

EPJ Plus
Focus Point on Nonlinear Physics Advances
S. Chibbaro, M.-C. Firpo, G. Napoli and S. Randoux (Guest editors)

Division Physique Non Linéaire

Société Française de Physique

Créée début 2021, la toute nouvelle Division de Physique Non Linéaire (DPNL) de la SFP a pour but de structurer la communauté du non-linéaire au sein d'une division transverse de la SFP qui a vocation à être interdisciplinaire.

Exemples : dynamique des fluides, mécanique, matière molle, optique, plasmas, biophysique, physique des interfaces…

DPNL

Le bureau de la DPNL (2021 – 2024) **11 membres**

Membre pendant 3 ans renouvelable une fois

• Axelle Amon (Université de Rennes)	Matière Molle	GDR IDE
• Médéric Argentina (Université Côte d'Azur)	Matière active	
• Mickaël Bourgoin (ENS de Lyon / CNRS)	Turbulence	GDR NS2.00
• Bérengère Dubrulle (CEA Saclay / CNRS)	Turbulence	
• Éric Falcon (Université de Paris / CNRS)	*Président/Trésorier*	
• Stéphan Fauve (ENS)	Dynamo - MHD	GDR Dynamo
• Marie-Christine Firpo (École Polytechnique)	Plasmas	
• Marc Lefranc (Université de Lille)	Biophysique	GDR AQV
• Chi-Tuong Pham (Université Paris Saclay)	Physique des interfaces	
• Stéphane Randoux (Université de Lille)	Optique non linéaire	
• Benoît Roman (ESPCI / CNRS)	Mécanique/Elasticité	GDR Méphy

Société Française de Physique

DIVISION PHYSIQUE NON LINÉAIRE

Quelques avantages d'adhérer à la Division de Physique Non Linéaire

- Pour un laboratoire adhérent à la SFP:

Chaque doctorant.e d'un laboratoire adhérent bénéficie d'une adhésion gratuite individuelle à la SFP

⇒ être informé des actualités de la division, rejoindre le réseau des doctorants, accéder au forum emploi de la SFP,

⇒ bénéficier du programme de mentorat de la SFP, réduction/gratuité d'enregistrement à des conférences

- Adhésion individuelle à la SFP (après 66% réduction d'impôt) : 9€ (Doct./Etudiant.e), 38€ (<35 ans), 50€ (>35 ans)

- **Pour tous: réductions/gratuité pour les événements organisés par les partenaires de la SFP tels que l'American Physical Society (DFD, March Meeting), l'Institut of Physics (IOP), l'European Physical Society (EPS).**

Comment rejoindre la nouvelle Division Physique Non Linéaire de la SFP ?

https://www.sfpnet.fr/inscription

SFP

Cas 1 : Je suis membre de la SFP
- Aller sur son espace membre SFP (login : "sfp" suivi de mon numéro d'adhérent)
- Cliquer sur l'onglet de gauche « mon activité à la SFP »
- Dans « S'informer », sélectionner : *Division Physique Non Linéaire,* valider

Cas 2 : Je ne suis pas membre de la SFP
- Renseigner le formulaire d'adhésion https://www.sfpnet.fr/inscription-adherent
- Cocher : *Physique Non Linéaire* au moment du choix des divisions thématiques

Cas 3 : Adhésion gratuite d'un doctorant.e d'un laboratoire adhérent
- remplir le formulaire en ligne https://www.sfpnet.fr/inscription-doctorant

Cas 4 : Pour devenir un laboratoire adhérent
https://www.sfpnet.fr/adhesions-laboratoires-et-autres-organisations

Société Française de Physique

DIVISION PHYSIQUE NON LINÉAIRE

Programme du mini-colloque

Programme de la 27^{e} Rencontre du Non-Linéaire

Nonlinear soft interfaces: Wetting, adhesion, flow, and fracture

Université Paris Cité, **18 mars 2024** – Amphithéâtre Buffon, 15 rue Hélène Brion, Paris 13e

We propose to discuss recent experimental and theoretical progress highlighting nonlinear effects in the mechanics of soft interfaces, which involve a wide range of phenomena crucial for numerous applications in wetting, imbibition, and adhesion processes. We will start notably on the coupling between surface tension and elasticity and go beyond by considering also the role of surface defects, multiphase complex materials as well as the deformation up to rupture of soft materials.

09h00 Start Invited talks are indicated in blue

09h15 – 09h40 Bruno Andreotti (LP ENS Paris) Statics and dynamics of soft wetting

09h40 – 10h05 Catherine Barentin (ILM, Lyon) Wetting of yield-stress fluids

10h05 – 10h30 Camille Duprat (LadhyX, Palaiseau) Drop spreading on poroelastic substrates

10h30 – 10h45 Coffee break and discussions

10h45 – 11h10 Jordi Ortin (Barcelona) Pressure-saturation hysteresis of two-phase flows in disordered media

11h10 – 11h35 Emmanuel Siéfert (Liphy, Grenoble) Dynamic elastocapillary coalescence of slender structures

Short talks (10 min)

11h35 Megan Delens, (GRASP, Liège) Superposition de ménisques capillaires : courber l'interface liquide pour micro-manipuler des objets flottants

11h45 Pierre Brice Bintein (MSC, Paris) Dynamiques de lignes de contact oscillantes

11h55 Alice Etienne-Simonetti (LPS) Surface deformation of a thin liquid film in the vicinity of a vertical fiber

12h05 Jiayu Wang (D'Alembert, Paris) Surface wrinkling of a thin liquid-infused membrane

12h15 – 13h45 Lunch

13h45 – 14h10 Matteo Ciccotti, (ESPCI, Paris) Soft coring: how to get a clarinet out of a flute?

14h10 – 14h35 Loic Vanel (ILM, Lyon) Nonlinear effects on crack propagation and interaction

Short talks (10 min)

14h35 Anthony Varlet (MSC, Paris) Dip-coating sur substrats déformables en mouillage partiel

14h45 Joséphine Van Hulle, (GRASP, Liège) Droplet spreading and transport: the role of substructures

14h55 Etienne Jambon-Puillet (LadHyX) Pendant droplets under a wet substrate pin on surface defects despite having no contact line

15h05 Friedrich Walzel (Strasbourg) Adhesive bubbles and drops between circular frames

15h15 – 15h45 Coffee break and discussions

15h45 – 16h10 Jacco Snoeijer (Twente) Soft wetting: Nonlinearity at large deformations

16h10 – 16h35 Thierry Ondarçuhu (Toulouse) Mouillage à l 'échelle nanométrique : désorption moléculaire à la ligne de contact

16h35 – 17h00 Axel Huerre (MSC Paris) Water dewetting on ice

Short talks (10 min)

17h00 Philippe Brunet (MSC Paris) Adhésion de la glace sur différents substrats

17h10 Kexin Zhao (PMMH, Paris) When marbles challenge pearls

17h20 Auriane Huyghes Despointes, (PMMH, Paris) Acrobatics of viscous marbles

17h30 End

Le mini-colloque de la RNL 2024 est organisé par Stéphane Santucci (ENS Lyon), Etienne Reyssat (PMMH).

27e Rencontre du Non-Linéaire

Université Paris Cité, 18 – 20 mars 2024

Bienvenue à la 27e Rencontre du Non-Linéaire 2024 qui aura lieu à l'Université Paris Cité, amphithéâtre Buffon, 15 rue Hélène Brion, Paris 13e.

Nous aurons 131 contributions se répartissant en 4 conférences invitées, 12 communications longues et 115 communications courtes.

Mardi 19 mars 2024

08h30 - 08h50 : Enregistrement
09h00 : **Introduction**
09h05 - 09h50 : **Conférence invitée 1 (40 + 5 min.)**
09h50 - 10h25 : Présentation des posters (2 min.) - 17 communications courtes
10h25 - 11h15 : **Pause café Posters** (50 min.)
11h15 - 11h55 : Présentation des posters (2 min.) - 20 communications courtes
11h55 - 12h40 : Exposés longs (20 + 2 min.) - 2 communications longues

12h40 - 14h00 : Déjeuner

14h00 - 14h45 : Exposés longs (20 + 2 min.) - 2 communications longues
14h45 - 15h50 : Présentation des posters (2 min.) - 32 communications courtes
15h50 - 17h00 : **Pause café Posters** (1h10)
17h00 - 17h45 : Exposés longs (20 + 2 min.) - 2 communications longues
17h45 - 18h30 : **Conférence invitée 2 (40 + 5 min.)**
18h30 - 20h30 : Cocktail

Mercredi 20 mars 2024

09h00 - 09h45 : **Conférence invitée 3 (40 + 5 min.)**
09h45 - 10h45 : Présentation des posters (2 min.) - 27 communications courtes
10h45 - 11h45 : **Pause café Posters** (1h00)
11h45 - 12h30 : Exposés longs (20 + 2 min.) - 2 communications longues

12h30 - 14h00 : Déjeuner

14h00 - 14h45 : Exposés longs (20 + 2 min.) - 2 communications longues
14h45 - 15h25 : Présentation des posters (2 min.) - 19 communications courtes
15h25 - 16h30 : **Pause café Posters** (1h05)
16h30 - 17h15 : Exposés longs (20 + 2 min.) - 2 communications longues
17h15 - 18h00 : **Conférence invitée 4 (40 + 5 min.)**

*Nous remercions **l'Université Paris Cité** de mettre à notre disposition les locaux de la RNL2024. Nous remercions également la **Division de Physique Non Linéaire** de la **SFP**, le laboratoire **de Physique de l'ENS**, le laboratoire **Matière et Systèmes Complexes (MSC),** le laboratoire **Physique et Mécanique des Milieux Hétérogènes (PMMH)**, le **Centre de Physique Théorique (CPT)**, le laboratoire de **Physique de ENS de Lyon,** l'Institut **Jean Le Rond d'Alembert,** les laboratoires **Phlam, LiPhy, LiSN,** et le **CNRS**.*
Cette année, nous sommes 212 inscrits au 11 mars 2024.

Le Comité d'Organisation de la RNL 2024 : Eric Falcon, Marc Lefranc, François Pétrélis et Chi-Tuong Pham.

Mardi 19 mars 2024

09h05 - 09h50 : Conférence invitée par Isabelle CANTAT (40 + 5 min.)
Flows in soap films

09h50 - 10h25 : Présentation des posters (2 min.) - 17 communications courtes

Laboratory granular landslides
L. Brivady, R. T. Cerbus, T. Faug et H. Kellay, présenté par Ludovic Brivady

Impact d'un jet liquide sur une surface chauffée
A. Goerlinger, F. Zoueshtiagh et A. Duchesne, présenté par Aurélien Goerlinger

Wave packets that do not move at the group velocity
G. Kozyreff, présenté par Gregory Kozyreff

Évaluation de la pertinence écologique des méthodes de calcul de la vitesse du changement climatique
L. Moinat, I. Gaponenko, S. Goyette et J. Kasparian, présenté par Jérôme Kasparian

Super-attracteurs d'ondes inertielles dans un frustum elliptique
B. Favier et S. Le Dizes, présenté par Benjamin Favier

Cheap turbulence modelling with quasi-singularities
W. Ruffenach, B. Dubrulle et L. Fery, présenté par Wandrille Ruffenach

La transition vers la turbulence induite par du bruit de l'écoulement de Couette plan contourne-t-elle les instantons ?
J. Rolland, présenté par Joran Rolland

Split societies
O. Devauchelle, P. Szymczak et P. Nowakowski, présenté par Olivier Devauchelle

Mesure du spectre des excitations autour d'un horizon acoustique
M. Jacquet, K. Falque, A. Delhom, Q. Glorieux, E. Giacobino et A. Bramati, présenté par Maxime Jacquet

Vertical velocities in quasi-geostrophic floating vortices
M. Aulnette, P. Le Gal et M. Le Bars, présenté par Marine Aulnette

Bacteria in liquid crystals: from the swimming mechanism of individuals to collective effects
G. Sintès, M. Góral, A. Lindner et T. López-León, présenté par Guillaume Sintes

Vertical structure of transport by ocean mesoscale turbulence
J. Meunier, B. Miquel et B. Gallet, présenté par Julie Meunier

Enhanced coupling power along manifolds in an intrinsically coupled system
M. C. de Sousa, A. B. Schelin, F. A. Marcus, R. L. Viana et I. L. Caldas, présenté par Meirielen C. de Sousa

Restitution coefficients of drops bouncing on a vibrating surface
T. Fullana, L. Molefe, F. Gallaire et J. M. Kolinski, présenté par Tomas Fullana

Large-Scale Turbulent Pressure Fluctuations Revealed by Ned Kahn's Artwork
J. Zhang et S. Perrard, présenté par Jishen Zhang

Couche limite turbulente sur réseaux logarithmiques
A. Lopez, A. Barral, G. Costa, Q. Pikeroen, B. Dubrulle et A.-L. Dalibard, présenté par Adrien Lopez

Suppression of wall modes in rapidly rotating Rayleigh-Bénard convection
L. Terrien, B. Favier et E. Knobloch, présenté par Louise Terrien

10h25 - 11h15 : Pause café Posters (50 min.)

11h15 - 11h55 : Présentation des posters (2 min.) - 20 communications courtes

Transmission anormale d'une onde acoustique à travers un choc faible
R. Delalande et F. Coulouvrat, présenté par Ronan Delalande

Champs multifractals : construction et déconstruction
S. Lakhal, L. Ponson, M. Benzaquen, J.-P. Bouchaud et M. M. Bandi, présenté par Samy Lakhal

Island myriads in periodic potentials
M. Lazarotto, I. Caldas et Y. Elskens, présenté par Matheus Lazarotto

Enstrophy conditioned extreme-event statistics and their morphology
B. Musci, J. Le Bris, A. Cheminet, C. Cuvier, P. Braganca, C. Wiertel-Gasquet, B. Dubrulle, présenté par Benjamin Musci

An experimental analogue of moist convection
V. Dorel, D. Lecoanet et M. Le Bars, présenté par Valentin Dorel

Dynamique d'une goutte sur une fibre verticale texturée
M. Leonard, J. Vanhulle et N. Vandewalle, présenté par Matteo Leonard

Reorganisation collective des dipoles dans une magnetostructure
A. Wafflard, E. Opsomer et N. Vandewalle, présenté par Adrien Wafflard

Numerical and experimental direct observation of vortex reconnection in a turbulent swirling flow
A. Harikrishnan, A. Cheminet, D. Geneste, A. Barlet, C. Cuvier, F. Daviaud, J. Foucaut, J. Laval, C. Wiertel, C. Nore, M. Creff, H. Faller, L. Cappanera, J. Guermond, B. Musci, J. Le Bris et B. Dubrulle, présenté par Abhishek P. Harikrishnan

Locally varying multifractality underlies intermittent energy dissipation in turbulence
S. Mukherjee, S. D. Murugan, R. Mukherjee et S. S. Ray, présenté par Siddhartha Mukherjee

Experimental observation of elastic rogue waves
M. Muralidhar, A. Naert et S. Aumaître, présenté par Murukesh Muralidhar

Etude expérimentale de moteurs à information mésoscopiques
A. Archambault, C. Crauste-Thibierge, S. Ciliberto et L. Bellon, présenté par Caroline Crauste-Thibierge

Equivalence between nonlinear dynamical systems and urn random processes
L. Brenig, présenté par Léon Brenig

Nonlinear interaction of turbulence and energetic particles in tokamak plasmas
A. Biancalani, A. Bottino, D. Del Sarto, M. V. Falessi, T. Hayward-Schneider, P. Lauber, A. Mishchenko, B. Rettino, J. N. Sama, F. Vannini, L. Villard, X. Wang, et F. Zonca, présenté par Alessandro Biancalani

Rheology of a particle laden soap film
J. Lalieu, A. Seguin, et G. Gauthier, présenté par Georges Gauthier

Un ratchet brownien à l'échelle humaine : une expérience de pensée historique en vrai !
A. Meynard, M. Lagoin, C. Crauste-Thibierge et A. Naert, présenté par Antoine Naert

Self-propulsion of floating ice blocks by melting
M. Chaigne, J. Jovet, M. Berhanu, A. Dawadi et A. Kudrolli, présenté par Michaël Berhanu

Impact de la rotation sur l'excitation stochastique des ondes acoustiques
L. Bessila, A. Deckx van Ruys, V. Buriasco, S. Mathis, L. Bugnet, R. García et S. Mathur, présenté par Leïla Bessila

Surface Quasi-Geostrophy: A Proxy for 3D Turbulence?
N. Valade, S. Thalabard et J. Bec, présenté par Nicolas Valade

Pendule de Doubochinski
D. B. Doubochinski et C. Raquin, présenté par Cyrille Raquin

Scale relativity applied to geophysical turbulence
W. Mouhali, T. Lehner, L. De Montera et L. Nottale, présenté par Waleed Mouhali

11h55 - 12h40 : Exposés longs (20 + 2 min.) - 2 communications longues

La turbulence d'ondes internes de gravité : un modèle pour la dynamique océanique à petite échelle ?
P.-P. Cortet et N. Lanchon, présenté par Pierre-Philippe Cortet

Trapping of Macroscopic Spinning Particles in Hydrodynamic Vortex Lattice
J.-B. Gorce, H. Xia, N. Francois, H. Punzmann, G. Falkovich et M. Shats, présenté par Jean-Baptiste Gorce

12h40 - 14h00 : DEJEUNER

14h00 - 14h45 : Exposés longs (20 + 2 min.) - 2 communications longues

Instabilité de vrillage et génération de courbure chez les plantes à vrilles
É. Dilly, J. Derr, S. Neukirch et D. Zanchi, présenté par Émilien Dilly

Use of metamaterials for surface wave control: Examples on backscattering reduction and boat wake absorption
S. Kucher, A. Kozluk, P. Petitjeans, A. Maurel, et V. Pagneux, présenté par Samantha Kucher

14h45 - 15h50 : Présentation des posters (2 min.) – 32 communications courtes

Bubble breakup probability in turbulence
A. Rivière et S. Perrard, présenté par Aliénor Rivière

Formation de film continu et homogène par coalescence de gouttes
A. Bouvier, E. Reyssat, J. Bico, B. Bouteille et J. Teisseire, présenté par Antoine Bouvier

Comment faire tourner un condensateur miniature déposé sur une surface d'eau ?
F. Mignolet et G. Lumay, présenté par Geoffroy Lumay

Inertia-gravity waves, a canonical example of nonlinear eigenvalue problems
J. Vidal et Y. Colin de Verdière, présenté par Jérémie Vidal

Profil d'un câble tracté
S. Villain-Guillot, présenté par Simon Villain-Guillot

Réflexion d'une onde de surface dans un domaine de profondeur variable
G. Ruiz Chavarria, présenté par Gerardo Ruiz Chavarria

The flexible sleeve
S. Neukirch, F. Dal Corso et Y. Vetyukov, présenté par Sébastien Neukirch

Observation en temps réel de la collision de solitons optiques dans une boucle de recirculation fibrée
F. Copie, P. Suret et S. Randoux, présenté par Francois Copie

A two-dimensional model for the dynamics of sand patches
C. Rambert, C. Narteau, J. Nield, G. Wiggs, P. Delorme, M. Baddock et P. Claudin, présenté par Camille Rambert

Mesure aérienne de la propagation d'une onde de surface dans une banquise fragmentée
S. Kuchly, E. Dumas-Lefebvre, D. Dumont, S. Perrard et A. Eddi, présenté par Sébastien Kuchly

Sedimentation of a single soluble particle at low Reynolds and high Peclet number
H. Nan, C. Yutong, W. David, D. Thierry, C. Philippe, S. Benoit, présenté par Nan He

Axisymmetric internal wave tunneling
S. Boury, B. R. Sutherland, S. Joubaud, P. Odier et T. Peacock, présenté par Samuel Boury

Sloshing instability driven by bubble plume
M. Cordelle Vacher, T. Boirot, S. Perrard et S. Ramananarivo, présenté par Marc Cordelle

Analyse statistique de l'endommagement sous choc dans des matériaux ductiles
C. Thouénon, A. Dubois, F. Willot et J. Besson, présenté par Corentin Thouénon

Réponse vibratoire d'ailes d'Odonates : mise en évidence d'un comportement non linéaire
C. Aracheloff, B. Thiria, R. Godoy-Diana, A. Nel et R. Garrouste, présenté par Camille Aracheloff

Thermo-mechanical influence on fracture propagation: integrating temperature effects through equilibrium statistical mechanics
C. Binetti, G. Florio, N. M. Pugno, S. Giordano et G. Puglisi, présenté par Claudia Binetti

Non-linéarité dans des systèmes micro-fluidiques par des valves
A. Bou Orm et B. Kaoui, présenté par Alaa Bou Orm

A hydrodynamic toy model for fish locomotion
B. Ventéjou, T. Métivet, A. Dupont, C. Graff et P. Peyla, présenté par Bruno Ventéjou

Numerical simulations of internal gravity wave turbulence
V. Labarre, G. Krstulovic et S. Nazarenko, présenté par Vincent Labarre

About the unsteady propulsion of an airfoil
G. Bertrand, R. Godoy-Diana, B. Thiria et M. Fermigier, présenté par Bertrand Gauthier

Transition topologique dans les oscillateurs paramétriques linéaires et non-linéaires
B. Apffel et R. Fleury, présenté par Benjamin Apffel

Flows in bursting soap film
A. Guillemot, J. Pierre et A. Bussonnière, présenté par Alexandre Guillemot

Interaction de gaz de solitons en eau profonde
L. Fache, F. Bonnefoy, G. Ducrozet, F. Copie, F. Novkoski, G. Ricard, E. Falcon, G. Roberti, P. Suret, G. El et S. Randoux, présenté par Loïc Fache

The influence of rotation on salt-fingers
S. Varghese, W. Bos et B. Miquel, présenté par Smiron Varghese

Correlations between scalar and vorticity reduce 2D mixing
X.-Y. Yin, W. Agoua, T. Wu et W. Bos, présenté par Wouter Bos

Lagrangian predictability in weakly ageostrophic surface ocean turbulence
S. Berti, M. Maalouly et G. Lapeyre, présenté par Stefano Berti

Turbulent convection and magnetically-driven flows in Europa's subsurface ocean
F. Daniel, C. Gissinger et L. Petitdemange, présenté par Florentin Daniel

Cooperation between two objects moving side-by-side in a granular medium
D. D. Carvalho, Y. Bertho, A. Seguin, E. M. Franklin et B. Darbois Texier, présenté par B. Darbois Texier

Envelope vector solitons in nonlinear flexible mechanical metamaterials
A. Demiquel, V. Achilleos, G. Theocharis, V. Tournat, présenté par Antoine Demiquel

3D tracking of microswimmers under flow and in a complex confinement
J. Moscatelli et F. Elias, présenté par Jeanne Moscatelli

Interaction between structures in a Couette-Poiseuille flow
B. Semin, T. Liu, R. Godoy-Diana et J. E. Wesfreid, présenté par Benoît Semin

Rheo-inertial transition to turbulence in pipe flow
A. Charles, J. Peixinho, T. Ribeiro, S. Azimi, V. Rocher, J.-C. Baudez et S. A. Bahrani, présenté par Antoine Charles

15h50 - 17h00 : Pause café Posters (1h10)

17h00 - 17h45 : Exposés longs (20 + 2 min.) - 2 communications longues

Getting a kick from water waves
G. P. Benham, O. Devauchelle et S. J. Thomson, présenté par Graham Benham

Oscillations de Bloch d'un soliton magnétique dans un mélange de bosons ultrafroids
F. Rabec, G. Chauveau, G. Brochier, S. Nascimbene, J. Dalibard et J. Beugnon, présenté par Jérome Beugnon

17h45 - 18h30 : Conférence invitée par Bertrand MAURY (40 + 5 min.)
Transport optimal et flots de gradient, un nouveau regard sur (une partie de) la physique

18h30 – 20h30 : Cocktail *(présentation du badge obligatoire)*

Mercredi 20 mars 2024

09h00 - 09h45 : Conférence invitée par David GUÉRY-ODELIN (40 + 5 min.)
The surprisingly rich physics of the modulated quantum pendulum

09h45 - 10h45 : Présentation des posters (2 min.) – 27 communications courtes

Nonlinear dynamics of zonal flows and geodesic acoustic modes in ITER
D. Gossard, A. Biancalani, A. Bottino, T. Hayward-Schneider, P. Lauber, A. Mishchenko, M. Pujol, M. Rampont, J. N. Sama et L. Villard, présenté par Didier Gossard

Détection de contact d'ordre élevé entre fibres
E. Hohnadel, O. Crespel, T. Métivet et F. Bertails-Descoubes, présenté par Emile Hohnadel

Le Collage dans des systèmes hamiltoniens : l'exemple de l'application standard
S. Rouvet, X. Leoncini et P. El-Kettani, présenté par Simon Rouvet

Bacterial exploration under confinement
R. Baillou, M. Pedrosa, Q. Guigue, S. Meinier, T. Darnige, G. Junot, F. Peruani et E. Clement, présenté par Renaud Baillou

Resonance of a floating object in a wave field
W. Reino, S. Kuchly, S. Perrard, G. Pucci et A. Eddi, présenté par Wilson Reino

Plasmas de fusion à l'équilibre thermodynamique : des particules au fluide.
Y. Lebouazda, A. Cordonnier, X. Leoncini et G. Dif-Pradalier, présenté par Yohann Lebouazda

Jet creation at the tip of a submerged plate forced by waves
D. Komaroff, G. Polly, A. Mérigaud, R. Godoy-Diana et B. Thiria, présenté par Diane Komaroff

Buoyancy effects in vertical soap films
A. Vigna-Brummer, A. Monier, C. Brouzet et C. Raufaste, présenté par Alexandre Vigna-Brummer

Rheology of a granular medium mixed with flexible fibers
L. Wierzchalek, B. Darbois-Texier et G. Gauthier, présenté par Ladislas Wierzchalek

Grain dispersion in smooth granular flows
K. Andrade, P. Jop, E. Kolb et S. Deboeuf, présenté par Klebbert Andrade

Bubble induced bifurcation in turbulent von Kármán flow
V. Mouet, F. Pétrélis et S. Fauve, présenté par Valentin Mouet

Aerodynamics of a fly swatter
A. Gayout, M. Bourgoin et N. Plihon, présenté par Ariane Gayout

Hydrodynamique généralisée et mesures de corrélations balistiques dans une boucle de recirculation fibrée
E. Charnay, P. Suret, B. Doyon, T. Bonnemain, F. Copie, présenté par Elias Charnay

Aiming of water waves in a time-varying metabathymetry
M. Koukouraki, A. Maurel, P. Petitjeans et V. Pagneux, présenté par Magdalini Koukouraki

Coalescence of viscous droplets under an elastic membrane
W-E. Khatla, E. Reyssat, A. Eddi, L. Duchemin, présenté par Wissem-Eddine Khatla

Non-linear scattering and nanojets in water waves using electrostriction
Q. Louis, C. Fraysse et E. Fort, présenté par Quentin Louis

Dynamics of two non miscible fluids inside a rotating cylinder
L. Gormit, I. Delbende, M. Rossi, présenté par Lyes Gormit

Towards broadband experimental wave index spatiotemporal modulation: Faraday waves in a modified gravity environment
E. Bontemps, Q. Louis et E. Fort, présenté par Eugénie Bontemps

Experimental investigation to test the static bell's inequality in a hydrodynamic system
S. K. Saroj, S. Perrard et M. Labousse, présenté par Sunil K. Saroj

Unveiling the wake of a surface swimming snake
V. Stin, G. Polly, A. Mérigaud, X. Bonnet, A. Herrel et R. Godoy-Diana, présenté par Vincent Stin

Particules solides et instabilités élasto-inertielles en écoulement de Taylor-Couette
C. Carré, T. Lacassagne, M. Moazzen, V. Thomy, S. Amir Bahrani, présenté par Charles Carré

Disambiguation of the different types of crossings in a mycelial branching network through complete identification of its spatio-temporal structure
T. Chassereau, F. Chapeland-Leclerc et E. Herbert, présenté par Thibault Chassereau

A very expressive plant: Spathiphyllum shape reactions to water stress
P. Marmottant, B. Dollet, O. Stephan, C. Quilliet et E. Siéfert, présenté par Philippe Marmottant

Bubble clouds generated by single and multi-plunging jets
N. Dev, J. John Soundar Jerome, H. Scolan, J.-P. Matas, présenté par Narendra Dev

Small coherent structures in rough turbulent convection
N. Carbonneau, J. Salort et A. Sergent, présenté par Nathan Carbonneau

Fluctuations du flux de chaleur en convection thermique à haut nombre de Rayleigh
M. Caelen, F. Pétrélis et S. Fauve, présenté par Martin Caelen

Numerical computation of a turbulent wind flow over buildings and estimation of its effect on drone's model
A. Ammar, A. Biancalani, A. Rabia, F. Chinesta, L. Chaozhen et S. Yahiaoui, présenté par Chaozhen Li

10h45 - 11h45 : Pause café Posters (1h00)

11h45 - 12h30 : Exposés longs (20 + 2 min.) - 2 communications longues

Dynamique d'une hélice acoustofluidique
S. Miralles, B. Vincent, A. Pothérat, D. Henry et V. Botton, présenté par Sophie Miralles

Spatio-temporal boundary dissipation measurements using Diffusing-Wave Spectroscopy
E. Francisco et S. Aumaître, présenté par Enzo Francisco

12h30 - 14h00 : DEJEUNER

14h00 - 14h45 : Exposés longs (20 + 2 min.) - 2 communications longues

La forme des bulles piégées dans la glace
V. Thiévenaz et A. Sauret, présenté par Virgile Thiévenaz

Compartment model of epidemic spreading in complex networks with mortality
T. Granger, T. Michelitsch, B. Collet, M. Bestehorn et A. Riascos, présenté par Thomas Michelitsch

14h45 - 15h25 : Présentation des posters (2 min.) – 19 communications courtes

Toy-model for the formation of rillenkarren by rainfall
S. Djambov et F. Gallaire, présenté par Simeon Djambov

Scaling laws of the plasma velocity in visco-resistive magnetohydrodynamic systems
A. Krupka et M.-C. Firpo, présenté par Anna Krupka

Noise sustained vs. self-sustained structures in rotor-stator flow
A. Gesla, L. Martin Witkowski, Y. Duguet et P. Le Quéré, présenté par Artur Gesla

Effet thermoélectrique à l'interface Gallium-Mercure
M. Vernet, S. Fauve et C. Gissinger, présenté par Marlone Vernet

How dynamic shape change effects the entry event
E. Gregorio, E. Balaras et M. C. Leftwich, présenté par Elizabeth Gregorio

In the search of magnetic reversals in a geodynamo model with a stably-stratified layer
N. P. Müller, F. Pétrélis et C. Gissinger, présenté par Nicolás Müller

Etats métastables d'un tricot relaxé : quelle est la forme de mon pull-over ?
Samuel Poincloux, Audrey Steinberger et Jerôme Crassous, présenté par Jérôme Crassous

Comment une singularité en temps fini peut "aveugler" : l'exemple des vortex ponctuels
P. El Kettani, X. Leoncini et E. Ugalde, présenté par Perla El Kettani

Spatiotemporal parametric modulation of a soft beam
E. Duval, J. Asnacios, S. Fauve, V. Tournat, F. Pétrélis et M. Lanoy, présenté par Éléonore Duval

Fluid response to the inner core's translational oscillations
P. Personnettaz, N. Schaeffer, D. Cébron et M. Mandea, présenté par Paolo Personnettaz

Dripping flow with solidification : an analogue system for the growth of tubular stalactites.
A. Mongruel, A. Eddi et P. Claudin, présenté par Anne Mongruel

Instabilities around a spheroid spinning in a rotating stratified fluid
A. Chauchat, M. Le Bars et P. Meunier, présenté par Antoine Chauchat

Topographic effects in planetary magneto-hydrodynamic flows
R. Monville, D. Cébron et D. Jault, présenté par Rémy Monville

Low-cost realization of a quantitative chaotic waterwheel
G. Le Lay, présenté par Grégoire Le Lay

Compétition entre convection naturelle et convection forcée en érosion par dissolution
M. Chaigne, M. Receveur, S. Courrech du Pont et M. Berhanu, présenté par Martin Chaigne

Caractérisation par mesure sismique de la banquise soumise à la houle
B. Auvity, S. Chekir, D. Dumont, L. Moreau, L. Duchemin, A. Eddi et S. Perrard, présenté par Baptiste Auvity

Internal wave instabilities and transition to turbulence in large aspect ratio wave attractors
I. Sibgatullin, S. Elistratov et T. Dauxois, présenté par Ilias Sibgatullin

Quantifying the flows in a freezing liquid foam
K. Bumma, A. Huerre, J. Pierre et T. Séon, présenté par Krishan Bumma

Investigating Tayler instability in a liquid metal experiment
G. Bermudez et C. Gissinger, présenté par Guillaume Bermudez

15h25 - 16h30 : Pause café Posters (1h05)

16h30 - 17h15 : Exposés longs (20 + 2 min.) - 2 communications longues

Mobile soap film drainage shows self-similarity
A. Monier, F.-X. Gauci, C. Claudet, F. Celestini, C. Brouzet et C. Raufaste, présenté par Antoine Monier

Taylor's Swimming Sheet near a Soft Wall
A. Jha, Y. Amarouchene et T. Salez, présenté par Aditya Jha

17h15 - 18h00 : Conférence invitée par Dominic VELLA (40 + 5 min.)
Some surprises in elastic snap-through

18h00 : FIN

Exposés invités de la 27^{e} Rencontre du Non-Linéaire

Flows in soap films

Isabelle Cantat

Institut de Physique de Rennes (IPR), UMR CNRS 6251, Université Rennes 1, 263, av. du Général Leclerc, 35042 Rennes Cedex
isabelle.cantat@univ-rennes1.fr

The thinning of the liquid films separating bubbles in a foam or in a bubbly liquid controls the coalescence process and the foam stability, and is highly relevant in many industrial processes. The spatiotemporal evolution of the film thickness is governed by nonlinear equations, whose solutions are still mostly unknown. In this talk we will discuss a few examples of flows in the plane of a horizontal foam film, driven by tiny capillary forces. These original flows will allow us to revisit the old problem of the 'marginal regeneration', a peculiar instability occurring between a flat film and a meniscus, which controls the film drainage.

The surprisingly rich physics of the modulated quantum pendulum

David Guéry-Odelin

Université Paul Sabatier - Toulouse 3, Laboratoire de Collisions - Agrégats - Réactivité, 118 Route de Narbonne, 31062 Toulouse cedex 9, France
dgo@irsamc.ups-tlse.fr

In classical mechanics, a pendulum whose parameters are modulated in time provides a standard example for introducing classical chaos, with the emergence of mixed or fully chaotic stroboscopic phase spaces. In quantum physics, although the Schrödinger equation is fully linear, the same Hamiltonian offers the possibility of studying weak and strong localization and chaos-assisted tunneling [1]. We will detail our recent results in this direction. Using quantum control techniques to drive the pendulum appropriately [2], we have recently extended the accessible physics in this system by demonstrating the production of squeezed states and matter wave transport with a quantum ratchet [3], performing qubit-based quantum computations and carrying out various quantum simulations based on Floquet Hamiltonian engineering including the generation of a synthetic and tunable cristal [4].

Références

1. M. Arnal, G. Chatelain, M. Martinez, N. Dupont, O. Giraud, D. Ullmo, B. Georgeot, G. Lemarié, J. Billy & D. Guéry-Odelin, Chaos-assisted tunneling resonances in a synthetic Floquet superlattice, *Sci. Adv.*, **6**, eabc4886 (2020).
2. N. Dupont, G. Chatelain, L. Gabardos, M. Arnal, J. Billy, B. Peaudecerf, D. Sugny & D. Guéry-Odelin, Quantum state control of a Bose–Einstein condensate in an optical lattice, *PRX Quantum*, **2**, 040303 (2021).
3. N. Dupont, L. Gabardos, F. Arrouas, N. Ombredane, J. Billy, B. Peaudecerf & D. Guéry-Odelin, A regular Hamiltonian halting ratchet for matter wave transport, *Phys. Rev. Lett.*, **131**, 133401 (2023).
4. N. Dupont, L. Gabardos, F. Arrouas, G. Chatelain, M. Arnal, J. Billy, P. Schlagheck, B. Peaudecerf & D. Guéry-Odelin, Emergence of a tunable crystalline order in a Floquet–Bloch system from a parametric instability , *Proc. Natl. Acad. Sci. USA*, **120**, e2300980120 (2023).

Transport optimal et flots de gradients, un nouveau regard sur (une partie de) la physique

Bertrand Maury

Laboratoire de Mathématiques, Université Paris-Saclay, 91405 Orsay Cedex
bertrand.maury@math.u-psud.fr

Formulé par Monge à la fin du XVIII^{e} siècle, le problème du transport optimal de masse a été « dormant » pendant plus d'un siècle, il a suscité un regain d'intérêt au milieu du XX^{e} siècle suite aux travaux fondateurs de Kantorovich en URSS, et a connu un troisième essor, fulgurant, il y a une trentaine d'années, il s'agit maintenant d'un domaine à part entière de l'analyse mathématique et du calcul des variations. Nous souhaitons présenter comment cette approche, qui vise au départ à estimer le coût de transport d'une distribution de masse donnée vers une zone d'accueil de cette masse, permet de définir une distance sur l'espace des mesures de probabilité (ou plus généralement des mesures positives d'une masse totale donnée). Il est alors possible de définir sur ce nouvel espace métrique des notions a priori réservées aux espaces euclidiens ou hilbertiens, comme la notion de flot de gradient (mouvement suivant la ligne de plus grande pente d'une fonction de « paysage » donnée). Cette approche jette une nouvelle lumière sur des équations hyperclassiques, comme l'équation de la chaleur, qui peut être vue dans ce contexte comme un flot de gradient pour la fonctionnelle d'entropie. Nous présenterons des extensions plus exotiques de cette approche, en particulier dans le domaine du mouvement de cellules ou de foules, ou de certains modèle fluides (écoulements de Hele-Shaw ou équations d'Euler sans pression avec contrainte de congestion).

Some surprises in elastic snap-through

Dominic Vella

Mathematical Institute, University of Oxford, Andrew Wiles Building, Radcliffe Observatory Quarter, Woodstock Road, Oxford, UK
dominic.vella@maths.ox.ac.uk

Elastic snap-through is familiar from everyday life ; whether it's the rapid inversion of an umbrella or the pop of a hair clip, we are familiar with the idea that some elastic objects have two equilibrium states and can be forced to 'snap' between them with a suitable load. These examples generally suggest that the motion occurs quickly, but trying to estimate this speed brings some surprises : if anything, the motion should happen *faster* than is typically observed. We show that this 'slow' snap-through occurs even without any viscous dissipation and gives a new route to control the state and behaviour of an elastic system using the rate of loading.

Exposés du Mini-colloque

« Nonlinear soft interfaces: wetting, adhesion, flow and fracture »

Statics and dynamics of soft wetting

Bruno Andreotti

LP ENS, ENS, PSL, 24 rue Lhomond, 75005 PARIS
andreotti@phys.ens.fr

Wetting of yield-stress fluids

Catherine Barentin

Institut Lumière Matière, Université de Lyon, Université Claude Bernard Lyon 1, CNRS
catherine.barentin@univ-lyon1.fr

Yield-stress fluids such as emulsions, suspensions, gels or foams exhibit interesting mechanical properties depending on the applied stress. Indeed they behave like an elastic deform plastically and finally flow like a liquid above it. This intermediate behavior solid/liquid makes them particularly interesting for applications (food industry, cosmetics, building industry), but fundamentally difficult to describe.

In many applications such as coating, printing, imbibition, interfaces between a solid surface and a complex fluid are encounted

In this presentation, I will study the wetting properties of yield stress fluids by performing three capillary experiments: a) capillary rise [1] , b) adhesion due to a capillary bridge [2] and c) spreading of a drop of a yied-stress fluid [3]. In the case of simple fluids, such experiments are classical and the wetting laws (Jurin's law or Young law) are well kown. Here I will study the influence of the yield stress on the final capillary rise or on the final contact angle. I will also show the strong impact of the dynamic history and of the boundary conditions [4]. More importantly, I will show that exploring the competition between surface tension, which is an equilibrium property, and yield stress effects that often keep the system out of thermodynamic equilibrium due to a dynamic arrest is possible as soon as force balances are performed.

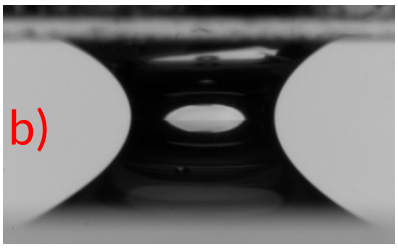

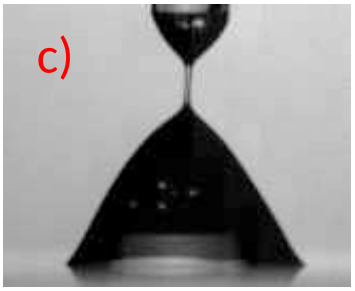

References

1. B. Géraud *et al.*, *Eur. Phys. Letters*, **107**, 58002 (2009).
2. L. Jorgensen *et al.*, *Soft Matter*, **11**, 5111 (2015).
3. G. Martouzet *et al.*, *Phys. Rev. Fluids*, **6**, 044006 (2021).
4. J. Péméja *et al.*, *Phys. Rev. Fluids* **4**, 033301 (2019).

Drop spreading on poroelastic substrates

Camille Duprat

LadHyX, École polytechnique, 91128 Palaiseau Cedex
duprat@ladhyx.polytechnique.fr

In many situations, drops spread on soft and porous substrates, such as paper, wood or gels. The wetting dynamics depends on a coupling between spreading, absorption and deformation of the substrate. Here, we consider the effect of swelling on the spreading dynamics of a drop deposited on a model poroelastic gel. When a drop is placed on a surface that it fully wets, it usually spreads until the height of the drop is comparable to the size of a single fluid molecule. However, when some fluid is absorbed by the substrate, the drop will reach a maximum radius that depends on the porous and elastic properties of the substrate. Furthermore, we show that the spreading is slowed down due to the deformation of the surface that modifies the apparent contact angle locally [1].

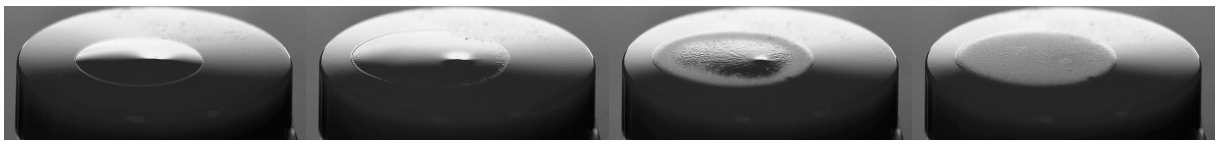

Figure 1. Chronophotography of the spreading and swelling dynamics of a drop of silicon oil ($\eta = 2.3$ mPa $\cdot$ s) on a flat elastomer (PVS of modulus $E = 0.9$ MPa). Time between successive images 1.8 s.

References

1. P. Van de Velde *et al.*, Spreading and absorption of a drop on a swelling surface, *Europhys. Lett.*, **144**, 33001 (2023).

Pressure-saturation hysteresis of two-phase flows in disordered media

Jordi Ortín

Departament de Física de la Matèria Condensada, Universitat de Barcelona, Spain and UBICS (Universitat de Barcelona Institute of Complex Systems) C/ Martí i Franqués 1, 08028 Barcelona, Spain
jordi.ortin@ub.edu

Fluid–fluid displacements in disordered media are found in a variety of natural and technological relevant situations, from the rise of sap in plants and wetting/drying processes in soils, to filtering and printing. On the other hand, displacements in disordered media exhibit complex phenomena at multiple scales, making them challenging and interesting also from a fundamental point of view.

In this talk I will focus the attention on the relationship across scales of pore-scale capillary events, spatially-extended collective displacements (avalanches or Haines jumps), and pressure vs saturation hysteresis cycles. I will show that the return-point memory property of quasistatic imbibition-drainage cycles provides a robust means to sort out and quantify the energy losses of capillary origin. The relative importance of viscous dissipation will be deduced by comparison with the results of nearly-quasistatic experiments.

The mechanisms identified here apply to a broad range of problems in hydrology, geophysics and engineering.

References

1. R. Holtzman, M. Dentz, R. Planet & J. Ortín, The origin of hysteresis and memory of two-phase flow in disordered media, *Commun. Phys.*, **3**, 1–7 (2020).
2. R. Holtzman, M. Dentz, R. Planet & J. Ortín, The relation between dissipation and memory in two-fluid displacements in disordered media, *Geophys. Res. Lett.*, **50**, 1–8 (2023).

Dynamic elastocapillary coalescence of slender structures

Emmanuel Siéfert, Béatrice Hua, Hadrien Bense, Basile Radisson, Lucie Domino, Fabian Brau

Nonlinear Physical Chemistry Unit, Université Libre de Bruxelles, B-1050 Bruxelles
emmanuel.siefert@gmail.com

Some small animals, such as bees, bats or passerine birds, are nectarivores. They feed by dipping periodically their hairy tongue - resembling a brush - in the nectar. As a first step to understand this intricate fluid capture mechanism, we consider a minimal tongue consisting of two hairs. I will first present the results in the quasi-static regime: when partially immersed, they interact with each other through the capillary force induced by their menisci. As they are removed from the bath, their dry length increases, and they become easier to bend until the capillary force is strong enough to trigger contact. Surprisingly, the structures snap to contact from a finite distance at a critical dry length. The transition to coalescence is thus subcritical and exhibits a large hysteresis loop between two stable states. An analytical coalescence criterion is derived and agrees well with experimental data.

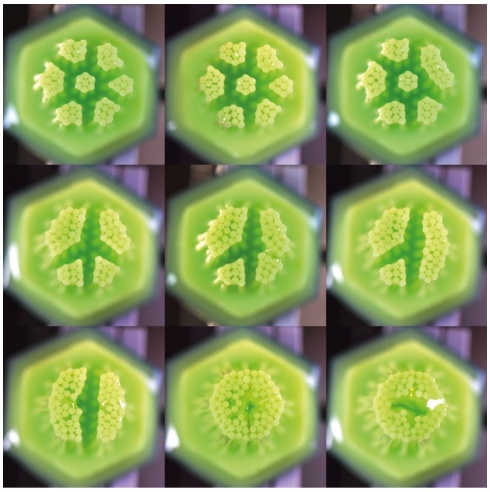

Figure 1. Aggregation of fibers in a brush with an increasing withdrawal speed (from top-left to right-bottom).

I will then consider the role of the withdrawing speed. We show that the capillary "Cheerios" force strongly increases with the retraction speed by up to a factor ten compared to the static case. This remarkable increase stems from the shape of the dynamical meniscus between the two fibers. We first study the dynamical meniscus around one fiber and obtain experimental and numerical scaling of its size increase with the capillary number, which is not captured by the classical Landau-Levich-Derjaguin theory. We then show that the shape of the deformed air-liquid interface around two fibers can be inferred from the linear superposition of the interface around a single fiber. These results yield an analytical expression for the attraction which compares well with the experimental data.

I will finally present preliminary results on the withdrawal of brushes containing many rigid and flexible fibers.

Soft coring: How to get a clarinet out of a flute?

Matteo Ciccotti[1], Frédéric Lechenault[2], Ilyad Ramdane[2], Sébastien Moulinet[2], M. Roman-Faure[1]

[1] Soft Matter Science and Engineering Laboratory, ESPCI Paris, Université PSL, CNRS, Sorbonne Université, 75005 Paris, France
[2] Laboratoire de Physique, ENS Paris, Université PSL, CNRS, Sorbonne Université, Université Paris Diderot, Sorbonne Paris Cité, 75005 Paris, France
matteo.ciccotti@espci.fr

Cutting mozzarella with a dull blade results in poorly shaped slices [1]: the process occurs in a configuration so deformed as to yield unexpectedly curved surfaces. We study the morphogenetics arising from such process through the example of coring [2]: when a thin cylindrical hollow punch is pushed into a soft elastomer, the large transverse expansion occurring during the cutting is responsible for the "clarinet-shape" of the extracted core, which reaches diameters far smaller than those of the tool (Fig. 1 (a)).

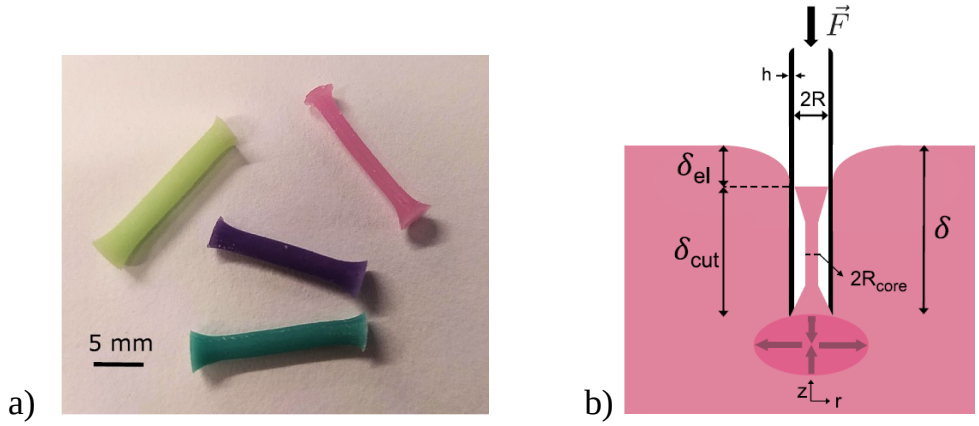

Figure 1. (a) Some examples of clarinet-shaped cores. (b) Sketch of the coring mechanism.

With contributions from fracture mechanics and large strain theory [3], we build a simple yet quantitative understanding of the observed discrepancy, which is shown to occur when the size of the punch is smaller than a characteristic, tomo-elastic length scale [2]. Moreover, material nonlinearity and friction appear to play a crucial role in this phenomenon [4].

References

1. T. Atkins, *The Science and Engineering of Cutting: The mechanics and processes of separating, scratching and puncturing biomaterials, metals and non-metals*, Butterworth-Heinemann (2009).
2. F. Lechenault, I. Ramdane, S. Moulinet, M. Roman-Faure & M. Ciccotti, *Extreme Mech. Lett.*, **61**, 101976 (2023).
3. C. Creton & M. Ciccotti, *Rep. Progr. Phys.*, **79**, 046601 (2016).
4. Y. Liu, C.-Y. Hui & W. Hong, *Extreme Mech. Lett.* **46**, 101343 (2021).

Nonlinear effects on crack propagation and interaction

C. Peretti[1], E. Lindas[1], O. Chaffard[1], Thierry Biben[1], A. Gravouil[2], Osvanny Ramos[1], Stéphane Santucci[3], Loïc Vanel[1]

[1] Université de Lyon, Université Claude Bernard Lyon 1, CNRS, Institut Lumière Matière, France
[2] Université de Lyon, LaMCoS, INSA-Lyon, CNRS, France
[3] Université de Lyon, École Normale Supérieure de Lyon, CNRS, Laboratoire de physique, France
loic.vanel@univ-lyon1.fr

The observed repulsive behaviour of two initially collinear cracks growing towards each other and leading to a hook-shaped path questioned recently the validity of the Principle of Local Symmetry within Linear Elastic Fracture Mechanics theory [1]. Theoretical and numerical work has solved this dilemma, providing the precise geometric conditions for the existence of the repulsive phase and revealing a multi-scale behaviour of the repulsive/attractive transition [2]. However, in polymer films, the repulsive phase depends strongly on the microscopic behaviour of the material, highlighting the crucial role of the fracture process zone [1]. At interaction distances larger than the process zone size, microscopic shape of the process zone tip controls crack repulsion. The maximum angle of repulsion is then systematically smaller than the one predicted by linear elasticity [2].

Nonlinear elastic materials such as elastomers also depart from the prediction of linear elasticity for interacting cracks. We performed experiments on PDMS film that indeed show a maximum angle of repulsion not only significantly smaller than the one of linear elasticity, but also smaller than the one observed in polymer films with a plastic process zone. Our FEM simulations on a Mooney–Rivlin material confirm that the nonlinear elastic response of PDMS modifies the crack path, reducing the repulsive strength between the two interacting cracks.

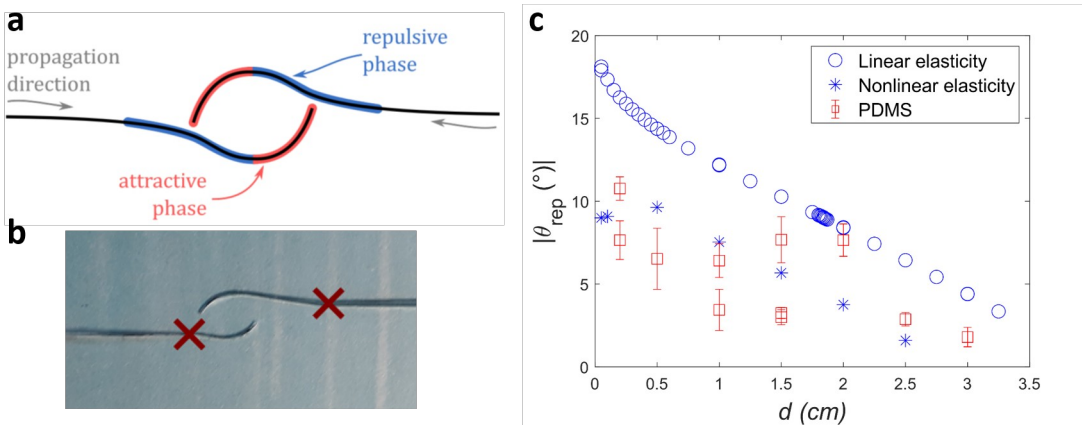

Figure 1. a. Repulsive and attractive phase (FEM). **b.** Example in PDMS film. **c.** Maximum repulsion angle in PDMS films and from FEM simulation of Mooney-Rivlin material as a function of the vertical separation of the two cracks (d=0 corresponds to perfectly aligned cracks).

References

1. M. J. Dalbe, J. Koivisto, L. Vanel, A. Miksic, O. Ramos, M. Alava & S. Santucci, *Phys. Rev. Lett.*, **114**, 205501 (2015).
2. M.-E. Schwaab, S. Santucci, T. Biben, A. Gravouil & L. Vanel, *Phys. Rev. Lett.*, **120**, 255501 (2018).

Soft wetting: Nonlinearity at large deformations

Jacco Snoeijer

Physics of Fluids group, Fac. of Science and Technology, University of Twente
j.h.snoeijer@utwente.nl

Wetting at the nanometer scale: Molecular desorption induced by a moving contact line

Sylvain Franiatte, Philippe Tordjeman, Thierry Ondarçuhu

Institut de Mécanique des Fluides de Toulouse, IMFT, 2 allée du Professeur Camille Soula, 31400 Toulouse
thierry.ondarcuhu@imft.fr

It is well established that the wetting properties of a surface by a liquid largely depend on the topographic and chemical nature of the substrate. In particular, the contact line motion is extremely sensitive to the presence of surface defects down to the nanometer scale. Here, we address the fundamental question of a possible action of the contact line on the surface at molecular scale.

We have shown recently that Atomic force microscopy (AFM) is a unique tool to study the dynamics of contact line or nanomeniscus down to the nanometer scale. The measurement of the capillary force exerted by the liquid on a nanoneedle carved at the apex of the AFM tip allows the monitoring of minute changes of surface wettability of the tip. In the present study, we continuously dip and withdraw the tip from the liquid a large number of times. We demonstrate that this leads to a change of the wettability of the surface chemistry while keeping the topography intact (see figure). Since the initial surface can be recovered when the tip is left in air, we interpret this behavior as a desorption of airborne contaminants by the liquid. Interestingly, using specific experiments, we unambiguously demonstrate that the desorption of physically sorbed molecules is induced at the contact line. The mechanism of molecules desorption is directly determined by the capillary force exerted at the contact line on the molecules. We also emphasize the potential of AFM to clearly decorrelate the effects of topographical and chemical defects and monitor, with a subsecond time resolution, the dynamics of molecules adsorption on a surface.

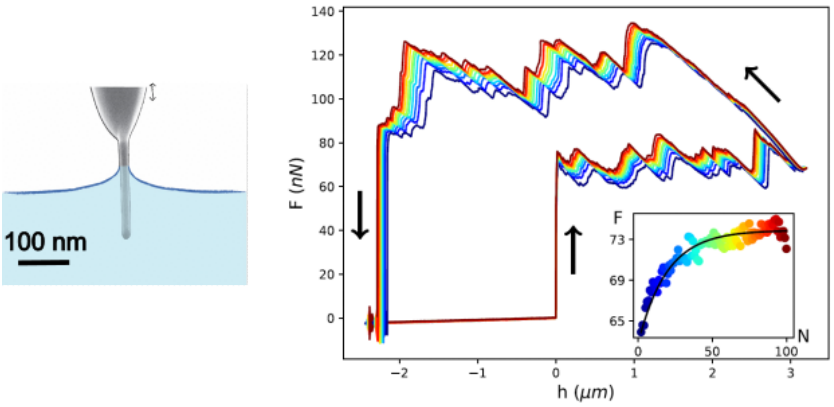

Figure 1. Left: sketch of the experiment; right: capillary force F measured as a function of the immersion depth h for a nanoneedle dipped in (increasing h) and withdrawn from (decreasing h) a liquid bath, for successive dipping cycles (from blue to red); inset: evolution of the force associated with a given peak of the force curve as a function of the number N of cycles.

References

1. S. Franiatte, P. Tordjeman, T. Ondarçuhu, *Phys. Rev. Lett.*, **127**, 065501 (2021).
2. S. Franiatte, P. Tordjeman, T. Ondarçuhu, *Langmuir*, **38**, 2614–2625 (2022).

Water dewetting on ice

Axel Huerre[1], Virgile Thiévenaz[2], Christophe Josserand[3], Rodolphe Grivet[3], Thomas Séon[4]

[1] MSC, Université Paris Cité, CNRS (UMR 7057), 75013 Paris, France
[2] PMMH, CNRS, ESPCI Paris, Sorbonne Université, Université Paris Cité, F-75005, Paris, France
[3] Laboratoire d'Hydrodynamique (LadHyX), IP Paris, CNRS-Ecole Polytechnique (UMR 7646), 91128 Palaiseau, France
[4] Institut Franco-Argentin de Dynamique des Fluides pour l'Environnement (IFADyFE), CNRS, UBA, CONICET (IRL 2027), CABA, Buenos Aires, Argentine.
axel.huerre@cnrs.fr

When considering a drop of melt on its own solid, intuition would lead to the conclusion that this drop will wet the solid completely. However, in the case of water on ice, experiments by Knight in 1966 showed that macroscopic water droplets can be observed on ice, suggesting a dewetting behaviour. We will see from recent experiments carried out in different configurations that the question of the contact angle of water on ice is still an open question. Experiments on the dewetting of a thin film of water on ice, with the formation of a droplet, will lead to the measurement of an angle between ice, liquid and air [2]. In a Landau–Levich coating experiment, we studied the removal of an ice plate from a water bath. Using a theoretical approach combining solidification and capillary fluid mechanics, we are able to identify a regime where a stable contact line of water on ice is maintained in a permanent regime. In this regime, the vertical position of the contact line depends on the angle between the three phases. This measurement finally allows us to propose a value for the contact angle of water on ice.

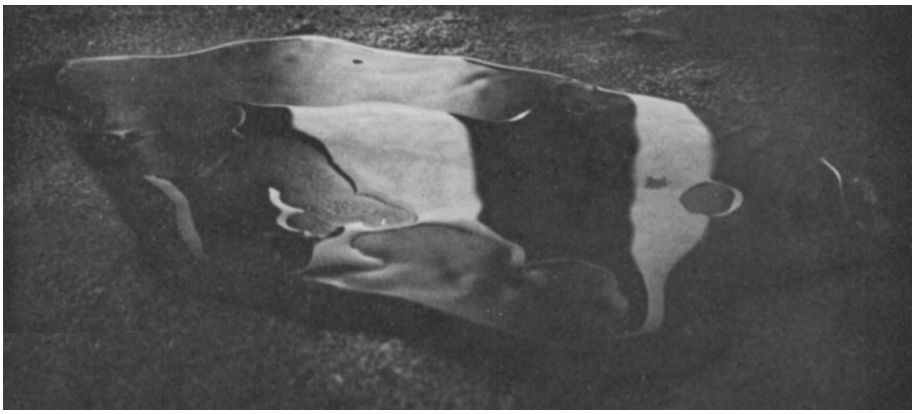

Figure 1. Historical experiment of a film of water dewetting on ice. [1]

References

1. C. A. Knight, *J. Colloid Interf. Sci.*, **25**, 280–284 (1966).
2. V. Thievenaz, T. Séon & C. Josserand, *Europhys. Lett.*, **132**, 24002 (2020).

Superposition des ménisques capillaires : courber l'interface liquide pour micromanipuler des objets flottants

Megan Delens, Axel Franckart, Nicolas Vandewalle

Laboratoire GRASP, Institut de Physique, Université of Liège, 19, Allée du six août, 4000 Liège, Belgique
megan.delens@uliege.be

La manipulation d'objets flottants, qu'ils soient solides ou liquides, allant des tailles microscopiques aux tailles mésoscopiques, revêt une importance considérable dans diverses applications de microfluidique et de microfabrication. Alors que les ménisques capillaires s'auto-assemblent naturellement [1] et transportent les particules [2] piégées aux interfaces liquides, leurs formes et tailles sont limitées. Effectivement à cause de la gravité, il est impossible d'incliner des liquides sur plus de quelques millimètres. Dans cette présentation, nous confrontons cette propriété fondamentale en courbant des liquides sans limite de taille ou de forme grâce à un réseau de pics de rayon submillimétrique imprimés en 3D. En effet, chacun de ces pics est le siège d'un ménisque capillaire et lorsque ceux-ci sont très proches, ils se superposent pour former un ménisque géant. En ajustant la géométrie des pics et du réseau, nous pouvons finement contrôler les gradients de hauteur sur la surface du liquide, permettant ainsi la création de tout type de topographie liquide, élémentaire ou artistique, à faible coût.

Les objets flottants à la surface de l'eau créant eux-mêmes un ménisque et étant sujets aux courbes de l'interface liquide, notre méthode est également un outil puissant pour manipuler des objets de toutes tailles [3].

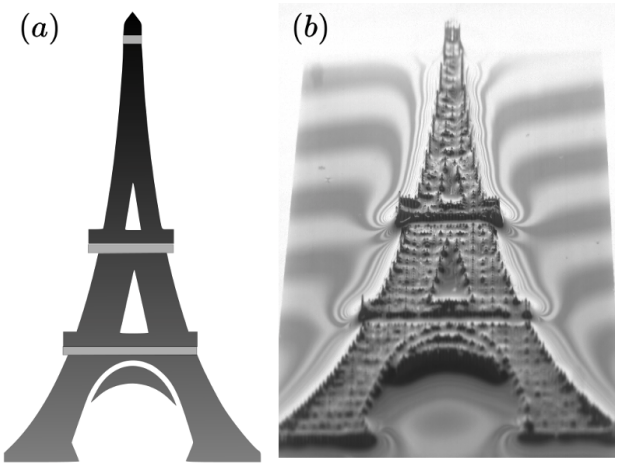

Figure 1. À partir de cette image 2D simplifiée du monument de la Tour Eiffel en niveaux de gris (a), un réseau de pics coniques tronquées a été conçu et imprimé en 3D. Au fur et à mesure que le liquide envahit le réseau, il s'élève pour reproduire la *Tour Eiffel* (b). Le code permettant de créer un réseau à partir d'une image et les fichiers STL sont disponibles sur notre GitHub à l'adresse `https://github.com/GRASP-LAB/3D-printed-spines`.

Références

1. D. Vella & L. Mahadevan, *Am. J. Phys*, **73**, 817 (2005).
2. D. L. Hu & J. W. Bush, *Nature*, **437**, 733 (2005).
3. M. Delens, A. Franckart & N. Vandewalle, Controlling liquid landscape with 3D-printed spines : A tool for micromanipulation, *Under review*, `https://doi.org/10.21203/rs.3.rs-3467162/v1` (2023).

Dynamiques de lignes de contact oscillantes

Pierre-Brice Bintein[1], Arnaud Grados[1], François Gallaire[2], Laurent Limat[1], Philippe Brunet[1]

[1] Laboratoire Matière et Systèmes Complexes, Université Paris Cité, CNRS, Paris
[2] LFMI-STI-IGM, EPFL, Lausanne
pierre-brice.bintein@u-paris.fr

Un liquide contraint d'avancer ou reculer sur une surface solide peut être observé dans notre environnement immédiat (ainsi les gouttes de pluie entraînées sur les vitres d'une voiture) comme dans certains procédés industriels (tels les revêtements de solides par dépôt liquide). Le mouvement du liquide est alors gouverné par la dynamique de mouillage de la ligne de contact (l'intersection des trois phases), qui est déterminé par l'hydrodynamique près de l'interface liquide-solide (soit la contrainte de cisaillement) et par les interactions physico-chimiques avec le substrat. L'angle de contact entre le liquide et le solide traduit macroscopiquement ces interactions moléculaires, et la relation entre l'angle de contact dynamique et la vitesse de la ligne de contact permet de comprendre et caractériser la dynamique de mouillage, qui a été beaucoup étudiée ces dernières années, à l'intersection de la mécanique des fluides, de la chimie et de l'ingénierie [1]. Des études spécifiques ont considéré l'influence de l'inertie sur une telle dynamique interfaciale [2, 3] qui peut survenir dans des conditions instationnaires.

Nous considérons ici la réponse d'une ligne de contact à un forçage oscillant horizontalement à basse fréquence. La goutte repose sur une surface non mouillante de faible hystérésis, et est accrochée par un capot adhésif, de sorte que la dynamique de la ligne triple implique une composante inertielle significative. En effet sous un tel forçage périodique, la loi de mobilité liant vitesse et angle de contact n'est plus dictée par un équilibre visco-capillaire classique (loi de Cox–Voinov) [2–4]. Afin de proposer des lois constitutives prenant l'inertie en compte, nous mesurons la dynamique de l'angle de contact en fonction de la vitesse de la ligne triple et relions les cycles d'hystérésis ainsi obtenus aux propriétés des oscillations (amplitude et fréquence), des liquides et des substrats.

Références

1. J. H. Snoeijer & B. Andreotti, Moving Contact Lines : Scales, Regimes, and Dynamical Transitions, *Annu. Rev. Fluid. Mech*, **45**, 269–292 (2013).
2. R. G. Cox, Inertial and viscous effects on dynamic contact angles, *J. Fluid. Mech.*, **357**, 249–278 (1998).
3. D. Fiorini, M. A. Mendez, A. Simonini, J. Steelant & D. Seveno, Effect of inertia on the dynamic contact angle in oscillating menisci, *Phys. Fluids*, **34**, 102116 (2022).
4. C.-L. Ting & M. Perlin, Boundary conditions in the vicinity of the contact line at a vertically oscillating upright plate: An experimental investigation, *J. Fluid. Mech.*, **295**, 263–300 (1995).

Surface deformation of a thin liquid film in the vicinity of a vertical fiber

Alice Étienne-Simonetti[1], Frédéric Restagno[1], Isabelle Cantat[2], Emmanuelle Rio[1]

[1] Laboratoire de Physique des Solides, Orsay, France
[2] Institut de Physique de Rennes, Rennes, France
alice.etienne-simonetti@universite-paris-saclay.fr

The deposition of homogeneous thin liquid films is a ubiquitous goal in the industry, for example, to confer mechanical or optical properties on a solid surface. A standard technique involves depositing a liquid film, which will dry and lead to the formation of the desired layer. Many heterogeneities can appear during the deposition of the liquid film or its drying [1], due to thickness instabilities [2] or particle accumulation, for example. Dust deposition can be an issue during such coating processes as it leads to thickness heterogeneities [3].

To study the impact of the shape and size of the solid defect, we deposit a cylindrical fiber vertically on a film of silicone oil that is spin-coated on a solid surface. We measure the thickness of the film in the region of the surface deformation by interferometry, using a hyperspectral camera.

We obtain thickness profiles at different times (see Fig. 1a), which exhibit a space-minimum thickness h_g for each time. Plotting this space-minimum thickness over time (see Fig. 1b) reveals that this minimum thickness is non-monotonic, allowing us to extract the time-minimum $h_\mathrm{g}^\mathrm{min}$, which is significant because if it reaches zero, the film will dewet.

We propose that the time-minimum thickness $h_\mathrm{g}^\mathrm{min}$ is reached when the meniscus formed at the bottom of the fiber reaches its equilibrium. This leads to a time-minimum thickness scaling with h_0^3/r_f^2, where h_0 is the initial thickness and r_f is the fiber radius, in good agreement with experimental data (see Fig. 1c).

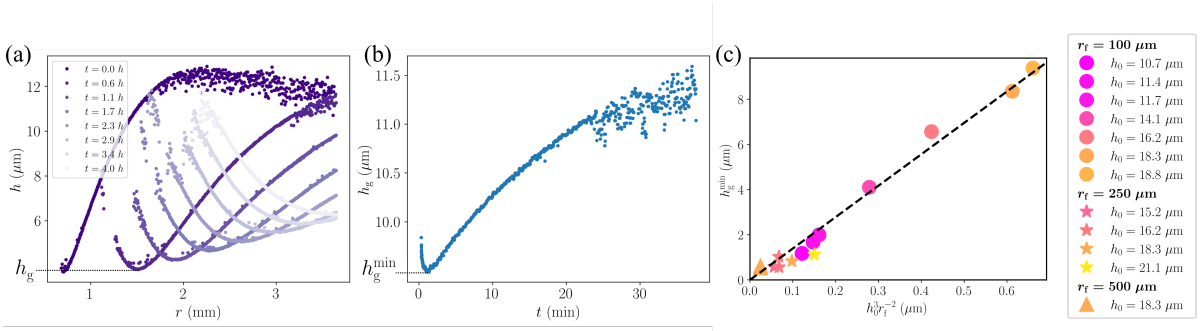

Figure 1. (a) Thickness profiles along the radial direction ($x = 0$ is the center of the fiber) at different times. First, the thickness decreases along the meniscus, then it reaches a minimum, and finally the thickness relaxes towards the initial thickness of the initial film. (b) The space-minimum thickness h_g as a function of time is non-monotonous and reaches a minimum. (c) Space-time-minimum thickness $h_\mathrm{g}^\mathrm{min}$ as a function of the theoretical value coming from the scaling law, for different initial thicknesses h_0 and fiber radii r_f.

References

1. S. F. Kistler & P. M. Schweizer, *Liquid Film Coating*, Springer, Dordrecht (1997).
2. C. Robert, *Ph.D. thesis, Sorbonne Université* (2022).
3. D. Garcia-Gonzalez, M. A. Hack, M. Kappl, H.-J. Butt & J. H. Snoeijer, *Soft Matter*, **19**, 1241–1248 (2023).

Surface wrinkling of a thin liquid-infused membrane

Jiayu Wang, Arnaud Antkowiak, Sébastien Neukirch

Institut Jean le Rond ∂'Alembert, Sorbonne Université, 75005, Paris, France
jiayu.wang@sorbonne-universite.fr

Elasto-capillary effects are due to the interactions between surface tension and elastic deformation of slender structures. Recent studies have highlighted diverse deformations induced by capillary forces, such as softening the sharp geometry of a soft substrate, bending and buckling of flexible fibers, and folding, wrapping, and wrinkling of thin sheets [1]. Our study builds upon experimental observations of a nano-fibrous liquid-infused tissue [2]. Under slight compression, it spontaneously develops wrinkles through elasto-capillarity effects. Upon further contraction, specific regions undergo substantial collapse, forming surface reservoirs that enhance the membrane's deformability. The remarkable deformability of this synthetic system closely resembles that of cell membranes, making it intriguing for applications in stretchable electronics, smart textiles, and soft biomedical devices.

To elucidate the underlying mechanism, we employ theoretical and numerical modeling. The system is simplified to a thickness-neglected, inextensible membrane confined within a liquid layer of constant volume. The configuration of the membrane-liquid system under certain compression is framed as an optimization problem and the nonlinear problem is solved with the help of the open-source tool CasADi [3].

The model reveals homogeneous wrinkles with slight compression. As compression increases beyond a certain threshold, wrinkles localize at one specific spot on the membrane. This transition provides insights into experimental observations, prompting further investigations into the behaviors of liquid-infused membranes.

References

1. J. Bico *et al.*, Elastocapillarity : When surface tension deforms elastic solids, *Annu. Rev. Fluid Mech.*, **50**, 629–659 (2018).
2. P. Grandgeorge *et al.*, *Science*, **360**, 296–299 (2018).
3. J. Andersson *et al.*, *Math. Program. Comput.*, **11**, 1–36 (2019).

Dip-coating sur substrats déformables en mouillage partiel : observation d'un retard à l'entraînement de film liquide

Anthony Varlet, Philippe Brunet, Laurent Limat, Julien Dervaux, Matthieu Roché

Laboratoire Matières et Systèmes Complexes (MSC), UMR 7057, Université Paris-Cité, France
anthony.varlet@u-paris.fr

La technique du *dip-coating* est un procédé couramment utilisé dans l'industrie pour, par exemple, enduire de liquide de grandes surfaces de tissus ou encore du matériel médical. En laboratoire, ce système est utilisé pour étudier des problèmes de mouillage dynamique : il permet d'obtenir une ligne de contact assez rectiligne et d'imposer une vitesse de mouillage ou de dé-mouillage de manière bien contrôlée. Le principe de ce dispositif est d'extraire un solide d'un bain liquide, à vitesse constante V, afin d'y déposer une couche fine de liquide. Les résultats d'expériences de dip-coating avec un solide rigide sont assez bien décrits. En mouillage total, le liquide recouvre systématiquement la surface du solide sous forme d'un film fin de liquide, d'épaisseur uniforme au dessus du ménisque relié au bain. Cette épaisseur est décrite par la relation de Landau–Levich–Derjaguin (LLD) et varie proportionnellement au nombre capillaire Ca à la puissance 2/3 [1] (nombre adimensionné de la vitesse du système comparant les forces visqueuses aux forces capillaires tel que $\mathrm{Ca} = \frac{\eta V}{\gamma}$, avec η la viscosité dynamique du fluide et γ la tension de surface ($\mathrm{J/m^2}$)). En mouillage partiel, un film au contour trapézoïdal est observé car la ligne de contact sur les côtés recède lors de l'extraction [2]. Cette couche de liquide est déposée lorsque Ca atteint une valeur seuil.

En revanche, l'enduisage de surfaces déformables est peu exploré [3]. Nous utilisons ici des substrats avec un module d'Young Y allant de l'ordre du kPa au MPa. Lorsqu'un liquide s'étale sur un tel substrat, une déformation (*ridge*) apparaît au niveau de la ligne triple, résultant de la compétition entre force capillaire et l'élasticité du substrat. La taille du ridge est défini par la longueur élastocapillaire $\ell_s \sim \frac{\gamma}{Y}$ [4, 5]. Si pour un substrat rigide ($Y \sim$ GPa) cette longueur est inférieure au nanomètre, considérée comme négligeable, pour nos substrats mous, elle peut aller à l'ordre de la dizaine de micromètre, assez significative pour pouvoir intervenir sur l'écoulement : sa présence et sa propagation conduisent à une dissipation d'énergie dans le solide.

Nos expériences ont mis en évidence le résultat suivant : contrairement au cas du solide rigide, où l'entraînement du liquide se fait instantanément, avec un substrat déformable, l'entraînement n'est pas instantané dans une plage de Ca intermédiaire, mais plutôt retardé. On assiste donc ici à l'émergence d'une nouvelle plage de solutions, dans laquelle le liquide est entraîné après un transitoire allant de la seconde à plusieurs dizaines de secondes, durée entre le début de l'extraction du solide et le moment où le liquide fini par être entraîné. Ce retard, que l'on nomme temps d'entraînement, semble décroître avec le nombre capillaire et présente une divergence en-deçà d'une valeur seuil Ca_1.

L'origine de ce retard reste encore à expliquer. Néanmoins, nous étudions la piste suivante : les substrats que nous utilisons contiennent des chaînes libres, qui peuvent contaminer la surface libre du liquide au cours de l'extraction [6], et ainsi modifier les conditions d'entraînement de liquide.

Références

1. L. Landau & B. Levich, Dragging of a liquid by a moving plate, *in Dynamics of Curved Fronts*, Academic Press, pp. 141–153 (1988).
2. J. H. Snoeijier, G. Delon, M. Fermigier, B. Andreotti, *Phys. Rev. Lett.*, **96**, 174504 (2006).
3. V. Bertin, J. H. Snoeijer, E. Raphaël & T. Salez, *Phys. Rev. Fluids*, **7**, L102002 (2022).
4. L. Limat, *Eur. Phys. J. E*, **35**, 1–13 (2012).
5. R. W Style & E. R. Dufresnes, *Soft Matter*, **8**, 7177 (2012).
6. A. Hourlier-Fargette, A. Antkowiak, A. Chateauminois, S. Neukirch, *Soft Matter*, **13**, 3484–3491 (2017).

Droplet spreading and transport: The role of substructures

Joséphine Van Hulle, Matteo Léonard, Cyril Delforge, Nicolas Vandewalle

GRASP, Institute of Physics, 19, Allée du 6 août, University of Liège, B4000 Liège, Belgium
jvanhulle@uliege.be

Efficient droplet transportation represents a significant challenge in the development of water collection devices [1]. It has been observed in nature that grooves favor droplet motion [2]. In this presentation, we investigate the dynamics of droplet spreading within 3D-printed grooves with varying curvatures [3]. We show that the type of curvature (convex or concave) significantly influences the droplet shape and the dynamics of spreading (see Fig. 1 (a)). Specifically, we show that the spreading of a droplet is faster inside a convex groove. Additionally, we examine the role of sub-structures in guiding droplet motion along vertical twisted threads [4]. Two fibers are twisted to create a helical groove along the bundle. We show that depending on the helical path the droplet exhibits a helical motion or a vertical descent (see Fig. 1 (b)). These findings underscore the crucial importance of substructures in manipulating droplets.

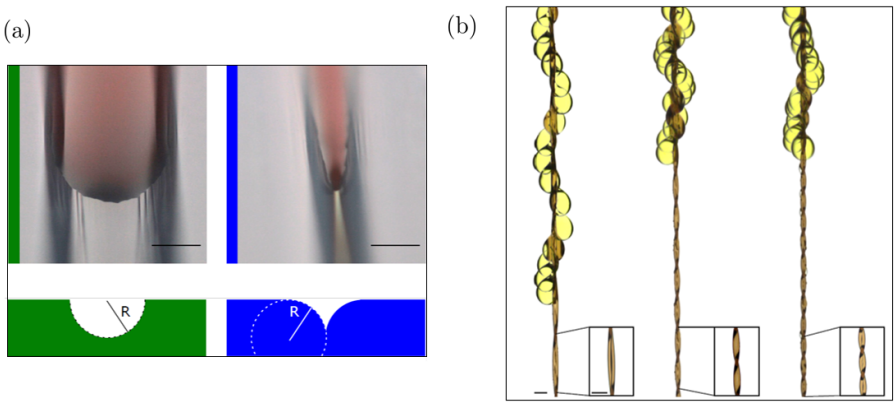

Figure 1. (a) Pictures of the liquid front of a red-dyed droplet spreading in a concave groove and a convex groove. Both grooves have the same radius of $R = 1.37$ mm. One observes that the groove's curvature influences the advancing front shape of the droplet. (b) Superposition of successive pictures of a droplet traveling down two twisted fibers with a helical groove substructure. From left to right, the number of fiber twists increases. With small twist values, the droplet adopts a motion that mirrors the underlying helical structure. However, at higher twist values, the droplet has a mixed motion of translations and rotations. Scale bars in the images represent 1 mm.

References

1. Y. Jiang, C. Machado, S. Savarirayan, N. A. Patankar & K.-C. Park, Onset time of fog collection, *Soft Matter*, **15**, 6779–6783 (2019).
2. H. Chen, T. Ran, Y. Gan, J. Zhou, Y. Zhang, L. Zhan, D. Zhang & L. Jiang, Ultrafast water harvesting and transport in hierarchical microchannels, *Nat. Mater.*, **17**, 935–942 (2018).
3. J. Van Hulle & N. Vandewalle, Effect of groove curvature on droplet spreading, *Soft Matter*, **19**, 4669 (2023).
4. J. Van Hulle, C. Delforge, M. Léonard & N. Vandewalle, Droplet helical motion on twisted fibers, under review (2024).

Pendant droplets under a wet substrate pin on surface defects despite having no contact line

Étienne Jambon-Puillet

LadHyX, CNRS, Ecole Polytechnique, Institut Polytechnique de Paris, Palaiseau, France
etienne.jambon-puillet@polytechnique.edu

Pendant drops spontaneously appear on the underside of wet substrates through the Rayleigh-Taylor instability. These droplets are unstationnary, they exchange liquid with the surrounding film and any perturbation will set them in motion [1]. Here, using experiments, numerical simulations, and theory I show that pendant drops sliding under a slightly tilted wet substrate can pin on surface defects, even though they do not have a contact line. Instead, this pinning force has a gravito-capillary origin that I rationalize for arbitrary substrate topographies with a semi-analytical convolution based theory. I finally demonstrate how to harness this pinning force to guide pendant drops using the substrate topography.

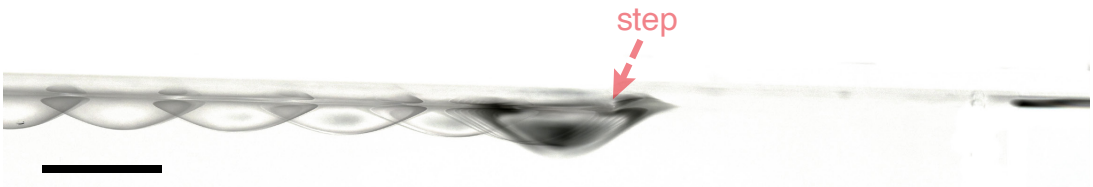

Figure 1. Chronophotography of a silicone oil pendant drop sliding under a wet surface inclined by 2.2 deg. The surface has a sharp step of height 330 µm (highlighted) that pins the drop. The images include reflexions of the drop on the wet substrate, scale bar 5 mm, time interval 2 min.

References

1. É. Jambon-Puillet, P. G. Ledda, F. Gallaire, P.-T. Brun, Drops on the underside of a slightly inclined wet substrate move too fast to grow, *Phys. Rev. Lett.*, **127**, 044503 (2021).

Adhesive bubbles and drops between circular frames: Shape, force and stability analysis

Friedrich Walzel, Jonathan Dijoux, Leandro Jacomine, Élodie Harle, Pierre Muller, Thierry Charitat, Wiebke Drenckhan

Institut Charles Sadron, University de Strasbourg/CNRS, Strasbourg, France
friedrich.walzel@etu.unistra.fr

We exploit the theory of axisymmetric constant mean curvature surfaces [1] to describe the mechanical interactions between drops, bubbles or capillary bridges [2,3] held by circular frames with radius R and distance $2h$ (see Fig. 1). We complement the theory with experimental and computational approaches [4]. The Figure 1 shows our obtained shape diagram, which indicates under which constraints the bubbles remain axisymmetric and in contact. Due to four different instabilities, the bubbles lose contact or lose their axisymmetry. Two of these four instabilities (2 and 3) have been discovered by us. Different contact angles between the bubbles θ are due to different adhesive forces between the bubbles. The shape diagrams of the two limiting cases with $\theta = 0°$ and $\theta = 180°$ have been obtained additionally to the case of $\theta = 60°$ (see Fig. 1). Using these diagrams and theory, the stability and mechanical properties of capillary bridges or bubbles in contact under tension or compression can be predicted [5]. The provided analysis holds equally for bubbles, drops or capillary bridges and gives an approach to investigate more complex interfaces with for example elastic skins.

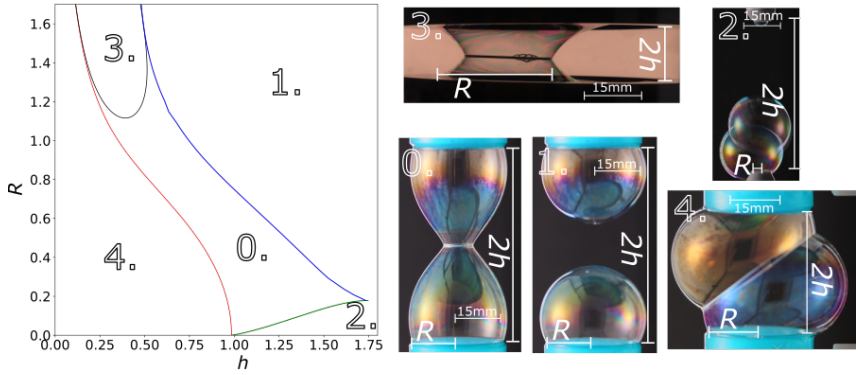

Figure 1. Shape diagram for two bubbles with a contact angle of 60° with 0. Delauney Surfaces 1. Bubble bubble detachment, 2. Bubble frame detachment, 3. Non axisymmetric shifting and 4. Non axisymmetric tilting.

References

1. B. G. Chen & R. D. Kamien, Nematic films and radially anisotropic Delaunay surfaces, *Eur. Phys. J. E*, **28**, 315–329 (2009).
2. M. A. Fortes, M. E. Rosa, M. F. Vaz & P. I. C. Teixeira, Mechanical instabilities of bubble clusters between parallel walls, *Eur. Phys. J. E*, **15**, 395–406 (2004).
3. F. Walzel *et al.*, Perturbing the catenoid: Stability and mechanical properties of nonaxisymmetric minimal surfaces, *Phys. Rev. E*, **106**, 014803 (2022).
4. K. A. Brakke, The surface evolver, *Exp. Math.*, **1**, 141–165 (1992).
5. F. Walzel, *Video V006: Kissing bubbles*, https://www.youtube.com/watch?v=iqRie9r4G80.

Adhésion de la glace sur différents substrats

Pierre-Brice Bintein[1], Arnaud Grados[1], Jordan Bonté[1], Laurent Royon[2], Philippe Brunet[1]

[1] Laboratoire Matière et Systèmes Complexes, UMR CNRS 7057, Université Paris Cité, 10 rue Alice Domon et Léonie Duquet 75205 Paris Cedex 13, France
[2] Laboratoire Interdisciplinaire des Energies de Demain, Université Paris Cité, 10 rue Alice Domon et Léonie Duquet 75205 Paris Cedex 13, France
philippe.brunet@univ-paris-diderot.fr

L'adhésion de la glace sur des solides demeure un problème avec de nombreuses questions mal résolues. Une revue sur ce sujet [1] concluait que la force d'adhésion de la glace dépend non seulement de la composition chimique, de la rugosité de la surface, des propriétés mécaniques et thermiques du substrat, mais dépend aussi de manière critique de la température et même du dispositif expérimental de mesure d'adhésion. Lorsqu'on explore la littérature sur le sujet depuis plus de 60 ans, on note que la température influence grandement la force avec laquelle la glace colle sur un solide, dans un intervalle entre $-20°C$ et $0°C$: la glace colle plus fort sur un solide plus froid. Quant au role de la rugosité de surface, il est ambivalent : pour certains solides (notamment les métaux), la glace adhère davantage sur un substrat plus rugueux, alors que sur certains plastiques c'est l'inverse.

Finalement, la nature chimique semble intervenir via l'affinité de l'eau liquide pour le solide, c'est à dire de la capacité de l'eau à s'étaler ou non sur sa surface, quantifiée par l'angle de contact. Une étude récente [2] a ainsi montré une forte corrélation entre l'angle de contact *en reculée* de l'eau liquide et la force d'adhésion de la glace sur le même substrat : plus l'eau à l'état liquide s'étale sur la surface d'un solide, plus la glace adhère sur ce solide.

Nous avons construit un dispositif macroscopique pour mesurer cette force d'adhésion sur différents substrats, à différentes températures. Un cube de glace de 1 cm de côté est laissé à température ambiante le temps d'avoir une couche d'eau liquide à sa surface, puis mis en contact avec la plaque froide sur laquelle il adhère en raison de la re-solidification. Puis il est poussé par un piston à force croissante jusqu'à ce qu'il se décroche : la force maximale est alors mesurée. Nous avons obtenu des résultats relativement reproductibles sur plusieurs substrats (dural de différentes rugosités, silicium) dans une gamme de température entre $-10°C$ et $0°C$. Néanmoins, la reproductibilité est beaucoup moins bonne à des températures plus froides. Nous essayons de comprendre ce phénomène en raison des conditions initiales mal maitrisées lors de la mise en contact.

Références

1. L. Makkonen, *J. Adhes. Sci. Technol.*, **26**, 413–445 (2012).
2. Adam L. Meuler *et al.*, *Appl. Mater. Interfaces*, **2**, 3100–3110 (2010).

When marbles challenge pearls

Kexin Zhao[1], David Quéré[2]

[1] LadHyX, CNRS, Ecole Polytechnique, Institut Polytechnique de Paris, Palaiseau, France
[2] Physique et Mécanique des Milieux Hétérogènes, UMR 7636 du CNRS, PSL Research University, ESPCI, 75005 Paris, France
kexin.zhao@espci.fr

The spectacular nature of non-wetting drops mainly arises from their extreme mobility, and quicksilver, for instance, was named after this property. There are two ways to make water non-wetting, and they both rely on texture: either we can roughen a hydrophobic solid, which makes drops looking like pearls, or we can texture the liquid with a hydrophobic powder that "isolates" the resulting marble from its substrate. We observe, here, races between pearls and marbles, and report two effects: (1) the static adhesion of the two objects is different in nature, which we interpret as a consequence of the way they meet their substrates; (2) when they move, pearls are generally quicker than marbles, which might arise from the dissimilarity of the liquid/air interface between these two kinds of globules.

References

1. E. B Dussan & R. T. P. Chow, On the ability of drops or bubbles to stick to non-horizontal surfaces of solids, *J. Fluid Mech.*, **137**, 1–29 (1983).
2. P. Aussillous & D. Quéré, Liquid marbles, *Nature*, **411**, 924–927 (2001).

Acrobatics of viscous marbles

Auriane Huyghues Despointes[1], Yui Takai[1], Shoko Ii[1], Timothée Mouterde[2], David Quéré[1]

[1] Physique et Mécanique des Milieux Hétérogènes, UMR 7636 du CNRS, PSL Research University, ESPCI-Paris, France
[2] Department of Mechanical Engineering, The University of Tokyo, Tokyo 113-8656, Japan
auriane.huyghues-despointes@espci.fr

While viscous drops are expected to be slow, their dynamics can be markedly different when they non-wet their substrate [1]. The Mahadevan–Pomeau model consists in two ideas. Firstly, non-wetting drops are flattened at their base due to gravity. Secondly, when the Reynolds number is below unity, the liquid exhibits solid-like rotation, characterized by minimal dissipation localized in the contact region. The law predicts the drop velocity to be proportional to the slope of the substrate, when considering its gravity-driven movement on a tilted plate.

As an archetype of non-wetting drops, we consider liquid marbles, obtained by shaking a drop on a bed of hydrophobic micrograins : the grains stick to the surface of the drop, which they armor without without however modifying its softness (and surface tension) [2]. In our experiment, a long wooden plate (a few meters in length) is inclined at an angle α, and we place a millimeter-sized marble of glycerol one thousand times more viscous than water at its top. We track the marble with a high-speed video camera as it moves down the slope. In Figure 1, we present two consecutive sequences showing side views of the marble moving on a plate inclined at 30°, with the camera tilted by the same angle. These chronophotographs allow us to capture both the instantaneous velocity and the shape of the droplet.

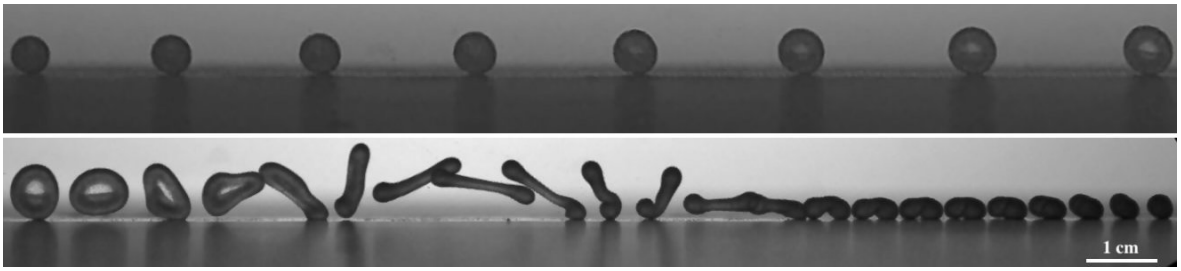

Figure 1. Chronophotography of a marble of glycerol (initial radius $R_o = 1.7\,\mathrm{mm}$) as it runs down a plate tilted by $\alpha = 30°$. Images are separated by (top) 32 ms and (bottom) 8 ms.

The experiment reveals that increasing the slope makes the drop speed 10 times quicker than expected from the Mahadevan-Pomeau model. This can be understood by taking into account the strong deformations of the marble, due to its centrifugations, whose effect is to minimize even further the solid/liquid contact –and thus the viscous dissipation. From an applied perspective, this means that non-wetting, viscous materials can be transported at speeds comparable to that of water.

References

1. L. Mahadevan & Y. Pomeau, Rolling droplets, *Phys. Fluids*, **11**, 2449–2453 (1999).
2. P. Aussillous & D. Quéré, Liquid marbles, *Nature*, **411**, 924–927 (2001).

Exposés longs de la 27^{e} Rencontre du Non-Linéaire

La turbulence d'ondes internes de gravité : un modèle pour la dynamique océanique à petite échelle ?

Pierre-Philippe Cortet, Nicolas Lanchon

Université Paris-Saclay, CNRS, FAST, 91405 Orsay, France
pierre-philippe.cortet@universite-paris-saclay.fr

Il est depuis longtemps proposé que la dynamique océanique à petite échelle résulte de processus non linéaires impliquant des ondes internes de gravité [1]. Les échelles en question, typiquement inférieures à quelques centaines de mètres dans la direction verticale, ne sont pas résolues dans les modèles océaniques globaux mais prises en compte par des paramétrisations ad hoc. Modéliser physiquement la dynamique turbulente de ces petites échelles constituerait ainsi un levier majeur d'amélioration des paramétrisations dans les modèles climatiques [2].

Dans ce contexte, la théorie la plus prometteuse est celle de la turbulence faible, aussi appelée turbulence d'ondes. Sa mise en œuvre dans le cas des ondes internes de gravité dans les fluides stratifiés en densité s'est toutefois révélée complexe et reste inaboutie. Elle est l'objet de questions analytiques délicates concernant la convergence de l'intégrale dite « de collision » qui pilote la dynamique dans les problèmes de turbulence d'ondes.

Dans cet exposé, nous examinons sous un nouvel angle la théorie de la turbulence faible dans un fluide linéairement stratifié. En partant de la formulation classique de cette théorie dans la limite des basses fréquences, nous dérivons une version simplifiée de l'équation cinétique de la turbulence d'ondes internes de gravité [3]. Cette équation nous permet de prédire des lois d'échelle pour les spectres spatiaux et temporels de l'énergie qui sont en accord avec les exposants typiquement mesurés dans les océans. La clé de notre description est l'hypothèse que les transferts d'énergie sont dominés par une classe d'interactions résonantes non locales, connues sous le nom de triades de « diffusion induite » et qui conservent le rapport entre la fréquence des ondes et leur nombre d'onde vertical. De manière remarquable, notre analyse montre que la cascade de la turbulence d'ondes internes est associée à un flux apparent d'action d'ondes constant.

Références

1. C. H. McComas & F. P. Bretherton, Resonant Interaction of Oceanic Internal Waves, *J. Geophys. Res.*, **82**, 1397–1412 (1977).
2. G. Dematteis, A. Le Boyer, F. Pollmann, K. L. Polzin, M. H. Alford, C. B. Whalen & Y. V. Lvov, Interacting internal waves explain global patterns of interior ocean mixing, arXiv:2310.19980 (2023).
3. N. Lanchon & P.-P. Cortet, Energy spectra of nonlocal internal gravity wave turbulence, *Phys. Rev. Lett.*, **131**, 264001 (2023).

Use of metamaterials for surface wave control: Examples on backscattering reduction and boat wake absorption

Samantha Kucher[1], Adrian Koźluk[12], Philippe Petitjeans[1], Agnès Maurel[3], Vincent Pagneux[4]

[1] Laboratoire de Physique et Mécanique des Milieux Hétérogènes, UMR CNRS 7636, ESPCI-Paris, Université PSL, Sorbonne Université, Université Paris Cité, 75005 Paris, France
[2] Institute of Aeronautics and Applied Mechanics, Warsaw University of Technology, 00-665 Warsaw, Poland
[3] Institut Langevin, UMR CNRS 7587, ESPCI-Paris, 75005 Paris, France
[4] Laboratoire d'Acoustique de l'Université du Mans, UMR CNRS 6613, 72085 Le Mans, France
samantha.kucher@espci.fr

Metamaterials are artificially architectured materials that affect the wave propagation in ways that are not usually found in nature. They initially emerged in the field of electromagnetism. However, they quickly spread to many other areas of physics since all waves share a fundamental nature. In the last years there has been an interest in the design of metamaterials for surface water waves. Such endeavour present both an advantage and a challenge. Surface waves are easily accessible as they are visible to the human eye. However, they are dispersive, which highly complexifies their dynamics. Here we pursue the challenge of controlling surface waves through metamaterials using a theoretical, numerical and experimental approach.

Two different, although closely related, wave control systems are studied: (i) the reduction of backscattering generated by a sharp bend in a channel thanks to an array of parallel plates, and (ii) the absorption of a boat wake by a microstructured wall consisting of resonant cavities. In both studies the periodic structure is carefully designed and described in terms of an effective medium using homogenization theory.

Firstly, we design a metamaterial consisting of a periodic array of parallel thin vertical plates, closely spaced. This array can be used to deflect waves at different angles depending on the thickness of the plates and the angle of incidence. We first study numerically the behavior of an infinite array of plates and then confine this array into a waveguide with two perpendicular turns. By placing the metamaterial in the central part we are able to reduce considerably the backscattering in the turns and thus obtain a high transmission [1].

Secondly, we consider the reflection coefficient in the complex frequency plane to design a microstructured wall capable of achieving perfect absorption [2]. Our wall consist of the repetition of resonant cavities and we use it to absorb the wake pattern of a boat. This system could be applied to coastal protection or on geometries with lateral confinement such as rivers.

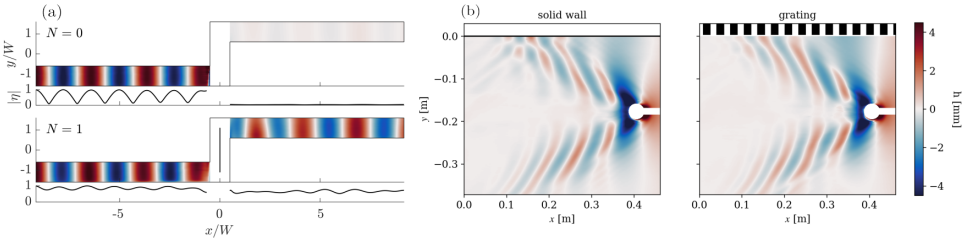

Figure 1. Measured free surface deformation fields: (a) Plane wave propagation in a channel with two perpendicular turns at a fixed frequency, in a configuration without the metamaterial and with one vertical plate. (b) Boat wake incidence on a solid wall and on a periodic grating made of resonant cavities.

References

1. S. Kucher, A. Koźluk, P. Petitjeans, A. Maurel & V. Pagneux, Backscattering reduction in a sharply bent water wave channel, *Phys. Rev. B*, **108**, 214311 (2023).
2. V. Romero-García, G. Theocharis, O. Richoux & V. Pagneux, Use of complex frequency plane to design broadband and sub-wavelength absorbers, *J. Acoust. Soc. Am.*, **139**, 3395–3403 (2016).

Trapping of macroscopic spinning particles in hydrodynamic vortex lattice

Jean-Baptiste Gorce[1,2], Hua Xia[2], Nicolas Francois[2], Horst Punzmann[2], Gregory Falkovich[3,4], Michael Shats[2]

[1] Université Paris Cité, CNRS, MSC, UMR 7057, F-75013 Paris, France
[2] Research School of Physics, The Australian National University, Canberra, ACT 2601, Australia
[3] Department of Physics, Weizmann Institute of Science, Rehovot 76100, Israel
[4] Photonics Center, Novosibirsk State University, Novosibirsk 630090, Russia
jean-baptiste.gorce@u-paris.fr

Recent advances in the confinement and manipulation of microparticles and ultracold atoms using optical waves have inspired new ideas related to the control of particles at liquid-gas interfaces using hydrodynamic vortex lattices [1]. These lattices consist of two orthogonal standing waves, which generate surface flows of counter-rotating vortices, guiding floating particles along closed trajectories. The specific shape and geometry of these vortices are determined by the phase shift and frequency of the waves, with the dimensions of the vortices corresponding to half of the wavelength.

The present study shows that by incorporating macroscopic active spinning disks, referred to as "spinners" into such vortex lattices, one can create a powerful tool for manipulating and self-assembling macroscopic spinning particles [2]. We will show that the spinners' orbits in the vortex lattice can be precisely tuned by changing their angular velocity while reversing the sign of the angular velocity moves the spinner to an adjacent vortex. In addition, multiple spinners within a vortex can self-organize into stable patterns orbiting around the center of the vortex.

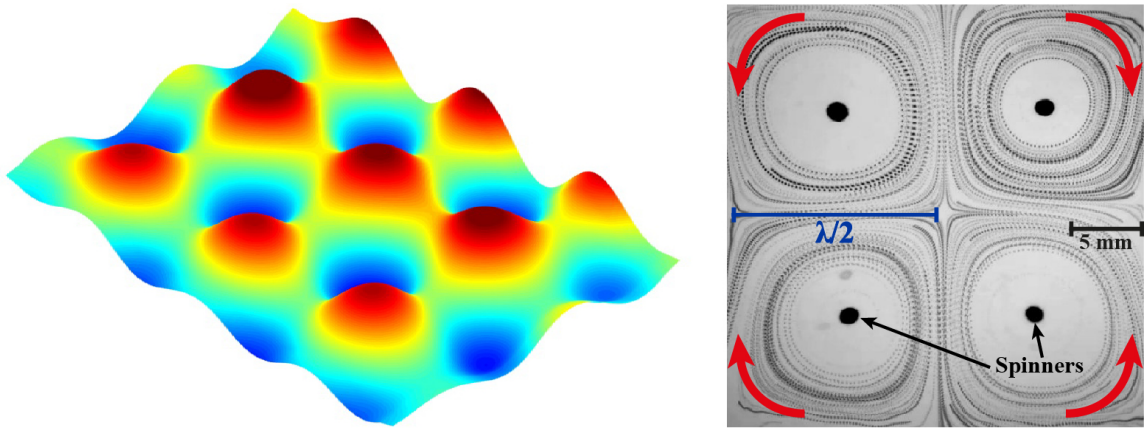

Figure 1. Left: Measured surface elevation snapshot of the vortex lattice derived from a diffusive light imaging analysis. The hot colors in the colormap correspond to peaks, while the cold colors represent troughs. Right: Trapping of 1 mm spinners within four different vortices. The red arrows represent the rotation direction of the vortices. The angular frequency of the spinners is 30 Hz.

References

1. N. Francois, H. Xia, H. Punzmann, P. W. Fontana & M. Shats, Wave-based liquid-interface metamaterials, *Nat. Commun.*, **8**, 14325 (2017).
2. J.-B. Gorce, H. Xia, N. Francois, H. Punzmann, G. Falkovich & M. Shats, Confinement of surface spinners in liquid metamaterials, *Proc. Natl. Acad. Sci. U.S.A.*, **116**, 25424–25429 (2019).

Instabilité de vrillage et génération de courbure chez les plantes à vrilles

Émilien Dilly[1], Julien Derr[2], Sébastien Neukirch[3], Dražen Zanchi[1]

[1] Laboratoire MSC, Université Paris Cité, 10, rue Alice Domon et Léonie Duquet, 75013 Paris
[2] Laboratoire Reproduction et Développement des Plantes, École Normale Supérieure de Lyon, 15, parvis René Descartes, 69342 Lyon
[3] Institut Jean Le Rond d'Alembert - Sorbonne Université, 4, Place Jussieu 75252 Paris Cedex 05
emilien.dilly@etu.u-paris.fr

Les plantes à vrilles, telles que les cucurbitacées (concombre, courgette, bryone), la vigne ou la passiflore, sont pourvues d'organes filiformes spécialisés, les vrilles, qui leur permettent de s'accrocher et de grimper. Après s'être attachée, par le biais d'une croissance différentielle sur sa section, la vrille continue de se courber. À une courbure critique, la tige droite devient instable, une connexion hélicoïdale se forme (voir fig. 1.a.). C'est l'instabilité de vrillage.

Pour reproduire cette instabilité, une expérience simple consiste à prendre une tige hélicoïdale élastique, la dérouler et la tirer de manière à la rendre droite. En rapprochant les deux extrémités, deux hélices de chiralités opposées apparaissent, reliées par une connexion appelée perversion (fig. 1.b). L'analyse non linéaire des équations de Kirchhoff pour les tiges inextensibles a démontré que cette instabilité de vrillage se manifeste à une valeur de tension axiale imposée finie [1]. Nos travaux rapportent des résultats sur la génération de ces perversions dans les tiges hélicoïdales en élastomère. Nous établissons expérimentalement et théoriquement un diagramme d'existence de tels objets en fonction de la rotation et de l'élongation imposées à la tige, en confirmant notamment le critère d'instabilité de vrillage [2].

Contrairement aux tiges en élastomère, chez les plantes, l'instabilité de vrillage est induite non pas par la réduction de la force axiale imposée aux extrémités, mais par la génération de courbure due à la croissance différentielle. Nous modélisons la dynamique du vrillage par un système bilame avec une lame en croissance et l'autre de longueur constante, la croissance étant elle-même sensible aux contraintes internes et donc à la tension imposée à ses extrémités. En imposant une force constante à la vrille et en suivant sa géométrie, nous décrivons la dynamique du vrillage et nous montrons l'existence d'une tension critique à partir de laquelle la vrille ne vrille plus. Nous expliquons cette observation à l'aide du critère d'instabilité mentionné précédemment et d'une loi phénoménologique de mécanosensibilité de la croissance.

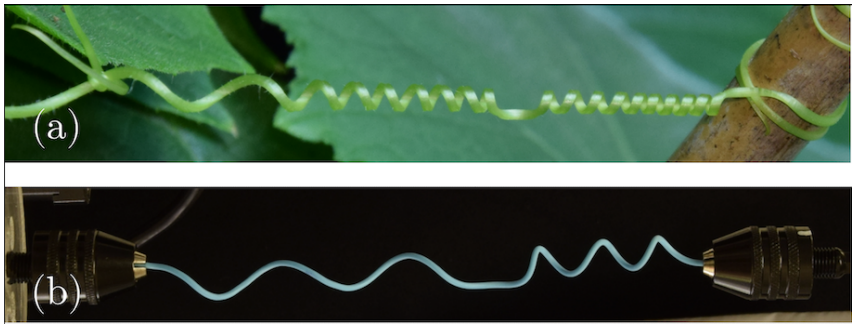

Figure 1. (a) Vrille de concombre présentant deux motifs hélicoïdaux reliés par une perversion (b) Tiges en élastomère avec perversion

Références

1. T. McMillen & A. Goriely, *J. Nonlinear Sci.*, **12**, 241 (2002).
2. É. Dilly, S. Neukirch, J. Derr & Dražen Zanchi, *Phys. Rev. Lett.*, **131**, 177201 (2023).

Getting a kick from water waves

Graham Benham[1], Olivier Devauchelle[2], Stuart Thomson[3]

[1] School of Mathematics and Statistics, University College Dublin, Dublin 4, Ireland
[2] Université de Paris, Institut de Physique du Globe de Paris, CNRS, F-75005 Paris, France
[3] School of Engineering Mathematics and Technology, University of Bristol, Ada Lovelace Building, University Walk, Bristol, BS8 1TW, UK
graham.benham@ucd.ie

Wave-driven propulsion occurs when a floating body, driven into oscillations at the fluid interface, is propelled by the waves generated by its own motion. Longuet-Higgins [1] first demonstrated this using a wave-making raft (see Fig. 1), proposing that the raft's forward thrust originates from the backward-radiation of wave momentum. More recently, wave-driven propulsion has been observed in the case of the waves generated by a honeybee trapped on the surface of water [2], in the case of *SurferBot*, a centimeter-scale interfacial robot that was inspired by the stricken honeybee [3], and at much larger scales, in the case of the waves generated by jumping up and down on a canoe, also known as *gunwale bobbing* [3], which are all illustrated in Fig. 1.

We propose a new theory for wave-driven propulsion based on coupling the equations of motion of a floating raft to a quasi-potential flow model of the fluid. Using this model, we derive expressions for the drift speed and propulsive thrust of the raft which in turn are shown to be consistent with global momentum conservation. We explore the efficacy of our model in describing the motion of *SurferBot*, demonstrating close agreement with the experimentally determined drift speed and oscillatory dynamics. The efficiency of wave-driven propulsion is then computed as a function of driving oscillation frequency and the forcing location, revealing optimal values for both of these parameters which await confirmation in experiments.

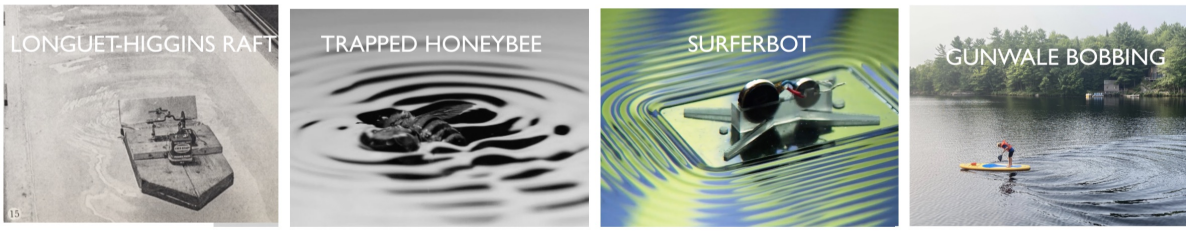

Figure 1. Examples of wave-driven propulsion, given by Refs. [1–4].

References

1. M. S. Longuet-Higgins, The mean forces exerted by waves on floating or submerged bodies with applications to sand bars and wave power machines, *Proc. R. Soc. A.*, **352**, 1671 (1977).
2. C. Roh & M. Gharib, Honeybees use their wings for water surface locomotion, *PNAS*, **116**, 49 (2019).
3. E. Rhee, R. Hunt, S. J. Thomson & D. M. Harris, SurferBot: a wave-propelled aquatic vibrobot, *Bioinspir. Biomim.*, **17**, 5 (2022).
4. G.P. Benham, O. Devauchelle, S. W. Morris & J. A. Neufeld, Gunwale bobbing, *Phys. Rev. Fluids*, **7**, 7 (2022).

Oscillations de Bloch d'un soliton magnétique dans un mélange de bosons ultrafroids

Jérôme Beugnon

Collège de France, CNRS, ENS-PSL University, Sorbonne Université, 11 Place Marcelin Berthelot, 75005 Paris, France
beugnon@lkb.ens.fr

La dynamique des gaz de bosons ultra-froids, lorsqu'ils sont dans un régime d'interaction faible et de température nulle, est très bien décrite par une équation de Schrödinger non-linéaire. Dans ce contexte, la non-linéarité est induite par les interactions entre particules. Dans notre équipe, nous manipulons des gaz dans des potentiels lumineux qui nous permettent de contrôler la dimensionnalité du gaz (2D ou 1D), sa géométrie et son profil de densité. Nous pouvons ainsi façonner des paquets d'ondes à souhait et étudier leur dynamique non-linéaire dans un profil de potentiel contrôlable. Cela nous a permis par exemple de découvrir l'existence de breather de l'équation de Schrödinger à non-linéarité cubique [1].

Récemment, nous avons étendu nos recherches aux mélanges binaires de bosons permettant ainsi d'étudier la dynamique non-linéaire de systèmes couplés. Nous avons par exemple démontré la réalisation du soliton de Townes, un exemple célèbre de soliton à deux dimensions [2]. Dans cette contribution, nous souhaitons présenter nos derniers résultats sur la dynamique d'un soliton magnétique.

Les solitons magnétiques ont été introduits dans le contexte des chaînes de spin ferromagnétiques mais ils sont aussi réalisables de façon analogue dans des mélanges binaires de bosons ultrafroids. Nous avons ainsi réalisé la première démonstration expérimentale de solitons magnétiques dans des mélanges non-miscibles à une dimension. Ces solitons présentent aussi une propriété remarquable que nous avons aussi observée. Lorsqu'ils sont soumis à une force constante ils vont subir un mouvement oscillant. Cette dynamique est proche de celles des oscillations de Bloch subies par un électron soumis à une force constante dans un solide mais il n'y a dans notre expérience aucun réseau pour expliquer cette oscillation [3, 4]. En jouant avec la géométrie du système nous avons mis en évidence le rôle central de la phase de la fonction d'onde du système sur le mouvement de ce système. Nous avons aussi démontré que la fréquence d'oscillation du soliton varie linéairement avec le nombre de particules constituant le soliton ce qui constitue un exemple très original de dynamique d'un système quantique dont la réponse à une force extérieure est collective.

Références

1. R. Saint-Jalm *et al.*, *Phys. Rev. X*, **9**, 021035 (2019).
2. B. Bakkali-Hassani *et al.*, *Phys. Rev. Lett.*, **127**, 023603 (2021).
3. A. M. Kosevich *et al.*, *Phys. Rep.*, **194**, 117 (1990).
4. S. Bresolin *et al.*, *Phys. Rev. Lett.*, **130**, 220403 (2023).

Spatio-temporal boundary dissipation measurements using Diffusing-Wave Spectroscopy

Enzo Francisco, Sébastien Aumaître

Service de Physique de l'Etat Condensée, CEA-Saclay, CNRS, 91191 Gif-sur-Yvette cedex, France
enzo.francisco@cea.fr

The determination of the velocity gradients provides valuable information in many aspects of fluid dynamics (dissipative structures, boundary layers, drag, etc). In particular, the norm of the strain rate tensor $\frac{\Gamma}{\sqrt{2}} = \sqrt{\sum_{i,j}\left[\frac{1}{2}\left(\partial_i v_j + \partial_j v_i\right)\right]^2}$ gives the viscous dissipation rate $\eta\Gamma^2$ of a Newtonian fluid flow. However, it is difficult to measure Γ to a sufficient level of spatial and temporal resolution. A promising technique, called Diffusing-Wave Spectroscopy (DWS), allows for its direct measurement. It exploits the diffusive nature of multiply scattered light in a turbid colloidal suspension. In a DWS measurement, the time autocorrelation of the scattered intensity is measured and decays because of the phase shift of light in time at each scattering event [1]. This decay is due on the one hand to the Brownian motion of particles and on the other hand to the fluid motion and more specifically to Γ, which can therefore be deduced [2,3].

We recently reported [4] the first spatially and temporally resolved measurements of the boundary dissipation using DWS with commercially available high-speed cameras. We demonstrated the method on a Taylor–Couette flow, characterizing the spatio-temporal dynamics of the boundary dissipation rate up to the wavy vortex flow (see Figure 1). We now perform such measurements in a wall-bounded turbulent flow, up to $\mathrm{Re} = 3 \times 10^5$, allowing the study of the dissipative structures and the temporal fluctuations of the boundary dissipation rate.

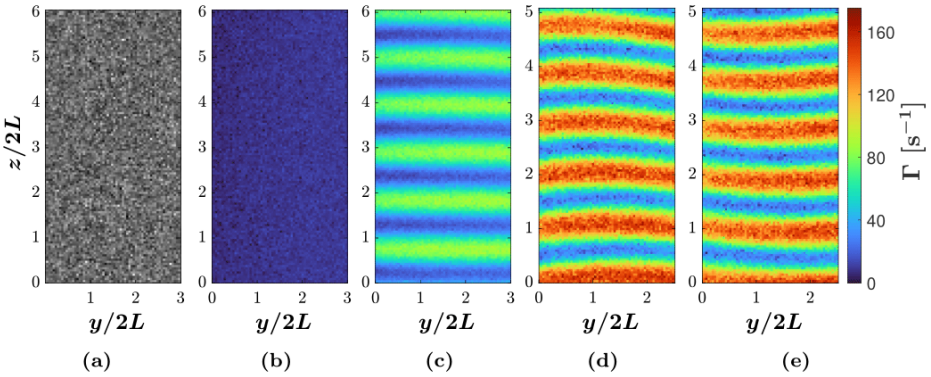

Figure 1. (a) Snapshot of the speckle pattern directly measured by the camera (arbitrary units of intensity). **(b)** Spatially resolved map of Γ in the linear regime ($\mathrm{Ta} = 188$), and **(c)** in the Taylor vortex regime ($\mathrm{Ta} = 3012$). **(d)(e)** Two spatially resolved map of Γ (0.25 s apart), in the wavy vortex regime ($\mathrm{Ta} = 4706$).

References

1. D. J. Pine, D. A. Weitz, J. X. Zhu & E. Herbolzheimer, *J. Physique*, **51**, 2101–2127 (1990).
2. X.-L. Wu, D. J. Pine, P. M. Chaikin, J. S. Huang & D. A. Weitz, *J. Opt. Soc. Am. B*, **7**, 15–20 (1990).
3. D. Bicout & G. Maret, *Physica A*, **210**, 87–112 (1994).
4. E. Francisco, V. Bouillaut, W. Tu & S. Aumaître, *Exp. Fluids*, **64**, 156 (2023).

La forme des bulles piégées dans la glace

Virgile Thiévenaz[1], Alban Sauret[2]

[1] PMMH, CNRS, ESPCI Paris, Sorbonne Université, Sorbonne Paris Cité, 7 quai Saint-Bernard, 75005 Paris
[2] Department of Mechanical Engineering, University of California Santa Barbara, 93106 Santa Barbara, USA
virgile.thievenaz@espci.fr

Un glaçon est rarement transparent, souvent opaque. Il contient de nombreuses petites bulles d'air [1]. Si l'on y regarde de près, ces bulles ne sont jamais sphériques mais allongées. Et deux bulles voisines peuvent avoir des tailles et des formes bien différentes. Certaines de ces bulles peuvent même former de longs cylindres, de plusieurs centimètres [2].

La plupart des gaz sont solubles dans l'eau mais très peu dans la glace. Ainsi, lorsque l'eau gèle, les gaz dissous sont expulsés et se concentrent devant le front de solidification. Des bulles s'y forment et sont capturées par la glace (Fig. 1). La combinaison entre solidification, capillarité, et diffusion du gaz donne aux bulles leurs formes spécifiques.

Nous montrons que sous certaines hypothèses, la forme des bulles peut être décrite par une seule équation différentielle ordinaire, fortement non linéaire. Cette équation met en jeu deux nombres sans dimensions liés à la sursaturation en gaz dissous et à la vitesse de solidification. Son étude permet d'expliquer certaines caractéristiques morphologiques communes à toutes les bulles comme l'arrondi de leur sommet. En-dessous d'une certaine vitesse de solidification se produit une bifurcation, après laquelle les bulles suffisamment grandes ne se referment jamais mais tendent vers une forme cylindrique.

Au-delà de l'étude mathématique, nous ajustons des solutions de cette équation différentielle à la forme de bulles observées expérimentalement. Cet ajustement est quantitatif dans la plupart des cas. Nous en déduisons la sursaturation ainsi que le rayon de nucléation des bulles. Cette méthode pourrait permettre de remonter dans l'histoire de bulles présentes dans des échantillons de glace, ainsi que de mieux contrôler la taille des pores de matériaux formés par trempe de solutions de gaz.

Figure 1. Bulles piégées dans la glace. Aucune n'est sphérique.

Références

1. A. E. Carte, *Proc. Phys. Soc.*, **77**, 757 (1961).
2. S. Bari & J. Halett, *J. Glaciol.*, **13**, 69, 489–520 (1974).

Dynamique d'une hélice acoustofluidique

Sophie Miralles[1], Bjarne Vincent[1,2], Alban Pothérat[2], Daniel Henry[1], Valéry Botton[1]

[1] Laboratoire de Mécanique des Fluides et d'Acoustique, INSA Lyon, CNRS, Ecole Centrale de Lyon, Universite Claude Bernard Lyon 1, UMR5509, 69621, Villeurbanne France
[2] Fluid and Complex Systems Research Centre, Coventry University, Coventry CV15FB, United Kingdom
sophie.miralles@insa-lyon.fr

Historiquement décrit par Faraday puis formalisé notamment par Lighthill et Eckart, l'*acoustic streaming* désigne les écoulements générés par la dissipation d'ondes acoustiques se propageant au sein d'un fluide. Un terme de force volumique, s'exprimant comme un tenseur de Reynolds basé sur le champ de vitesse acoustique, permet de rendre compte du mécanisme de conversion d'une partie de l'énergie acoustique en énergie mécanique. Suivant la configuration on peut d'ailleurs évoquer certaines analogies avec d'autres forces volumiques telles que les forces de flottabilité, les forces électromagnétiques ou encore le streaming accompagnant les ondes internes en milieu stratifié.

Lorsque l'onde acoustique est générée par une source plane de diamètre fini, l'écoulement prend la forme d'un jet qui peut se déstabiliser avec l'amplitude du forçage. Des instationnarités sont observées par plusieurs auteurs, notamment des oscillations basses fréquences, mais sont rarement détaillées.

En cavité fermée, l'orientation judicieuse du faisceau acoustique complexifie la géométrie du forçage et de l'écoulement en tirant parti des réflexions sur les parois. On peut ainsi observer un écoulement « carré » [1] (figure 1, gauche) ou encore en hélice [2] (figure 1, droite) avec une source ultrasonore unique. Les champs de vitesse, caractérisés expérimentalement par des mesures PIV et PTV3D résolues en temps, prennent au premier ordre la forme du champ de force lorsqu'ils sont moyennés en temps et montrent également une riche dynamique (figure 1, milieu), ouvrant la perspective au mélange chaotique [3, 4].

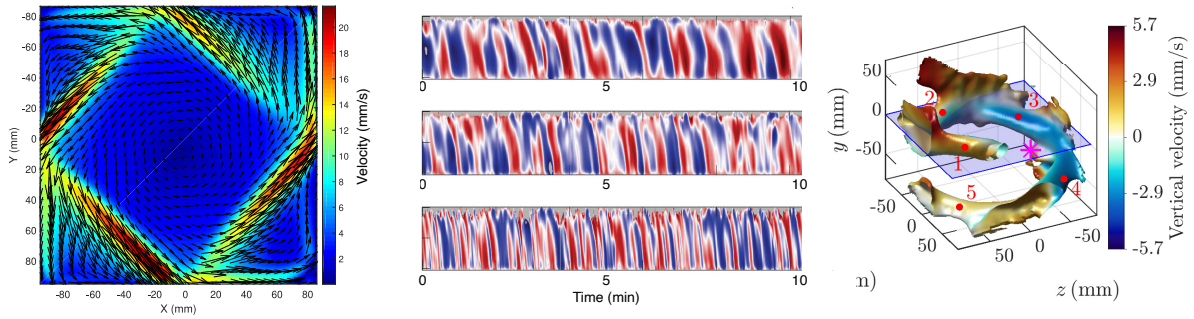

Figure 1. Gauche : Champ de vitesse moyenné en temps, résultant de la réflexion du faisceau d'ultrasons ($f = 2$ MHz) sur les 4 parois de la cavité carrée [1]. Milieu : Diagramme spatiotemporel de l'écart au champ moyen sur un jet [1]. Droite : Isocontour de vitesse moyenne obtenu par PTV 3D, sur un écoulement en géométrie hélicoidale [2].

Références

1. T. Cambonie *et al.*, From flying wheel to square flow: Dynamics of a flow driven by acoustic forcing, *Phys. Rev. Fluids*, **2**, 123901 (2017).
2. B. Vincent *et al.*, Experimental study of a helical acoustic streaming flow, soumis à *Phys. Rev. Fluids* (2023).
3. G. Launay *et al.*, Transition to chaos in an acoustically driven cavity flow, *Phys. Rev. Fluids*, **4**, 044401 (2019).
4. J. Qu *et al.*, Chaotic mixing in an acoustically driven cavity flow, *Phys. Rev. Fluids*, **7**, 064501 (2022).

Compartment model of epidemic spreading in complex networks with mortality

Téo Granger[1], Thomas M. Michelitsch[1], Bernard Collet[1], Michael Bestehorn[2], Alejandro P. Riascos[3]

[1] Sorbonne Université, Institut Jean le Rond d'Alembert, CNRS UMR 7190, 4 Place Jussieu, 75252 Paris Cedex 05, France
[2] Brandenburgische Technische Universität Cottbus-Senftenberg, Institut für Physik, Erich-Weinert-Straße 1, 03046 Cottbus, Germany
[3] Departamento de Física, Universidad Nacional de Colombia, Bogota, Columbia
michel@lmm.jussieu.fr

We study epidemic spreading in complex networks by a multiple random walker's approach. Each random walker performs an independent simple random walk on a connected complex random graph such as the Barabasi-Albert (BA), Erdös-Rényi (ER) and Watts-Strogatz (WS) type graphs. We assume, both walkers and nodes can be infected. They are in one of the compartments, susceptible (S) or infected (I) representing their states of health. The transmission of the disease happens as follows. Susceptible nodes may be infected by visits of infected walkers, and susceptible walkers may be infected by visiting infected nodes. No direct transmission among walkers are possible. This model mimics the class of diseases such as Dengue and Malaria with transmission via vectors (mosquitos).

In addition, for infected walkers, we account for the possibility that they may die during a random duration of their infection time (by introducing an additional compartment of dead walkers), whereas infected nodes never die and always recover after a random period of infection. We implement this random walk model (using PYTHON NetworkX library) and perform simulations to explore the compex interplay of the topology of the network and the propagation of the disease. An animated simulation can be seen by clicking on following link: https://drive.google.com/file/d/1dQNvxT4mEhGR64eOI1rJJT-dmFXZ5rQf/view.

References

1. W. O. Kermack, A. G. McKendrick, A contribution to the mathematical theory of epidemics, *Proc. Roy. Soc. A*, **115**, 700–721 (1927).
2. T. Granger, T. M. Michelitsch, M. Bestehorn, A. P. Riascos & B. A. Collet, Four-compartment epidemic model with retarded transition rates, *Phys. Rev. E*, **107**, 044207 (2023).
3. M. Bestehorn, T. M Michelitsch, B. A. Collet, A. P. Riascos & A. F. Nowakowski, Simple model of epidemic dynamics with memory effects, *Phys. Rev. E*, **105**, 024205 (2022).
4. M. Bestehorn, A. P. Riascos, T.M. Michelitsch & B. A Collet, A Markovian random walk model of epidemic spreading, *Cont. Mech. Therm.*, Springer Verlag (2021). https://cnrs.hal.science/hal-02968842
5. Supplementary materials (Simulation films and Python Codes): https://sites.google.com/view/scirs-model-supplementaries/accueil

Mobile soap film drainage shows self-similarity

Antoine Monier[1], François-Xavier Gauci[1], Cyrille Claudet[1], Franck Celestini[1], Christophe Brouzet[1] and Christophe Raufaste[1,2]

[1] Université Côte d'Azur, CNRS, Institut de Physique de Nice (INPHYNI), 06200 Nice, France
[2] Institut Universitaire de France (IUF), 75005 Paris, France
antoine.monier@univ-cotedazur.fr

Liquid foams are widely used in industry because of their remarkable thermal and mechanical properties. Although, predicting their stability remains a challenge as it results from diverse mechanisms. One of which is liquid film thinning under the effect of drainage, that is still lacking today full understanding.

We study a unique soap film in a rectangular frame draining under the effect of gravity. Our study focuses on 'mobile' soap films that exhibit a smooth thickness profile at their center along with the presence of an instability near the borders of the frame, next to the meniscii, called marginal regeneration [2]. This instability creates locally thinner film elements surrounded by thicker film. Subject to gravity, in vertical films, these thinner elements rise due to buoyancy force. This phenomenon generates an upward flux along the borders inside the frame, contrasting with the overall downward motion of the colored interference fringes in the center of the films [3]. We aim to address how to characterize these two opposite flows and understand how they are coupled, dictating the time scale of the thinning process.

In our work, we precisely study the spatio-temporal features of the thinning process thanks to color interferometry. We show that there is an equivalence between looking at the descent dynamics of the interference fringes and looking at the thinning dynamics at given positions. We also show that the drainage dynamics is self-similar gathering all data onto a single curve regardless of the solution properties and frame dimensions. Finally, data from literature also align with ours, suggesting a universal soap film shape during the drainage. To conclude, draining films all have the same shape with a thinning rate that is a function of the experimental parameters [4]. These results pave the way towards a better understanding on how marginal regeneration governs soap film drainage.

References

1. I. Cantat, S. Cohen-Addad, F. Elias, F. Graner, R. Höhler, O. Pitois, F. Rouyer & A. Saint-Jalmes, *Foams: Structure and dynamics*, Oxford University Press, Oxford (2013).
2. K. J. Mysels, K. Shinoda & S. Frankel, *Soap films: Studies of their thinning and a bibliography*, Pergamon Press (1959).
3. J. Seiwert, R. Kervil, S. Nou & I. Cantat, Velocity field in a vertical foam film, *Phys. Rev. Lett.*, **118**, 048001 (2017).
4. A. Monier, F.-X. Gauci, C. Claudet, F. Celestini, C. Brouzet & C. Raufaste, Self-similar and universal dynamics in drainage of mobile soap films, arXiv:2401.03931 (2024).

Taylor's swimming sheet near a soft wall

Aditya Jha, Yacine Amarouchene, Thomas Salez

LOMA, UMR 5798, Universitè de Bordeaux, Talence 33405, France
aditya.jha@u-bordeaux.fr

In 1951, G. I.Taylor [1] modelled swimming organisms by hypothesizing a 2D infinite sheet swimming due to a wave passing through it. This simple model not only captured the ability to swim as a result of wavy motion of the flagella but further development into the model captured the optimal nature of metachronal waves observed in ciliates. While the effect of confinement near rigid walls was studied by Katz [2] and Reynolds [3], we focus on the correction to swimming velocity generated due to the softness of the wall. By following the analysis akin to the studies on lift forces observed near soft gels and elastomers, we explore whether this softness of the boundary can enhance the swimming velocity of the micro-organism or not, for a small compliance of the wall.

References

1. G. I. Taylor, Analysis of the swimming of microscopic organisms, *Proc. R. Soc. Lond. A*, **209**, 447–461 (1951).
2. D. F. Katz, On the propulsion of micro-organisms near solid boundaries, *J. Fluid Mech.*, **64**, 33–49 (1974).
3. A. J. Reynolds, The swimming of minute organisms, *J. Fluid Mech.*, **23**, 241–260 (1965).

Exposés courts de la 27^{e} Rencontre du Non-Linéaire

Laboratory granular landslides

Ludovic Brivady[1], Rory T. Cerbus[2], Thierry Faug[3], Hamid Kellay[1]

[1] Laboratoire Ondes et Matière d'Aquitaine (LOMA), UMR 5798 Univ. Bordeaux et CNRS, 351 cours de la Libération, 33405 Talence, France
[2] RIKEN Center for Biosystems Dynamics Research (BDR), 2-2-3 Minatojima-minamimachi, Chuo-ku, Kobe 650-0047, Japan
[3] Univ. Grenoble Alpes, CNRS, INRAE, IRD, Grenoble INP, IGE, 38000 Grenoble, France
ludovic.brivady@u-bordeaux.fr

A main objective in landslide research is to predict how far they will travel. A well-known feature first reported by Albert Heim in 1932 [1] is the positive correlation between landslide volume and landslide runout, so that larger landslides can travel many times further than one can naively predict using the energy balance between initial potential energy and frictional dissipation (cf. Fig. 1). Different mechanisms have been suggested [2, 3]. An obstacle for these explanations is that it is difficult to test them by a systematic and independent study of the parameters for naturally occurring landslides.

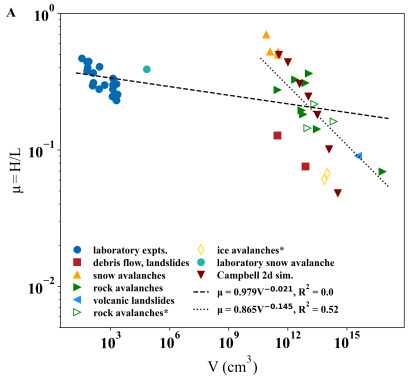

Figure 1. Comparison of experiments with field data using the usual normalized runout (the ratio between the travel distance and the initial height of the mass) showing the scale separation in the landslide size.

We used a simplified geometry for granular landslide laboratory experiments and focus on the maximum travel distance, the landslide runout, that is of primary interest for hazard management. Despite the apparent scale separation, we first managed to reproduce the decrease in friction with the landslide size observed in nature for large landslide sizes. Then by taking part of the relative simplicity of our set-up, we study the influence of substrate roughness and initial mass height. Our results suggest that a decrease in the apparent friction still occurs for rough sliding slopes or different dropping heights albeit with a shift in the critical landslide size needed to make this appear. The versatility of the set-up enables us to study the motion of the mass and particularly the non-trivial relations between the flow thickness, the speed of the landslide front and the landslide size. These results provide scaling laws that might be useful to test the validity of proposed mechanisms for the increase in mobility.

References

1. A. Heim, *Der Bergsturz und Menschenleben*, Fretz und Wasmuth (1932).
2. C. Johnson & C.S. Campbell & H. J. Melosh, The reduction of friction in long runout landslides as an emergent phenomenon, *J. Geophys. Res. Earth Surf.*, **121**, 881 (2016).
3. S. Parez & E. Aharonov, Long runout landslides: A solution from granular mechanics, *Front. Phys.*, **3**, 80 (2015).

Impact d'un jet liquide sur une surface chauffée

Aurélien Goerlinger, Farzam Zoueshtiagh, Alexis Duchesne

Univ. Lille, CNRS, Centrale Lille, Univ. Polytechnique Hauts-de-France, UMR 8520 - IEMN - Institut d'Electronique de Microélectronique et de Nanotechnologie, F-59000 Lille, France
aurelien.goerlinger@univ-lille.fr

Lorsqu'un jet liquide vertical impacte une surface chaude horizontale, différents phénomènes peuvent être observés comme par exemple la caléfaction [1]. Nous nous intéressons ici à l'impact d'un jet d'eau déminéralisée sur un disque en Duralumine chauffé à l'aide d'une plaque chauffante. Le rayon du jet a varie entre 85 µm et 250 µm et la température du disque en Duralumine varie entre 300°C et 500°C. Un pousse-seringue permet de faire varier le débit Q au niveau du jet. Dans nos expériences, nous utilisons le nombre de Weber associé au jet et défini comme $\mathrm{We} = \frac{2\rho Q^2}{\pi^2 \gamma a^3}$ où ρ est la densité de l'eau et γ sa tension de surface. Nous observons alors deux régimes différents en fonction du nombre de Weber. Pour des nombres de Weber faible ($\lesssim 35$), une unique goutte se forme sous le jet, grossit, puis se détache en laissant place à une autre goutte (voir figure 1a). Inversement, pour des nombres de Weber assez grands ($\gtrsim 35$), nous observons l'éjection d'une multitude de petites gouttelettes (voir figure 1b). Alors que l'observation de ces régimes dépend fortement du nombre de Weber, nous montrons que la température de la plaque n'a aucun impact sur nos observations, tandis que l'impact du rayon du jet est relativement limité. Enfin, nous tentons que rationnaliser nos observations en obtenant des lois d'échelle à partir de modèles jouet.

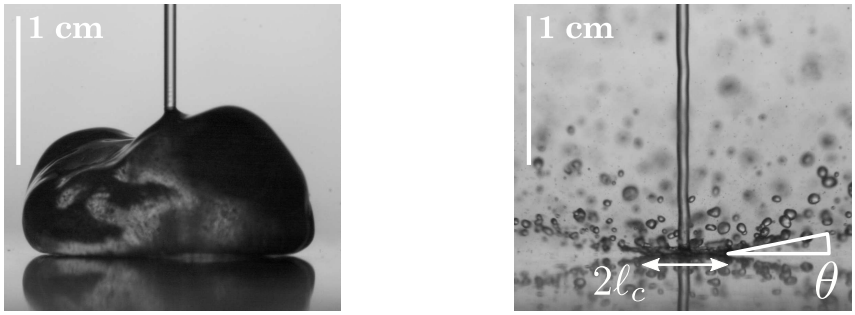

(a) We $\simeq 24$ (b) We $\simeq 98$

Figure 1. Impact d'un jet d'eau de rayon 195 µm impactant un disque en Duralumine chauffé à 350°C pour deux nombres de Weber de jet différents. (a) Une unique goutte reste sous le jet, grossit puis se détache, laissant place à une nouvelle goutte. (b) Une nappe liquide, de rayon ℓ_c, se forme sous le jet et se brise en une multitude de petites gouttelettes qui sont éjectés avec un angle θ par rapport à l'horizontale.

Références

1. C. Agrawal, Surface quenching by jet impingement – A review, *Steel Res. Int.*, **90**, 1800285 (2023).

Wave packets that do not move at the group velocity

Gregory Kozyreff

Département de physique, Université libre de Bruxelles, Campus de la Plaine, CP 231, 1050 Bruxelles.
gregory.kozyreff@ulb.be

The group velocity is an important unifying concept in wave phenomena. It yields the speed of wave packets and generally differs from that of the phase velocity of the underlying oscillations. Moreover, its validity carries over to the realm of weakly nonlinear wave packets through the universal nonlinear Schrödinger equation (NLS). However, this communication reports that in this general frame, the group velocity, and hence the NLS, ceases to describe the dynamics of soliton wave packets when the group and phase velocities are sufficiently close to one other.

We will demonstrate our result on the following general class of wave equations

$$\frac{\partial^2 E}{\partial x^2} + \int_{-\infty}^{\infty} \beta^2(\omega)\hat{E}(x,\omega)e^{-i\omega t}\,\mathrm{d}\omega = N[E,\epsilon]\,,$$

where

$$\hat{E}(x,\omega) = \frac{1}{2\pi}\int_{-\infty}^{\infty} E(x,t)e^{i\omega t}\,\mathrm{d}t$$

is the Fourier transform of the scalar field $E(x,t)$ of interest and $N[E,\epsilon]$ is the nonlinearity, which tends to zero as $\epsilon \to 0$. The linear properties of the wave system is contained in the dispersion function $\beta(\omega)$ and the results are derived in a region of parameters such that the relative difference between the group and phase velocities is $O\left(\epsilon^{-1/2}\exp(-\pi/4\epsilon)\right)$. In that region, not only do solitonic wave packets depart from the group velocity, but worse than that: they do not even move at a constant speed. In this presentation, we will provide a physical argument for this behaviour and sketch the derivation based on exponential asymptotics [1]. The final result is that the motion of the wave packet is governed by a surprisingly simple and familiar equation.

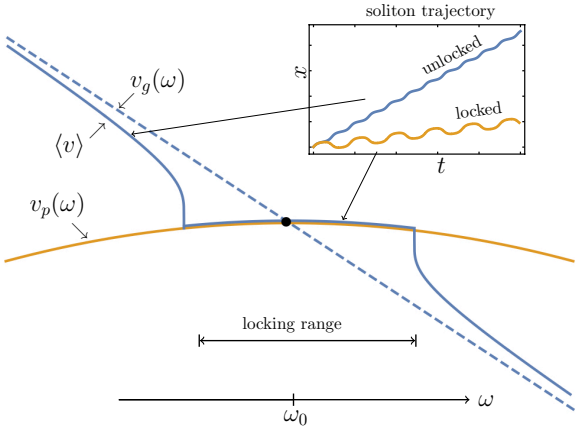

Figure 1. v_g: group velocity, v_p: phase velocity, $\langle v\rangle$: average soliton velocity. Inset: soliton trajectory.

References

1. G. Kozyreff, Speed of wave packets and the nonlinear Schrödinger equation, *Phys. Rev. E*, **107**, 014219 (2023).

Évaluation de la pertinence écologique des méthodes de calcul de la vitesse du changement climatique

Laure Moinat[1,2], Iaroslav Gaponenko[3], Stéphane Goyette[1,2], Jérôme Kasparian[1,2]

[1] Institut des Sciences de l'Environnement, Université de Genève, bd Carl Vogt 66, 1211 Genève 4, Suisse
[2] Groupe de Physique Appliquée, Université de Genève, Rue de École de Médecine 20, 1211 Genève 4, Suisse
[3] DQMP, Université de Genève, Quai Ansermet 24, 1211 Genève 4, Suisse
jerome.kasparian@unige.ch

Le changement climatique influe sur les aires de répartition des espèces. La vitesse de ces déplacements est liée au changement climatique, et notamment au déplacement des isothermes vers les pôles. Mais les valeurs météorologiques à court-terme, la topographie ou d'autres barrières jouent également un rôle. De plus, la direction et la norme de la vitesse de déplacement des isothermes n'est pas définie de manière univoque. Elles dépendent d'hypothèses implicites sur lesquelles se fondent les calculs, notamment pour déterminer la direction du vecteur vitesse. L'approche classique qui suppose que le déplacement se fait parallèlement au gradient de température [1] montre de sérieuses limitations, en particulier dans les zones de faible gradient où la vitesse diverge [2]. Cela nous a récemment amenés à introduire une méthode alternative qui maximise la régularité du champ de vitesses : Monte-cArlo iTerative Convergence metHod (MATCH) [3].

Cependant, cette méthode étant basée sur des arguments mathématiques, sa pertinence écologique doit être évaluée soigneusement. Nous nous sommes intéressés aux aires de répartition des oiseaux nord-américains, sur la base des observations du *Audubon Christmas Bird Count*, ainsi que sur les espèces marines observées dans la zone de pêche Atlantique Nord Est du *NOAA fisheries survey*. Pour chaque espèce, nous avons déterminé le centroïde de l'aire de répartition à deux plages de temps, et nous en avons déduit la norme et la direction du déplacement correspondant, ainsi que sa vitesse. Nous avons également calculé à chaque lieu d'observation le décalage des isothermes de la température : température de l'air de surface pour les oiseaux et température de surface de l'océan pour les espèces marines. Nous en avons déduit une vitesse moyenne de dérive des isothermes, avec la méthode du gradient ainsi qu'avec la méthode MATCH.

En comparant les déplacements des aires de répartition des espèces avec ceux des isothermes, nous avons seulement trouvé une corrélation positive statistiquement significative entre le décalage latitudinal des espèces marines et le déplacement des isothermes calculé avec la méthode MATCH. Ni l'approche classique basée sur le gradient, ni les décalages en longitude, ni les déplacements d'aires de répartition des oiseaux, n'ont montré de corrélation significatives. Nos résultats suggèrent donc que la méthode MATCH est préférable pour les applications écologiques. Nous confirmons également des observations antérieures montrant que les espèces marines suivent davantage le changement climatique que les espèces terrestres. Ces résultats pourraient aider à anticiper les changements d'aires de répartition des espèces, et donc à mieux cibler les mesures de conservation.

Références

1. S. R. Loarie *et al.*, *Nature*, **462**, 1052 (2009).
2. J. Rey, G. Rohat, M. Perroud, S. Goyette & J. Kasparian, *Env. Res. Lett.*, **15**, 034027 (2020).
3. I. Gaponenko, G. Rohat, S. Goyette, P. Paruch & J. Kasparian, *Sci. Rep.*, **12**, 2997 (2022).

Super-attracteurs d'ondes inertielles dans un frustum elliptique

Benjamin Favier, Stéphane Le Dizès

Aix Marseille Univ, CNRS, Centrale Marseille, IRPHE, Marseille, France
benjamin.favier@univ-amu.fr

Les attracteurs sont des singularités bien connues des fluides stratifiés ou en rotation [1, 2], souvent étudiés en deux dimensions. Ils sont une conséquence des lois de propagation inhabituelles des ondes internes ou inertielles, dont la réflection sur une paroi inclinée mène à leur focalisation le long d'un cycle limite qui dépend de la géométrie considérée. Nous présentons la généralisation de ces attracteurs à des cas tridimensionels, et montrons en particulier l'existence de super-attracteurs, qui attire l'ensemble des rayons du volume, quelle que soit leur position initiale.

Nous considérons pour cela des ondes inertielles se propageant dans un fluide en rotation contenu dans une cavité tri-dimensionnelle non axisymétrique. Nous nous concentrons sur le cas particulier d'un fluide contenu dans un tronc de cône, qui est le volume situé entre deux plans parallèles horizontaux coupant un cône droit. Bien que cette géométrie ait été étudiée par le passé, nous la généralisons en brisant son axisymétrie et en considérant le cas d'un cône elliptique dont les sections horizontales sont des ellipses et non des cercles. Le problème est d'abord abordé à l'aide d'un tracé de rayons où les paquets d'ondes locaux sont géométriquement propagés et réfléchis sans atténuation à l'intérieur du volume. Ces résultats sont complétés par une analyse asymptotique locale et des simulations numériques du problème linéaire visqueux d'origine. Nous montrons que les attracteurs, bien connus dans les domaines bidimensionnels ou axisymétriques, peuvent être piégés dans un plan particulier en trois dimensions à condition que l'axisymétrie du domaine soit brisée. Contrairement aux exemples précédents d'attracteurs dans des domaines tridimensionnels [3–5], tous les rayons convergent vers le même cycle limite, quelles que soient leurs conditions initiales.

Références

1. L. R. M. Maas & F.-P. Lam, Geometric focusing of internal waves, *J. Fluid Mech.* **300**, 1–41 (1995).
2. L. R. M. Maas, Wave attractors : Linear yet nonlinear, *Int. J. Bifurc. Chaos*, **15**, 2757–2782 (2005).
3. A. M. Manders & L. R. M. Maas, On the three-dimansonal structure of the inertial wave filed in a rectangular basin with one sloping boundary, *Fluid Dyn. Res.*, **35**, 1–21 (2004).
4. G. Pillet, E. V. Ermanyuk, L. R. M. Maas, I. N. Sibgatullin & T. Dauxois, Internal wave attractors in three-dimensional geometries: Trapping by oblique reflection, *J. Fluid Mech.*, **845**, 203–225 (2018).
5. G. Pillet, L. R. M. Maas & T. Dauxois, Internal wave attractors in 3d geometries: A dynamical systems approach, *Eur. J. Mech. B*, **77**, 1–16 (2019).

Cheap turbulence modelling with quasi-singularities

Wandrille Ruffenach[1,2], Bérengère Dubrulle[2], Lucas Fery[2,3]

[1] Department of Physics, École Normale Supérieure de Lyon, 69364, Lyon, France
[2] SPEC/IRAMIS/DSM, CEA, CNRS, University Paris-Saclay, CEA Saclay, 91191 Gif-sur-Yvette, France
[3] Laboratoire des Sciences du Climat et de l'Environnement, CEA Saclay l'Orme des Merisiers, UMR 8212 CEA-CNRS-UVSQ, Université Paris-Saclay & IPSL, 91191, Gif-sur-Yvette, France
wandrille.ruffenach@ens-lyon.fr

Turbulent flow exhibit spatio-temporal intermittent energy dissipation and transfers. This makes their modelling challenging, as capturing these events require high temporal and spatial resolution. In this contribution, we present a cheap modelling strategy, using the scale separation between the large scale flow and these small scale extreme events. Specifically, we represent these events by localized Lagrangian quasi-singularities of vorticity. The dynamics of these particles is adapted from the vorton model of Novikov [1], to include self-regularization and interaction with a mean flow. As a first application, we consider the case where the large-scale is a pure shear flow. In that case, we observe a transition between a laminar regime where the regularization scale $\eta(t)$ grows like $\sqrt{t}$ and a turbulent regime in which η stabilizes at a statistically steady value solely determined by the Reynolds number. By construction, our modelling strategy is cheap and is yet able to reproduce key features of turbulence.

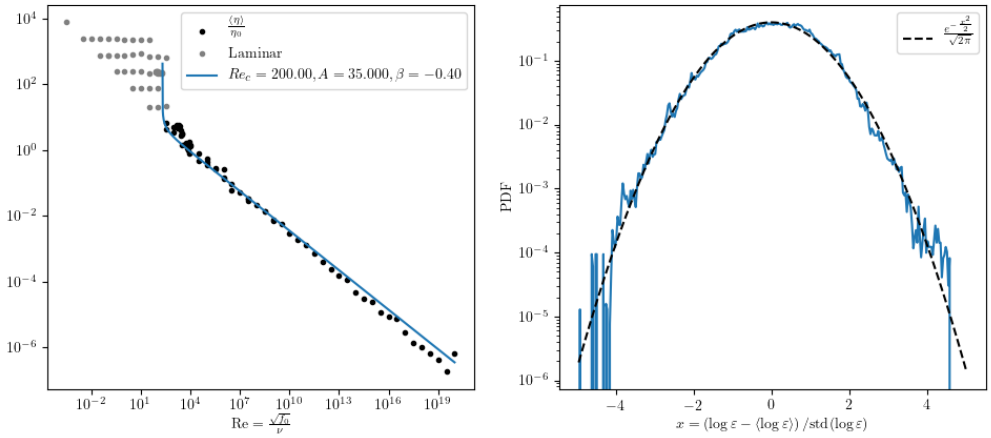

Figure 1. Left: Average regularisation lengthscale in the turbulent (black) and laminar (grey) states. In the laminar state, a plateau of order $\sqrt{\nu t_{\mathrm{simul}}}$ is reached. Right: Lognormal behavior of the energy dissipation rate.

References

1. E. A. Novikov, Generalized dynamics of three-dimensional vortical singularities (vortons), *Zh. Eksp. Teor. Fiz.*, **84**, 981 (1983).
2. G. S. Winckelmans, Contributions to vortex particle methods for the computation of three-dimensional incompressible unsteady flows, *J. Comput. Phys.*, **109**, 247–273 (1993).

La transition vers la turbulence induite par du bruit de l'écoulement de Couette plan contourne-t-elle les instantons ?

Joran Rolland

Univ. Lille, CNRS, ONERA, Arts et Métiers Institute of Technology, Centrale Lille, UMR 9014 - LMFL - Laboratoire de Mécanique des Fluides de Lille - Kampé de Fériet, F-59000 Lille, France.
joran.rolland@centralelille.fr

Comme d'autres écoulements de paroi, l'écoulement de Couette plan, d'un fluide de viscosité cinématique ν entre deux parois séparées d'une distance $2h$ se déplaçant à vitesse $\pm U$, a une transition particulière vers la turbulence. L'écoulement de base laminaire est linéairement stable pour tout nombre de Reynolds $R = \frac{hU}{\nu}$, le principal paramètre de contrôle adimensionné. Cependant, la turbulence peut exister de manière localisée en espace dès que $R \gtrsim 330$. Dans ce cas, son existence est transitoire, avec un temps de vie qui augmente extrêmement rapidement avec le nombre de Reynolds et avec les tailles longitudinales L_x et transverses L_z du domaine de l'écoulement.

On a ainsi une situation bistable entre l'écoulement laminaire et l'écoulement turbulent. Nous considérons ici le passage de l'écoulement laminaire vers l'écoulement turbulent sous un forçage stochastique principalement contrôlé par son taux d'injection d'énergie ϵ [3]. Lorsque le taux d'injection d'énergie est réduit, l'observation d'une trajectoire allant du voisinage de l'écoulement laminaire vers la turbulence devient rare. Ces trajectoires sont donc systématiquements échantillonnées à l'aide d'une méthode de simulation d'évènements rares [2], accompagnée de validations.

De manière surprenante, les trajectoires échantillonnées n'ont que partiellement les propriétés des instantons, les trajectoires les plus probables structurants les évènements de métastabilité dans la limite $\epsilon \to 0$. Si l'on observe entre autre une croissance exponentielle avec $\frac{1}{\epsilon}$ du temps d'attente T avant un évènement, et une concentration des trajectoires à ϵ donné, des élements clefs sont manquants. Ainsi, la trajectoire autour de laquelle les évènements se concentrent évolue lentement avec ϵ. De plus, si ces trajectoires traversent la séparatrice entre écoulement laminaire et turbulent, elles le font relativement loin du point col le plus proche, au contraire d'un instanton. Le lent déplacement des trajectoires dans l'espace des phases laisse penser qu'elles peuvent rejoindre un instanton, mais qu'elles le feraient à des ϵ très petits et des temps d'attente excessivement longs. Ce comportement est observé dans des domaines de tailles $L_x \times L_z$ minimales et dans des domaines de tailles croissantes où de la coexistence laminaire-turbulente se manifeste. Ce comportement pourrait être similaire à celui décrit pour la première fois dans le cadre plus simple de la transition induite par du bruit, d'une onde non linéaire vers l'écoulement de base de l'écoulement de Poiseuille plan. Dans ce cas, les instantons passent par un état médiateur près de la séparatrice, où les trajectoires traversent effectivement [4]. Il est comparable à celui décrit dans des modèles à quelques degrés de libertés motivés par la géophysique [1].

Références

1. R. Börner, R. Deeley, R. Römer, T. Grafke, V. Lucarini & U. Feudel, arXiv:2311.10231 (2023).
2. F. Cérou, A. Guyader, *Stoch. Anal. Appl.* **25**, 417–443 (2007) .
3. J. Rolland, arXiv:2401.05555 (2024).
4. X. Wan, H. Yu, W. E, *Nonlinearity*, **28**, 1409 (2015).

Split societies

Olivier Devauchelle[1], Piotr Szymczak[2], Piotr Nowakowski[3]

[1] Université Paris Cité, Institut de Physique du Globe de Paris, 1 rue Jussieu, CNRS, F-75005 Paris, France.
[2] Institute of Theoretical Physics, Faculty of Physics, University of Warsaw, Poland.
[3] Group for Computational Life Sciences, Division of Physical Chemistry, Ruđer Bošković Institute, Zagreb, Croatia and Max Planck Institute for Intelligent Systems, Stuttgart, Germany.

devauchelle@ipgp.fr

Elections are often surprisingly tight, and sometimes split the electorate into two solidly opposed camps [1]. These camps are not necessarily connected, but election maps generally show consistent clusters. Here, inspired by a recent contribution [2], we draw an analogy with the statistical behavior of magnets, wherein atoms tend to orient their spins with those of their neighbors.

Adapting the classical Ising model to account for the influence of opinion polls on a voter, we find that a new phase appears, in which two equal-sized camps solidify (figure 1, left). This ordered phase exists when the temperature is low enough, that is, when voters are strongly influenced by others (figure 1, right). Surprisingly, the susceptibility of this phase remains continuous, like that of the classical paramagnetic phase. Combining the fluctuation–dissipation theorem with a continuous model of the split-society phase, one can, in principle, estimate the influence of opinion polls from the fluctuations of their results.

Of course, such a simplistic model can only treat a voter's inner feelings as noise, but it nonetheless suggests that the outcome of modern elections reflects the feedback between voters and polls. We test this hypothesis against publicly-available election data.

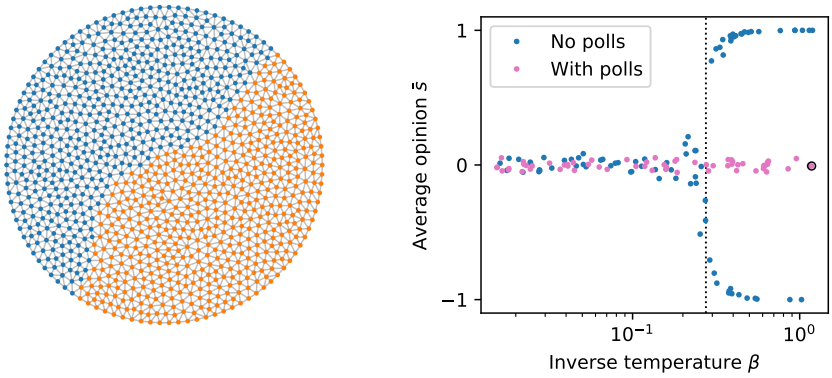

Figure 1. Left: Split-society phase on a triangular mesh (1046 nodes). Each node is a voter, connected to its neighbors as shown by gray lines. Blue and orange colors indicate the state of each voter ($s = +1$ or -1). Right: Average opinion $\bar{s}$ of the electorate shown on the left panel, as a function of the inverse temperature (numerical simulations using the Glauber algorithm). Blue dots: classical Ising model (no opinion polls). Pink dots: opinion polls influence voters. Dotted black line: critical temperature for the classical Ising model on a triangular mesh [3]. The black circle corresponds to the state shown on left panel.

References

1. S. A. Levin, H. V. Milner & C. Perrings, *Proc. Natl. Acad. Sci. USA*, **118**, e2116950118 (2021).
2. N. Araújo, J. Andrade Jr & H. Herrmann, *PLOS One*, **5**, e12446 (2010).
3. G. Wannier, *Phys. Rev.*, **79**, 357 (1950).

Vertical velocities in quasi-geostrophic floating vortices

Marine Aulnette, Patrice Le Gal, Michael Le Bars

Aix Marseille University, CNRS, Centrale Marseille, IRPHE, Marseille, France
marine.aulnette@univ-amu.fr

Oceanic structures subjected to the Earth's rotation are driven by geostrophic equilibrium which allows large-scale oceanographic models to successfully reproduce the near-two-dimensional dynamics of large eddies and currents. However, fine-scale ocean structures, such as vortices, fronts, filaments, waves emerge and escape this description. They generate three-dimensional movements which therefore break the geostrophic equilibrium. Measurements and understanding of these fine-scale vertical motions are one of the main open questions among the oceanography community, as they are most likely responsible for ocean mixing and have a strong impact on the transport of biologic and chemical components as well as on the climate evolution.

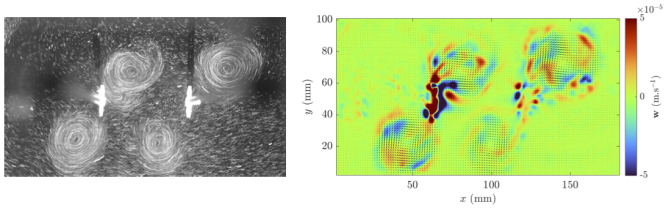

Figure 1. (a) Superimposition of raw images of four floating vortices. (b) Resulting $\mathbf{w}$ (m/s) field obtained from the ω-equation model (Eq. (1)).

We focus here on three-dimensional motions in floating vortices resulting from the balance between the Coriolis force and the density gradients [1]. If the most intense velocities are horizontal as we would expect from geostrophy, their shape is connected to small vertical velocities. Therefore, the aim of this study is to measure experimentally these vertical motions. This is especially challenging because vertical velocities are smaller by several orders of magnitudes compared to the horizontal velocities. The floating vortices will be produced by injecting dyed pure water at the surface of a salt water rotating volume (Fig. 1). PIV and particle tracking are the method of choice to measure horizontal and vertical velocity fields and LIF is used to measure density fields. The results are then compared to predictions from oceanographers model given by the ω-equation [2] :

$$N^2\nabla_h^2\mathbf{w} + f^2\frac{\partial^2\mathbf{w}}{\partial z^2} = 2\nabla_h \cdot (\nabla_h\mathbf{u_g} \cdot \nabla_h\rho) \tag{1}$$

with $\mathbf{w}$ the ageostrophic vertical velocity, $\mathbf{u_g}$ the geostrophic horizontal velocity field, ρ the density, f the Coriolis frequency, N the Brunt–Väisälä frequency and ∇_h the horizontal gradients.

Acknowledgments: This work received financial support from the French government under the France 2030 investment plan, as part of the Initiative d'Excellence d'Aix–Marseille Université – AMIDEX AMX-21-RID-035.

References

1. H. M. de la Rosa Zambrano, A. Cros, R. Cruz Gómez, M. Le Bars & P. Le Gal, A laboratory study of floating lenticular anticyclones, *Eur. J. Mech. B*, **61**, 1–8 (2017).
2. B. J. Hoskins, I. Draghici & H. C. Davies, A new look at the ω-equation, *Q. J. R. Meteorol. Soc.*, **104**, 31–38 (1978).

Bacteria in liquid crystals: from the swimming mechanism of individuals to collective effects

Guillaume Sintès[1,2], Martyna Góral[1,2], Anke Lindner[1], Teresa López-León[2]

[1] PMMH, ESPCI, 10 rue Vauquelin 75005 Paris
[2] Gulliver, ESPCI, 10 rue Vauquelin 75005 Paris
guillaume.sintes@espci.fr

Despite the importance of bacterial dynamics in anisotropic environments, very common in biology, many important questions remain unresolved. Water-soluble liquid crystals have proven to be a model system to study the influence of anisotropy on the swimming and space exploration behavior of the micro-swimmers. Recent studies have showed that bacteria are forced to follow the nematic director, inhibiting their intrinsic run and tumble exploration dynamics. We show that, in these highly anisotropic media, bacteria can reverse their swimming direction by relocating at least one flagellum on the other side of their bodies.

Liquid crystals also enable the emergence of new types of collective behavior, such as the spontaneous formation of self-propelled trains of bacteria. We compare these dynamic structures to those formed by the passive self-assembly of particles in liquid crystals and investigate the mechanism enabling their self-propulsion. Finally, we show that more complex collective behaviors emerge when the liquid crystal is confined to spherical liquid crystal droplets and shells, where bacteria are forced to interact with topological defects.

Vertical structure of transport by ocean mesoscale turbulence

Julie Meunier[1], Benjamin Miquel[2], Basile Gallet[1]

[1] Université Paris-Saclay, CNRS, CEA, Service de Physique de l'Etat Condensé, 91191, Gif-sur-Yvette, France
[2] Univ Lyon, CNRS, Ecole Centrale de Lyon, INSA Lyon, Université Claude Bernard Lyon 1, LMFA, UMR5509, 69130, Ecully, France.
julie.meunier@cea.fr

Ocean mesoscale eddies — vortices of size tens of kilometers — play a significant role in the transport of heat, salt and tracers across latitudes. Despite this significant impact on the global ocean, most climate models do not resolve mesoscale vortices and rely on crude parametrizations of the associated turbulent transport.

We revisit this turbulent transport problem based on the asymptotic dynamics of rotating stratified flows. We propose a direct derivation of the diffusion tensor relating the turbulent fluxes to the background gradients of an arbitrary tracer, together with constraints on the vertical structure of the associated transport coefficients [1]. Based on these constraints, we derive a perturbative prediction for the vertical structure of the turbulent heat flux within the water column. We quantitatively validate these predictions by comparison with Direct Numerical Simulations of an isolated patch of ocean [2]. The resulting physically-based parametrization is currently being implemented in a global ocean model.

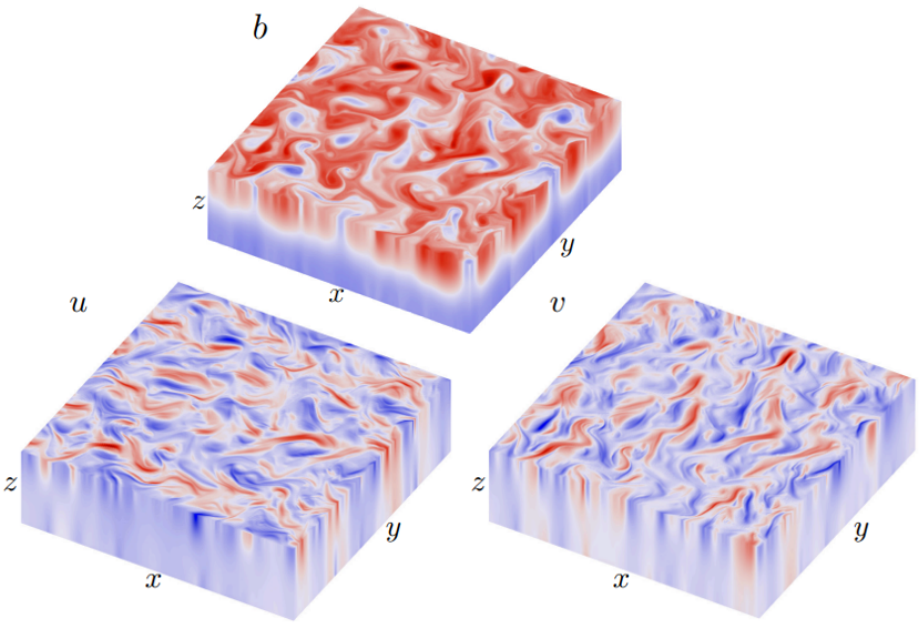

Figure 1. Visualisations of mesoscale eddies in a simulation of an idealized patch of ocean: snapshots of buoyancy departure b, zonal velocity departure u and meridional velocity departure v.

References

1. J. Meunier, B. Miquel & B. Gallet, A direct derivation of the Gent–McWilliams/Redi diffusion tensor from quasi-geostrophic dynamics, *J. Fluid Mech.*, **963**, A22 (2023).
2. J. Meunier, B. Miquel, B. Gallet, Vertical structure of buoyancy transport by ocean baroclinic turbulence, *Geophys. Res. Lett.*, **50**, e2023GL103948 (2023).

Restitution coefficients of drops bouncing on a vibrating surface

Tomas Fullana[1], Lebo Molefe[1,2], François Gallaire[1], John Martin Kolinski[2]

[1] Laboratory of Fluid Mechanics and Instabilities, School of Engineering, Ecole Polytechnique Fédérale de Lausanne, Lausanne, 1015, Switzerland
[2] Engineering Mechanics of Soft Interfaces, School of Engineering, Ecole Polytechnique Fédérale de Lausanne, Lausanne, 1015, Switzerland
tomas.fullana@epfl.ch

Drops exhibit fascinating rebound behavior when interacting with superhydrophilic solid surfaces, such as atomically smooth mica sheets [1]. Experimental observations show that drop bouncing occurs without the drop ever touching the solid and there is a nanometer-scale film of air that separates the liquid and solid. At touchdown, the drop experiences both primary and secondary reaction forces, strongly influencing its deformation and subsequent jump-off mechanism [2]. In the case of a vibrating stage, the drop can either remain in a 'bound' state, that will eventually lead to contact, or enter a sustained 'bouncing' state triggering harmonic oscillations. We investigate the bouncing and period-doubling thresholds up until chaos for varying accelerations γ/g, with γ the peak stage acceleration, and vibration numbers $2\pi f/\sqrt{\sigma/\rho R^3}$ corresponding to the ratio between the forcing frequency and the characteristic drop oscillation frequency. We use the free software basilisk [3] to solve the two-phase Navier-Stokes equations in an axisymmetric formulation by the Volume-Of-Fluid method on quadtree adaptive meshes. The numerical results demonstrate a remarkable agreement with experimental observations, facilitating a comprehensive exploration of the system's dynamics and allowing us to extend the regime diagram of previous work on a similar setup [4]. Extracting the coefficient of restitution C_R and the characteristic 'contact-time' τ_C, we are able to cast a simplified nonlinear spring model that accurately predicts the drop center oscillation for any given set of parameters. The exact nonlinearities pertaining to this reduced-order model are compared to those deduced from the application of a state-of-the-art data-driven learned model.

References

1. J. M. Kolinski, L. Mahadevan & S. M. Rubinstein, *Europhys. Lett.*, **108**, 24001 (2014).
2. B. Zhang, V. Sanjay, S. Shi, Y. Zhao, C. Lv, X.-Q. Feng & D. Lohse, *Phys. Rev. Lett.*, **129**, 104501 (2022).
3. S. Popinet, *J. Comput. Phys.*, **190(2)**, 572-600 (2003).
4. J. Moláček & J. Bush, *J. Fluid Mech.*, **727**, 582-611 (2013).

Large-scale turbulent pressure fluctuations revealed by Ned Kahn's artwork

Jishen Zhang, Stéphane Perrard

Physique et Mécanique des Milieux Hétérogènes, ESPCI, Paris 6, UMR CNRS 7635, 75231 Paris cedex 5, France
jishen.zhang@espci.fr

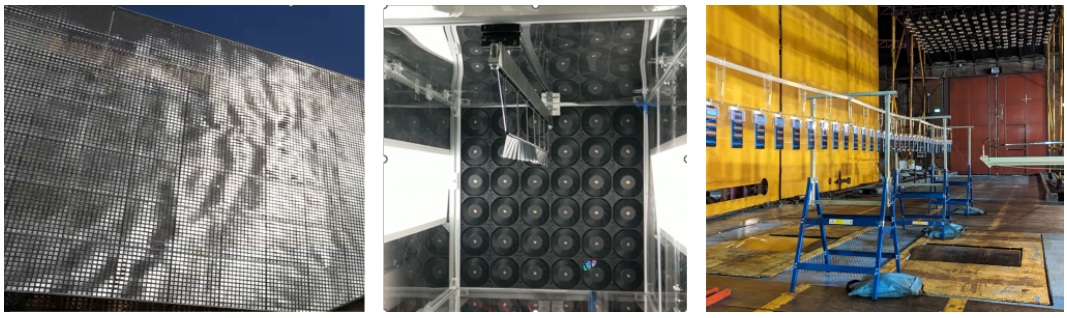

Figure 1. (left) One of Ned Kahn's kinetic facade exhibits, wave like patterns can be seen. (middle) Photography of our 1-dimensional chain of pendulums located at the center of the wind tunnel's test section. (right) large scale chain of telephones measurements in IAT wind tunnel.

Ned Kahn is an American artist who has implemented numerous exhibits inspired by the ephemeral nature. Amongst his works is the kinetic facade, which is composed of a matrix of small aluminium plates that cover facades of buildings. As the wind blows over the wall, the plates oscillate freely creating some wave-like large scale patterns (Fig. 1 (left)), that could be either wind generated waves [1], or the signature of turbulent pressure fluctuations [2].

To unravel the physical origin of these deformations, we designed in a wind tunnel a one-dimensional chain of coupled pendulum in a reduced version composed of rectangular plastic thin plates. We use fine nylon fishing wires to achieve a weak coupling between plates. In the absence of wind, the dispersion relation of the chain oscillatory motions follows the theoretical prediction (discrete sine-Gordon equation):

$$\omega_0^2 = \omega_p^2 + 4\omega_w^2 \sin^2\left(\frac{kW}{2}\right), \tag{1}$$

Where ω_p denotes the natural frequency of a single pendulum, ω_w the elastic coupling frequency and W the distance between two plates. At the laboratory scale under the wind action, the dynamical response is either dominated by a resonance phenomenon, or a linear response to pressure fluctuations. From amateur video analysis on large-scale kinetic facades, we show that the plate oscillation is driven by the same resonant response mechanisms and the apparent wavy pattern corresponds to the most energetic Fourier mode propagating at the advection speed of pressure fluctuations. To better characterize the large scale turbulence, we have equally fabricated a large-scale chain of pendulums of 10 meters using smartphone embedded accelerometers and we have performed long measurements in the IAT large aerodynamic wind tunnel.

References

1. M. J. Shelley & J. Zhang, Flapping and bending bodies interacting with fluid flows, *Annu. Rev. Fluid Mech.*, **43**, 449–465, (2011).
2. S. Perrard, A. Lozano-Duran, M. Rabaud, M. Benzaquen & F. Moisy, Turbulent windprint on a liquid surface, *J. Fluid. Mech.*, **873**, 1020–1054(2019).

Couche limite turbulente sur réseaux logarithmiques

Adrien Lopez[1], Amaury Barral[1], Guillaume Costa[1], Quentin Pikeroen[1], Bérengère Dubrulle[1], Anne-Laure Dalibard[2]

[1] Université Paris-Saclay, CEA, CNRS, SPEC, 91191 Gif-sur-Yvette, France
[2] Laboratoire Jacques-Louis Lions, Sorbonne Université, 75252 Paris, France
adrien.lopez@cea.fr

Introduite en 2019 [1], la méthode des réseaux logarithmiques est un modèle idéalisé pour simuler les fluides dans un régime de turbulence développée, apparentée à une généralisation multidimensionnel des modèles en couche. Elle consiste en un échantillonement exponentiel des modes de Fourier, permettant d'économiser la mémoire, le temps de calcul et d'atteindre des valeurs de paramètres astronomiques ou géophysiques. Telle qu'elle a été formulée à l'origine, la méthode accomode difficilement les conditions aux bords, qui sont indispensables pour une modélisation géophysique fidèle. En effet, la formulation est purement spectrale et le lien avec l'espace réel est compromis par la décimation des modes. Dans la continutation de [1], nous proposons une méthode alternative pour implémenter ces conditions aux bords. Nous nous restreindrons à des bords plans. Afin de préserver la structure du produit de convolution, nous utilisons également une méthode des images qui impose un choix de modes par symmétrie. Pour imposer les conditions souhaitées, nous avons choisi de modifier le Laplacien numérique par un changement de base. Ainsi, nous arrivons maintenant à implémenter des conditions de glissement avec friction, dites de Navier, utiles pour modéliser des surfaces rugueuses et des conditions de Robin pour les champs scalaires.

Nous présenterons le résultats de simulations donnant des lois d'échelle obtenues dans un écoulement bidimensionnel forcé à la Poiseuille. En particulier nous étudierons s'il y a un changement de régime autour d'une valeur critique du frottement de Navier comme suggéré par les équations de Prandtl.

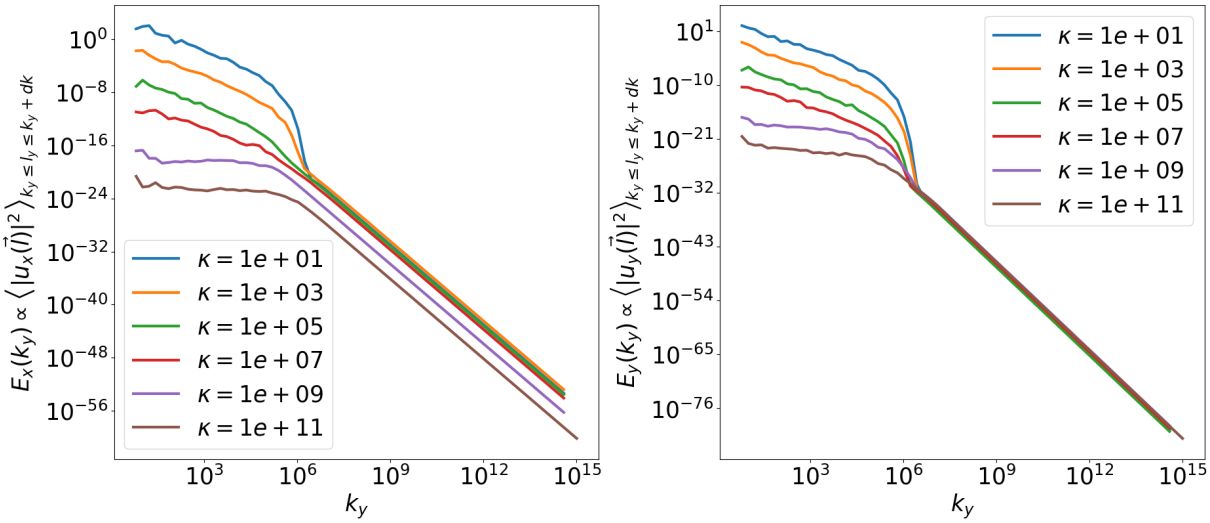

Figure 1. Spectres d'énergie (renormalisés) moyenné sur la direction parallèle au bord pour un écoulement bidimensionnel forcé à $\mathrm{Re} = 10^{10}$ avec des conditions de Navier avec le coefficient de friction κ.

Références

1. C. S. Campolina, *Fluid Flows and Boundaries on Logarithmic Lattices*, Instituto de Matemática Pura e Aplicada—IMPA (2022)

Suppression of wall modes in rapidly rotating Rayleigh–Bénard convection

Louise Terrien[1], Benjamin Favier[1], Edgar Knobloch[2]

[1] Aix Marseille Univ, CNRS, Centrale Marseille, IRPHE, Marseille, France
[2] Department of Physics, University of California at Berkeley, Berkeley, California 94720, USA
louise.terrien@univ-amu.fr

Studying heat transport in rapidly rotating Rayleigh–Bénard convection is of major importance for geophysical flows. In order to make laboratory measurements of the bulk heat flux in the geostrophic turbulence regime, experiments are performed in tall (to increase to Rayleigh number) and thin (to avoid centrifugal effects) cylinders. However, robust wall modes localized at the vertical boundaries develop [1,2] and perturb the measurement of the heat flux which can represent 60% of the total heat flux. These modes are very robust to perturbations of the overall shape of the container [3] which might be due to their topological origin. We show that adding narrow horizontal fins on the vertical walls allows us to reduce sufficiently the contribution of the wall modes heat flux making it negligible compared to the bulk heat flux in the geostrophic turbulence regime [4] .

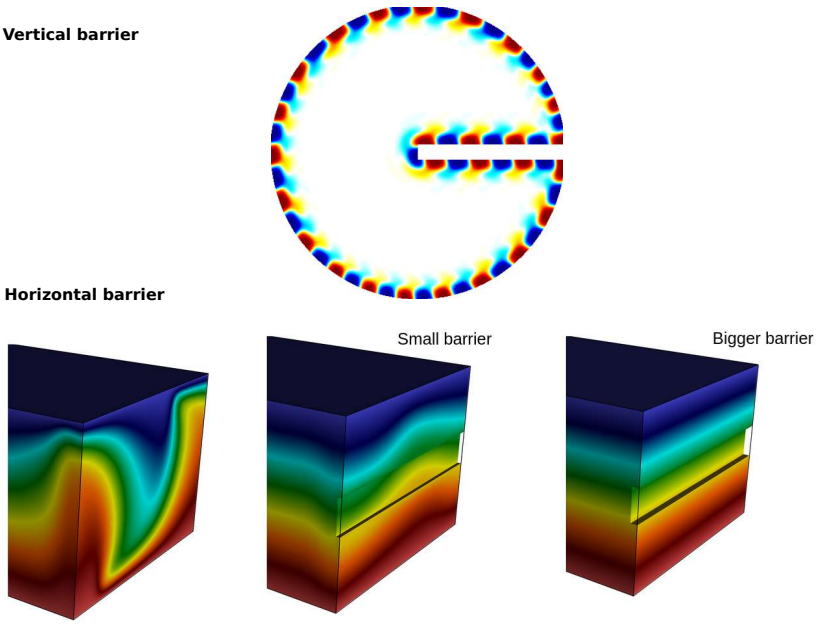

References

1. X. Zhang, R. E. Ecke & O. Shishkina, *J. Fluid Mech.*, **915**, A62 (2021).
2. B. Favier & E. Knobloch, *J. Fluid Mech.*, **895**, R1 (2020).
3. F. Zhang & J.-H. Xie, Submitted (2023).
4. L. Terrien, B. Favier & E. Knobloch, *Phys. Rev. Lett.*, **130** , 174002 (2023).

Transmission anormale d'une onde acoustique à travers un choc faible

Ronan Delalande[1,2], François Coulouvrat[1]

[1] Sorbonne Université, Institut Jean le Rond d'Alembert, CNRS, 4 place Jussieu, 75005 Paris France
[2] Arts et Metiers Institute of Technology, CNAM, PIMM, HESAM University, F-75013 Paris, France
francois.coulouvrat@sorbonne-universite.fr

Au milieu du XXème siècle, J. M.Burgers [1] puis J. Brillouin [2] se sont intéressés à l'interaction entre une onde de choc et une onde acoustique dans un fluide en considérant une incidence normale. Différentes études, par exemple McKenzie et Westphal [3], ont par la suite étendu le modèle au cas de l'incidence oblique. Ces travaux sont à la base des modèles de stabilité des chocs aérodynamiques. Toutefois, jusqu'à présent, seul le cas des ondes de chocs fortes a été analysé, avec des nombres de Mach acoustiques proches de l'unité, voire bien au-delà. Dans la présente étude, nous examinons le cas de l'interaction non linéaire entre un choc faible et une onde acoustique linéaire contra-propagative, en incidence oblique (figure 1).

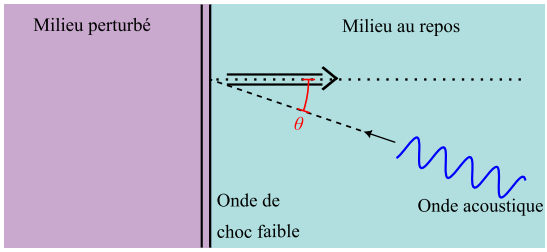

Figure 1. Interaction entre un choc faible et une onde acoustique contra-propagative sous une incidence θ

Une telle configuration interdit l'existence d'ondes réfléchies sur le choc, ce dernier se propageant à vitesse supersonique vis-à-vis du milieu au repos. L'interaction peut toutefois aboutir à la génération de modes de vorticité et d'entropie dans le milieu perturbé, auxquels s'ajoute l'onde acoustique transmise. L'onde acoustique incidente perturbe également le choc lui-même. Les relations de Rankine–Hugoniot permettent de déterminer les amplitudes des ces quatre modes. La conservation du nombre d'onde tangent au choc détermine la direction de l'onde transmise et l'amplitude de l'effet Doppler. L'ensemble est gouverné par l'amplitude du choc, l'angle d'incidence et les paramètres caractérisant la non-linéarité de l'équation d'état du milieu. Les cas particuliers de l'eau et de l'air sont considérés, aboutissant en indicence normale à des comportement opposés. Pour l'air, l'onde acoustique pompe de l'énergie au choc, alors qu'elle en cède pour l'eau. En incidence oblique, on observe plusieurs régimes de transmission anormaux, n'existant pas en régime acoustique. Dans certains cas la vitesse de phase de l'onde transmise s'inverse, celle-ci se propageant alors dans la même direction que le choc. Qualitativement, certaines de ces observations sont en accord avec des expériences préliminaires quantifiant le phénomène dans le cas des solides [4].

Références

1. J. M. Burgers, On the transmission of sound waves through a shock wave, *Selected Papers of J. M. Burgers* (1995).
2. J. Brillouin, Réflexion et refraction d'ondes acoustiques par une onde de choc, *Acta Acust. United Ac.*, **5**, 149–163 (1955).
3. J. F. McKenzie & K. O. Westphal, Interaction of linear waves with oblique shock waves, *Phys. Fluids*, **11**, 2350–2362 (1968).
4. M. Ducousso *et al.*, Bulk probing of shock wave spatial distribution in opaque solids by ultrasonic interaction, *Physic. Rev. Appl.*, **15**, L051002 (2021).

Champs multifractals : construction et déconstruction

Samy Lakhal[1,2,3,6], Laurent Ponson[2], Michael Benzaquen[1,3,4], Jean-Philippe Bouchaud[3,4,5], Mahesh M. Bandi[6]

[1] LadHyX, UMR CNRS 7646, Ecole Polytechnique, 91128 Palaiseau Cedex, France
[2] Institut Jean Le Rond d'Alembert, UMR CNRS 7190, Sorbonne Université, 75005 Paris, France
[3] Chair of EconophysiX & Complex Systems, Ecole Polytechnique, 91128 Palaiseau Cedex, France
[4] Capital Fund Management, 23 rue de l'Université, 75007 Paris, France
[5] Académie des Sciences, Quai de Conti, 75006 Paris, France
[6] Nonlinear and Non-equilibrium Physics Unit, OIST Graduate University, Onna, Japon
samy-lakhal@oist.jp

De nombreux systèmes naturels, sociaux et physiques peuvent manifester des régimes invariants d'échelle. Dans le cas de systèmes linéaires décrits par des observables physiques, cette *fractalité* et les exposants la décrivant peuvent se déduire par analyse harmonique ou stochastique. Cependant dans un cas non linéaire, des interactions inter-échelles peuvent mener à l'apparition inattendue de tels régimes fractals, voire multifractals si leur invariance est décrite par un spectre continu d'exposants. Ces régimes sont souvent caractérisés par *(i)* leurs statistiques non gaussiennes et intermittentes, *(ii)* l'auto-similarité de leurs fonctions de structure et (iii) la forte corrélation spatiale ou temporelle de l'enveloppe de leurs fluctuations [1].

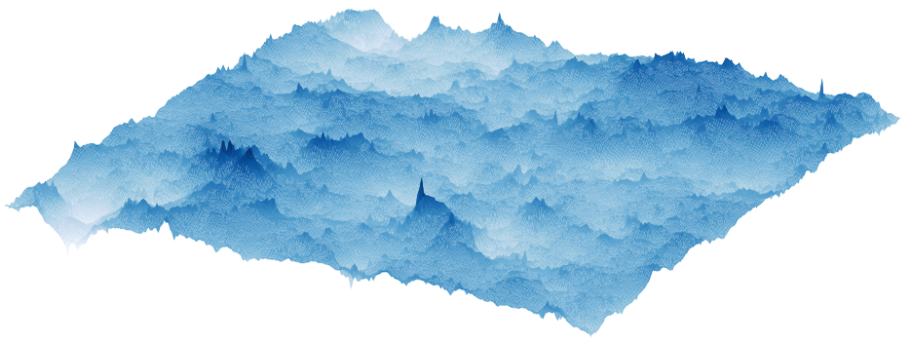

Figure 1. Surface multifractale synthétique

Nous proposons une méthode de construction de champs multifractals reproduisant les principales propriétés observées dans les données expérimentales [2] (e.g. Fig. 1). Appliquée inversement, notre méthode permet la déconstruction des signaux expérimentaux en champs stationnaires décrivant l'amplitude locale des fluctuations. Nous illustrons cette méthode par l'analyse de deux types de signaux : (i) le champs des hauteurs des surfaces de rupture, et (ii) les relevés de vitesse du vent, récemment employés dans l'analyse statistique de la puissance produite par les énergies éoliennes [3]. La comparaison entre données synthétiques et expérimentales révèle des différences fondamentales dans l'organisation spatiale et temporelle de l'intermittence statistique.

Références

1. E. Bacry, J. Delour & J. Muzy, Multifractal random walk, *Phys. Rev. E*, **64**, 026103 (2001).
2. S. Lakhal, L. Ponson, M. Benzaquen & J.-P. Bouchaud, Wrapping and unwrapping multifractal fields, arXiv:2310.01927 (2023).
3. M. Bandi, Spectrum of wind power fluctuations, *Phys. Rev. Lett.*. **118**, 028301, (2017).

Island myriads in periodic potentials

Matheus Lazarotto[1,2], Iberê Caldas[2], Yves Elskens[1]

[1] Aix-Marseille Université, CNRS, UMR 7345 PIIM, F-13397, Marseille cedex 13, France
[2] Instituto de Física, Universidade de São Paulo, Rua do Matão 1371, São Paulo 05508-090, Brazil
matheus_jean_l@hotmail.com

A phenomenon of emergence of stability islands in phase-space was identified for two periodic potentials with tiling symmetries, one square and other hexagonal, as inspired by bidimensional Hamiltonian models of optical lattices. The structures found, here named as island myriads, resemble web-tori with notable fractality and arise at energy levels reaching that of unstable equilibrium points 1. In general, the myriad is an arrangement of concentric island chains with properties relying on the translational and rotational symmetries of the potential functions [1, 2]. In the square system, orbits within the myriad come in isochronous pairs and can have different periodic closure, either returning to their initial position or jumping to identical sites in neighbor cells of the lattice, therefore impacting transport properties. As seen when compared to the generic case, i.e. the rectangular lattice, the breaking of square symmetry disrupts the myriad even for small deviations from its equilateral configuration. For the hexagonal case, the myriad was found but in attenuated form, mostly due to extra instabilities in the potential surface that prevent the stabilization of orbits forming the chains.

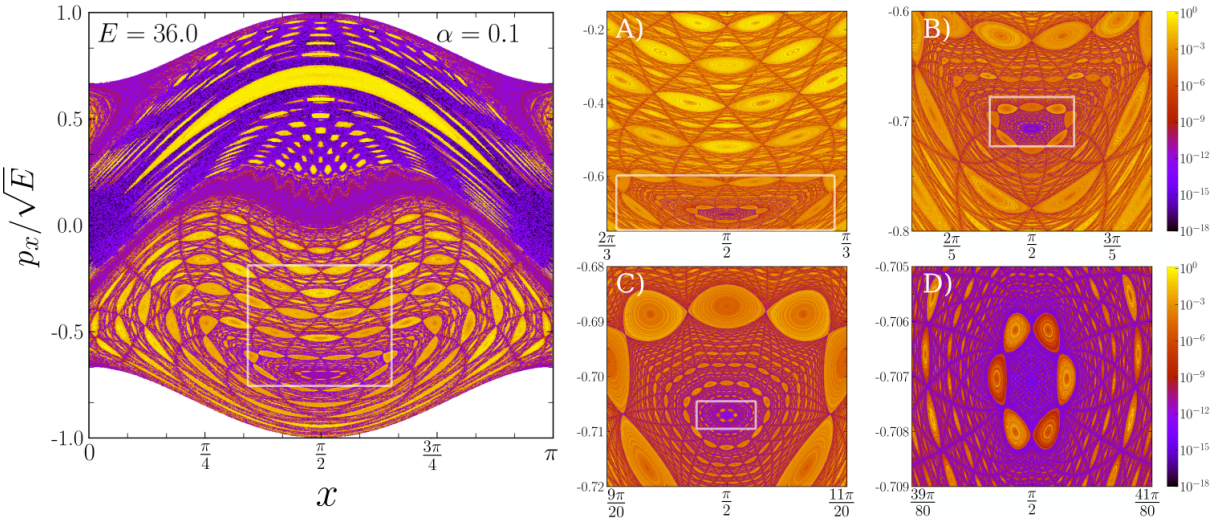

Figure 1. Colorized phase-space showing the island myriad and successive zooms (white rectangles) into the myriad core.

References

1. M. Lazarotto, I. Caldas & Y. Elskens, Diffusion transitions in a 2D periodic lattice, *Commun. Nonlinear Sci. Numer. Simul.*, **112**, 106525 (2022).
2. M. Lazarotto, I. Caldas & Y. Elskens, Island myriads in periodic potentials, ArXiV:2311.04227 (2023).

Enstrophy conditioned extreme-event statistics and their morphology

Benjamin Musci[1], Jean Le Bris[1], Adam Cheminet[1], Christophe Cuvier[2], Pierre Bragança[2], Cécile Wiertel–Gasquet[1], Bérengère Dubrulle[1]

[1] SPHYNX Lab, CEA-Saclay, 91191 Gif-sur-Yvette
[2] LMFL, Centrale Lille, 59655 Villeneuve d'Ascq
benjamin.musci@cea.fr

A key problem in our understanding of turbulence is the existence of the so-called dissipative anomaly [1, 2]. One possible explanation to this could be the existence of quasi-singularities (or extreme-events) in the flow, which are able to dissipate energy inertially, near or below the Kolmogrov scale [1]. Mathematicians also link the possible existence of these singularities in the equations of motion to the violent phenomenon of "spontaneous stochasticity" [1]. However, to date, there is no experimental demonstration of this phenomenon, nor any proof of its link with singularities or quasi-singularities.

This work aims to help fill this void with state-of-the-art experimental results from the Giant-von-Kármán (GvK) facility at CEA Paris-Saclay [3]. The resulting data covers a range of Reynolds number (6,000–150,000) at resolved scales rarely reached in experimental flows (down to 1/4 Kolmogorov). By performing 4D Particle Tracking Velocimetry at these very high spatial resolutions, the time-resolved velocity fields are used to better understand the occurrence of extreme events in turbulence, both statistically and instantaneously. The fine resolution achieved in this work is crucial for helping to better answer the elusive description of the smallest scales in turbulent flows.

We statistically investigate the amplification of vorticity gradients occurring during intermittent extreme events. By conditioning these statistics using enstrophy, we allow for a better understanding of the vortex stretching mechanisms specifically in those regions where intermittency occurs, and exclude quiescent regions [4]. Additionally, we re-investigate the possible universality of the alignment of vorticity vector with the intermediate strain-rate eigenvector [5].

This work also investigates individual extreme-event morphologies to better understand amplification processes in such events. The identification of an event in time and space allows for the tracking of this event spatio-temporally. With this tracking, the changing alignment of the strain and vorticity vectors can be used to answer questions about extreme-event generation and enstrophy production.

References

1. B. Dubrulle, Beyond Kolmogorov cascades, *J. Fluid Mech.*, **867**, P1 (2019).
2. B. Pearson, P.-A. Krogstad & W. van de Water, Measurements of the turbulent energy dissipation rate, *Phys. Fluids*, **14**, 1288–1290 (2002).
3. A. Cheminet *et al.*, Eulerian vs Lagrangian irreversibility in an experimental turbulent swirling flow, *Phys. Rev. Lett.*, **129**, 124501 (2022).
4. D. Buaria & A. Pumir, Nonlocal amplification of intense vorticity in turbulent flows, *Phys. Rev. Res.*, **3**, L042020 (2021).
5. A. Pumir, H. Xu & E. D. Siggia, Small-scale anisotropy in turbulent boundary layers, *J. Fluid Mech.*, **804**, 5–23 (2016).

An experimental analogue of moist convection

Valentin Dorel[1], Daniel Lecoanet[2], Michael Le Bars[1]

[1] CNRS, Aix Marseille Univ., Centrale Marseille, IRPHE, Marseille, France
[2] Department of Engineering Sciences and Applied Mathematics & CIERA, Northwestern University, Evanston, IL 60208, USA
valentin.dorel@univ-amu.fr

Large scale motions of the lower part of the atmosphere (the troposphere) are partly due to moist convection. In this type of convection, the source of buoyancy is the latent heat released by condensation of water droplets. This type of convection is very different from the classical Rayleigh-Bénard case: the heating is internal and associated to a saturation threshold. Strong and localised updrafts appear whereas downdrafts are slow and more diffuse [1]. A correct parametrisation of the lateral scales associated to moist convection is one of the key ingredients for correct mid and long term climate forecasts.

Yet, the full dynamic of such a complex system is barely accessible to 3D direct numerical simulations in large aspect ratio domains. We built an experimental analogue of moist convection to identify the important physical processes behind these complex atmospheric motions.

Inspired by the simple model of moist convection derived by Vallis et al. [2] and the experimental study of conditional instability by Krishnamurti [3] we reproduced the key ingredients of moist convection in the laboratory. Our experimental setup is a rectangular tank filled with water, stratified in temperature. A pH indicator (bromothymol blue) is dissolved, it is yellow at low pH and blue at high pH. A DC power supply applies a constant voltage between the copper plate at the bottom and the grid of stainless steel wire at the top. This voltage induces the water electrolysis at both electrodes: the water close to the top one becomes more acidic and the water close to the bottom one becomes basic hence blue. A sodium lamp placed at the top heats internally the basic (blue) fluid which rises in the stratified ambient because of buoyancy. Simultaneously it mixes, dilutes, becomes more acid, and turns yellow once pH becomes lower than a given threshold around 7. Hence the main ingredients of moist convection, including internal heating, the competition between mixing and increasing buoyancy, and the existence of a threshold in buoyancy production, are reproduced.

The analytical modelling of our system shows the similarities between our setup and the moist convection model of Vallis *et al.* [2] The system is also studied with linear stability analysis and direct numerical simulations using the pseudospectral solver Dedalus [4].

References

1. O. Pauluis & J. Schumacher, Self-aggregation of clouds in conditionally unstable moist convection, *Proc. Natl. Acad. Sci.* **108**, 12623–12628 (2011).
2. G. K. Vallis *et al.*, A simple system for moist convection: the Rainy–Bénard model, *J. Fluid Mech.*, **862**, 162–199 (2019).
3. R. Krishnamurti, Convection induced by selective absorption of radiation: a laboratory model of conditional instability, *Dyn. Atmos. Oceans*, **27**, 367–382 (1996).
4. K. J. Burns *et al.*, Dedalus: A flexible framework for numerical simulations with spectral methods, *Phys. Rev. Res.*, **2**, 023068 (2020).

Dynamique d'une goutte sur fibre verticale texturée

Léonard Matteo, Van Hulle Joséphine, Vandewalle Nicolas

GRASP, Université de Liège, Belgique
matteo.leonard@uliege.be

L'eau est un enjeu majeur de ce siècle. Dans les situations où elle se fait rare, la Nature nous surprend par la diversité des solutions qu'elle met en œuvre. Ainsi, elle s'illustre par le réseau de canyons lilliputiens texturant le dos du lézard *Texas Hornet* [1] ou par la structure multidimensionnelle des épines de cactus [2]. L'homme puise continuellement dans cette source d'inspiration pour innover et relever les défis contemporains.

Dans cette étude [3], nous nous penchons sur la dynamique d'une goutte qui s'enveloppe autour d'une fibre verticale et dévale celle-ci sous l'effet de la gravité. Il s'agit d'une situation que l'on rencontre fréquemment, que ce soit sur une soie d'araignée baignée de rosée ou le long des fibres d'un filet à nuage. Grâce au travail effectué en amont [4], cette recherche introduit une complexité supplémentaire dans le système. Plutôt que de considérer une fibre simple, nous examinons une fibre *texturée*. Pour ce faire, de deux à quatre fibres sont assemblées pour créer un faisceau. Ce dernier peut être assimilé à une fibre composite, unique, dotée d'un nombre précis et équitablement réparti de rainures. Ainsi, il est possible d'ajuster facilement le nombre et la profondeur des rainures en choisissant judicieusement le diamètre et le nombre de fibres composant le faisceau.

Nous vous invitons à découvrir l'interaction entre une goutte et cette nouvelle structure, qui, bien que paraissant simple, dévoile une complexité fascinante. Que ce soit le profil de la goutte, le sillage qu'elle laisse derrière elle ou sa vitesse, toutes ces propriétés pourraient bien réagir de manière surprenante à cette nouvelle texture...

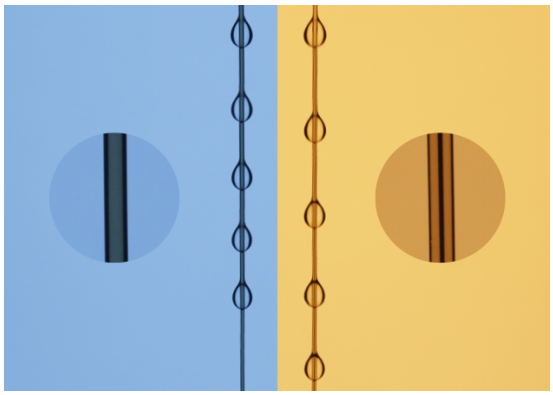

Figure 1. Lorsque l'on maintient le périmètre total d'une fibre tout en introduisant une sous-structure, comme des rainures dans ce cas-ci, cela entraîne une modification de la dynamique de la goutte.

Références

1. P. Comanns *et al.*, *J. Roy. Soc. Interface*, **12**, 415 (2015).
2. J. Ju *et al.*, *Nat. Commun.*, **3**, 1247 (2012).
3. M. Leonard *et al.*, *Phys. Rev. Fluids*, **8**, 103601 (2023).
4. T. Gilet *et al.*, *Eur. Phys. J. E*, **31**, 253–262 (2010).

Réorganisation collective des dipôles dans une magnétostructure

Adrien Wafflard, Eric Opsomer, Nicolas Vandewalle

GRASP, Université de Liège, B5a, Allée du 6 août, 4000 Liège, Belgique
adrien.wafflard@uliege.be

Jouer avec de petits aimants sphériques en néodyme, que l'on peut trouver dans les magasins de jouets, se révèle très addictif. En faisant l'hypothèse qu'elles sont uniformément magnétisées, les billes magnétiques peuvent être assimilées à des dipôles ponctuels. Pour les scientifiques, ces petits objets montrent comment des particules dipolaires s'auto-assemblent en une large variété de structure, depuis les chaînes 1D aux cristaux 3D. On peut montrer que les magnétocristaux et les magnétotubes peuvent changer de géométrie au delà d'un certain rapport d'aspect. Les différents dipôles changent collectivement leurs orientations, modifiant la stabilité mécanique du système entier. Grâce à des simulations numériques et en reproduisant expérimentalement les structures, nous avons identifié les conditions pour lesquelles ces phénomènes se produisent, en particulier pour des tubes.

Références

1. N. Vandewalle & S. Dorbolo Magnetic ghosts and monopoles, *New J. Phys.*, **16** 013050 (2014).
2. A. Wafflard, N. Vandewalle & E. Opsomer, Collective dipole reorganization in magnetostructures, *New J. Phys.*, **25**, 063024 (2023).
3. D. Vella, E. Pontavice, C. L. Halland & A. Goriely, The magneto-elastica: Drom self-buckling to self-assembly, *Proc. Roy. Soc. A*, **470**, 2162 (2014).
4. R. Messina, L. Abou Khalil & I. Stankovic, Self-assembly of magnetic balls: From chains to tubes, *Phys. Rev. E*, **89**, 011202 (2014).

Numerical and experimental direct observation of vortex reconnection in a turbulent swirling flow

Abhishek Harikrishnan[1], Adam Cheminet[1], Damien Geneste[1], Antoine Barlet[1], Christophe Cuvier[2], François Daviaud[1], Jean-Marc Foucaut[2], Jean-Philippe Laval[2], Cécile Wiertel–Gasquet[1], Caroline Nore[3], Melvin Creff[3], Hugues Faller[1], Loïc Cappanera[4], Jean-Luc Guermond[5], Benjamin Musci[1], Jean Le Bris[1], Bérengère Dubrulle[1]

[1] Service de Physique l'Etat Condensé, CEA Saclay, 91191 Gif-sur-Yvette, France
[2] Laboratoire de Mécanique des Fluides de Lille, 59655 Villeneuve d'Ascq, France
[3] Université Paris-Saclay, LISN, CNRS, UMR 9015, France
[4] Dep. of Mathematics, University of Houston, Texas 77204, USA
[5] Dep. of Mathematics, Texas A&M University, Texas 77843, USA
abhishek.harikrishnan@fu-berlin.de

The energy budget for weak solutions of incompressible Navier–Stokes derived by Duchon and Robert [1] has been instrumental in studying local in space, scale and time energy transfers (denoted D_l^I where l is the probed scale) and dissipation (denoted D_l^ν) in turbulent flows. At scales smaller than the Kolmogorov scale η, a downscale (positive) transfer of energy can potentially identify the presence of singularities or quasisingularities within the flow. Dubrulle [2] examined the experimental datasets of the von Kármán flow and linked large values of D_l^I and D_l^ν with coherent structures having a shock-like (or front-like) and spiral-like geometry. Recently, Harikrishnan *et al.* [3] analysed numerical and experimental datasets of the von Kármán flow and showed that strong $|D_l^I|$ events, defined $|D_l^I| > \tau(q = 0.95)$ where τ is a threshold associated with a quantile q, can be seen at the plane of reconnecting vortices.

In this work, we will extend the analysis of Harikrishnan *et al.* [3] to study the links between vortex reconnection and energy transfer. To this end, a tracking technique with region-based correspondence capable of automatically identifying reconnecting pairs of vortices is developed. A change in the order of the components of enstrophy is used as an indicator for vortex reconnection as shown in Fig. 1. This technique is applied to numerical and experimental datasets of the von Kármán flow, the latter of which is performed on a much larger tank thereby allowing for the exploration of scales close and below η.

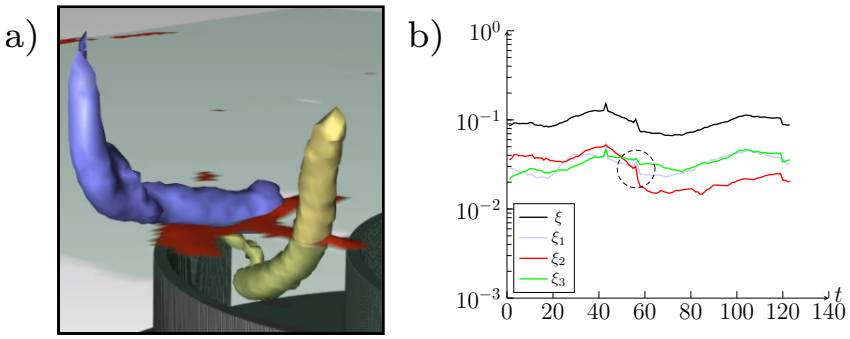

Figure 1. (a) Strong $|D_l^I|$ (red patch) can be seen at the plane of reconnection of the blue and yellow vortex structures. (b) Enstrophy ξ and its components ξ_1, ξ_2, ξ_3 versus time t.

References

1. J. Duchon & R. Robert, *Nonlinearity*, **13**, 1 (2000).
2. B. Dubrulle, *J. Fluid Mech*, **867**, P1 (2019).
3. A. Harikrishnan *et al.*, Tracking singularities: A journey through the scales. *Gallery of fluid motion*, (2022).

Locally varying multifractality underlies intermittent energy dissipation in turbulence

Siddhartha Mukherjee[1,2], Sugan Murugan[2], Ritwik Mukherjee[2], Samriddhi Sankar Ray[2]

[1] Université Côte d'Azur, CNRS, LJAD, Nice 06000, France
[2] International Centre for Theoretical Sciences (ICTS-TIFR), Bengaluru 560089, India
siddhartha.mukherjee@univ-cotedazur.fr

Understanding turbulence rests delicately on the conflict between Kolmogorov's 1941 theory of non-intermittent, space-filling energy dissipation characterised by a unique scaling exponent and the overwhelming evidence to the contrary of intermittency, multiscaling and multifractality. Strangely, multifractality is not typically envisioned as a local flow property, variations in which might be clues exposing inroads into the fundamental unsolved issues of anomalous dissipation and finite time blow-up. Using a simple construction, we show that the multifractal analysis can be fundamentally extended as a tool for educing entire fields of generalized dimensions and fractal measures underlying the energy dissipation field. For instance this allows us, for the first time, to reveal the spatial variation in the correlation dimension across the flow, as seen below in Fig. 1A. By defining a suitable measure $\Phi(\mathbf{x})$ of the spatial variation of multifractality (illustrated in Fig. 1B), we show that this grows logarithmically with the extent to which the energy dissipation varies locally around $\mathbf{x}$. In other words, much of the dissipation field remains surprisingly monofractal à la Kolmogorov, while multifractality appears as small islands in this calm sea. These results suggest new ways to understand how singularities could arise and provide a fresh perspective on anomalous dissipation and intermittency. The simplicity and adaptability of our approach also holds great promise in applications ranging from climate sciences to medical data analysis.

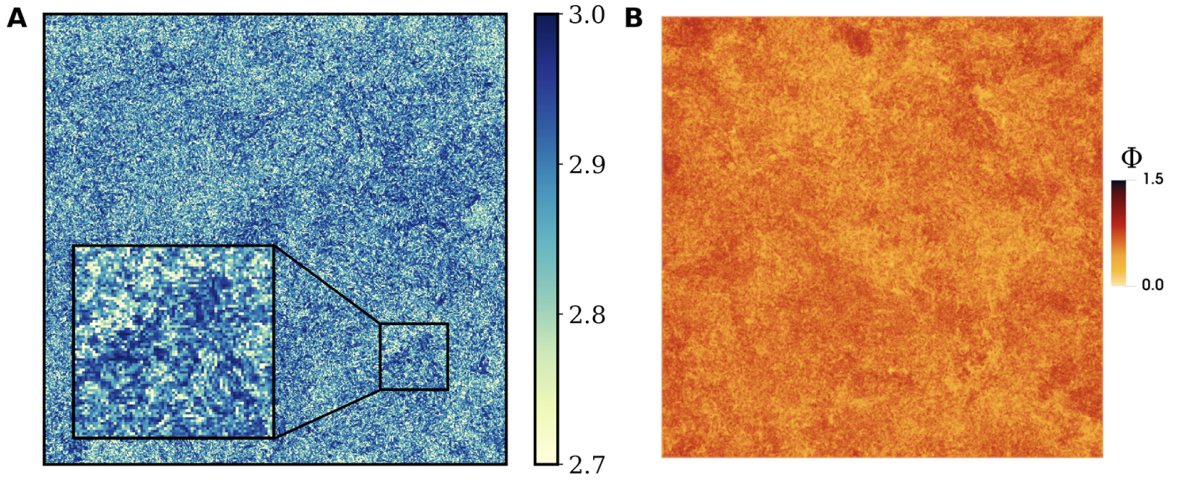

Figure 1. (A) Correlation dimension (D_2) revealed as a field using the local analysis and **(B)** Variation in the degree of multifractality, showing that turbulence is not *uniformly* multifractal.

References

1. S. Mukherjee, S. D. Murugan, R. Mukherjee & S. S. Ray, Turbulent flows are not uniformly multifractal, arXiv:2307.06074 (2023).

Experimental observation of elastic rogue waves

Murukesh Muralidhar[1,2], Antoine Naert[1], Sébastien Aumaître[2]

[1] Laboratoire de Physique, ENS de Lyon, UMR-CNRS 5672, 46 allée d'Italie, 69007 Lyon, France
[2] Service de Physique de l'Etat Condensé, DSM, CEA-Saclay, UMR 3680 CEA-CNRS, 91191 Gif-sur-Yvette, France
murukesh.muralidhar@cea.fr

Rogue waves are exceptionally large & extreme waves that take place in seas and oceans. A more classical definition is, waves with heights exceeding twice the significant height of a given sea state. [1]. These rare, destructive events demand an understanding of their underlying physical mechanism for their prediction, particularly considering their impact on seafaring and structures. This study aims to explore the existence and possibly characterize rogue waves in an analogous system—a thin, elastic stainless steel plate.

The elastic plate adheres to wave turbulence theory, assuming a 4-wave process. Despite analogies to surface waves, differences exist, notably the absence of an inverse cascade in these elastic waves. For waves longer than the plate's thickness, this dispersive media is considered two-dimensional, governed by a dispersion relation: $\omega = \lambda k^2$, with λ as the efficient coefficient measuring the plate's response to external force [2]. A large electromagnetic shaker sustains the plate in a steady state of motion, out of equilibrium. Laser vibrometers are used to measure the displacement and velocity at different points. Questions arise regarding the system's ability to exhibit extreme states and the physical mechanisms involved. Can occurrences be quantified, and are the same mechanisms applicable to ocean waves? Addressing the effect of forcing frequency and amplitude on rogue wave observation is a primary focus. Determining the proper wave description—geometrical or kinematic—is also crucial.

We show the first experimental observation of elastic rogue waves and characterize it. As expected, the spectral density of the displacement signal reveals a slope of -2 for the low frequency regime, lower than the excitation frequency, indicating the equipartition of energy at these frequencies [3]. Interestingly, the occurrence of rogue events is not strictly associated with the highest steepness of the waves, which may seem counter-intuitive. Another intriguing finding is that the asymptotic value of the percentage of occurrence of rogue waves appears independent of the forcing frequency, marking a significant inference. Future work would involve a more comprehensive description of such waves, particularly in terms of energy considerations.

References

1. G. Michel, F. Bonnefoy, G. Ducrozet & E. Falcon, Statistics of rogue waves in isotropic wave fields, *J. Fluid Mech.*, **943**, A26 (2022).
2. S. Nazarenko, *Wave turbulence*, Springer (2011).
3. B. Miquel, A. Naert & S. Aumaître, Low-frequency spectra of bending wave turbulence, *Phys. Rev. E*, **103**, L061001 (2021).

Étude expérimentale de moteurs à information mésoscopiques

Aubin Archambault, Caroline Crauste–Thibierge, Sergio Ciliberto, Ludovic Bellon

Laboratoire de Physique CNRS UMR 5672, ENS de Lyon, 46 allée d'Italie, 69007 Lyon
caroline.crauste @ ens-lyon.fr

Les lois de la thermodynamique usuelles sont robustes et s'appliquent à une vaste gamme de systèmes à l'échelle macroscopique. Cependant dès lors que l'amplitude des fluctuations thermiques devient comparable aux phénomènes étudiés, ces lois ne décrivent plus qu'un comportement moyen.

S'il est macroscopiquement impossible d'extraire de l'énergie des seules fluctuations thermiques, l'exploitation d'une mesure permet d'outrepasser cette limite en adaptant les protocoles utilisés à la réalisation exacte du bruit thermique. Je présenterai ici une réalisation expérimentale de moteurs à information, c'est à dire des cycles monothermes dont l'évolution dépend du résultat d'une mesure sur le système. Ces cycles seront effectués grâce à une particule unique, mésoscopique, qui peut être modélisée comme une particule brownienne évoluant à une dimension selon une dynamique sous-amortie dans un puit de potentiel harmonique. Cette particule est soumise à la fois au bruit thermique et à une force de rétroaction.

Je montrerai qu'il est alors possible d'extraire de l'énergie des fluctuations thermiques, et d'explorer différents régimes en optimisant l'extraction du travail. Ces mesures testent la validité de travaux théoriques récents, et explorent le régime sous-amorti peu étudié car plus complexe à aborder.

Nonlinear interaction of turbulence and energetic particles in tokamak plasmas

Alessandro Biancalani[1], A. Bottino[2], D. Del Sarto[3], M. V. Falessi[4], T. Hayward-Schneider[2], P. Lauber[2], A. Mishchenko[5], B. Rettino[2], J. N. Sama[3], F. Vannini[2], L. Villard[6], X. Wang[2], F. Zonca[4,7].

[1] Léonard de Vinci Pôle Universitaire, Research Center, 92916 Paris La Défense, France
[2] Max-Planck Institute for Plasma Physics, 85748 Garching, Germany
[3] Institut Jean Lamour- UMR 7168, University of Lorraine - BP 239, F-54506 Vandoeuvre les Nancy, France
[4] Center for Nonlinear Plasma Science and ENEA C. R. Frascati, 00044 Frascati, Italy
[5] Max-Planck Institute for Plasma Physics, 17491 Greifswald, Germany
[6] Ecole Polytechnique Fédérale de Lausanne (EPFL), Swiss Plasma Center (SPC), CH-1015 Lausanne, Switzerland
[7] Institute for Fusion Theory and Simulation and Department of Physics, Zhejiang Univ., Hangzhou, China
alessandro.biancalani@devinci.fr

Gradients in the temperature and density profiles, drive drift-waves unstable in tokamak plasmas. These micro-instabilities nonlinearly interact forming turbulence. The mitigation of turbulence is considered an important step towards the achievement of controlled nuclear fusion in magnetic confinement devices. A byproduct of turbulence is the generation of zonal, i.e. axisymmetric, flows (ZF). ZFs are recognized as one of the main mechanisms of turbulence saturation [1]. Energetic particles (EPs), are present in tokamak plasmas due fusion reactions and external heating mechanisms. EP can drive electromagnetic oscillations like unstable Alfvén Modes (AM) [2, 3].

In this work, we show how EPs can indirectly affect turbulence. We consider two mechanisms, both mediated by the EP-driven AMs: (i) the nonlinearly excitation of ZF [4,5]; (ii) the nonlinear modification of the equilibrium profiles [6]. The numerical tool used to perform the numerical simulations is the multispieces electromagnetic gyrokinetic particle-in-cell code ORB5 [3, 7]. This theoretical model paves the way for different points of view on the interpretation of experimental results such as the turbulence reduction in the presence of EPs, in experimentally relevant cases.

References

1. A. Hasegawa, C. G. Maclennan & Y. Kodama, *Phys. Fluids*, **22**, 2122 (1979).
2. K. Appert *et al.*, *Plasma Phys.*, **24**, 1147 (1982).
3. L. Chen & F. Zonca, *Rev. Mod. Phys.*, **88**, 015008 (2016).
4. A. Biancalani *et al.*, *46th EPS Conference on Plasma Physics*, July 8–12 2019, Milan, Italy, I5.J602.
5. J. N. Sama *et al.*, *49th EPS Conference on Plasma Physics*, July 3–8 2023, Bordeaux, France, O4.104.
6. A. Biancalani *et al.*, *J. Plasma Phys.*, **89**, 905890602 (2023).
7. A. Mishchenko *et al.*, *Comp. Phys. Commun.*, **238**, 194 (2019).
8. E. Lanti *et al.*, *Comp. Phys. Commun.*, **251**, 107072 (2020).

Rheology of a particle laden soap film

Jonathan Lalieu, Antoine Seguin, Georges Gauthier

Labo FAST, Université Paris Saclay, Bât 530, Rue André Rivière, 91405 ORSAY
georges.gauthier@universite-paris-saclay.fr

Particle laden interfaces are ubiquitous in industry (e.g. oil recovery, filtration processes, armored drops used as microreactors, or concrete foams) for which interface stabilization effect have to be controlled. Recent studies [1, 2], have shown that mechanical properties of particle-laden films differ from those of single particle laden interface, though the origin of the differences remains unclear. We study experimentally the rheology of a macroscopic particle-laden soap film constituted of slightly polydisperse polystyrene spheres trapped in a single film made of a tetradecyl trimethyl ammonium bromide (TTAB) and glycerol aqueous mixture of the same density as the particles. The particles are larger than the typical film thickness, they cross both interfaces and capillarity gives rise to attractive interactions between the particles. To study the strain-stress relation of such particle laden film, it is stretched in an annular rheometer cell and sheared at imposed velocity, measuring the stress. The strain-stress results are compared with local shear rate measured through image correlation. We show that, at dense particle volume fraction, the granular film exhibits a complex visco-plastic behavior which is largely influenced by interfacial parameters such as surface tension and surface viscosity of the carrying fluid. To account for the non-local rheology of the particle laden soap film, we confront the particle velocity fields to kinetic theory extended to dense granular media [3].

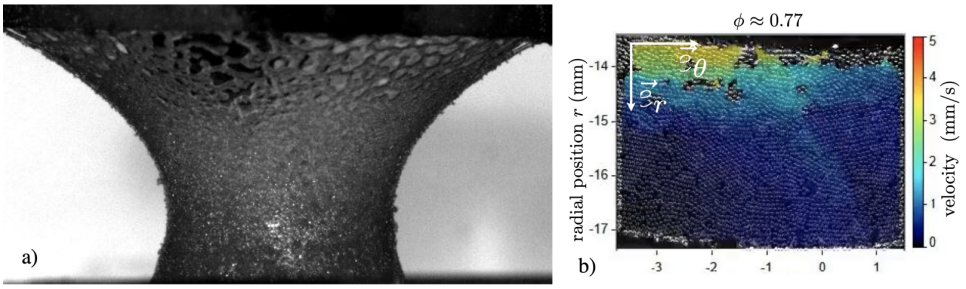

Figure 1. (a) Pinch-off of a granular film. (b) Velocity field of a granular film stretched in the rheometer cell for an imposed velocity Ω0. Hz using DIC software.

References

1. N. Taccoen, F. Lequeux, D. Gunes & C. Baroud, Probing the mechanical strength of an armored bubble and its implication to particle-stabilized foams, *Phys. Rev. X*, **1**, 011010 (2016).
2. Y. Timounay, O. Pitois & F. Rouyer, Gas marbles: much stronger than liquid marbles, *Phys. Rev. Lett.*, **118**, 228001 (2017).
3. W. Losert, L. Bocquet, T. C. Lubensky & J. P. Gollub, Particle dynamics in sheared granular matter, *Phys. Rev. Lett.*, **85**, 1428–1431 (2000).

Un ratchet brownien à l'échelle humaine : une expérience de pensée historique en vrai !

Adrian Meynard, Marc Lagoin, Caroline Crauste–Thibierge, Antoine Naert

ENSL, CNRS, Laboratoire de physique, F-69342 Lyon, France.
antoine.naert@ens-lyon.fr

Nous avons réalisé expérimentalement le célèbre *ratchet* de Feynman, à l'échelle macroscopique. Dans notre système, la rotation d'un objet brownien 1D de 2cm de diamètre dans un gaz granulaire qui joue le rôle d'un thermostat est détectée par un convertisseur électromécanique (dynamo), qui produit une tension proportionnelle à la vitesse angulaire. Le courant généré par cette rotation aléatoire est redressé par un dispositif électronique (démon), de sorte que seul le courant positif passe : c'est du redressement simple alternance. Un travail peut donc être produit. L'avantage de ce dispositif macroscopique est de permettre de mesurer toutes les observables en fonction du temps : la puissance utile (travail), la chaleur extraite du bain, et enfin le rendement du moteur thermique équivalent. La rétroaction permettant la conversion de la chaleur en travail s'exprime comme un biais sur la rotation brownienne. L'observation des opérations du démon lui-même permet d'étudier la chaleur dégagée vers la source froide, ou encore sur le taux de production d'entropie d'information.

Self-propulsion of floating ice blocks by melting

Martin Chaigne[1], Jérôme Jovet[2], Michael Berhanu[1], Amit Dawadi[3], Arshad Kudrolli[3]

[1] Laboratoire Matière et Systèmes Complexes, Université Paris Cité, CNRS, 10, rue Alice Domon et Léonie Duquet, 75013 Paris
[2] UFR Physique, Université Paris Cité, CNRS, 10, rue Alice Domon et Léonie Duquet, 75013 Paris
[3] Department of Physics, Clark University, Worcester, Massachusetts 01610, USA
michael.berhanu@u-paris.fr

The melting of icebergs floating on the ocean is often accompanied by buoyant convection flows [1], as temperature and salinity variations modify locally the water density. Significant gravity driven currents occur thus at the vicinity of iceberg below the water surface. As these currents carry momentum, they can participate to the drift of the iceberg, in addition to the more important contribution of the wind and oceanic currents. Previously, Dorbolo *et al.*related the spinning of floating ice disks to the convection flow driven by melting [2]. However due to the symmetric shape, no propulsion was reported. Then, Mercier *et al.* [3] showed the self-propulsion of a floating asymmetric solid with an embedded local heat source that generates thermal convection.

Recently, we demonstrate that an inclined boat incorporating an inclined plate made of a solute material like salt and sugar can propel more rapidly due to the solutal convection flow driven by the dissolution [4]. Here, we investigate now, the propulsion of asymmetric floating ice blocks. For a water bath at a temperature of about $T_b = 20°$, we report typically propulsion velocity of order 5 mm/s for ice prisms of width about 10 cm with a rectangular triangle base of diagonal about 20 cm. We use a shadowgraph imaging setup to simultaneously track the motion, evaluate the melting rate and visualize the buoyancy convection flow (Fig. 1). A phenomenological model relating the melting rate to the transitional speed explains the magnitude of the reported propulsion velocities.

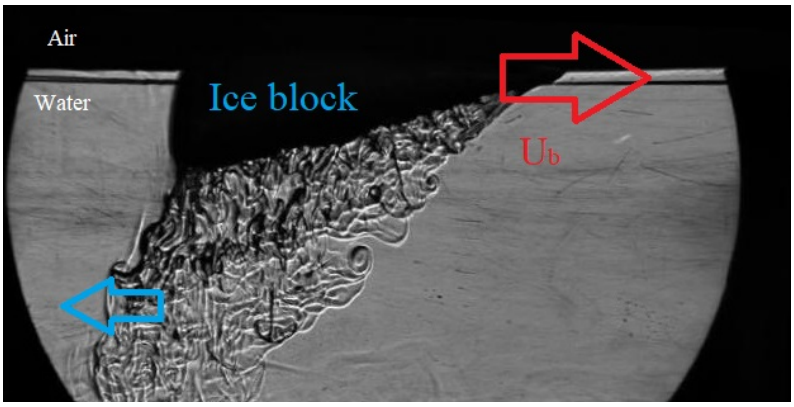

Figure 1. Shadowgraph imaging of a floating ice block (width 9 cm, diagonal 21 cm) during its melting in a bath at $T_b = 20°$. Due to the inclined melting surface, the convection flow is deviated on the left direction. Consequently, the block self-propel at a velocity of 4 mm/s (red arrow).

References

1. C. Cenedese & F. Straneo, Icebergs Melting, *Annu. Rev. Fluid Mech.*, **55**, 377–402 (2022).
2. S. Dorbolo, N. Adami, C. Dubois, H. Caps, N. Vandewalle & B. Darbois-Texier, Rotation of melting ice disks due to melt fluid flow, *Physical Review E*, **93**, 033112 (2016).
3. M. J. Mercier, A. M. Aderkani, M. R. Allshouse, B. Doyle & T. Peacock, Self-propulsion of immersed objects via natural convection, *Phys. Rev. Lett.*, **12**, 204501 (2014).
4. M. Berhanu, M. Chaigne & A. Kudrolli, *Proc. Natl Acad. Sci.*, **120**, e2301947120 (2023).

Impact de la rotation sur l'excitation stochastique des ondes acoustiques

Leïla Bessila[1], Adrien Deckx van Ruys[1,2], Valentin Buriasco[1,3], Stéphane Mathis[1], Lisa Bugnet[4], Rafael García[1], Savita Mathur[5,6]

[1] Université Paris-Saclay, Université Paris Cité, CEA, CNRS, AIM, F-91191, Gif-sur-Yvette, France
[2] Ecole polytechnique, Institut Polytechnique de Paris, Palaiseau, France
[3] ENSTA Paris Tech, Institut Polytechnique de Paris, Palaiseau, France,
[4] Institute of Science and Technology Austria (IST Austria), Am Campus 1, Klosterneuburg, Austria
[5] Instituto de Astrofísica de Canarias (IAC), E-38205, La Laguna, Tenerife, Spain
[6] Universidad de La Laguna (ULL), Departamento de Astrofísica, E-38206 La Laguna, Tenerife, Spain
leila.bessila@cea.fr

Dans les milieux naturels, les ondes acoustiques sont excitées de manière stochastique par les mouvement d'un champ turbulent. Ce phénomène a de nombreuses applications en géophysique et en astrophysique : les ondes acoustiques sont générées dans les régions convectives des astres et apportent des informations sur leurs structures internes. Cependant, l'action de la rotation est négligée dans la plupart des modèles théoriques d'excitation stochastique. La rotation exerce une inflence significative sur la convection turbulente, qui a alors tendance à être inhibée.

Nous présentons un formalisme théorique pour modéliser l'excitation stochastique, qui est applicable à tous types d'ondes en géométrie sphérique. Nous incluons l'impact de la rotation sur la dynamique de l'excitation par la convection turbulente. Nous montrons que les amplitudes des modes diminuent significativement en présence de rotation.

À titre d'illustration, nous examinons le cas d'une étoile similaire au Soleil. Ces résultats s'inscrivent dans la continuité des observations de la mission spatiale *Kepler*, qui ont révélé une absence de signaux des modes acoustiques dans une fraction importante d'étoiles en rotation rapide. Les ondes acoustiques sont pourtant primordiales pour caractériser les étoiles et leurs systèmes planétaires.

Références

1. S. Mathur *et al.*, *Front. Astron. Space Sci.*, **6**, 6–11 (2019).

Surface Quasi-Geostrophy: A Proxy for 3D Turbulence?

Nicolas Valade[1], Simon Thalabard[2], Jérémie Bec[1,2]

[1] Université Côte d'Azur, Inria, CNRS, Calisto team, Sophia Antipolis
[2] Université Côte d'Azur, CNRS, Institut de Physique de Nice
nicolas.valade@inria.fr

The Surface Quasi-Geostrophic equations (SQG), describing the two-dimensional transport of a scalar temperature field θ under strong rotation and stratification, are known to share formal similarities with the incompressible three-dimensional (3D) Navier–Stokes (NS) system [1,3]. The analogy is formally mediated by the scalar gradient, which undergoes stretching $\nabla\theta \cdot \nabla\mathbf{u}$ along Lagrangian trajectories, akin to the vortex stretching $\boldsymbol{\omega} \cdot \nabla\mathbf{u}$ constitutive of 3D-NS. Recent studies [2] have also pointed out that, when subject to suitable large-scale forcing and small-scale dissipation, SQG settles into a statistical steady state displaying hallmark signatures of canonical 3D homogeneous isotropic turbulence.

In essence, the SQG steady-state has finite energy; It is sustained by finite injection and (anomalous) dissipation $\epsilon > 0$ through a direct cascade of kinetic energy associated with an approximate $k^{-5/3}$ power-law scaling, as prescribed by the classical Kolmogorov 1941 theory of turbulence. Here, we present a new series of highly resolved direct numerical simulations of SQG, employing up to $16,384^2$ grid points on a doubly-periodic domain. Our purpose is to expand upon previous observations, and compile the turbulent signatures observed in the forced-dissipated SQG system into a refined statistical phenomenology of SQG turbulence.

On the one hand, our numerics substantiate quantitative statistical similarities between SQG scalars and 3D-NS velocity fields. These include dissipative anomaly, negatively skewed distributions, spatial multiscaling and refined self-similarity. As dissipation vanishes, those features are observed over an increasing (inertial) range of scales delimited on the ultraviolet side by the Taylor scale λ. We argue that λ characterizes the typical size of vortex patches, originating from temperature filaments breaking up into smaller scales due to internal shearing by the underlying turbulent flow.

On the other hand, our work highlights three caveats originating from the specifics of the SQG dynamics, in particular its two-dimensionnal setting and inviscid conservation laws. (i) The analogy between SQG and NS holds, strictly speaking, at the level of the advected SQG scalar field only. While both the scalar and the velocity fields are multifractal, only the SQG scalar field is negatively skewed. (ii) Effects of finite dissipation in SQG are more pronounced than in 3D-NS. (iii) SQG turbulence appears less universal than 3D-NS turbulence, with likely dependence upon injection scheme.

As such, while framed in a 2D setting, SQG shares the essential statistical signatures of 3D turbulence, but, unfortunately, also its numerical challenges.

References

1. P. Constantin, A. J. Majda & E. Tabak,, Formation of strong fronts in the 2-D quasigeostrophic thermal active scalar, *Nonlinearity*, **7**, 1495 (1994).
2. G. Lapeyre, Surface Quasi-Geostrophy, *Fluids*, **2**, 7 (2017).
3. N. Valade, S. Thalabard & J. Bec, Anomalous dissipation and spontaneous stochasticity in deterministic surface quasi-geostrophic Flow, *Ann. Henri Poincaré*, **25**, 1261–1283 (2023).

Pendule de Doubochinski

Danil Doubochinski[1], Cyrille Raquin[2]

[1] QUANTIX, 73 rue de Watignies, Paris
[2] SECURENGY, Huillat, 23170 Auge
c.raquin@securengy.com

Le pendule de Doubochinski permet de valider l'existence de couplages entre des oscillateurs non linéaires avec création de nouveaux états de stabilité dynamique. Ces nouveaux modes oscillatoires ne sont ni forcés, ni paramétriques. Leur utilisation dans le cadre des applications débouche sur d'importantes applications industrielles qui seront présentées devant le poster(table de présentation du pendule et des applications) [1, 2].

Références

1. J. Tennenbaum & D. Doubochinski, A new dynamical conception of physical objects and their interactions, *Quantum Matter*, **4**, 251–257–11 (2015).
2. D. Doubochinski & J. Tennenbaum, The macroscopic quantum effect in non linear oscillating systems, *International Workshop on atomic structure*, 1–19 (2007).

Bubble breakup probability in turbulence

Aliénor Rivière, Stéphane Perrard

PMMH, ESPCI, 10 rue Vauquelin, 75005, Paris
alienor.riviere@espci.fr

Bubbles play a crucial role in mass transport across interfaces. By increasing the surface of exchange they lead chemical and gas transfers in various industrial processes, as homogenizers, and geophysical situations, such as rivers, waterfalls and oceans. Since the gas exchanges are bubble size dependent, predicting breakups is central to first understand the bubble size distribution and then quantify the transfers. In turbulence, bubble fate is controlled by the ratio between inertial and capillary forces, namely, the Weber number, We. Bubbles tend to deform for large We, while they are statistically stable for low We. The limit between these two regimes is defined in a statistical sense as, in theory, any bubble can encounter a large enough pressure fluctuation and break.

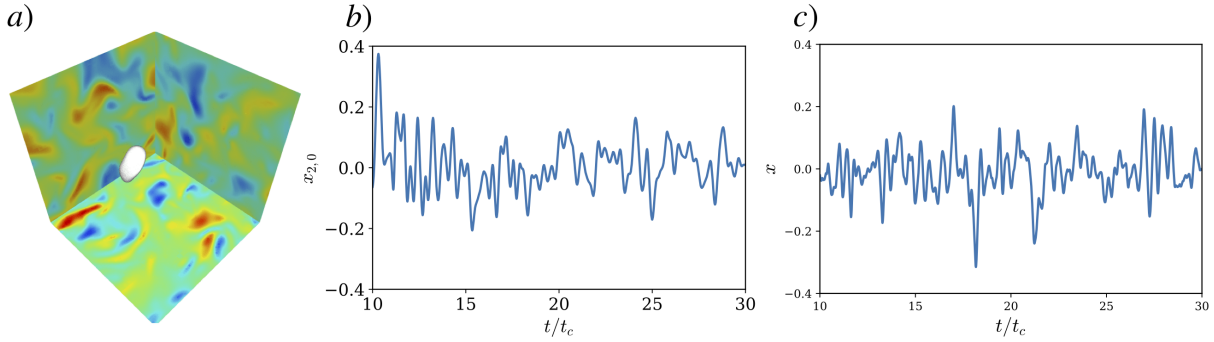

Figure 1. a) Snapshot of a bubble in a turbulent flow. The bubble is in white. The velocity field can be visualized with the three background planes. b) Typical temporal evolution of the mode $(2, 0)$ at $\mathrm{We} = 0.71$ in the DNS. c) Typical temporal evolution given by our reduced linear model for the same Weber number.

Using direct numerical simulations (DNS) of a single bubble in an homogeneous and isotropic turbulent flow, we quantify the probability that a bubble breaks within a time window by modeling bubble deformations. We decompose the bubble surface onto the spherical harmonics base and show that each mode stochastic dynamics can be well described by a damped linear oscillator randomly forced by turbulence. We measure the values of the natural frequency and the damping factor, together with the statistical properties of the stochastic forcing. Then, by simulating these reduced dynamics for the five most relevant bubble modes, corresponding to oblate-prolate oscillations, we show that bubble breakup in turbulence is a memoryless process. The associated breakup rate varies exponentially with We^{-1} suggesting a mechanism of random activation process, which has been similarly observed in drop breakups [1]. Eventually, we find a quantitative agreement between our predicted breakup rate and several experimental datasets on bubble breakups. Our model can then be used to quantify the probability for a bubble to break, in homogeneous turbulence as well as in more realistic turbulent flows, which are non stationary and inhomogeneous.

References

1. A. Vela-Martín & M. Avila, Memoryless drop breakup in turbulence, *Sci. Adv.*, **8**, p.eabp9561 (2022).

Inertia-gravity waves, a canonical example of nonlinear eigenvalue problems

Jérémie Vidal[1], Yves Colin de Verdière[2]

Université Grenoble Alpes, CNRS, ISTerre, 38000 Grenoble, France
Université Grenoble Alpes, CNRS, Institut Fourier, 38000 Grenoble, France
jeremie.vidal@univ-grenoble-alpes.fr

Global rotation and density stratification are ubiquitous in natural systems (e.g. in the Earth's oceans and atmosphere, in fluid planetary interiors or in stars). Consequently, geophysical flows are often shaped by the action of the so-called inertia-gravity waves (IGWs). From a mathematical viewpoint, IGWs offer a canonical example to investigate the physics of quadratic eigenvalue problems (QEP) of the form [1]

$$\lambda^2 \boldsymbol{u} + \lambda \mathcal{A}(\boldsymbol{u}) + \mathcal{B}(\boldsymbol{u}) = \boldsymbol{0},$$

where $[\mathcal{A}, \mathcal{B}]$ are two linear operators with specific symmetries, and with the eigenvalue $\lambda \in \mathbb{C}$. Here, we study the properties of IGWs that can exist in pancake-like stratified vortices, which are often generated by turbulence in geophysical environments. Typical applications are oceanic eddies (e.g. the Meddies) or Jovian vortices (e.g. the Great Red Spot in Jupiter). We consider a fluid enclosed within a rigid triaxial ellipsoid, which is stratified in density with a constant Brunt-Väisälä frequency (using the Boussinesq approximation) and uniformly rotating along a (possibly) tilted axis with respect to gravity. Despite the corresponding QEP is generically is an ill-posed Cauchy problem, we find that the spectrum is pure point in ellipsoids (i.e. only consists of eigenvalues) with smooth polynomial eigenvectors. Then, we fully characterise the spectrum using numerical calculations and microlocal analysis [3, 4]. In addition to the usual IGWs (which exist in unbounded fluids), we report the existence of gravito-inertial (surface) waves whose energy is maximum near the boundary. These waves appear similar to the Kelvin waves in oceanography [5], and we show that they owe their existence to a non-trivial mathematical property satisfied by the pressure on the boundary [6]. Finally, we aim to explore whether parametric instabilities (e.g. the elliptical instability or the triadic resonant instability), which are also governed by a QEP in the linear theory, could sustain a transition towards (wave) turbulence in such stratified vortices.

References

1. E. M. Barston, *J. Math. Phys.*, **8**, 523–532 (1967).
2. S. Vantieghem, *Proc. R. Soc. A*, **470**, 20140093 (2014).
3. J. Vidal & Y. Colin de Verdière, *Proc. R. Soc. A*, In press (2024).
4. Y. Colin de Verdière & J. Vidal, *J. Spectr. Theory*, ArXiv:2305.01369 (2024).
5. W. Thomson, *Proc. R. Soc. Edinburgh*, **10**, 92–100 (1880).
6. Y. Colin de Verdière & J. Vidal, *J. Contemp. Math*, Preprint (2024).

Formation de film continu et homogène par coalescence de gouttes

Antoine Bouvier[1,2], Étienne Reyssat[1], José Bico[1], Barbara Bouteille[2], Jérémie Teisseire[2]

[1] Laboratoire de Physique et Mécanique des Milieux Hétérogènes, PMMH UMR 7636 CNRS, ESPCI Paris, PSL, Sorbonne Université, Université Paris Cité, 7 Quai Saint-Bernard, 75005, Paris
[2] Saint-Gobain Research Paris, 39 Quai Lucien Lefranc, 93300 Aubervilliers
antoine.bouvier@espci.fr

Recouvrir une surface par un film initialement liquide est très important en industrie car cela permet de protéger ou de fonctionnaliser des surfaces. Ces films peuvent être obtenus par coalescence de gouttes déposées avec un spray ou par impression jet d'encre. Dans un spray, les gouttes sont distribuées en taille et en position [1] tandis que l'impression jet d'encre permet un grand contrôle du dépôt de chaque goutte [2]. La coalescence a déjà été largement étudiée dans le cas de deux gouttes sessiles [3,4]. Toutefois, les mécanismes impliquant plus de gouttes restent une question ouverte. Toutes les gouttes doivent fusionner pour obtenir un film continu et éviter la présence de trous ou de défauts. Nous présentons ici des expériences modèles de coalescence réalisées avec un petit nombre de gouttes. Un montage expérimental a été conçu pour déposer automatiquement des gouttes de glycérol sur une plaque de verre selon des motifs précis. La figure 1 montre un dépôt de deux gouttes déposées sur une plaque de verre.

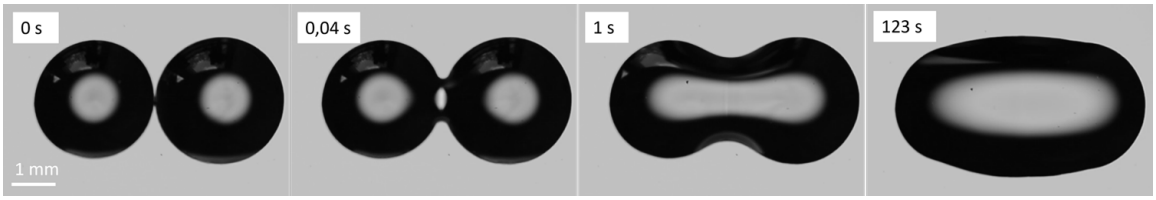

Figure 1. Coalescence de deux gouttes de glycérol sur une plaque de verre.

Nous mesurons la dynamique de coalescence ansi que les dimensions et la géométrie du dépôt liquide dans l'état final. Au cours de la coalescence, des ponts de liquide se forment entre les deux gouttes. Nos expériences suggèrent que, dans un régime visqueux, la largeur du pont de liquide suit une relaxation exponentielle jusqu'à un état final. Le nombre de gouttes et le motif de dépôt ont une grande influence sur la coalescence. De plus, la présence d'hystérésis d'angle de contact joue un rôle majeur dans la géométrie de l'état final en limitant les mouvements de la ligne triple après coalescence. Prendre en compte la géométrie et la chronologie apporte un nouveau point de vue sur les coalescence multiples.

Références

1. A. Dalili, K. Sidawi & S. Chandra, Surface coverage by impact of droplets from a monodisperse spray, *J. Coat. Technol. Res.*, **17**, 207–217 (2020).
2. B. Derby, Inkjet printing of functional and structural materials: Fluid property requirements, feature stability, and resolution, *Annu. Rev. Mater. Res.*, **40**, 395–414 (2010).
3. J. F. Hernandez-Sanchez, L. A. Kubbers, A. Eddi & J. H. Snoeijer, Symmetric and asymmetric coalescence of drops on a substrate, *Phys. Rev. Lett.*, **109**, 184502 (2012).
4. W. D. Ristenpart, P. M. McCalla, R. V. Roy & H. A. Stone, Coalescence of spreading droplets on a wettable substrate, *Phys. Rev. Lett.*, **97**, 064501 (2006).

Profil d'un câble tracté

Simon Villain-Guillot

LOMA, Université de Bordeaux, 351 cours de la Libération 33405 Talence Cedex, France
simon.villain-guillot@u-bordeaux.fr

On s'intéresse à un cable homogène et souple tracté à vitesse constante, par exemple sous l'eau par un chalutier [1], que ce soit un filet de pèche ou une fibre optique, ou bien dans les airs pour un câble tracté par un hélicoptère [2].

Nous allons nous intérésser au profil stationnaire de ce câble, qu'il entraine ou non un objet, par exemple un sonar ou un chalut pour un bateau, ou une charge de matériel pour un hélicoptère. Ce profil nous permettra notamment de calculer la tension le long de ce câble. Pour l'obtenir, nous allons déterminer l'équation régissant localement la forme du câble puis nous en étudierons les différents type de solutions.

Cet article, inspiré d'un travail de Daniel Reyss (19 juin 1936–27 avril 2021), lui est dédié.

Références

1. L. Laubier, J. Martinais & D. Reyss, Publication du Centre National pour l'Exploitation des Océans (CNEXO), Série : Rapports scientifiques et techniques n° 03 (1971).
2. Vidéo : https://www.youtube.com/watch?v=q-_7yOWUnW4

Réflexion d'une onde de surface dans un domaine de profondeur variable

Gerardo Ruiz Chavarria

Facultad de Ciencias, Universidad Nacional Autonoma de Mexico. Av. Universidad 3000, 04510 Ciudad de México, Mexique
gruiz@unam.mx

Dans cette contribution on présente une étude de la réflexion d'ondes de surface qui se déplacent dans un domaine de profondeur variable. Les expériences ont été conduites dans un bassin de 120 cm $\times$ 50 cm $\times$ 15 cm, dans lequel on a mis une couche d'eau d'une épaisseur $H = 11$ cm. Afin d'avoir une profondeur variable, on a placé dans le bassin un triangle fait en plexiglass de façon que la profondeur du domine varie de H a une valeur minimale inferieure a 1 cm. Pour produire les ondes on a utilisé un batteur plat qui est forcée a des fréquences entre 4 et 8 Hz. Finalement pour reconstruire la forme de la surface libre on a utilisé la méthode de Schlieren synthétique. Due au fait que cette méthode est limitée à des faibles amplitudes (par rapport à la longueur d'onde) nous avons fait des expériences avec une amplitude maximale de 1 mm. On a trouvé une réflexion des ondes au voisinage du sommet du triangle. L'amplitude de l'onde réfléchie dépend de l'amplitude de l'onde incident et du rapport entre la longueur d'onde et la profondeur minimale. On discute les difficultés pour la mesure des propriétés des ondes au sommet du triangle et on présente les propriétés de l'onde transmise.

Rheology of a granular medium mixed with flexible fibers

Ladislas Wierzchalek, Baptiste Darbois Texier, Georges Gauthier

Laboratoire FAST Rue André Rivière Orsay CEDEX 91405, Université Paris-Saclay
ladislas.wierzchalek@universite-paris-saclay.fr

The introduction of a small amount of flexible fibers into a granular medium is an effective and inexpensive technique to reinforce the mechanical resistance of these materials. This technique is widely used for civil engineering applications to reinforce non-cohesive soils against erosion, to increase the compressive strength of natural adobes and mortars and to develop high-performance concretes. Although the effect of fibers on the yield stress material has been investigated, the way fibers affect the flowing properties of the material is much unknown. To fill this gap, we measure the flowing response of a model material made of glass beads (radius of order 150 µm) and polypropylene fibers. Those fibers are flexible and have a high aspect ratio, about 100. We use a shear vane geometry which has been already use to characterize the rheology of pure grains [1, 2]. We impose the rotation speed and measure the torque required to shear the granular material mixed with fibres. After a transient regime, the torque reaches a stationary value. We study the influence of different parameters on the stationary torque : the rotation speed, the volume fraction of the fibres and their aspect ratio. Finally, we attempt to analyse these results within the framework of $\mu(I)$ rheology developed for dry granular flows [3].

Références

1. R. C. Daniels, A. P. Poloski & A. E. Saez, *Powder Technol.*, **181**, 237–248 (2008).
2. F. Qi, S.K de Richter, M. Jenny & B. Peters, *Powder Technol.*, **366**, 722–735 (2020).
3. O. Pouliquen, C. Cassar, P. Jop, Y. Forterre & M. Nicolas, *J. Stat. Mech.*, **2006**, 07020 (2006).

Observation en temps réel de la collision de solitons optiques dans une boucle de recirculation fibrée

François Copie, Pierre Suret, Stéphane Randoux

Univ. Lille, CNRS, UMR8523 - PhLAM - Physique des Lasers Atomes et Molécules, F-59000 Lille, France
francois.copie@univ-lille.fr

Les solitons dans les fibres optiques sont des impulsions lumineuses qui se propagent indéfiniment tout en conservant leur forme grâce à un parfait équilibre entre dispersion et non-linéarité. De manière quasi-concomitente à la prédiction de leur existence il y a 50 ans [1], Zakharov et Shabat ont développé le cadre théorique qui permet de décrire la propagation de tels solitons en résolvant exactement l'équation de Schrödinger non linéaire unidimensionnelle [2]. Un des résultats remarquables est le fait que les solitons « collisionnent » élastiquement, ce qui signifie qu'ils émergent après leur interaction complètement inchangés, à l'exception de décalages de position déterminés uniquement par leur amplitude et leurs vitesses relatives.

Nous présentons ici des expériences axées sur la génération et l'observation en temps réel de différents scénarios de collisions entre solitons grâce à la configuration de boucle de recirculation fibrée. Des impulsions solitoniques sont générées qui sont ensuite modulées en phase, permettant le controle individuel de leurs vitesses. L'injection de ces impulsions dans une boucle de recirculation et l'enregistrement de leur évolution tour à tour permet d'observer avec précision leur dynamique spatiotemporelle [3].

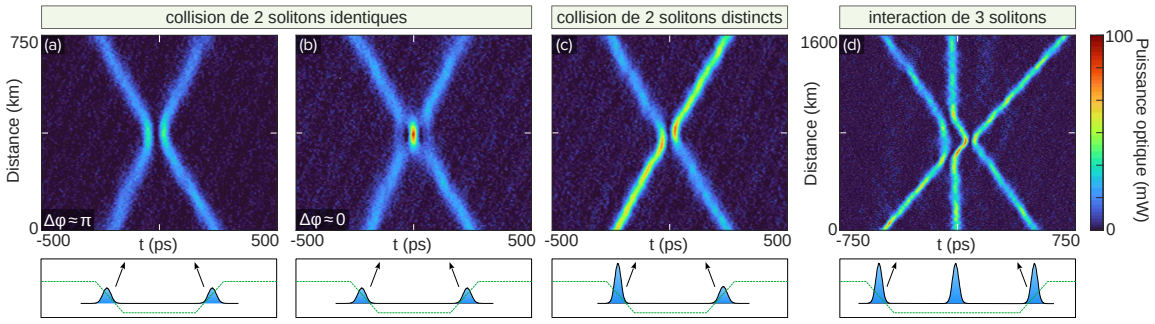

Figure 1. Enregistrements expérimentaux de la dynamique spatio-temporelle de solitons en collision dans différentes configurations. Les impulsions bleues et les lignes pointillées vertes dans les panneaux inférieurs illustrent schématiquement l'intensité initiale et la modulation de phase appliquée respectivement

La figure 1 montre des extraits de nos résultats expérimentaux, à savoir l'interaction de 2 solitons identiques ou distincts ainsi que le scénario plus complexe de l'interaction entre un petit ensemble de solitons confirmant la prédiction remarquable que le résultat de multiples collisions de solitons n'est paramétrisé que par les interactions par paires.

Ce travail présente des confirmations expérimentales originales de certaines propriétés fondamentales de l'interaction de solitons 1D en utilisant une boucle de recirculation fibrée. Par la suite, la dynamique de champs d'ondes optiques plus complexes constitués de grands ensembles de solitons peut être étudiée en utilisant cette plateforme.

Références

1. A. Hasegawa & F. Tappert, *Appl. Phys. Lett.*, **23**, 142 (1973).
2. V.E. Zakharov & A.B. Shabat, *JETP*, **34**, 72 (1972).
3. F. Copie, P. Suret & S. Randoux, *Opt. Commun.*, **545**, 129647 (2023).

A two-dimensional model for the dynamics of sand patches

Camille Rambert[1], Clément Narteau[2], Joanna Nield[3], Giles Wiggs[4], Pauline Delorme[5], Matthew Baddock[6], Philippe Claudin[7]

[1] Physique et Mécanique des Milieux Hétérogènes, ESPCI Paris, Paris, France
[2] Institut de physique du Globe de Paris, Université de Paris, CNRS, Paris, France
[3] School of Geography and Environmental Science, University of Southampton, Southampton, UK
[4] School of Geography and the Environment, Univeristy of Oxford, Oxford, UK
[5] Energy and Environment Institute, University of Hull, Hull, UK
[6] Geography and Environment, Loughborough University of Technology, Loughborough, UK
[7] Physique et Mécanique des Milieux Hétérogènes, CNRS, ESPCI Paris, PSL Research University, Sorbonne Université, Université de Paris, Paris, France

camille.rambert@espci.fr

Sand patches are one of the early stages of aeolian bedforms. They form on non-erodible surfaces in both desert and coastal environments. Their initiation is associated with the change of saltation transport law on rigid and granular beds [1]. Here we present a two-dimensional model that couples these surface-dependent transport laws with the feedback of the bed elevation on the wind flow. Analysing the spatio-temporal evolution of an initial very flat sand patch, we emphasise the central role of the input flux as well as the lengthscale over which occurs the transition between the two transport laws. We also show that, for adjusted parameters of the model, we are able to reproduce the growth and the propagation of these small metre-scale bedforms over time, in quantitative comparison with field measurements.

References

1. P. Delorme, J. M. Nield, G. F. S. Wiggs, M. C. Baddock, N. R. Bristow, J. L. Best, K. T. Christensen & P. Claudin, Field evidence for the initiation of isolated aeolian sand patches, *Geophys. Res. Lett.*, **50**, e2022GL101553 (2023).

Mesure aérienne de la propagation d'une onde de surface dans une banquise fragmentée

Sébastien Kuchly[1], Élie Dumas-Lefebvre[2], Dany Dumont[2], Stéphane Perrard[1], Antonin Eddi[1]

[1] Laboratoire de Physique et Mécanique des Milieux Hétérogènes, PMMH, ESPCI Paris, 7 Quai Saint-Bernard, 75005, Paris, France
[2] Institut des Sciences de la Mer de Rimouski (ISMER), UQAR, 310 Allée des Ursulines, Rimouski, Canada
sebastien.kuchly@espci.fr

Les Zones Marginales Glaciaires (Marginal Ice Zones MIZ) sont des régions polaires océaniques couvertes de glace fragmentée. Ces milieux complexes s'étendent sur plusieurs centaines de kilomètres et forment la frontière entre l'océan libre et les banquises continues arctiques et antarctiques. De part leur proximité avec l'océan, les MIZ sont soumises à différentes contraintes : vents, courants océaniques et champs de vagues environnant, tous capables de briser les étendues de glace continues. Les MIZ sont susceptibles de protéger la glace continue en absorbant l'énergie des vagues. Cependant, le caractère multi-échelle des MIZ rend difficile la prévision de l'atténuation d'une onde de surface par une répartition de fragments.

Afin de mieux caractériser ces milieux fragmentés, notre équipe a effectué des mesures de terrain dans l'estuaire du Saint-Laurent, près de Rimouski au Canada. Des séquences vidéos aériennes de zones de glace de mer fragmentée ont été réalisées à l'aide d'un drone en vol stationnaire (voir figure 1).

Figure 1. Vue aérienne d'une région de glace fragmentée réalisée dans la Baie du Haha ! Canada

Par corrélation d'images digitales (DIC) [1], nous sommes capables d'extraire le champ de vitesse induit par les vagues sur l'ensemble de la zone filmée. À partir de ces champs de vitesse, nous observons que la relation de dispersion des vagues en eau libre n'est pas modifiée par la présence de fragments de surface. Cependant, nous observons une atténuation spatiale de l'onde qui dépend des fréquences composant l'onde incidente. L'amplitude de l'onde décroit de façon exponentielle : $A \approx \mathrm{e}^{-\alpha(f)x}$. Dans la zone étudiée, ce coefficient d'atténuation α évolue avec la fréquence incidente selon la loi de puissance suivante $\alpha(f) \approx af^{3.33}$. Cette loi d'évolution est cohérente avec des observations précédemment réalisées en Arctique à l'aide de bouées de vagues [2].

Références

1. B. Pan, K. Qian, H. Xie & A. Asundi, Two-dimensional digital image correlation for in-plane displacement and strain measurement, *Meas. Sci. Technol.*, **6**, 062001 (2009).
2. M. H. Meylan, L. G. Bennetts, J. E. M. Mosig, W. E. Rogers and M. J. Doble & M. A. Peter, Dispersion relations, power laws, and energy loss for waves in the marginal ice zone, *J. Geophys. Res. Oceans*, **123**, 3322–3335 (2018).

Sedimentation of a single soluble particle at low Reynolds and high Péclet numbers

Nan He, Yutong Cui, David Wai Quan Chin, Thierry Darnige, Philippe Claudin, Benoît Semin

PMMH, CNRS, ESPCI Paris, PSL Research University, Sorbonne Université, Université Paris Cité, F-75005, Paris, France
nan.he@espci.fr

We investigate experimentally the dissolution of an almost spherical butyramide particle during its sedimentation, in the low Reynolds high Péclet regime. The particle sediments in a quiescent aqueous solution, and its shape and position are measured simultaneously by a camera attached to a translation stage, as shown in Fig. 1(a). The particle is tracked in real time, and the translation stage moves accordingly to keep the particle in the field of the camera. The measurements from the particle image show that the radius shrinking rate is constant with time, as shown in Fig. 1(b), and independent of the initial radius of the particle. We explain this with a simple model, based on the sedimentation law in the Stokes' regime and the mass transfer rate at low Reynolds and high Péclet numbers. The theoretical and experimental results are consistent within 20%. We introduce two correction factors to take into account the non-sphericity of the particle and the inclusions of air bubbles inside the particle, and reach quantitative agreement. With these corrections, the indirect measurement of the radius shrinking rate deduced from the position measurement is also in agreement with the model. We discuss other correction factors, and explain why there are negligible in the present experiment. We also compute the effective Sherwood number as a function of an effective Péclet number and show agreement with the power law $\mathrm{Pe}^{1/3}$ predicted by the theory. More information can be found in the pre-print paper [1].

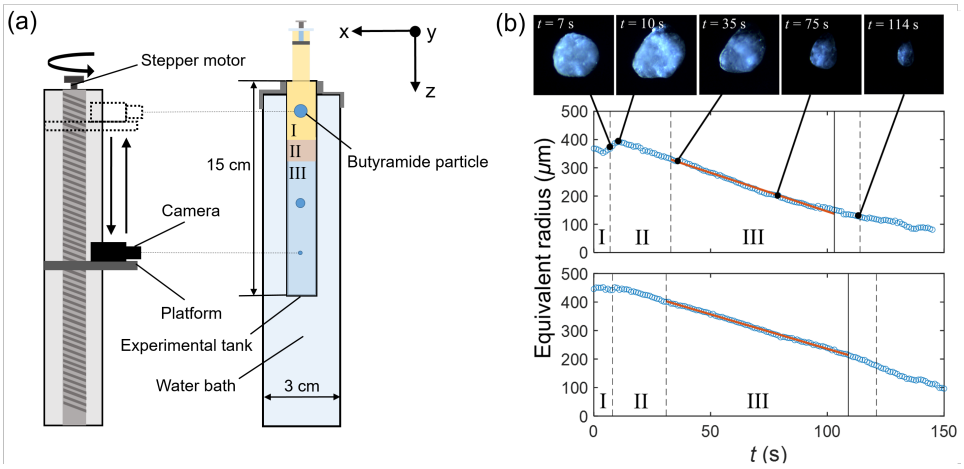

Figure 1. (a) Schematic diagram of the experimental setup; (b) Two examples of radius of the particle versus time. The blue points represent the equivalent radius from the projection of the particle, and the red line is a linear fit. Regime I corresponds to the saturated butyramide solution. Regime II corresponds to the intermediate transition of two layers. Regime III corresponds to the low concentration NaCl solution.

References

1. N. He, Y. Cui, D. Wai Quan Chin, T. Darnige, P. Claudin & B. Semin, Sedimentation of a single soluble particle at low Reynolds and high Péclet number, ArXiv:2310.14737V1 (2023).

Axisymmetric internal wave tunneling

Samuel Boury[1], Bruce R. Sutherland[2], Sylvain Joubaud[3], Philippe Odier[3], Thomas Peacock[4]

[1] Université Paris-Saclay, CNRS, FAST, 91405 Orsay, France
[2] Departments of Physics and of Earth and Atmospheric Sciences, University of Alberta, Edmonton, AB, Canada T6G 2E1
[3] Univ Lyon, ENS de Lyon, Univ Claude Bernard, CNRS, Laboratoire de Physique, F-69342 Lyon, France
[4] Department of Mechanical Engineering, Massachusetts Institute of Technology, Cambridge, MA 02139, USA
samuel.boury@universite-paris-saclay.fr

The various mechanisms through which inertia-gravity waves can propagate through geophysical fluids trigger a constantly renewed interest due to their assumed significant role in energy transport and dissipation processes, notably in the oceans. In this context, numerous studies have been devoted to such waves in stratified fluids, i.e. fluids that exhibit a density gradient. Idealized linear stratifications, with constant density gradients, or piece-wise stratifications, linear by parts, are particularly interesting to understand and model the propagation of internal gravity wave through a column of stratified fluid. In the oceans, stratifications are fundamentally non-linear and often display density interfaces with, sometimes, layers of constant density that should inhibit internal waves propagation. In-situ measurements as well as experimental and numerical observations, however, show that internal waves can propagate through such barrier-layers in particular situations, through a process called wave tunneling [3, 4], analoguous to the well-known tunneling effect at play in quantum mechanics.

This study extends the results of Sutherland and Yewchuk [4] on 2D Cartesian internal wave tunneling to the case of 3D axisymmetric wave fields. Using an experimental apparatus that has been proven capable of generating axisymmetric internal wave fields [1] and that has been used previously to study internal wave transmission through density gradient interfaces [2], along with numerical simulations, we show quantitatively that such waves can efficiently tunnel through constant density layers and still conserve their structure. We propose a simple three-layer model allowing for the computation of transmission coefficients for the velocity fields, and we test it on a case study. We notably show that there exists a smooth transition between the fully propagating and the tunneling regimes.

References

1. S. Boury, T. Peacock & P. Odier, Excitation and resonant enhancement of axisymmetric internal waves, *Phys. Rev. Fluids*, **4**, 034802 (2019).
2. S. Boury, P. Odier & T. Peacock, Axisymmetric internal wave transmission and resonant interference in non-linear stratifications, *J. Fluid Mech.*, **886**, A8 (2020).
3. T. Mixa, A. Dörnbrack & M. Rapp, Nonlinear simulations of gravity wave tunneling and breaking over Auckland Island, *J. Atmos. Sci.*, **78**, 1567–1582 (2021).
4. B. R. Sutherland & K. Yewchuck, Internal wave tunnelling, *J. Fluid Mech.*, **511**, 125–134 (2004).

Sloshing instability driven by bubble plume

Marc Cordelle Vacher[1,2,3], Thomas Boirot[1], Stéphane Perrard[2], Sophie Ramananarivo[1]

[1] Laboratoire d'Hydrodynamique, École Polytechnique, boulevard des Maréchaux, 91120, Palaiseau
[2] Physique et Mécanique des Matériaux Hétérogène, École Supérieure de Physique et de Chimie Industrielles de la ville de Paris, 10 rue Vauquelin, 75005 Paris
[3] Saint-Gobain Recherche, Saint-Gobain, 39 quai Lucien Lefranc, 93300, Aubervilliers, France
marc.vacher@polytechnique.edu

Some molten glass furnaces are stirred by gas flames in the volume, leading to surface instabilities that can have important industrial consequences. We design and built an analog experiment with water and air as working fluids. A sparger is immersed in a water tank and injects air vertically at a constant air flow rate. An air plume is then created : air bubbles rise up towards the water surface. Above a certain flow rate, a sloshing mode grows at the water surface, due to a complex interaction with the air plume, as previously observed in a similar geometry by Aoki *et al.* [1].

In this study, we aim at identifying when and why the surface destabilizes. Our main control parameters are the air flow rate and the tank aspect ratio, $R = h_0/L$, where h_0 is the static water height and L the tank width. To measure the bubble trajectories and the free surface position, we use shadowgraphy techniques.

Figure 1. Planar view of the bubble plume with self-induced sloshing

We characterize the instability by measuring the critical air flow rate as a function of tank aspect ratio, and the oscillating frequency. To identify the instability mechanism, we performed a spectral analysis in time of both the jet and the surface. We show that the sloshing frequency is incompatible with low frequency oscillations of bubble wakes, which occurs in mixing bubble columns used in chemical engineering for example [2]. We eventually propose a phenomenological model of coupled oscillators to explain what motors this instability.

References

1. R. Aoki, S. Fujioka & K. Terasaka, Experimental study and prediction by computational fluid dynamics on self-induced sloshing due to bubble flow in a rectangular vessel, *J. Chem. Eng. Jap.*, **54**, 51–57 (2021).
2. L. Liu, H. Yan, T. Ziegenhein, H. Hessenkemper, Q. Li & D. Lucas, A systematic experimental study and dimensionless analysis of bubble plume oscillations in rectangular bubble columns, *Chem. Eng. J.*, **372**, 352–362 (2019).

Analyse statistique de l'endommagement sous choc dans des matériaux ductiles

Corentin Thouénon[1,2], Alizée Dubois[1], Jacques Besson[2], François Willot[2]

[1] CEA DAM DIF, F-91297 Arpajon, France, Université Paris-Saclay, CEA, Laboratoire Matière en Conditions Extrêmes, F-91680 Bruyères-le-Châtel, France
[2] MINES ParisTech, PSL Research University, MAT - Centre des matériaux, CNRS UMR 7633, BP 87 91003 Evry, France
corentin.thouenon@cea.fr

L'écaillage constitue le principal phénomène d'endommagement observé dans les matériaux soumis à un chargement dynamique. La variation de certains paramètres expérimentaux, tels que la vitesse de déformation et la pression de choc, est rendue possible grâce à différentes méthodes de génération de chocs, comme l'impact mécanique ou le choc laser. Ces méthodes permettent de modifier les propriétés de rupture. Dans les matériaux ductiles, le mécanisme microscopique à l'origine des fissures d'écaillage implique la nucléation, la croissance et la coalescence de pores dans le plan traversé par les ondes de relaxation et l'onde de choc réfléchie. De nombreux modèles d'endommagement supposent un ensemble de pores indépendants, négligeant les potentiels effets collectifs entre ces derniers [1–4]. L'approche statistique proposée vise à mettre en évidence des corrélations dans la distribution spatiale des tailles de pores et à étudier les variations de la densité surfacique de pores en fonction de la vitesse de déformation. En utilisant la microscopie électronique à balayage et l'imagerie stéréoscopique, cette méthode permet une analyse statistique de reconstructions 3D post-mortem de surfaces écaillées [5]. L'objectif est d'améliorer les modèles d'endommagement ainsi que notre compréhension des mécanismes fondamentaux sous-jacents.

Figure 1. Image électronique d'une surface écaillée d'aluminium obtenue par choc laser

Références

1. A. Molinari & S. Mercier, Micromechanical modelling of porous materials under dynamic loading, *J. Mech. Phys. Solids*, **49**, 1497–1516 (2001).
2. A. Molinari & S. W. Wright, A physical model for nucleation and early growth of voids in ductile materials under dynamic loading, *J. Mech. Phys. Solids*, **53**, 1476–1504 (2005).
3. H. Trumel, F. Hild, G. Roy, Y.-P. Pelligrini & C. Denoual, On probabilistic aspects in the dynamic degradation of ductile materials, *J. Mech. Phys. Solids*, **57**, 1280–1998 (2009).
4. S. W. Wright & K. T. Ramesh, Dynamic void nucleation and growth in solids : A self-consistent statistical theory, *J. Mech. Phys. Solids*, **56**, 336–359 (2008).
5. L. Ponson & D. Bonamy, Crack propagation in brittle heterogenous solids : Material disorder and crack dynamics, *Int. J. Fract.*, **162**, 21–31 (2010).

Réponse vibratoire d'ailes d'Odonates : mise en évidence d'un comportement non linéaire

Camille Aracheloff[1,2], Benjamin Thiria[1], Ramiro Godoy-Diana[1], André Nel,[2], Romain Garrouste[2]

[1] Physique et mécanique des milieux hétérogènes (PMMH), ESPCI, Paris, France
[2] Institut de Systématique, Évolution, Biodiversité (ISYEB), MNHN, Paris, France
camille.aracheloff@espci.fr

Les Odonates (ordre d'insectes comprenant les libellules et les demoiselles) ont des capactités de vol remarquables [1] qui sont le résultat d'interactions fluide–structure complexes, notamment entre leurs ailes et l'air. Les ailes sont des structures hétérogènes flexibles composées d'une membrane et d'un réseau de nervures qui influencent localement la rigidité. Leurs caractéristiques (taille, géométrie, réseau de nervures, présence de structures spécifiques...) présentent une grande diversité du fait du nombre d'espèces d'Odonates et de leur répartition géographique extrêmement large. L'objectif de notre étude est de comprendre le rôle de différents paramètres impliqués dans la production de force aérodynamique [2], ainsi que le lien entre les caractéristiques des ailes, les environnements et les modes de vie de différentes Odonates actuelles. Ces résultats pourront être extrapolés aux formes passées des Odonatoptera, dont les plus anciens fossiles datent du Carbonifère (325–324 Ma) [3], afin d'avoir une meilleure compréhension de leur vol, de leur environnement et de leur évolution.

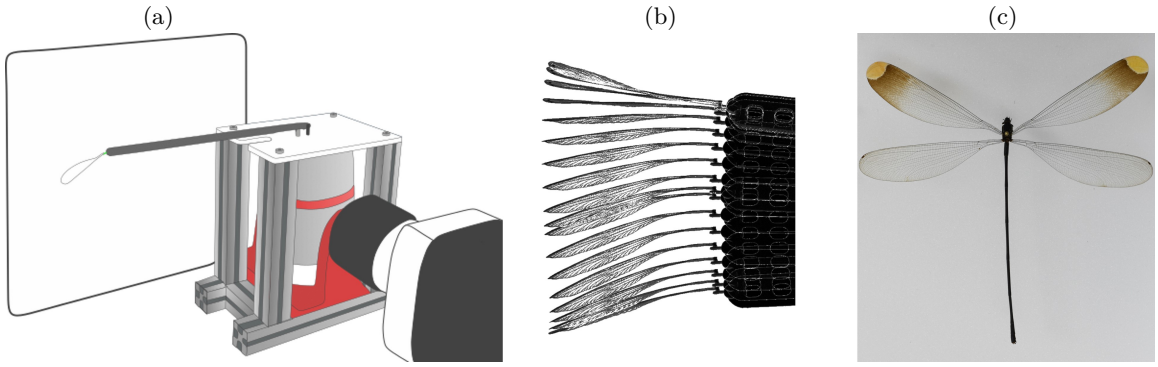

Figure 1. (a) Dispositif expérimental de mise en vibration où un pot vibrant impose un mouvement à la base d'une aile via un bras de levier qui va permettre d'atteindre des grandes amplitudes d'oscillation. (b) Aile mise en mouvement. (c) *Microstigma rotundatum* (*Odonata : Pseudostigmatidae*).

Le vol des Odonates est un vol battu où les ailes subissent de grands déplacements et ainsi que d'importantes déformations. La forme prise au cours du vol a un impact sur la production de force aérodynamique, or cette forme est liée aux propriétés mécaniques de l'aile. Dans un premier temps nous avons étudié des ailes provenant de 23 spécimens venant de 7 familles différentes via des tests de vibration en faible amplitude, permettant de determiner leur fréquence de resonnance dans le cadre linéaire. Puis nous nous sommes penchés sur une famille de demoiselles (*Pseudostigmatidae*) pour laquelle une étude en grande amplitude a pu être menée mettant en évidence un comportement non linéaire des ailes.

Références

1. E. Salami, T. A. Ward, E. Montazer & N. N. N. Ghazali, *Proc. Inst. Mech. Eng. C*, **233**, 6519–6537 (2019).
2. R. Antier, B. Thiria & R. Godoy-Diana, *J. Fluids Struct.*, **124**, 104043 (2024).
3. A. Nel, G. Fleck, R. Garrouste, G. Gand, J. Lapeyrie, S. M. Bybee & J. Prokop, *Palaeontogr. Abt. A*, **289**, 89–121 (2009).

Thermo-mechanical influence on fracture propagation: Integrating temperature effects through equilibrium statistical mechanics

Claudia Binetti[1,2], Giuseppe Florio[2,3], Nicola Maria Pugno[4,5], Stefano Giordano[1], Giuseppe Puglisi[2]

[1] University of Lille, CNRS, Centrale Lille, Univ. Polytechnique Hauts-de-France, UMR 8520 - IEMN - Institut d'Électronique, de Microélectronique et de Nanotechnologie, Lille, F-59000, France
[2] Department of Civil Environmental Land Building Engineering and Chemistry, DICATECh, Polytechnic of Bari, Via Orabona 4, Bari, 70125, Italy
[3] INFN, Section of Bari, I-70126, Italy
[4] Laboratory for Bioinspired, Bionic, Nano, Meta Materials & Mechanics, Univ. of Trento, Via Mesiano 77, Trento, 38123, Italy
[5] School of Engineering and Materials Science, Queen Mary Univ. of London, Mile End Road, London, E1, U.K.
claudia.binetti@iemn.fr

The study of the impact that thermal fluctuations have on fracture propagation represents an intriguing yet intricate subject, presenting both theoretical and experimental challenges across diverse scales of interest. Despite the plethora of experimental studies and numerical simulations analyzing the correlation between thermal fluctuations and mechanical properties, a notable absence of a robust theoretical framework in fracture mechanics that integrates temperature effects persists. In response to this gap, our study endeavors to elucidate the influence of temperature on material failure using the tools of equilibrium statistical mechanics. We employ a multi-scale approach to study how fracture propagation at the micro scale determines the macroscopic failure of the solid. Specifically we develop a discrete model that mimics crack propagation within a medium at the micro scale. This model consists of n successive units, each comprising an elastic spring (stiffness k_e) replicating the solid's elastic properties and a breakable unit (stiffness k_t) simulating fracture propagation. We underline that although the model is initially developed in the discrete form, mainly to account for the entropic effects, we also study the continuum limit (number of units of the system tending to infinity), which enables a more simple and compact analytical description of the physical phenomenon. We investigate the thermo-mechanical response of the system under a distributed force F, yielding a total mechanical energy expression

$$g = \frac{1}{2}k_t \sum_i (1-\chi_i)\, w_i^2 + \frac{1}{2}k_e \sum_i (w_{i+1}-w_i)^2 - F\sum_i w_i,$$

where, following the approach used in [1], we have introduced an internal spin variable χ_i which assumes value 0 when the link is intact and 1 when it is broken. After exploring the equilibrium configuration through energy minimization for a given crack length, we compute the stress required for fracture propagation, according to the traditional Griffith energy criterion [2]. The novelty in our model lies in extending this well-known criterion to incorporate thermal fluctuations. Thus, by employing equilibrium statistical mechanics, we integrate entropic effects into the overall energy balance. Specifically, we write the partition function in the Gibbs ensemble as

$$\mathcal{Z} = \int_{\mathbf{R}^n} \exp\left[-g/(k_{\mathrm{B}}T)\right] \mathrm{d}w_1 \ldots \mathrm{d}w_n,$$

which relates the mechanical energy of the system to a thermodynamic quantity, which is the Gibbs free energy $\mathcal{G} = H - TS = k_{\mathrm{B}}T \ln \mathcal{Z}$. The crucial point of integrating thermal fluctuations into traditional fracture mechanics involves substituting the total mechanical energy with the Gibbs free energy. This approach enables us to derive fully analytical results describing the analytical dependence of the fracture threshold on temperature and, in particular, revealing the existence of a critical temperature, in correspondence of which the system undergoes a phase transition — the spontaneous rupture of the system without applying a mechanical load. This behavior reflects known experimental phenomena, including fracture in high and medium entropy alloys and nanowires, cell detachment, DNA and RNA denaturation.

References

1. G. Florio, G. Puglisi & S. Giordano, *Phys. Rev. Res.*, **2**, 033227 (2020).
2. A. A. Griffith, *Philos. Trans. R. Soc. A*, **221**, 163–198 (1921).

Non-linéarité dans des systèmes micro-fluidiques par des valves

Alaa Bou Orm, Badr Kaoui

Biomécanique et Bioingénierie, CNRS, Université de Technologie de Compiègne, 60200 Compiègne, France
alaa.bou-orm@utc.fr, badr.kaoui@utc.fr

L'écoulement des fluides dans les canaux des systèmes micro-fluidiques s'opère en régime stationnaire et linéaire en raison du faible nombre de Reynolds, caractéristique de l'absence d'effets inertiels à petite échelle. Un intérêt croissant émerge pour l'exploration des phénomènes non linéaires dans les systèmes micro-fluidiques, en particulier pour des applications variées de contrôle des débits [1]. En complément des techniques déjà proposées dans la littérature, nous suggérons l'utilisation de valves bicuspides, composées de deux feuillets, similaires à celles trouvées dans les veines et les vaisseaux lymphatiques [2–4], afin de prévenir un reflux. À ce stade, notre étude est purement numérique. Nous avons développé une méthode numérique basée sur la méthode de Boltzmann sur réseau, mieux adaptée à la prédiction de l'écoulement se développant dans des géométries complexes telles que celles des systèmes micro-fluidiques. La mécanique d'ouverture–fermeture des valves est calculée par la méthode des ressorts, avec un couplage fort avec l'écoulement via la méthode des frontières immergées [5]. Les résultats obtenus par des simulations en 2D pour les performances d'une jonction en T, avec et sans valve, sont présentés dans les figures 1 (a) et 1 (b), ainsi que le débit de sortie Q_{out} en fonction du gradient de pression $\Delta P = P_1 - P_{\text{out}}$ entre les entrées et la sortie de la jonction, illustré dans la Fig. 1 (c). Le débit obtenu à la sortie est non linéaire en présence des valves. En outre, nous présentons un cas plus fascinant, à savoir l'évolution du régime d'écoulement dans une cascade de jonctions, comme illustré dans la Fig. 1 (d). Pour cette configuration, nous examinons la nature du débit à la sortie, qu'il soit stationnaire ou non, en fonction de l'amplitude et de la fréquence de l'aspect oscillatoire des écoulements au niveau des entrées multiples. Cette étude nous aidera à prévoir et à analyser le drainage de la lymphe au sein des réseaux de vaisseaux lymphatiques [2, 3].

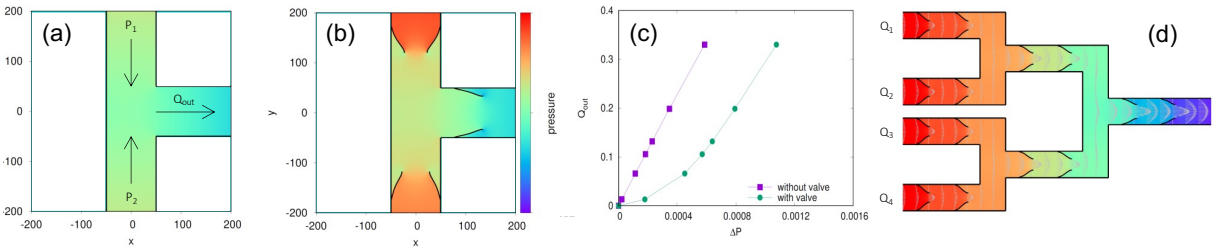

Figure 1. (a) Champ de pression calculé dans une jonction en T sans valve. (b) Pression en présence des valves. (c) Débit à la sortie Q_{out} en fonction du gradient de pression imposé entre les entrées et la sortie de la jonction $\Delta P = P_1 - P_{\text{out}}$. (d) Champs de pression et de vitesse se développant dans une cascade de jonctions.

Références

1. B. Sarah, D. A. Weitz & G. M. Whitesides, Nonlinear phenomena in microfluidics, *Chem. Rev.*, **122**, 6921–6937 (2022).
2. T. P. Padera, E. F. J. Meijer & L. L. Munn, The lymphatic system in disease processes and cancer progression, *Annu. Rev. Biomed. Eng.*, **18**, 125–158 (2016).
3. J. E. Moore & C. D. Bertram, Lymphatic system flows, *Annu. Rev. Fluid Mech.*, **50**, 459–582 (2018).
4. S. C. Hofferberth *et al.*, A geometrically adaptable heart valve replacement, *Sci. Transl. Med.* **12**, eaay4006 (2020).
5. A. Bou Orm & B. Kaoui, Computer simulations of the lymphatic vessels and valves dynamics, *The 18th International Conference for Mesoscopic Methods in Engineering and Science*, June 27th–July 1st 2022, La Rochelle, France.

A hydrodynamic toy model for fish locomotion

Bruno Ventéjou[1], Thibaut Métivet[2], Aurélie Dupont[1], Christian Graff[3], Philippe Peyla[1]

[1] University Grenoble Alpes, CNRS, LIPhy, Grenoble, France
[2] Université Grenoble Alpes, INRIA, CNRS, Grenoble INP, LJK, Grenoble, France
[3] University Grenoble Alpes, CNRS, LPNC, Grenoble, France
bruno.ventejou@univ-grenoble-alpes.fr

The social interaction of fish has been mainly studied in 2D without hydrodynamic interactions [1,2] or with hydrodynamic interactions in the limit of the far-field [3]. As a fish swims, it affects the flow around its body in a complex manner at distances much larger than the typical fish scale. Thus, it could compete with cognitive interaction. Some efforts have been done to describe precisely the flow generated around a fish [4,5]. But, the high cost of hydrodynamic simulations prevents the use of such models to study schools of fish.

We propose a toy model , that is able to generate the vortex wake induced by the fish locomotion (Fig. 1) and which is light compare to solving the fish tail flapping. We describe the fish as a rigid body by a penalty method and achieve the description of the tail flapping by exerting a torque in the fluid compensated in the body. The trajectory of the fish is determined by the position of the tail in relation to the body. We perform a full characterization of the toy model and compare it to the scaling found in the animal kingdom [6].

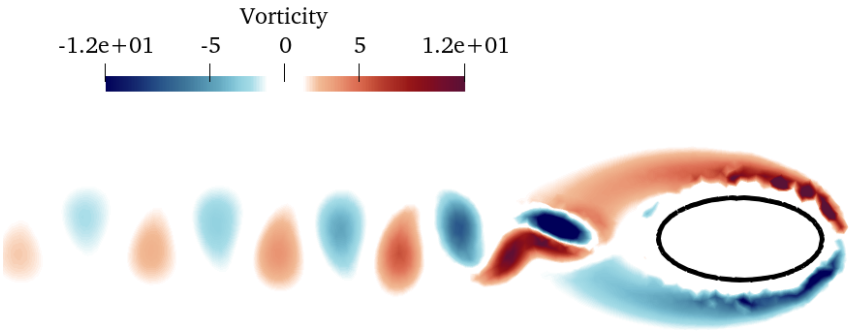

Figure 1. Illustration of the vortex wake behind a rigidbody with the minimal model developed.

Références

1. J. Gautrais *et al.*, Analyzing fish movement as a persistent turning walker, *J. Math. Biol.*, **58**, 429–445 (2009).
2. D. S. Calovi *et al.*, Swarming, schooling, milling : Phase diagram of a data-driven fish school model, *New J. Phys.*, **16**, 015026 (2014).
3. A. Filella *et al.*, Hydrodynamic interactions influence fish collective behavior, *Phys. Rev. Lett.*, **120**, 198101 (2018).
4. M. Bergmann *et al.*, Effect of caudal fin flexibility on the propulsive efficiency of a fish-like swimmer, *Bioinspir. Biomim.*, **9**, 046001 (2014).
5. G. Novati *et al.*, Synchronisation through learning for two self-propelled swimmers, *Bioinspir. Biomim.*, **12**, 036001 (2017).
6. M. Gazzola *et al.*, Scaling macroscopic aquatic locomotion, *Nat. Phys.*, **10**, 758–761 (2014).

Numerical simulations of internal gravity wave turbulence

Vincent Labarre[1], Giorgio Krstulovic[1], Sergey Nazarenko[2]

[1] Université Côte d'Azur, Observatoire de la Côte d'Azur, CNRS, Laboratoire Lagrange, Boulevard de l'Observatoire CS 34229–F 06304 Nice Cedex 4, France
[2] Université Côte d'Azur, CNRS, Institut de Physique de Nice (INPHYNI), 17 rue Julien Lauprêtre 06200 Nice, France
vincent.labarre@oca.eu

Stratified flows support the propagation of internal gravity waves, which are important in many geophysical applications such as mixing in the deep ocean [1]. Yet, simulating waves directly is too expensive for climate modeling due to the space and time scale separation, so their effects are parameterized. In the limit of weak nonlinearity, the Weak Wave Turbulence theory describes the evolution of the system with a kinetic equation

$$\dot{n}_{\boldsymbol{k}} = \int \left[\mathcal{R}^{\boldsymbol{k}}_{12} - \mathcal{R}^{1}_{\boldsymbol{k}2} - \mathcal{R}^{2}_{\boldsymbol{k}1}\right] \, \mathrm{d}^3\boldsymbol{k}_1 \, \mathrm{d}^3\boldsymbol{k}_2 + f_{\boldsymbol{k}} - d_{\boldsymbol{k}},$$
$$\mathcal{R}^{\boldsymbol{k}}_{12} = 4\pi \; \delta(\boldsymbol{k} - \boldsymbol{k}_1 - \boldsymbol{k}_2) \; \delta(\omega_{\boldsymbol{k}} - \omega_1 - \omega_2) \; |V^{\boldsymbol{k}}_{12}|^2 \; (n_1 n_2 - n_{\boldsymbol{k}} n_1 - n_{\boldsymbol{k}} n_2) \, ,$$

$n_{\boldsymbol{k}}$ being the wave action spectrum, $f_{\boldsymbol{k}}$ the forcing, $d_{\boldsymbol{k}}$ the dissipation, $\omega_{\boldsymbol{k}}$ the wave frequency, and $V^{\boldsymbol{k}}_{12}$ the interaction coefficients between wave modes [2]. The kinetic equation gives directly the wave dynamics on very large time scales which is hardly obtained by direct numerical simulations, and could help us to estimate energy transfers and mixing due to waves without using ad-hoc parameters [3]. Using a large scale and localized forcing, we observe that the spectrum develops through successions of nonlocal energy transfers (cf. Fig. 1), namely the Elastic Scattering (ES), Parametric Subharmonic Instability (PSI) and Induced Diffusion (ID) [4]. It leads to the formation of strongly anisotropic spectra.

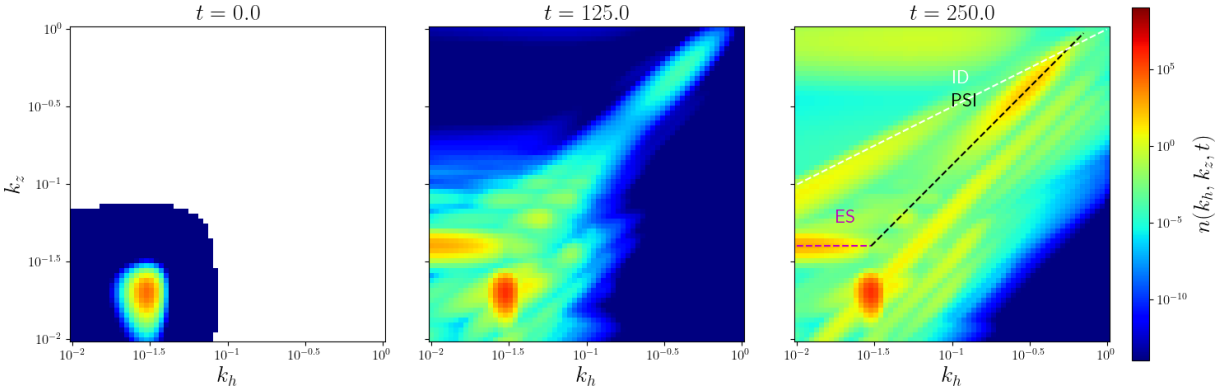

Figure 1. Wave action spectrum in one of our kinetic equation simulations at different times. k_h and k_z are the horizontal and vertical wave-vector modulus. The lines correspond to nonlocal interactions with the forced mode.

References

1. J. A. MacKinnon *et al.*, Climate process team on internal wave–driven ocean mixing, *Bull. Amer. Meteor. Soc.*, **98**, 2429–2454 (2017).
2. V. Labarre, N. Lanchon, P.-P. Cortet, G. Krstulovic & S. Nazarenko, Kinetics of internal gravity waves beyond hydrostatic regime, arXiv:2311.14370 (2023).
3. G. Dematteis & Y. Lvov, The structure of energy fluxes in wave turbulence, *J. Fluid Mech.*, **954**, A30 (2023).
4. C. H. McComas & F. P. Bretherton, Resonant interaction of oceanic internal waves, *J. Geophys. Res.*, **82**, 1397–1412 (1977).

About the unsteady propulsion of an airfoil

Gauthier Bertrand, Ramiro Godoy-Diana, Benjamin Thiria, Marc Fermigier

Laboratoire de Physique et Mécanique des Milieux Hétérogènes, ESPCI-PSL, CNRS, Sorbonne Université, Université Paris-Cité, 7 Quai Saint-Bernard, 75005 Paris.
gauthier.bertrand@espci.fr

Unsteady aerodynamic problems have been studied extensively for swimming and fighting animals observed in nature, but also for helicopter rotors, wind turbines or micro air vehicles. For all these topics, the aim is to optimise the propulsive loads and the efficiency of the unsteady effects. In this way, we are interested in unsteady propulsion for sailing boats and, more specifically, for windsurfing.

The competitive practice of sailing and windsurfing is developing. It can be attributed to the willingness to break records, which increases the performance of sailing boats. At the start of a race or in light winds, to get or keep the board in foiling mode, for example after a tack change, athletes use intermittent propulsion by pumping the sail, i.e. periodically changing the angle of incidence of the sail relative to the wind. The flapping motion of the sail, and more generally of a foil, destabilises the flow and generates a flow dominated by a vortex alley in its wake. Depending on the flapping parameters, different types of wake are possible. Some even allow the generation of a thrust. At the very least, they all influence the aerodynamic forces acting on the wing [1]. We experimentally characterise the aerodynamics of the sail and its propensity to generate thrust for the boat.

Our aim is to compare the sailing (C_{drive}, C_{drift}) and aerodynamic (C_{drag}, C_{lift}) coefficients between a static and an oscillating sail [2]. We have obtained data on the forces acting on the foil using force sensors.

References

1. J. M. Anderson, K. Streitlien, D. S. Barrett & M. S. Triantafyllou, Oscillating foils of high propulsive efficiency, *J. Fluid Mech.*, **360**, 41–72 (1998).
2. R. R. Schutt, *Unsteady Aerodynamics of Sailing Maneuvers and Kinetic Techniques*, PhD Thesis, Cornell University, pp. 57–70 (2019).

Transition topologique dans les oscillateurs paramétriques linéaires et non linéaires

Benjamin Apffel, Romain Fleury

Institute of Electrical and Micro Engineering, Laboratory of Wave Engineering, École Polytechnique Fédérale de Lausanne (EPFL), Station 11, 1015 Lausanne, Switzerland
benjamin.apffel@epfl.ch

Un oscillateur paramétrique est un exemple simple d'oscillateur forcé extérieurement dont on trouve des réalisations dans de nombreux domaines d'application (optique, mécanique quantique, hydrodynamique, mécanique...). Lorsque le forçage externe est accordé en fréquence et suffisamment intense, la réponse de l'oscillateur croît exponentiellement tout en oscillant à la fréquence moitié de celle du forçage [1]. La phase de cette oscillation n'est pas arbitraire mais fixée, à π près, par le forçage externe. Il existe donc deux cycles limites oscillant en opposition de phase, et le choix de l'un ou l'autre dépend des conditions initiales. Cette dégénérescence de phase a par exemple été utilisée dans les machines d'Ising cohérentes comme analogue d'un spin 1/2 [2].

On propose ici d'étudier la possibilité d'effectuer une transition entre ces deux cycles limites lorsque le forçage externe est perturbé continûment. Plus précisément, on s'intéresse au comportement de l'oscillateur lorsque l'excitation oscillant à la fréquence f_0 est désaccordée de λf_0 durant un temps $1/\lambda f_0$. Lorsque le paramètre λ varie, on observe ou non une transition de l'oscillateur de l'un vers l'autre cycle limite. Il existe ainsi des valeurs critiques λ_c pour lesquelles le comportement change brusquement. De manière intéressante, il existe une interprétation topologique à ce phénomène que l'on discutera. Les différences entre oscillateurs linéaires et non linéaires sont également mises en lumière. On propose une réalisation expérimentale avec l'instabilité de Faraday observée sur un bain de liquide vibré. Les cas linéaires et non linéaires sont sondés expérimentalement et comparés avec les prédictions théoriques. Ces transitions se rapprochent de d'autres travaux dans le contexte de « *bit flip* » dans les machines d'Ising [3] et étendent les effets topologiques à des systèmes non linéaires modulés en temps.

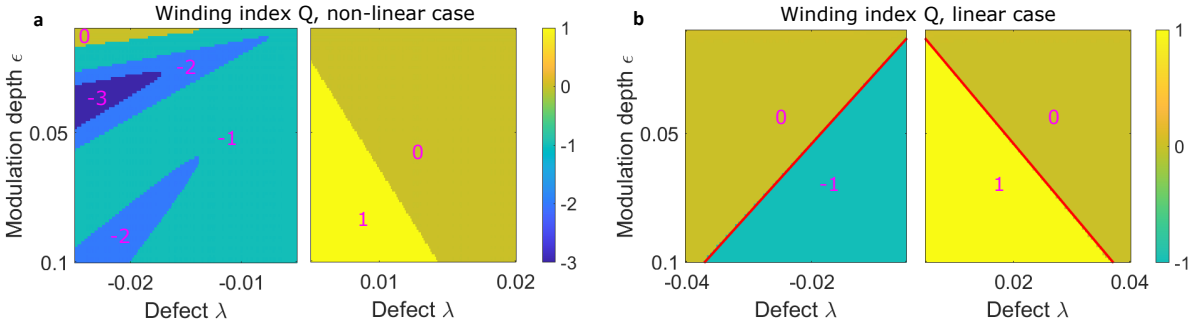

Figure 1. Exemple de diagramme de transition en fonction du paramètre de perturbation λ et du forçage adimensionné ϵ dans le cas d'un oscillateur paramétrique non linéaire (gauche) et linéaire (droite). Le nombre Q indique le changement de phase (normalisé par π) entre l'état initial et final, qui ne peut être qu'un nombre entier.

Références

1. S. Fauve, *Hydrodynamics and Nonlinear Instabilities*, Cambridge University Press, pp. 387—492 (1998).
2. E. Goto, The parametron, a digital computing element which utilizes parametric oscillation, *Proc. IRE*, **47**, 1304–1316 (1959).
3. M. Frimmer *et al.*, Rapid flipping of parametric phase states, *Phys. Rev. Lett.*, **123**, 254102 (2019).

Flows in bursting soap film

Alexandre Guillemot[1], Juliette Pierre[1], Adrien Bussonnière[2]

[1] Institut ∂'Alembert, Sorbonne Université - UMR 7190, 75005 Paris, France
[2] Matière et Systèmes Complexes, Université Paris Cité, UMR 7057, 75013, Paris, France
alexandre.guillemot@dalembert.upmc.fr

A soap film is a thin layer of liquid with surfactant at its interface. Surfactants lower its surface tension and stabilize it. When a liquid film without surfactant molecules is punctured, a hole appears and grows at a well-defined speed called Taylor–Culick velocity, resulting from the balance between surface tension forces and inertia [1]. With surfactant the film retraction is more complex. Indeed, during the film bursting, a flow can sometimes be observed ahead of the hole edge, called the rim, while the area containing the flow is named the aureole [2].

This flow arises from the reduction in surface tension within the aureole, i.e. Marangoni flow, and is leading to a local thickening of the film. It does not come without an impact on the film's opening speed, as it decreases at the same time. The variation in surface tension is caused by the rapid bursting of the film (the film area decreases and vanishes in few ms), which compresses the surfactants at the interface, making it a completely out-of-equilibrium phenomenon [3]. The relation between surface tension and the degree of film compression is referred to as elasticity.

A dedicated setup has been built to track the aureole dynamics and various concentration of insoluble surfactant has been used to vary the elasticity. Deviations from the self-similar Frankel model are observed. After a transient regime, two different behaviours are observed. For low insoluble concentration, the aureoles are of constant size, while for higher concentration, aureoles increase in size but are smaller than expected in Frankel theory. We rationalize these two regimes by invoking the surfactant desorption.

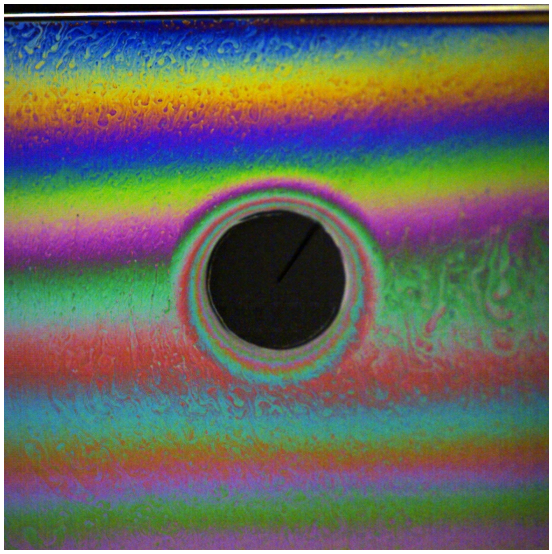

Figure 1. Aureole of a bursting soap film

References

1. F. E. C. Culick, Comments on a ruptured soap film, *J. Appl. Phys.*, **31**, 1128–1129 (1960).
2. W. R. McEntee & K. J. Mysels, Bursting of soap films. I. An experimental study, *J. Phys. Chem.*, **73**, 3018–3028 (1969).
3. S. Frankel & K. J. Mysels, Bursting of soap films. II. Theoretical considerations, *J. Phys. Chem.*, **73**, 3028–3038 (1969).

Interaction de gaz de solitons en eau profonde

Loïc Fache[1], Félicien Bonnefoy[2], Guillaume Ducrozet[2], Francois Copie[1], Filip Novkoski[3], Guillaume Ricard[3], Éric Falcon[3], Giacomo Roberti[4], Pierre Suret[1], Gennady El[4], Stéphane Randoux[1]

[1] Univ. Lille, CNRS, UMR 8523 - PhLAM - Physique des Lasers Atomes et Molécules, F-59 000 Lille, France
[2] Nantes Université, École Centrale Nantes, CNRS, LHEEA, UMR 6598, F-44 000 Nantes, France
[3] Université Paris Cité, CNRS, MSC, UMR 7057, F-75 013 Paris, France
[4] Department of Mathematics, Physics and Electrical Engineering, Northumbria University, Newcastle upon Tyne, NE1 8ST, United Kingdom
loic.fache@univ-lille.fr

Nous présentons des expériences hydrodynamiques étudiant l'interaction entre deux ensembles statistiques de solitons (ondes non linéaires localisées), appelés gaz de solitons, et considérons un cas particulier composé de solitons d'amplitudes identiques, mais ayant des vitesses opposées, appelés gaz monochromatiques, interaction étudiée théoriquement en 2005 [1]. Notre étude consiste à enregistrer l'évolution spatio-temporelle de ces deux gaz de solitons dans un bassin long de 140 mètres, où la dynamique, à l'ordre premier, est décrite par l'équation intégrable de Schrödinger non linéaire focalisante à une dimension (NLS-1d). Pour modifier la force d'interaction des deux gaz, nous faisons varier la vitesse initiale relative de ceux-ci.

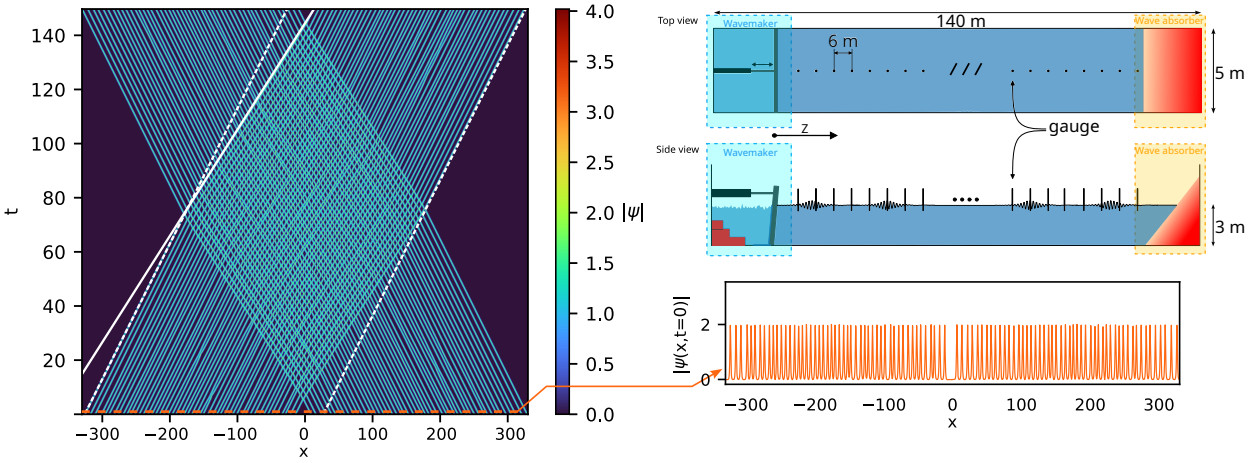

Figure 1. Simulation numérique de NLS-1d avec pour condition initiale deux faisceaux monochromatiques de gaz de solitons avec des vitesses opposées. Schématisation du bassin hydrodynamique.

Dans cette étude, nous avons mesuré les changements de densité macroscopique des gaz ainsi que les changements de vitesses induits par l'interaction [2]. Nos résultats expérimentaux sont en bon accord quantitatif avec les prédictions de la théorie cinétique des gaz de solitons [1]. Nous trouvons aussi que ces résultats sont robustes à la présence d'effets non linéaires perturbatifs qui rompent l'intégrabilité de la dynamique des ondes. La figure 1 montre le principe de la collision de deux gaz monochromatiques, en présentant son évolution spatio-temporelle ainsi que le changement de vitesse relative induit.

Références

1. G. A. El & A. M. Kamchatnov, Kinetic equation for a dense soliton gas, *Phys. Rev. Lett.*, **95**, 204101 (2005).
2. L. Fache, F. Bonnefoy, G. Ducrozet, F. Copie, F. Novkoski, G. Ricard, G. Roberti, É. Falcon, P. Suret, G. El & S. Randoux, Interaction of soliton gases in deep-water surface gravity waves , *Phys. Rev. E*, **109**, 034207 (2024).

The influence of rotation on salt-fingers

Smiron Varghese, Wouter Bos, Benjamin Miquel

CNRS, École Centrale de Lyon, INSA Lyon, Université Claude Bernard Lyon 1, Laboratoire de Mécanique des Fluides et d'Acoustique, UMR5509, 69130, Ecully, France
smiron.varghese@ec-lyon.fr, benjamin.miquel@cnrs.fr

Salt-fingering convection is one example among the broad class of doubly–diffusive instabilities: when a stable stratification ($\partial_z \rho < 0$) results from a stable temperature stratification and an antagonistic unstable chemical composition stratification, the diffusivity ratio may drive the growth of slender structures, coined salt-fingers in the oceanographic context. This instability is also expected to occur in other geo- and astrophysical systems such as planetary and stellar cores [1] where rotation plays a crucial role [2].

In order to model the polar region of a planet or star, we study salt-fingering convection in a horizontal layer of fluid rotating about a vertical axis, as a step of intermediate complexity towards the spherical problem [3,4]. In this simplified geometry, we present the scalings obtained by linear stability analysis for both the threshold of the instability and the wavelength at onset. Different regimes exist, including one regime reminiscent of rapidly rotating Rayleigh–Bénard convection [2]. In addition, these predictions from linear theory are illustrated by 3D direct numerical simulations in the statistically-stationary regime [5].

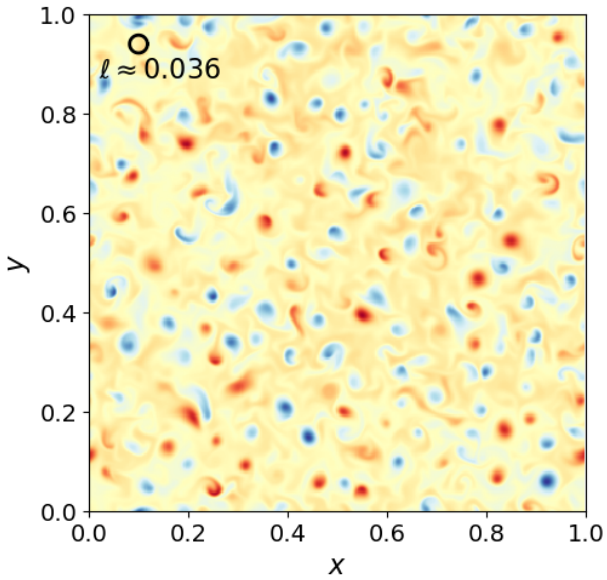

Figure 1. Salinity in the horizontal plane at mid-depth of a rapidly rotating layer in the stationary regime. Compared to the bottom surface, the top surface is kept at larger temperature (a stabilizing effect) and salinity (destabilizing). The black circle has a diameter representing the characteristic scale $\ell \approx 0.036$ of the fastest growing mode predicted by linear theory.

References

1. P. Garaud, Double-diffusive convection at low Prandtl number, *Annu. Rev. Fluid Mech.*, **50** 275–298 (2018).
2. S. Chandrasekhar, *Hydrodynamic and Hydromagnetic Stability*, Clarendon Press, Oxford (1961).
3. R. Monville, J. Vidal, D. Cébron & N. Schaeffer, Rotating double-diffusive convection in stably stratified planetary cores, *Geophys. J. Int.*, **219**, S195–S218 (2019).
4. C. Guervilly, Fingering convection in the stably stratified layers of planetary cores, *J. Geophys. Res. Planets*, **127**, e2022JE007350 (2022).
5. B. Miquel, Coral: A parallel spectral solver for fluid dynamics and partial differential equations, *J. Open Source Soft.*, **6**, 2978 (2021).

Correlations between scalar and vorticity reduce 2D mixing

Xi–Yuan (Bruce) Yin[1], Wesley Agoua[1], Tong Wu[2], Wouter J. T. Bos[1]

[1] CNRS, École Centrale de Lyon, INSA Lyon, Universite Claude Bernard Lyon 1, Laboratoire de Mécanique des Fluides et d'Acoustique, UMR5509, 69130, Ecully, France
[2] Theoretical Physics I, University of Bayreuth, Bayreuth, Germany
wouter.bos@ec-lyon.fr

Invariants play a major role in the study of turbulence and turbulent mixing. The correlation $Q = \langle \omega \phi \rangle$ between a passive scalar ϕ and the vorticity ω of the flow is an invariant of the two-dimensional Euler equations advecting a passive scalar. The question we address in the present investigation is: "how does this correlation affect the mixing rate".

We first consider mixing in a Galerkin truncated Euler system, i.e. the dynamics of a finite number of Fourier modes advecting a passive scalar. This system allows rigorous treatment by equilibrium statistical mechanics. The results point to the importance of Q and the initial energy distribution for mixing. For most initial conditions it is shown that a strong correlation Q results in bad mixing.

To investigate the dynamics, we use a recently developed numerical method [1] to investigate the non-truncated Euler and advection equations. Simulations (See Fig. 1) confirm the insights from statistical mechanics: the initial correlation Q is of major importance for mixing [2] and strong initial correlations dramatically reduce the mixing rate. Implications are discussed for the generation of helicity in anisotropic turbulence [3], a system which turns out to be directly related to 2D mixing.

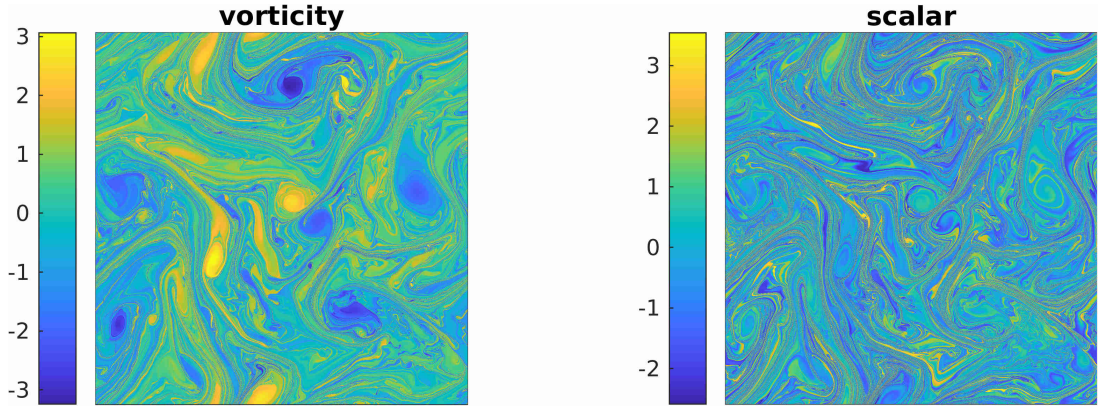

Figure 1. Vorticity and scalar field, computed using the characteristic mapping method. Initial correlations between the fields are conserved and will strongly affect the mixing rate.

References

1. X.-Y. Yin, O. Mercier, B. Yadav, K. Schneider & J.-C. Nave, A characteristic mapping method for the two-dimensional incompressible Euler equations, *J. Comput. Phys.*, **424**, 109781 (2021).
2. X.-Y. Yin, W. Agoua, T. Wu & W. J. T. Bos, The influence of the vorticity-scalar correlation on mixing, in preparation.
3. W. Agoua, B. Favier, A. Delache, A. Briard & W. J. T. Bos, Spontaneous generation and reversal of helicity in anisotropic turbulence, *Phys. Rev. E*, **103**, L061101 (2021).

Lagrangian predictability in weakly ageostrophic surface ocean turbulence

Stefano Berti[1], Michael Maalouly[1], Guillaume Lapeyre[2]

[1] Univ. Lille, ULR 7512, Unité de Mécanique de Lille Joseph Boussinesq (UML), F-59000 Lille, France
[2] LMD/IPSL, CNRS, Ecole Normale Supérieure, PSL Research University, 75005 Paris, France
stefano.berti@polytech-lille.fr

Upper-ocean turbulent flows at horizontal length scales smaller than the deformation radius (the submesoscale range) depart from geostrophic equilibrium and develop important vertical velocities, which are key to marine ecology and climatic processes. Due to their small size and fast temporal evolution, these fine scales are difficult to measure from satellites and in oceanographic campaigns. New, high-resolution satellite altimetry has very recently started to reveal them. However, to compute horizontal transport properties or surface energy exchanges, it is crucial to assess how well the horizontal velocities provided by the satellite compare to actual surface currents and down to what length scale. Indeed, the satellite-derived velocities should represent the geostrophic flow component, and the impact of unresolved ageostrophic motions on transport and dispersion features needs to be assessed. In this study, we investigate ocean submesoscale turbulence from a Lagrangian point of view, relying on numerical simulations of a model including (weakly) ageostrophic motions [1,2]. The model originates from a Rossby-number expansion of the primitive equations and recovers the surface quasi-geostrophic one [3], a paradigm of submesoscale dynamics, in the limit of vanishing Rossby number. We focus on the predictability of the full Lagrangian trajectories when using a filtered flow, where ageostrophic motions are artificially removed. Specifically, we consider Lagrangian tracer dynamics for particles advected by either the total velocity field or by its geostrophic component only, to perform a systematic comparison of the flow transport properties, in terms of single and two-particle statistics. Our results indicate that, over long times, both the particle mean-square displacement and relative dispersion are only weakly affected by the ageostrophic component of the velocity field. However, advection by the geostrophic-only flow tends to overestimate the typical pair-separation rate. We then provide a characterization of the temporary particle clusters that form due to ageostrophic motions, showing that Lagrangian tracers preferentially accumulate in cyclonic frontal regions, in agreement with observations from real drifters. We further find that, while compressibility is always small in our simulations, due to the smallness of the Rossby numbers explored, the intensity of clustering can be relevant. Our analysis suggests that, in this system, clustering is essentially due to the interplay between the (small) flow compressibility and the existence of long-lived structures that trap particles, enhancing their aggregation.

References

1. G. J. Hakim, C. Snyder & D. J. Muraki, A new surface model for cyclone-anticyclone asymmetry, *J. Atmos. Sci.*, **59**, 2405–2420 (2002).
2. M. Maalouly, G. Lapeyre, B. Cozian, G. Mompean & S. Berti, Particle dispersion and clustering in surface ocean turbulence with ageostrophic dynamics, *Phys. Fluids*, **35**, 126601 (2023).
3. G. Lapeyre, Surface quasi-geostrophy, *Fluids*, **2**, 7 (2017).

Turbulent convection and magnetically-driven flows in Europa's subsurface ocean.

Florentin Daniel[1], Christophe Gissinger[1,2], Ludovic Petitdemange[3]

[1] Laboratoire de Physique de l'École normale supérieure, ENS, Université PSL, CNRS, Sorbonne Université, Université de Paris, Paris, France
[2] Institut Universitaire de France (IUF), Paris, France
[3] Laboratoire d'Études du Rayonnement et de la Matière en Astrophysique et Atmosphères (LERMA), Observatoire de Paris, PSL, CNRS, Sorbonne Université, Paris, France
florentin.daniel@phys.ens.fr

Jupiter's icy moons (Ganymede, Callisto, Europa) have been the focus of recent space missions and telescope observations, which have suggested the existence of liquid oceans beneath the outer layer of ice. However, the fact that water can remain liquid under the ice crust is not fully understood. The classic explanation is that the disintegration of silicate mantle rocks provides a significant radiogenic heat flux from the seafloor. The associated thermal convection modifies heat transfer in the ocean and therefore has an impact on the thickness of the ice crust, possibly influencing the generation of water plumes at the surface [1]. Two other effects have proved important for ocean dynamics: tidal forces [2] and Jupiter's magnetic influence on the conducting ocean, which generates a substantial jet of a few cm/s near the equator and consequent ohmic heating [3]. This magnetohydrodynamic effect could be partly responsible for the dynamics of the cracks visible on Europa's surface. This jet could rival that due to convection within a certain range of parameters.

Using direct numerical simulations of Europa's subsurface ocean, we will discuss how the nonlinear coupling of thermal convection with magnetohydrodynamic effects impacts the resulting zonal flow and heat transport in the ocean. Emphasis will be placed on the generation of turbulence in the flow, and on how this turbulence modifies the spatial distribution of heat flux within the ocean. In the perspective of upcoming JUICE and CLIPPER space missions data, these realistic nonlinear direct numerical simulations aim to provide a model that is directly comparable with observational data. In particular, our DNS could provide informations on turbulent dissipation in the ocean, thought to be linked to the structures observed at the surface and the thickness of the ice.

References

1. K. Soderlund, B. E. Schmidt, J. Wicht & D. D. Blankenship, Ocean-driven heating of Europa's icy shell at low latitudes, *Nat. Geosci.*, **7**, 16–19 (2013).
2. D. Lemasquerier, C. J. Bierson & K. M. Soderlund, Europa's ocean translates interior tidal heating patterns to the ice-ocean boundary, *AGU Adv.*, **4**, e2023AV000994 (2023).
3. C. Gissinger & L. Petitdemange, A magnetically driven equatorial jet in Europa's ocean, *Nat. Astron.*, **3**, 401–407 (2019).

Cooperation between two objects moving side-by-side in a granular medium

Douglas D. Carvalho[1,2], Yann Bertho[1], Antoine Seguin[1], Erick M. Franklin[2], Baptiste Darbois Texier[1]

[1] Université Paris-Saclay, CNRS, Laboratoire FAST, 91405 Orsay, France.
[2] Faculdade de Engenharia Mecânica, Universidade Estadual de Campinas (UNICAMP), Rua Mendeleyev, 200 Campinas, SP, Brazil
baptiste.darbois-texier@universite-paris-saclay.fr

Various practical situations involve the movement of several objects in a granular medium, such as animal locomotion or civil engineering applications. Interactions between objects moving close to each other in grains have been the topic of several studies. In the case where the objects move freely, it has been shown that they repel each other at short distances and attract each other at intermediate distances [1]. These observations have motivated the study of the side force experienced by two threaded objects placed side-by-side into grains [2]. Numerical simulations have also shown that the interaction between objects has an impact on the drag they experience [3]. However, experimental confirmation of this effect on drag force has yet to be established.

Figure 1. Two spheres (20 mm in diameter) moving side-by-side close to the surface of a granular medium.

In order to fill this gap, we investigate experimentally the drag experienced by a pair of spherical intruders moving side-by-side into grains at constant depth and constant velocity (Fig. 1). We quantify the influence of the separation distance between the spheres and their depth below the granular surface. When the intruders are sufficiently far apart, they do not interact and the average drag felt by each of them corresponds to that of a single intruder. However, for a small separation between the intruders, the mean drag is reduced, confirming the existence of a cooperative effect that facilitates motion. In addition, the relative drag reduction is observed to increase with burial depth. We propose a model for the drag reduction of a pair of intruders based on the breakup of contact chains caused by the shear generated by the neighbouring intruder. These results provide new insights into the interaction between solid objects that move together in grains, as in the case of animal locomotion in sand or the growth of plant roots in soil.

References

1. F. Pacheco-Vázquez & J. C. Ruiz-Suárez, *Nat. Commun.*, **1**, 123 (2010).
2. G. A. Caballero-Robledo, M. F. Acevedo-Escalante, F. Mandujano & C. Málaga, *Phys. Rev. Fluids*, **6**, 084303 (2021).
3. D. D. Carvalho & E. M. Franklin, *Phys. Fluids*, **34**, 123306 (2022).

Envelope vector solitons in nonlinear flexible mechanical metamaterials

Antoine Demiquel, Vassos Achilleos, Georgios Theocharis, Vincent Tournat

Laboratoire d'Acoustique de l'Université du Mans (LAUM), UMR 6613, Institut d'Acoustique - Graduate School (IA-GS), CNRS, Le Mans Université, France
antoine.demiquel@univ-lemans.fr

Nonlinear flexible mechanical metamaterials (flexMMs) are architected materials consisting of highly deformable soft elements connected to stiffer ones. Their capacity to undergo large local deformations implies a geometric nonlinearity. Both nonlinear and linear behaviors can be tuned by changing the geometry and the materials of the structure (cf. Fig. 1 (a)). Various nonlinear wave effects have been studied and unveiled, including pulse vector solitons, rarefaction solitary waves, transition waves, and topological solitons through bistable structures [1]. Many interesting wave phenomena are expected to occur, including the manifestation of modulation instability (MI) [2]; up to now theoretically described and numerically observed. Moreover the formation of localized waves, such as discrete envelope solitons (bright and dark solitons) or breather solitons [3] represent intriguing phenomena that hold the potential for yielding conclusive results in the flexMM thematic.

In this presentation, we are interested in modulated wave propagation along flexMMs. Using a lump element approach, we formulate discrete equations that describe the longitudinal and rotational displacements of each individual rigid unit mass constituing the chain. In a second part, analytical and numerical tools employed in order to find an effective nonlinear Schrödinger (NLS) equation are discussed. The final equation describes the envelope of weakly dispersive and nonlinear waves. Leveraging on the bright and dark soliton solutions of the NLS equation, we can ascertain the required initial conditions for propagating these solitons within the lattice see Fig. 1 (b).

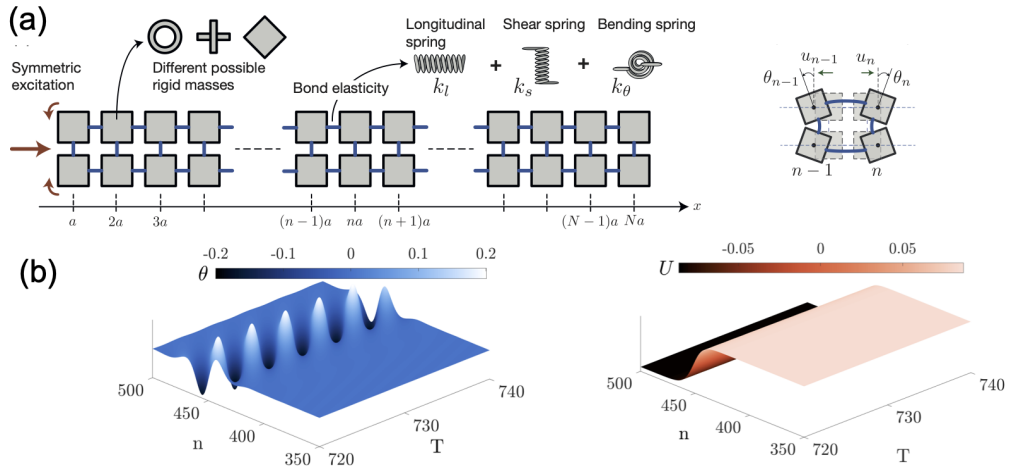

Figure 1. (a) Sketch of the flexMM under consideration. (b) Propagation of a lattice bright envelope vector soliton along the structure.

References

1. B. Deng, J. R. Raney, K. Bertoldi & V. Tournat, Nonlinear waves in flexible mechanical metamaterials, *J. Appl. Phys.*, **130**, 040901 (2021).
2. A. Demiquel, V. Achilleos, G. Theocharis & V. Tournat, Modulation instability in nonlinear flexible mechanical metamaterials, *Phys. Rev. E*, **107**, 054212 (2023).
3. N. Boechler, G. Theocharis, S. Job, P. G. Kevrekidis, M. A. Porter & C. Daraio, Breathers in one-dimensional diatomic granular crystals, *Phys. Rev. Lett.*, **104**, 244302 (2009).

3D tracking of microswimmers under flow and in a complex confinement

Jeanne Moscatelli, Florence Elias

Laboratoire PMMH, ESPCI, 7 quai Saint Bernard 75005 Paris
jeanne.moscatelli@espci.fr

Weather permitting, a natural, very persistent foam may appear on the seashore, due to the bloom of certain microalgae in the water. During this period, a decrease in the diversity and quantity of microalgae is observed in the environment. This observation and our previous experiments [1, 2] lead us to believe that microalgae are trapped in the interconnected channels known as Plateau borders, which lie between the foam bubbles. As these microalgae are motile, our study aims to understand the interactions between foam and active matter. We conduct our experiments on a model biflagellate microalgae, *Chlamydomonas reinhardtii*. We place the latter with a concentration of 10^6 cells $\cdot$ L^{-1} in a 200 µm vertical square capillary, so that the microswimmers are exposed to a confinement resembling the one inside foams and to a complex space geometry including corners, similar to Plateau borders (cf. Fig. 1). In addition, we track individuals under different flow speeds, from no flow to an average speed of 125 µm $\cdot$ s^{-1}, which corresponds to the typical flow velocity in the Plateau borders of a freely draining foam. To visualize the 3D trajectories of the microswimmers, we use a laser that we pass through the capillary to excite the natural fluorescence of the chlorophyll found in the microalgae. By placing two mirrors on either side of the capillary, we can visualize the projections of the individuals' positions on two parallel planes, enabling us to reconstruct the trajectories in three dimensions. Thanks to this system, we can quantify the interaction of the swimming motion with the walls and with the Poiseuille flow, and compare these measurements with existing theoretical predictions [3]. So we intend to compare our experimental data with these predictions. We also look at the density of presence in the capillary and the behaviors in the corners to understand the effects of complex geometry and gravity on swimming.

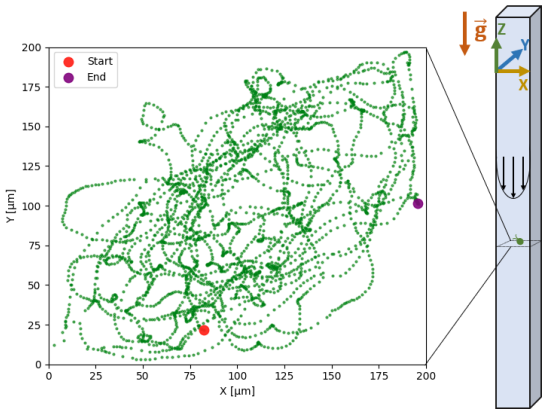

Figure 1. The trajectory of one algea in a Poiseuille flow, seen from above, for a duration of 1 minute ($\bar{v}_{\text{Poiseuille}} = 42$ µm $\cdot$ s^{-1})

References

1. Q. Roveillo, J. Dervaux, Y. Wang, F. Rouyer, D. Zanchi, L. Seuront, F. Elias , Trapping of swimming microalgae in foam, *J. R. Soc. Interface*, **17**, 20200077 (2020).
2. A. Théry, Y. Wang, M. Dvoriashyma, C. Eloy, F. Elias, E. Lauga, Rebound and scattering of motile Chlamydomonas algae in confined chambers, *Soft Matter*, **17**, 4857–4873 (2021).
3. A. Zöttl, H. Stark, Nonlinear dynamics of a microswimmer in Poiseuille flow, *Phys. Rev. Lett.*, **108**, 218104 (2012).

Interaction between structures in a Couette–Poiseuille flow

Benoît Semin, Tao Liu, Ramiro Godoy-Diana, José Eduardo Wesfreid

PMMH, CNRS, ESPCI Paris, Université PSL, Sorbonne Université, Université Paris Cité, F-75005, Paris, France
benoit.semin@espci.fr

In the transition regime, active turbulence is localized in turbulent spots in wall-bounded shear flows, which are for instance flows between two parallel plates. They contain coherent structures, such as streamwise vortices called rolls and modulations of the streamwise velocity called streaks. Many theoretical and numerical works have shown that the nonlinear interaction between these structures is responsible for the self-sustaining process (SSP) of the turbulence, but experimental studies are scarce. We investigate experimentally the interaction between these coherent structures using two sets of experiments.

We perform the experiments in a plane Couette-Poiseuille channel in which the flow is driven by a moving belt and connected to two reservoirs so that the mean flux is zero (fig. 1A). The direction of the moving belt defines the streamwise direction x, z is the spanwise direction and y the wall-normal direction. The streaks are quantified by the streamwise velocity fluctuations u_x, and the rolls by the spanwise velocity u_z and by the wall-normal velocity u_y.

In the first set of experiments, we study the decay of turbulence using a 'quench' protocol, i.e. an abrupt decrease of the Reynolds number Re from a fully turbulent state to a laminar regime [1]. We show that the rolls decay faster than the streaks. The streaks have two decay stages in the decay process. During the first stage of the decay, the remaining rolls slow down the decay of the streaks. This is consistent with the lift-up effect, i.e. the formation of streaks by linear advection of the rolls.

In a second set of experiments, we study the waviness of streaks using vortex generators to induce unstable wavy streaks [2]. The evolution of the streaks becoming wavy from a straight state is characterized using stereoscopic PIV, and processed using a new method that we developed. Using spatial Fourier filtering, we define a proxy for the waviness $\langle|\omega_{y,\mathrm{wavy}}|\rangle$. Our experimental results show that the wall-normal velocity, which is a proxy for the rolls, is correlated to the increase of the waviness of the streaks, as expected from SSP models (fig. 1B). Moreover, for streaks of low waviness, the value of $|u_y|$ is small and related to the amplitude of the streak $|u_x|$, as expected for linear lift-up.

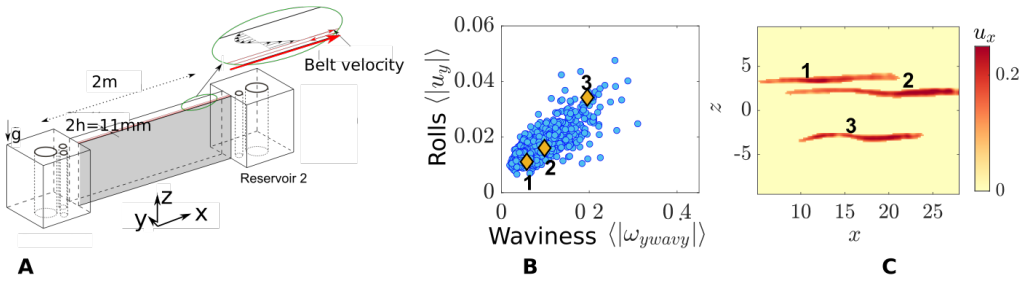

Figure 1. A: schematic view of the experimental set-up. B: link between rolls and waviness, a point corresponds to the average on a streak. C: corresponding streaks for the three points indicated in B.

References

1. T. Liu, B. Semin, L. Klotz, R. Godoy-Diana, J. E. Wesfreid & T. Mullin, Decay of streaks and rolls in plane Couette–Poiseuille flow, *J. Fluid Mech.*, **915**, A65 (2021).
2. T. Liu, B. Semin, R. Godoy-Diana & J. E. Wesfreid, Lift-up and streak waviness drive the self-sustained process in wall-bounded transition to turbulence, *Phys. Rev. Fluids*, **9**, 033901 (2024).

Rheo-inertial transition to turbulence in pipe flow

Antoine Charles[1], Jorge Peixinho[2], Thierry Ribeiro[3], Sam Azimi[4], Vincent Rocher[4], Jean-Christophe Baudez[1], S. Amir Bahrani[1]

[1] IMT Nord Europe, Institut Mines Télécom, Univ. Lille, Center for Energy and Environment, F-59000 Lille
[2] Arts et Métiers Institute of Technology, CNRS, CNAM, PIMM, HESAM Université, Paris, France
[3] Institut Polytechnique UniLaSalle, Université d'Artois, ULR 7519, 19 rue Pierre Waguet, 60000 Beauvais, France
[4] SIAAP - Service public pour l'assainissement francilien, Direction Innovation, 82 avenue Kléber, 92700 Colombes, France

antoine.charles@imt-nord-europe.fr

The transition to turbulence in cylindrical pipes is still not fully understood despite extensive studies since the Reynolds experiment in the early 1880s [1], even more for non-Newtonian fluids, see recent reviews [2,3]. We focused here on the mechanism leading to the transition to turbulence in pipe for yield-stress shear-thinning fluids. This transition occurs for purely shear-dependant viscosity fluids (without elastic effects) due to their rheological behaviors, so called here *rheo-inertial transition to turbulence*. An experimental setup allowed us to identify flow regimes in a cylindrical pipe, by combining flow structures visualisations and pressure drops measurements. We observed a new regime in the rheo-inertial laminar-turbulent transition, triggered below the turbulent puffs onset. This pre-transition regime is characterised by a flow asymmetry [4–6] in which its position and degree evolve with the Reynolds number [7]. The origin for the rheo-inertial regime stability could be due to a favourable competition between the non-linear contributions of rheological behavior and flow inertia. Beyond this regime, we quantified the puff transit intermittence. It revealed the delay to turbulence caused by the yield stress. It also revealed for the first time a different rheo-inertial transitional behavior in the intermittency evolution versus Reynolds, with a smoother transition on a broader Reynolds hydrodynamical range. Finally the increasing delay to the onset of turbulent puffs with the yield stress is highlighted.

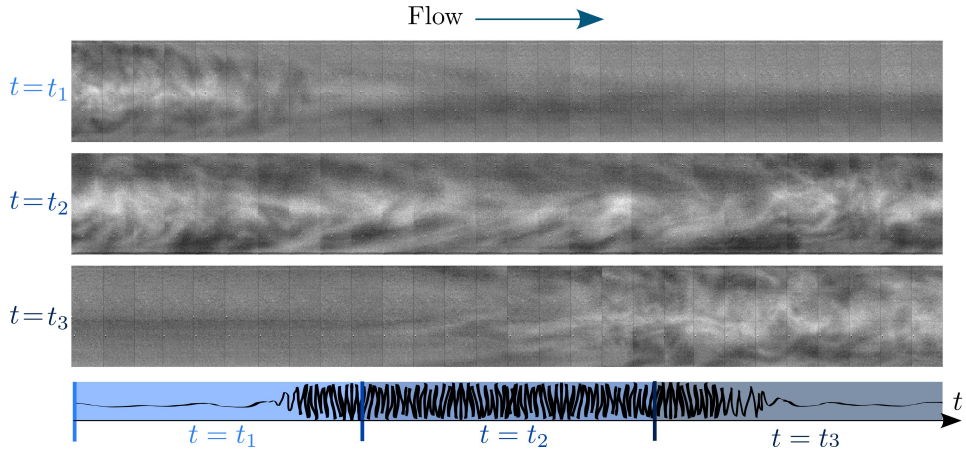

Figure 1. Flow visualisations on a yield-stress fluid at Re = 3,875.

References

1. O. Reynolds, *Philos. Trans. R. Soc.*, **174**, 935–982 (1883).
2. B. Eckhardt, *Physica A*, **504**, 121–129 (2018).
3. M. Avila, D. Barkley & B. Hof, *Annu. Rev. Fluid Mech.*, **5**, 575–602 (2022).
4. M. P. Escudier *et al.*, *J. Nonnewton. Fluid Mech.*, **127**, 143–155 (2005).
5. J. Peixinho, C. Nouar , C. Desaubry & B. Théron, *J. Nonnewton. Fluid Mech.*, **128**, 172–184 (2005).
6. S. A. Bahrani & C. Nouar, *J. Appl. Fluid Mech.*, **7**, 1–6 (2014).
7. C. Wen, R. Poole, A. P. Willis & D. J. C. Dennis, *Phys. Rev. Fluids*, **2**, 1–8 (2017).

Nonlinear dynamics of zonal flows and geodesic acoustic modes in ITER

Didier Gossard[1], Alessandro Biancalani[2], Alberto Bottino[3], Thomas Hayward-Schneider[3], Philipp Lauber[3], Alexey Mishchenko[4], Martin Pujol[1], Martin Rampont[1], Juvert N. Sama[5], Laurent Villard[6]

[1] École Supérieure d'Ingénieurs Léonard de Vinci, 92916 Paris La Défense, France
[2] Léonard de Vinci Pôle Universitaire, Research Center, 92916 Paris La Défense, France
[3] Max Planck Institute for Plasma Physics, 85748 Garching, Germany
[4] Max Planck Institute for Plasma Physics, 17491 Greifswald, Germany
[5] Institut Jean Lamour UMR 7198, Université de Lorraine-CNRS, Nancy 54011, France
[6] École Polytechnique Fédérale de Lausanne, Swiss Plasma Center, CH-1015 Lausanne, Switzerland
didier.gossard@devinci.fr

Turbulence develops in tokamak plasmas, due to the gradients of the density and temperature profiles. Zonal, i.e. axisymmetric, flows take part in the nonlinear saturation of turbulence. Two kinds of zonal flows exist: zero frequency zonal flows (ZFZF) [1], and finite frequency geodesic acoustic modes (GAM) [2]. GAMs can also be driven by energetic particles (EP) due to inverse Landau damping, taking the name of EP-driven GAMs (EGAM). In this paper, we investigate the dynamics of zonal flows in the absence and in the presence of EPs with the gyrokinetic particle-in-cell code ORB5 [3]. The ITER pre-fusion-power-operation plasma scenario [4] is considered for these numerical simulations. The nonlinear interaction of EPs and EGAMs is investigated. We observe the EP redistribution in phase space, once the EGAM has reached saturation. The corresponding amplitude of EGAMs is estimated for this ITER experimental regime.

References

1. A. Hasegawa, C. G. Maclennan & Y. Kodama, Nonlinear behavior and turbulence spectra of drift waves and Rossby waves, *Phys. Fluids*, **22**, 2122–2129 (1979).
2. N. Winsor, J. L. Johnson & J. M. Dawson, Geodesic acoustic waves in hydromagnetic systems, *Phys. Fluids*, **11**, 2448–2450 (1968).
3. E. Lanti etal., Orb5: A global electromagnetic gyrokinetic code using the PIC approach in toroidal geometry, *Comp. Phys. Commun.*, **251**, 107072 (2020).
4. T. Hayward-Schneider, Ph. Lauber, A. Bottino & A. Mishchenko, Multi-scale analysis of global electromagnetic instabilities in ITER pre-fusion-power operation plasmas, *Nucl. Fusion*, **62**, 112007 (2022).

Détection de contact d'ordre élevé entre fibres

Emile Hohnadel, Octave Crespel, Thibaut Métivet, Florence Bertails-Descoubes

Univ. Grenoble Alpes, Inria, CNRS, Grenoble INP, LJK
emile.hohnadel@inria.fr

Dans ce travail, nous cherchons à évaluer et améliorer la précision des forces de contact calculées dans une assemblée de fibres. Nous identifions la phase de détection de collision comme une source importante d'artefacts numériques dans la réponse en force lorsque la détection se fait entre primitives de bas degré géométrique, typiquement des segments. Nous quantifions ces artefacts sur un scénario contrôlé (test du trois points), en comparant deux modèles de fibre (Super-Hélice [2] et Discrete Elastic Rod [3]) couplés à un solveur non régulier de contact frottant [4], voir figure 1 à gauche.

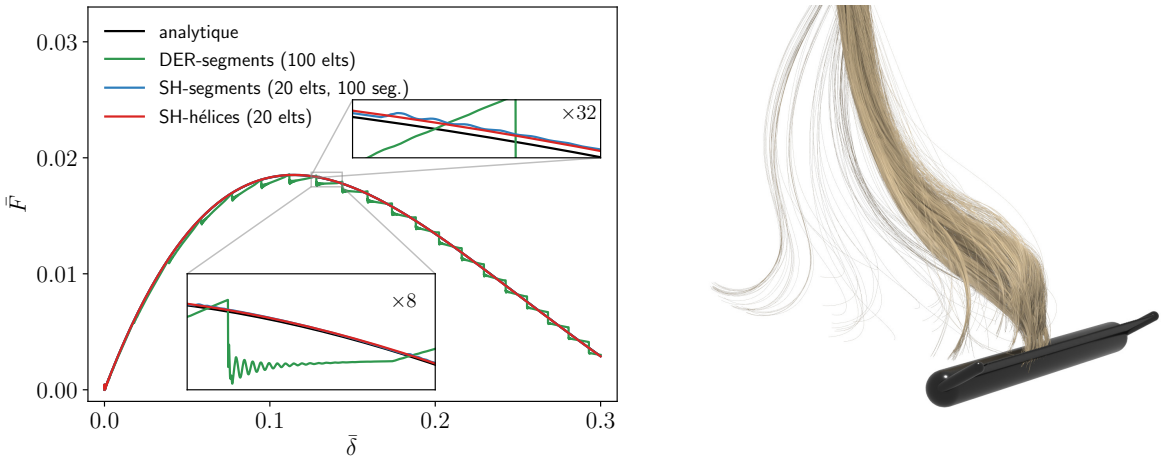

Figure 1. À gauche : Comparaison de la réponse en force normalisée $\bar{F}$ en fonction de l'indentation normalisée $\bar{\delta}$ du test du trois points avec plusieurs méthodes de détection de contact. Les sauts visibles résultent des jonctions non lisses entre les primitives de détection (segments), et sont d'autant plus visibles que la courbure de la fibre est importante. À droite : Peignage d'une mèche de cheveux ; notre algorithme permet la simulation robuste de plusieurs milliers de fibres en contact frottant avec évaluation précise des forces de contact.

Afin d'éliminer ces artefacts, nous proposons un algorithme efficace [1] pour calculer la distance entre deux courbes lisses, que nous appliquons au modèle lisse de Super-Hélice. Nous démontrons enfin la validité et la robustesse de notre méthode dans des scénarios 3D complexes mettant en jeu des dizaines de milliers de points de contact, comme le peignage d'une mèche de cheveux, voir figure 1 à droite.

Références

1. O. Crespel, E. Hohnadel, T. Metivet & F. Bertails-Descoubes, Contact detection between fibres : High order makes a difference, soumis, https://hal.science/hal-04364565v1/ (2023).
2. F. Bertails, B. Audoly, M.-P. Cani, B. Querleux, F. Leroy & J.-L. Lévêque, Super-helices for predicting the dynamics of natural hair, *ACM Trans. Graph.*, **25**, 1180–1187 (2006).
3. M. Bergou, M. Wardetzky, S. Robinson, B. Audoly & E. Grinspun, Discrete elastic rods, *ACM Trans. Graph.*, **27**, 1–12 (2008).
4. G. Daviet, F. Bertails-Descoubes & L. Boissieux, A hybrid iterative solver for robustly capturing coulomb friction in hair dynamics, *ACM Trans. Graph.*, **30**, 1–12 (2011).

Le collage dans des systèmes hamiltoniens : l'exemple de l'application standard

Simon Rouvet, Xavier Leoncini, Perla El Kettani

Aix-Marseille Université, Université de Toulon, CNRS, CPT, Marseille, France
simon.rouvet@cpt.univ-amu.fr

Le pari de la Physique Statistique consiste à décrire un système possédant $O(10^{23})$ degrés de liberté microscopiques à l'aide de $O(1)$ degrés de liberté macroscopiques. Le passage des variables microscopiques (p, q) vers les variables macroscopiques $(E, P, V, T, ...)$ tient à la condition que le système soit ergodique, c'est-à-dire qu'il se comporte de manière "suffisamment" aléatoire.

On propose de rediscuter cette hypothèse pour un système dynamique connu : l'Application Standard [1]. Des travaux récents [2] montrent que des pseudo-pièges habitent l'espace des phases : les zones de collage [3]. Ces zones de collage engendrent du transport anomal à la manière des vols de Lévy (persistence des fluctuations). De plus, elle se déploient au coeur d'une fractale dans le voisinage des îlots de stabilité.

L'enjeu de ce travail est d'identifier ces zones de collage et de clarifier leur rôle vis-à-vis de la relaxation du système vers l'équilibre. La méthode utilisée consiste à exploiter des distributions de moyennes temporelles en temps finis d'une observable $s(p, q)$ [4]. Ces distributions révèlent des pics très localisés qui correspondent exactement aux zones de collage. Or, l'ergodicité nous assure que ces pics de collage doivent disparaître aux temps longs, néanmoins, leur influence sur la dynamique et le transport reste très forte. En somme, on explore de nouveaux angles d'études vers la physique statistique hors d'équilibre.

Références

1. B. V. Chirikov, Universal instability of many-dimensional oscillator systems, *Phys. Rep.*, **52**, 263–379 (1979).
2. L. Bouchara, O. Ourrad, S. Vaienti & X. Leoncini, Anomalous transport and observable average in the standard map, *Chaos Solit. Fractals*, **78**, 277–284 (2005).
3. G. M. Zaslavsky, *The Physics of Chaos in Hamiltonian Systems*, Imperial College Press, 2nd edition (2007).
4. X. Leoncini, C. Chandre & O. Ourrad, Ergodicité, collage et transport anormal, *C. R. Mécanique*, **336**, 530–535 (2008).

Bacterial exploration under confinement

Renaud Baillou[1], Marta Pedrosa García-Moreno[2], Quentin Guigue[1], Solene Meinier[1], Thierry Darnige[1], Gaspard Junot[1], Fernando Peruani[2], Éric Clément[1]

[1] Laboratoire PMMH-ESPCI Paris, Sorbonne Université, 7, quai Saint-Bernard, Paris, France.
[2] CY Cergy Paris Université, Laboratoire de Physique Théorique et Modélisation, UMR 8089.
renaud.baillou@espci.fr

E. coli undergo run and tumble kinematics, alternating between 3D swimming and quasi-2D exploration of surfaces (see figure 1). In the absence of boundaries and in a chemically uniform environment, the combination of run and tumble leads to a 3D diffusive process. In numerous practical situations, such as mucus barriers, low-dimensional substrates alters this simple picture and appears as a key to control the large-scale transport and contamination properties.

Here, we address this fundamental question by combining experiment and theory using a simple prototypical setup in which bacteria swim in an environment bounded only by the presence of two parallel surfaces separated by a height H .

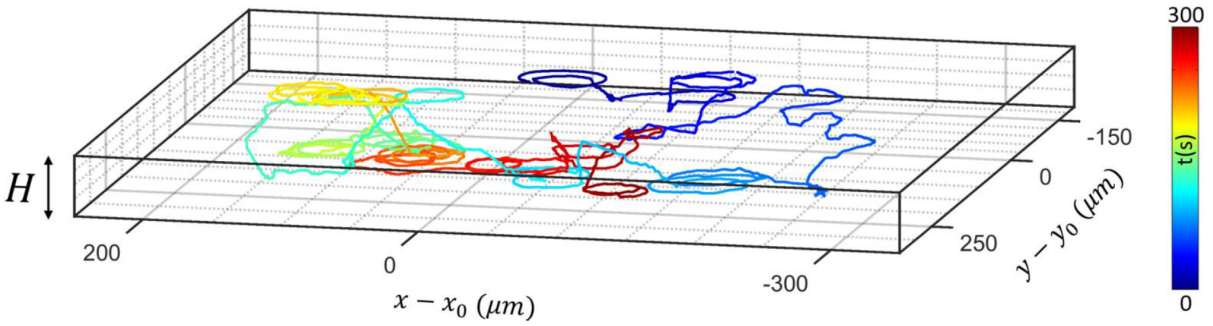

Figure 1. 3D trajectory of duration $T = 300$s of a E. coli bacterium spreading laterally between two parallel plates separated by a distance $H = 50\mu$m. Motion is circular at surfaces, straight in the bulk, and interrupted by reorientations.

We show that the emerging dispersion process along the plane differs from the boundless limit and explicitly depends on the confinement height as well as on specific features of the surface kinematics. To describe the exploration process, we use the "behavioral variability" (BV) model [1], which has recently been shown to be successful in describing bacterial residence time [3] and backflow contamination [2]. This model incorporates the fluctuations of a slowly varying internal molecular variable, called "the mood", that triggers the run-to-tumble events. In this work we have adapted it to additionally take into account the circular kinematics at surfaces.

References

1. N. Figueroa-Morales *et al.*, 3D spatial exploration by *E. coli* echoes motor temporal variability, *Phys. Rev. X*, **10**, 021004 (2020).
2. N. Figueroa-Morales *et al.*, *E. coli* super-contaminates narrow ducts fostered by broad run-time distribution, *Sci. Adv.*, **6**, eaay0155 (2020).
3. G. Junot *et al.*, Run-to-tumble variability controls the surface residence times of *E. coli* bacteria, *Phys. Rev. Lett.*, **128**, 248101 (2022).

Resonance of a floating object in a wave field

Wilson Reino[1,2], Sébastien Kuchly[3], Stéphane Perrard[3], Giuseppe Pucci[2], Antonin Eddi[3]

[1] Dipartimento di Fisica, Università della Calabria, Via P. Bucci, Cubo 31C, 87036 Rende (CS), Italia.
[2] Consiglio Nazionale delle Ricerche - Istituto di Nanotecnologia (CNR-NANOTEC), Via P. Bucci 33C, 87036 Rende (CS), Italy.
[3] PMMH, CNRS, ESPCI Paris, Université PSL, Sorbonne Université, Université de Paris Cité, F-75005, Paris, France.

wilson.reino.c@gmail.com

The evolution of the Earth's climate is causing a gradual decline in sea ice coverage in the Arctic and Antarctic. As the ice diminishes, it becomes increasingly vulnerable to environmental stresses such as winds, ocean currents, and waves. These factors contribute to ice fracturing and to the formation of the Marginal Ice Zone (MIZ), a complex region where various physical phenomena occur, including ice floes, clusters, and wave damping among others [1, 2]. Studying how a single floe deflects and attenuates incoming waves provides valuable insights into the complex processes governing the evolution of the marginal ice zone and their implications for the climate.

We designed a laboratory-scale experiment using floating plastic cylinders that simulate ice floes. Each cylinder behaves as a dynamic resonator within the wave field, absorbing energy from surrounding waves. We analyzed the interaction between surface waves and the floating object using Fast Checkerboard Demodulation (FCD), a surface reconstruction technique that extracts the pixel displacement field from a sequence of images, and enables surface topography reconstruction via the refraction at the air-liquid interface [3, 4].

We determined the resonance frequency of the floating cylinders through controlled impacts and analyzed their impulsive response in terms of the generated wave field. We mapped out the resonance frequency as a function of height and radius of the cylinders. We then explored the behavior of these plastic ice floe while interacting with incoming waves generated by a linear motor. By systematically varying the frequency of incoming waves, we quantified the response wave field generated by the floating object, identified by its maximum wave amplitude. Remarkably, we observed a distinct attenuation in this response wave field in the vicinity of the previously determined resonance frequency, indicating minimal wave generation by the floating object approximately at these frequencies. Furthermore, in this same regime the waves experienced minimal deviation near the cylinders compared with other frequencies.

These observations suggest efficient energy transmission to the object's motion when the incoming waves oscillate at the object's resonance frequency, resulting in minimal wave generation by the plastic floes when they interact with incoming waves.

References

1. V. Squire, J. Dugan, P. Wadhams, P. Rottier, & A. Liu, Of ocean waves and sea ice, *Annu. Rev. Fluid Mech.*, **27**, 115–168 (1995).
2. D. Dumont, Marginal ice zone dynamics: History, definitions and research perspectives, *Philos. Trans. R. Soc. A*, **380**, 20210253 (2022).
3. F. Moisy, M. Rabaud & K. Salsac, A synthetic Schlieren method for the measurement of the topography of a liquid interface, *Exp. Fluids*, **46**, 1021–1036 (2009).
4. S. Wildeman, Real-time quantitative Schlieren imaging by fast Fourier demodulation of a checkered backdrop, *Exp. Fluids*, **59**, 97 (2018).

Plasmas de fusion à l'équilibre thermodynamique : des particules au fluide

Yohann Lebouazda[1], Aurélien Cordonnier[1], Xavier Leoncini[1], Guilhem Dif-Pradalier[2]

[1] Aix Marseille Univ, Université de Toulon, CNRS, CPT, Marseille, France.
[2] CEA, IRFM, Saint-Paul-lez-Durance, F-13108, France.
yohann.lebouazda@cpt.univ-mrs.fr

Que pouvons-nous apprendre des équilibres thermodynamiques de plasmas ? On s'intéresse d'abord à la cinétique des plasmas de fusion : les propriétés de la dynamique collective de particules chargées interagissant via un champ magnétostatique moyen. Ensuite, aux écoulements de fluide chargé correspondant aux solutions à l'étude.

On se place dans une colonne de plasma, à symétrie cylindrique. Les équilibres cinétiques en question sont modélisés par des solutions stationnaires de l'équation de Boltzmann (sans collisions) maximisant l'entropie du système en accord avec les quantités conservées lors des trajectoires :

$$\frac{\mathrm{d}f}{\mathrm{d}t} = 0 \ ; \ \delta\left(S[f] - \beta E[f] - \gamma P[f] - \mu N[f]\right) = 0, \tag{1}$$

d'où la qualification de « thermodynamique ». $f(x, p, t)$ est la distribution d'états, E, P sont respectivement des contraintes de convservation de l'énergie et de moment cinétique, et N la conservation du nombre de particules. Ce travail est présenté plus en profondeur dans [1].

Côté fluide chargé, ces solutions équivalent à des écoulements non nuls et non visqueux. Pour arriver à cette conclusion, on étudie le même modèle qu'en cinétique dans un contexte de magnétodynamique des fluides idéale.

Références

1. A. Cordonnier, X. Leoncini, G. Dif-Pradalier & X. Garbet, Full self-consistent Vlasov–Maxwell solution, *Phys. Rev. E*, **106**, 064209 (2022).

Jet creation at the tip of a submerged plate forced by waves

Diane Komaroff[1], Gatien Polly[1], Alexis Mérigaud[2], Ramiro Godoy-Diana[1], Benjamin Thiria[1]

[1] Laboratoire de Physique et Mécanique des Milieux Hétérogènes (PMMH), Paris, France
[2] IFP Energies nouvelles, Rueil-Malmaison, France
diane.komaroff@espci.fr

Wave energy is a very good candidate for a renewable energy source because it carries enormous amounts of energy. In the case of Europe, it could make a significant contribution to electricity supply, with an estimated capacity of 300-400 GW along the European Atlantic coasts alone [1]. However, there are currently no wave energy converters (WECs) capable of harnessing wave energy on a large scale and at relatively low cost. A promising new WEC design consists of a flexible plate immersed near the free surface and exposed to the swell. For example, Shoele [2] investigated how a plate made of piezoelectric material could be used for energy harvesting. In our laboratory at PMMH, we are experimentally studying the behaviour of a flexible polycarbonate plate immersed in a wave field with a single held edge. Our system is not designed for energy recovery, but to better understand and quantify the interaction between the wave field and the plate.

Our study shows that the presence of the plate in the wave field strongly dissipates the incident wave energy. In particular, we have observed that for certain wave frequencies a significant fraction of the wave energy is dissipated by vortices shed at the edges of the plate, giving rise to a jet similar to that observed for a flapping fin, see figure 1. The wave field is measured using a Synthetic Schlieren technique [3]. In order to study and characterize in greater detail the jet created by waves forcing the flexible plate we use 2D Particle Image Velocimetry (PIV), which provides the instantaneous velocity field of particles in the fluid. Measurements are performed for plates of length $L = 19$ cm and $L = 28$ cm in different configurations of wave frequencies and amplitudes. Our experiments show that the size of the jet, its orientation and intensity depend on the membrane studied, the frequency and the amplitude of the waves. It is largest in the frequency range where wave energy dissipation is greatest. Finally, we have performed additional PIV experiments, this time in the plane orthogonal to the direction of wave propagation. Preliminary results show the existence of non-negligible transverse effects.

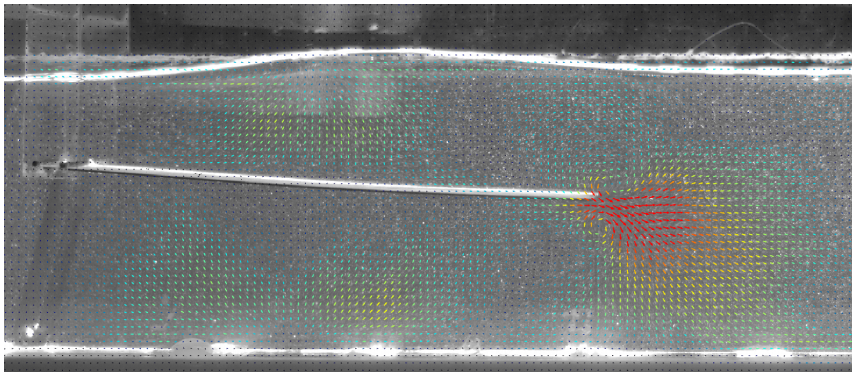

Figure 1. Example of a mean velocity field over four wave periods for waves of frequency $f = 2.4$ Hz for a plate of length $L = 19$ cm.

References

1. A. Babarit, *Ocean Wave Energy Conversion*, ISTE Press, Elsevier (2018), chap. 1.
2. K. Shoele, Hybrid wave/current energy harvesting with a flexible piezoelectric plate, *J. Fluid Mech.*, **968**, A31 (2023).
3. F. Moisy, M. Rabaud & K. Salsac, A synthetic Schlieren method for the measurement of the topography of a liquid interface, *Exp. Fluids*, **46**, 1021–1036 (2009).

Buoyancy effects in vertical soap films

Alexandre Vigna–Brummer[1,2], Antoine Monier[1], Christophe Brouzet[1], Christophe Raufaste[1,2]

[1] Institut de Physique de Nice - INPHYNI, 17, rue Julien Lauprêtre, 06200 Nice
[2] Université Côte d'Azur - UniCA, 28, avenue Valrose, 06108 Nice
alexandre.vigna-brummer@univ-cotedazur.fr

An analogy can be drawn between density stratified fluids, like oceans or atmosphere, with vertical soap films, which are stratified in thickness. To study this analogy, we have built an experimental set up to create large steady soap films, with frame sizes up to 15×25 cm^2. Fed from the top by a syringe pump, each film typically shows a lifetime from a few minutes up to one hour with stationary thickness profiles characterized by interferometry. This experimental set up allows usto introduce hair rings in the soap film to probe buoyancy effects. In particular, we study the presence of an effective Archimede's force, as each ring stabilizes at an equilibrium thickness in the film. This equilibrium position is measured experimentally as a function of ring properties (mass and radius) and compared to theoretical predictions. Additionally, by displacing the rings from their equilibrium position, we study how the ring relaxes to this position.

References

1. N. Adami & H. Caps, Capillary-driven two-dimensional buoyancy in vertical soap films, *Europhys. Lett.*, **106**, 46001 (2014).
2. Y. Couder, J.-M. Chomaz & M. Rabaud, On the hydrodynamics of soap films, *Physica D*, **37**, 384–405 (1989).

The mysterious sliding sleeve

Sébastien Neukirch[1], Francesco dal Corso[2], Yury Vetyukov[3]

[1] d'Alembert Institute for Mechanics, Sorbonne University, Paris, France
[2] DICAM-University of Trento, via Mesiano 77, I-38123 Trento, Italy
[3] Institute of Mechanics, TU Wien, Austria
sebastien.neukirch@cnrs.fr

Je souhaite montrer qu'une tige élastique, lorsqu'elle entre dans une gaine, subit une force qui tend à l'expulser de la gaine, et ce même si la gaine est sans frottement. Pour ce faire, je compare deux cas classiques de flambement de tige élastique, l'un sans gaine, et l'autre avec. Je finirai en parlant rapidement du cas où la gaine elle-même est flexible.

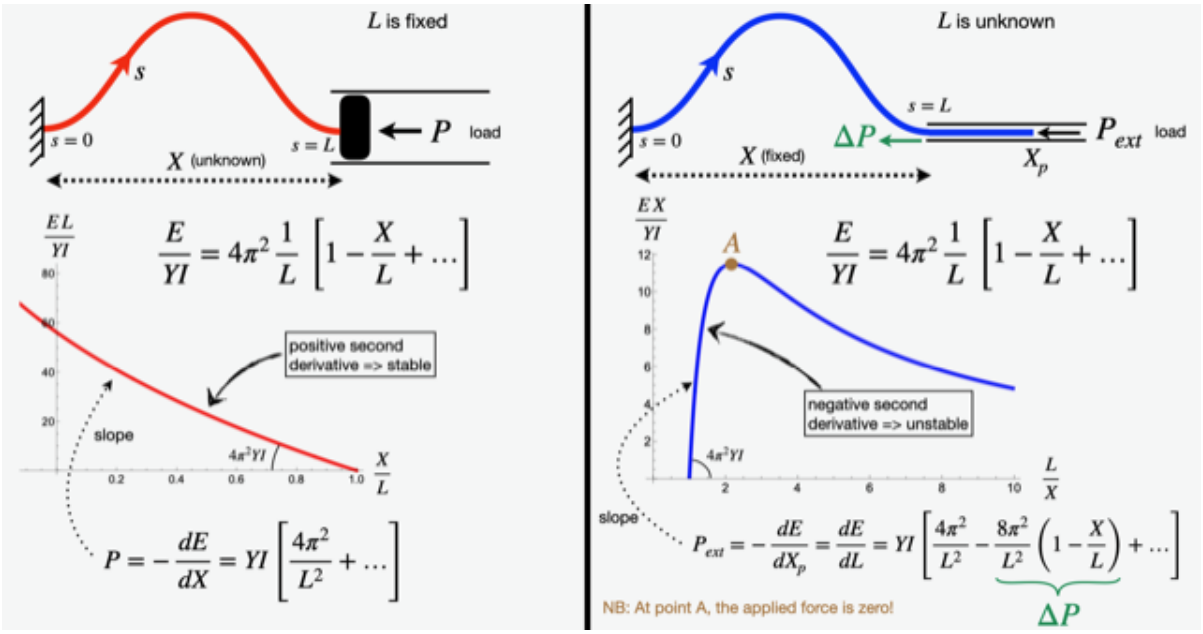

Figure 1. (à gauche) Cas classique du flambement d'une tige élastique dans le plan avec conditions de bords d'encastrement aux deux extrémités. (à droite) Cas du flambement à travers une gaine sans frottement où l'on voit apparaitre une force de compression engendrée à la sortie de la gaine.

Grain dispersion in smooth granular flows

Klebbert Andrade[1], Pierre Jop[1], Evelyne Kolb[2], Stéphanie Deboeuf[3]

[1] Surface du Verre et Interfaces, CNRS/Saint-Gobain, UMR 125, 93303 Aubervilliers, France.
[2] Physique et Mécanique des Milieux Hétérogènes, UMR 7636, 75005, Paris, France
[3] Institut Jean Le Rond d'Alembert, Place Jussieu 75252 Paris Cedex 05, Paris, France
klebbert.andrade@saint-gobain.com

Mixing plays a crucial role in various industrial processes, such as glass and concrete manufacturing, where inadequate homogenization of raw materials can significantly impact product quality. Chaotic flows are known to enhance the mixing at low Reynolds number through advection and diffusion [1]. Quantitative analysis of the homogenization processes can be made following the concentration field [2].

While numerous studies have explored mixing in different fluids, the description of granular mixing in smooth flows remains limited [3]. Differences between fluids and grains, such as the discrete nature, the lack of thermal agitation and the shear-related diffusion, contribute to a poorly understanding of the interplay between advection and diffusion, while the Peclet number is low compared to classical fluid experiments.

We developed a 2D dry granular experiment in a closed configuration to study their dispersion using a figure-eight protocol to stir the grains (Fig. 1a). Following each grains, we quantify the separation of Lagrangian trajectories and the evolution of a initially tagged particles toward a homogeneous state, focusing on the role of a global rotation of the system. Our results underscore the potential for refining dispersion models in smooth granular flows through further analysis of variance decay.

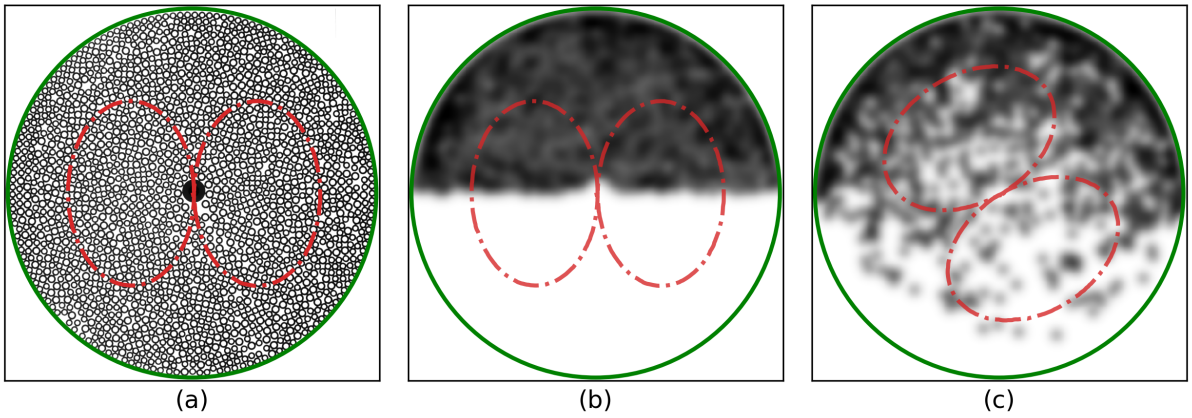

Figure 1. (a) 2D granular experiment confined in a circular closed configuration (green line), where the grains are stirred by moving the rod using a figure-eight protocol (red line). (b) Tagged particles at the initial state of the system. (c) Dispersion of the tagged particles after 40 cycles of the rotated protocol.

References

1. H. Aref, Stirring by chaotic advection, in *Hamiltonian Dynamical Systems*, pp. 725–745 (1987).
2. E. Villermaux, Mixing versus stirring, *Annu. Rev. Fluid Mech.*, **51**, 245–273 (2019).
3. J. Ottino & D. Khakhar, Mixing and segregation of granular materials, *Annu. Rev. Fluid Mech.*, **32**, 55–91 (2000).

Bubble induced bifurcation in turbulent von Kármán flow

Valentin Mouet, François Pétrélis, Stéphan Fauve

Laboratoire de Physique de l'ENS, 24 rue Lhomond, 75005 Paris
valentin.mouet@phys.ens.fr

Bubbly flows are ubiquitous in nature and have been shown to control gas fluxes between the atmosphere and the ocean [1]. For this particular situation as for many others, there is a strong coupling between the large scale flow, the bubble size distribution and the gas transfer. For a given geometry and a given forcing, adding bubbles to an initially single-phase flow can have drastic impacts on energy fluxes within the flow [2] or fluid-structure interactions [3]. We present an experimental study of large scale flow bifurcation induced by bubble migration. A turbulent von Kérmán flow is generated by two counter- rotating disks fitted with blades. This flow has been investigated extensively as a model for turbulence because of its high shear rate in the middle plane, creating a strongly turbulent mixing zone. The torque Γ required to turn one disk at rotation rate Ω in single phase turbulent von Kármán flow, follows the asymptotic behaviour in the high Re limit:

$$\Gamma = C(\theta)\rho R^2\Omega^2,$$

where R is the radius, ρ is the liquid density and θ is the ratio of the disks rotation rates [4]. In turbulent two-phase flows with given fluids, the function C also depends on the void fraction α and the Reynolds number. We show experimentally that bubble migration induce a bifurcation of the large scale flow and result in a drastic reduction of energy input in the system when void fraction exceed a certain threshold α_c. The nature of the bifurcation depends on θ and can lead to a reduction of energy input up to 30 % compared with a single phase flow at the same effective density.

References

1. D. W. R. Wallace & C. D. Wirick, Large air–sea gas fluxes associated with breaking waves, *Nature*, **356**, 694–696 (1992).
2. B. Gvozdic *et al.*, Experimental investigation of heat transport in homogeneous bubbly flow, *J. Fluid Mech.*, **845**, 226–244 (2018).
3. M. E. McCormick & R. Bhattacharyya, Drag reduction of a submersible hull, *Naval Eng. J.*, **85**, 11–16 (1973).
4. O. Cadot *et al.*, Energy injection in closed turbulent flows: Stirring through boundary layers versus inertial stirring, *Phys. Rev. E*, **56**, 427 (1997).

Aerodynamics of a fly swatter

Ariane Gayout[1], Mickaël Bourgoin[2], Nicolas Plihon[2]

[1] Biomimetics, ESRIG, University of Groningen, Nijenborgh 7, 9747AG Groningen, Netherlands
[2] Laboratoire de Physique, ENS de Lyon, UMR CNRS 5672, 46, allée d'Italie, F-69364 Lyon
a.m.m.gayout@rug.nl

Our everyday life provides us with the perfect example of a porous object moving in a flow over a wide range of angles of attack: the fly-swatter. While its holes were originally introduced for durability and elasticity, their aerodynamic function is scarcely discussed, despite being well-known for strongly influencing aerodynamic properties. Through partially covering the holes of a square-shaped fly-swatter (Fig. 1. a), we investigate experimentally the effect of the porosity pattern on the fly-swatter aerodynamics, and in particular on the development of stall in a tri-dimensional context.

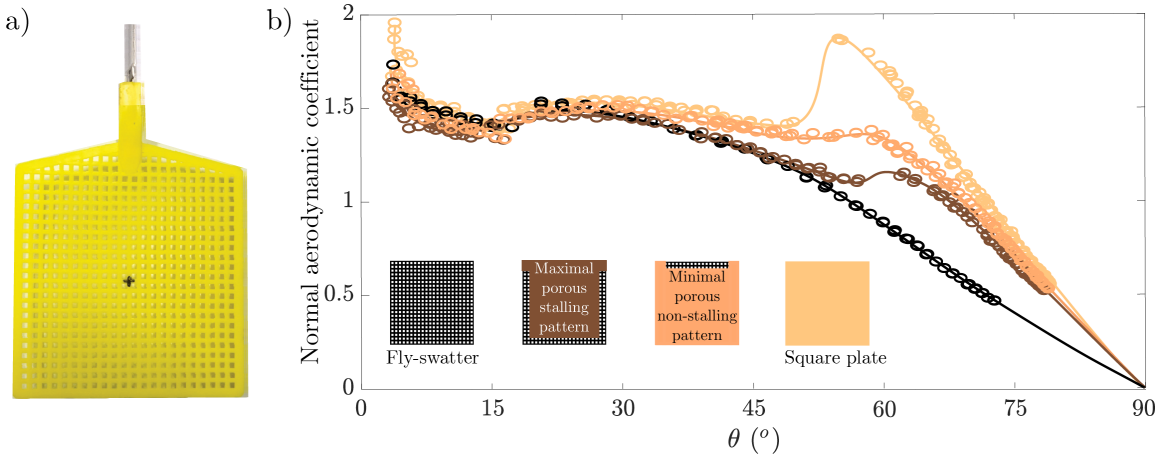

Figure 1. a) Fly-swatter used in the experiments. b) Angular evolution of the normal aerodynamic coefficient C_N for four different porous configurations. A sharp stall is observed for the square plate (beige) and the maximally porous stalling pattern (brown) while a smooth evolution is found for the fly-swatter (black) and the minimally porous non-stalling pattern (orange). Holes on the leading-edge are sufficient to hamper stall, by destabilizing the formation of the leading-edge vortex. To trigger stall, the whole leading-edge needs to be flat, especially its corners, suggesting that the trailing vortices need to find grounds to attach and interact with the leading-edge vortex for stall to occur.

By taping progressively the holes of the fly-swatter over 19 pattern configurations, we identified sufficient conditions for the absence of sharp stall and necessary conditions for its appearance. The aerodynamic coefficients of four configurations are presented in Fig. 1. b). Preliminary PIV measurements were also conducted for the fly-swatter and full plate configurations, and showed wide discrepancies in wake structure along the lift branch ($\theta > 50°$), supporting our hypotheses based on the aerodynamic coefficient.

References

1. A. Gayout, M. Bourgoin & N. Plihon, Influence of the porosity pattern on the aerodynamics of a square-shaped fly-swatter, *Phys. Fluids*, **36**, 0179009 (2024).

Hydrodynamique généralisée et mesures de corrélations balistiques dans une boucle de recirculation fibrée

Elias Charnay[1], Pierre Suret[1], Benjamin Doyon[2], Thibault Bonnemain[2], François Copie[1]

[1] Univ. Lille, CNRS, UMR 8523 - PhLAM - Physique des Lasers Atomes et Molécules, F-59 000 Lille, France
[2] Department of Mathematics, King's College London, Strand, London WC2R 2LS, UK
elias.charnay@univ-lille.fr

L'Hydrodynamique Généralisée a apporté avec succès une nouvelle description macroscopique de la thermodynamique et hydrodynamique des systèmes intégrables [1]. Une de ses forces est l'expansion hydrodynamique, permettant l'introduction de termes cassant faiblement l'intégrabilité, tels que les pièges ou les potentiels extérieurs. De ce fait, elle est devenue un domaine de recherche très actif en atomes froids et dans les systèmes à N-corps quantiques. Elle prédit de plus des corrélations à grande échelle [2].

Nous pouvons calculer des corrélations spatio-temporelles à deux points pour l'infinité de constantes du mouvement des équations intégrables. En particulier dans le cas de l'équation de Schrödinger non linéaire, la masse $\int |\psi(x,t)|^2 \, \mathrm{d}x$ est conservée, et sa corrélation connectée dans l'état stationnaire statistique est donnée par :

$$C_v(t) = \left\langle |\psi(x-vt,t)|^2 \, |\psi(0,0)|^2 \right\rangle - \left\langle |\psi(x-vt,t)|^2 \right\rangle \left\langle |\psi(0,0)|^2 \right\rangle \sim_{t,x\to\infty} \frac{\alpha_v}{t} \tag{1}$$

où α_v est un coefficient dépendant des statistiques de la condition initiale [3]. Cette forme balistique est liée au fait que les solitons, en tant que quasi-particules, se propagent avec une vitesse effective v, modifiée par les interactions.

Nous proposons ici des expériences dans une boucle de recirculation fibrée [4] permettant la mesure de ces corrélations d'intensité. Notre système nous permet la génération de condition initiale arbitraire, en intensité et en phase, puis sa propagation avec peu de pertes. A chaque tour, le signal parcourt 5 kilomètres de fibre optique standard où les pertes sont compensées par un laser Raman contrapropagatif, puis nous extrayons 10 % de ce signal pour reconstruire le diagramme spatio-temporel de l'intensité. À partir de ces données, il devient simple de calculer les corrélations. Nous montrons que celles-ci suivent bien une loi polynomiale, en α/t, démontrant le transport balistique dans ce système et une preuve supplémentaire de la validité de cette théorie.

Références

1. O. A. Castro-Alvaredo, B. Doyon & T. Yoshimura, Emergent hydrodynamics in integrable quantum systems out of equilibrium, *Phys. Rev. X*, **6**, 041065 (2016).
2. T. Bonnemain, B. Doyon & G. El, Generalized hydrodynamics of the KdV soliton gas, *J. Phys. A*, **55**, 374004 (2022).
3. R. Koch, J.-S. Caux & A. Bastianello, Generalized hydrodynamics of the attractive non-linear Schrödinger equation, *J. Phys. A*, **55**, 134001 (2022).
4. A. E. Kraych, D. Agafontsev, S. Randoux & P. Suret, Statistical properties of the nonlinear stage of modulation instability in fiber optics, *Phys. Rev. Lett.*, **123**, 093902 (2019).

Aiming of water waves in a time-varying metabathymetry

Magdalini Koukouraki[1], Agnès Maurel[2], Philippe Petitjeans[1], Vincent Pagneux[3]

[1] Laboratoire de Physique et de Mécanique des Milieux Hétérogènes, ESPCI, 7 Quai Saint-Bernard, 75005 Paris
[2] Institut Langevin, ESPCI, 1 Rue Jussieu, 75005 Paris
[3] Laboratoire d'Acoustique de l' Université du Mans, Av. Olivier Messiaen, 72085 Le Mans
magdalini.koukouraki@espci.fr

We investigate both analytically and numerically the two-dimensional propagation of shallow water waves over a time-varying medium, which switches from isotropic to anisotropic at a given time. Motivated by the study of Pacheco-Peña *et al.* [1], where temporal waveguides were designed for electromagnetic waves, we propose here a water-wave analog. The anisotropy is established with the abrupt appearance of a plate array at the fluid bottom, which changes the effective water depth in each direction in the long-wavelength limit [2]. Depending on the wavenumber angle incident on the plate array, the angle of the energy flow will change, allowing us to deflect the wave. A schematic representation of such a deviation is depicted in Figure 1. Note that isotropic time variation of the water wave speed has been explored in [3] and [4]. Finally, an experimental setup has also been designed, which allows the plate array to be suddenly lifted at the fluid bottom.

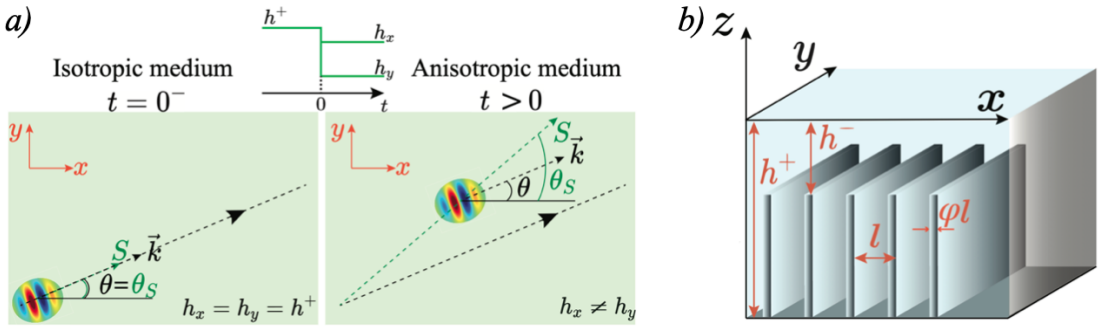

Figure 1. a) Wave packet deviation from its initial trajectory due to the anisotropy introduced at $t = 0$. b) Representation of the plate array at the fluid depth.

References

1. V. Pacheco-Peña & N. Engheta, Temporal aiming, *Light Sci. Appl.*, **9**, 129 (2020).
2. A. Maurel, J.-J. Marigo, P. Cobelli, P. Petitjeans & V. Pagneux, Revisiting the anisotropy of metamaterials for water waves, *Phys. Rev. B.*, **96**, 134310 (2017).
3. V. Bacot, M. Labousse, A. Eddi, M. Fink & E. Fort, Time reversal and holography with spacetime transformations, *Nat. Phys.*, **12**, 972–977 (2016).
4. B. Apffel & E. Fort, Frequency conversion cascade by crossing multiple space and time interfaces, *Phys. Rev. Lett.*, **128**, 129 (2022).

Coalescence of viscous droplets under an elastic membrane

Wissem-Eddine Khatla, Étienne Reyssat, Antonin Eddi, Laurent Duchemin

PMMH Laboratory, CNRS, ESPCI, PSL University, Sorbonne University, Paris, France
wissem.khatla@espci.fr

The spreading of viscous fluids under an elastic membrane is an essential phenomenon underpinning many processes, both technical-industrial [1] and geological, such as certain laccolithic structures [2].

A particularly interesting case for this type of flow involves the study of the formation of two pockets of fluid between a rigid substrate on the one hand and an elastic membrane on the other. The drops generated will spread out until they eventually merge when their respective fronts meet. From this point onwards, a bridge of increasing height is formed.

This configuration is analogous to its capillary equivalent in the case of coalescence of free-surface drops. It was shown in [3] that the height of this bridge between the drops increases linearly with time, this process being described by a self-similar solution which has been made explicit in the same study.

We therefore propose to revisit this experiment in the case where we consider, not the surface tension, but the elasticity induced by the presence of the membrane.

We inject a fluid of viscosity μ and density ρ at a constant flow rate Q through a glass plate onto which a membrane of millimetric thickness d has been deposited. The evolution of the fluid's height profile $h(r,t)$ is therefore governed by the thin-film equation, where D and T represent the membrane's flexural modulus and tension respectively:

$$\frac{\partial h}{\partial t} = \frac{1}{12\mu r}\frac{\partial}{\partial r}\left[rh^3\left(\rho g\frac{\partial h}{\partial r} + D\frac{\partial}{\partial r}(\Delta_r^2 h) - T\frac{\partial}{\partial r}(\Delta_r h)\right)\right] + w(r, z=0, t). \tag{1}$$

Two drops are thus formed in the case of a double injection through two intrusions of diameter $e = 1$ mm and separated by a distance $L_{gap} = 3$ cm (cf. Fig. 1). We define the initial time t_0 of coalescence as the instant when the height of the bridge h_0 is non-zero.

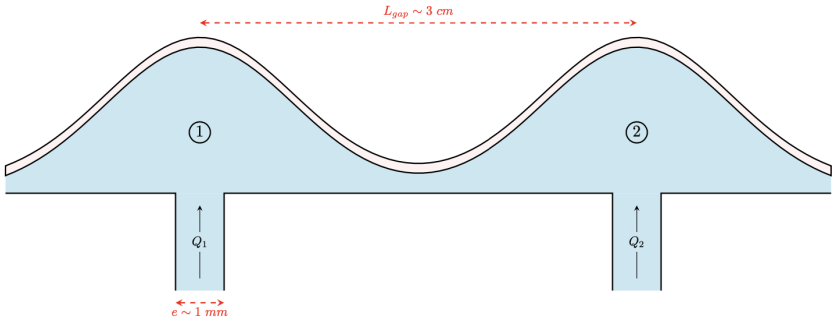

Figure 1. Simplified scheme representing the usual configuration of the study

We will show that the elasticity of the membrane is responsible for the relaxation of the drops as they merge by making explicite a power law confirming this dependancy. We will explain a simple geometric model that illustrates the self-similar behavior of the shape of the bridge joining the two blisters. We will try to confront the obtained results both experimentally and numerically.

References

1. E. Fortunato, P. Barquinha & R. Martins, *Adv. Mater.*, **24**, 2945–2986 (2012).
2. J. M. Castro, C. Ian & T. S. Tuffen, *Nat. Commun.*, **7**, 13585 (2016).
3. L. A. Hernández-Sánchez, A. Eddi & J. H. Snoeijer, *Phys. Rev. Lett.*, **109**, 184502 (2012).

Dynamics of two non miscible fluids inside a rotating cylinder

Lyes Gormit, Ivan Delbende, Maurice Rossi

Sorbonne-Université, Institut Jean Le Rond D'Alemebert, 4, Place Jussieu 75252 Paris
lyes.gormit@sorbonne-universite.fr

We study the dynamical behavior of a two-phase vortex, namely a light fluid core embedded within a denser fluid flow environment. Such vortices can be seen in nature and in industrial applications, for example, cavitating helical vortices in the wake of ship propellers. Since such configuration is complex, we opt to investigate a simplified configuration where the vortex core is straight and confined. Two non-miscible fluids are placed within a rotating cylindrical container, with the axis of rotation oriented perpendicular to the gravitational field. When the rotation is sufficient, the centrifugal force maintains the lighter fluid around the axis of rotation with a slight shift of the bubble below the center of the tank. At the interface between the two fluids, waves are found to propagate.

Previous studies examined this configuration experimentally. The pioneering work by Phillips [1] proposed a linearized analytical solution to the problem of the base flow perturbed by gravity, together with a decoupled wave study in the axisymmetric configuration (without gravity); the problem was simplified by considering only the outer fluid in the inviscid framework, and the fluid surface as a free surface. Experimental results were given for the air-water system. Kozlov *et al.* [2] performed experiments with two non-miscible liquids, and derived an analytical dispersion relation for interfacial waves between the two fluids, yet neglecting gravity, viscosity and surface tension.

Our approach involves numerical simulations of the same system using the CFD Basilisk flow solver [3] in a two-dimensional configuration. The solver is well known for its efficiency in computing multiphase flows. We can vary the density contrast between the two fluids, their viscosity contrast, the surface tension and the confinement ratio (inner fluid radius divided by outer cylinder radius).

We choose parameters for which a stationary state exists, and focus on the establishment of this state: trajectory of the lighter fluid towards the equilibrium state, and interfacial wave motions. Following Phillips and Kozlov, we propose an analytical solution in the inviscid framework, now taking into account surface tension effects. Numerical simulations are compared to analytical solutions. Excellent agreement was found between numerical and theoretical steady states.
In addition to the above stable state, other regimes might occur, depending on the problem parameters (Froude number, Reynolds number, density ratio, confinement). These regimes observed experimentally can also be captured numerically. To understand them, an instability study has to be conducted.

References

1. O. M. Phillips, Centrifugal waves, *J. Fluid Mech.*, **7**, 340–352 (1960).
2. N. V. Kozlov, A. N. Kozlova & D. A. Shuvalova, Dynamics of immiscible liquids in a rotating horizontal cylinder, *Phys. Fluids*, **28**, 112102 (2016).
3. S. Popinet, The basilisk code (2013).

Towards broadband experimental wave index spatiotemporal modulation: Faraday waves in a modified gravity environment

Eugénie Bontemps[1], Quentin Louis[2], Emmanuel Fort[2]

[1] ESPCI Paris, Université PSL, CNRS, Paris, France.
[2] Institut Langevin, ESPCI Paris, Université PSL, Paris, France.
emmanuel.fort@espci.fr

Finding a material capable of supporting arbitrary broadband spatial and temporal variations of its index would prove important for wave physics and its numerous applications [1]. Time-varying media physics is demanding for experimentalists because of the need for the index change to happen on smaller timescales than a wave period. Photonic and acoustic experiments are currently limited while a few experimental explorations have been fruitful using water waves with electrostriction and vertical vibration [2–5]. However, both methods are limited in either frequency range or integral displacement.

Here, we use a separation of scales method between high and low frequencies to provide a broadband index change actionable fast in front of the low frequency wave timescale. The mechanism is that found in the Kapitza pendulum. We measure and characterize the effect using Faraday waves.

In our one dimensional setup, an additional effect appears: the bath showcases resonances typical of the excitation of an elongated object under periodic excitation. A vibro-equilibrium of the fluid height emerges, and we can observe a gradient of Faraday wavelength.

In addition to time-variations, spatial structuration of the index in water waves was so far only possible using either bathymetry or spatially structuring electrodes with either limitations in damping or modulation amplitude. Lifting this limitation along with unlocking the additional degree of freedom in time opens up exciting new possibilities for broadband spatiotemporal wave physics.

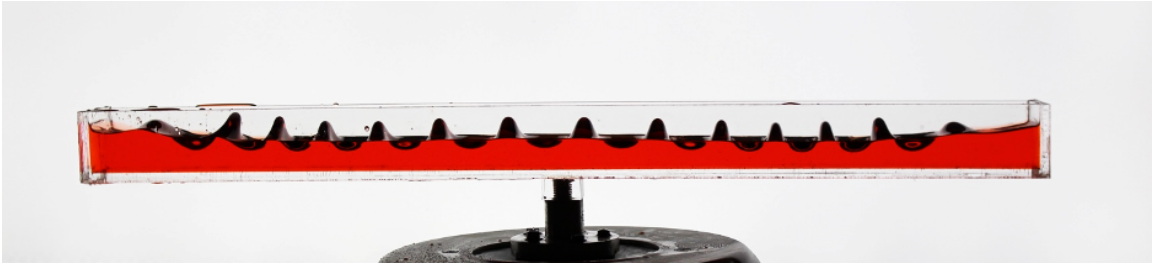

Figure 1. Colored Faraday waves gradient in an elongated 1D bath under high-frequency excitation. Experimental values: Faraday half-frequency at $f_F = f_E/2 = 8$ Hz, high frequency excitation at $f_h = 157$ Hz, bath length $L = 60$ cm.

References

1. N. Engheta, Four-dimensional optics using time-varying metamaterials, *Science*, **379**, 1190–1191 (2023).
2. H. Moussa, G. Xu, S. Yin, E. Galiffi, Y. Ra'di & A. Alù, Observation of temporal bontempslection and broadband frequency translation at photonic time interfaces, *Nat. Phys.*, 1–6 (2023).
3. V. Bacot, M. Labousse, A. Eddi, M. Fink & E. Fort, Time reversal and holography with spacetime transformations, *Nat. Phys.*, **12**, 972–977 (2016).
4. B. Apffel, S. Wildeman, A. Eddi & E. Fort, Experimental implementation of wave propagation in disordered time-varying media, *Phys. Rev. Lett.*, **128**, 094503 (2022).
5. B. Apffel & E. Fort, Frequency conversion cascade by crossing multiple space and time interfaces, *Phys. Rev. Lett.*, **128**, 064501 (2022).

Experimental investigation to test the static Bell's inequality in a hydrodynamic system

Sunil Kumar Saroj[1,2], Stéphane Perrard[2], Matthieu Labousse[1]

[1] Gulliver, CNRS, ESPCI Paris, Université PSL, 75005, Paris, France
[2] PMMH, CNRS, ESPCI Paris, Université PSL, Sorbonne Université, Université de Paris, 75005, Paris, France
sunil.kumar-saroj@espci.fr

A sub-millimetric bouncing droplet can walk on the surface of the fluid due to the resonant interaction with its own wave field [1]. The present experimental study investigates the wave coupling behavior of two droplets bouncing in two different cavities and their associated trajectory.

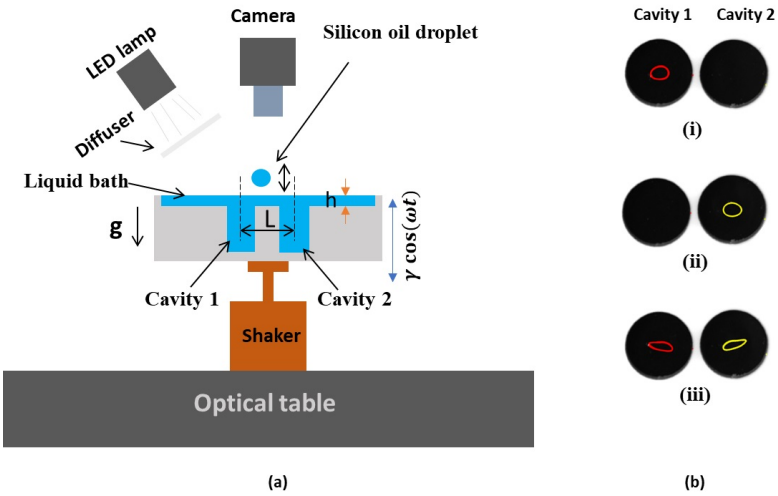

Figure 1. (a) Sketch of the experimental arrangement. (b) Trajectories of the droplets: (i) droplet present in cavity 1, (ii) droplet present in cavity 2 and (iii) droplets present in both cavities.

Figure 1 (a) illustrates the experimental arrangement of a vibrating bath with two cavities submerged in it. The center distance (L) between the cavities and memory both affect the trajectories. For example: the circular trajectory when a droplet is bouncing in the cavity 1 (see Fig. 1 (b) i). The trajectory is exactly identical if the droplet from cavities 1 is transferred to the cavity 2 (see Fig. 1 (b) ii). The trajectories are modified when the droplet present in both the cavities (see Fig. 1 (b) iii). This is due to the mediated wave interaction between two droplets that bounce into their respective cavities [2]. This correlation between two droplets is significantly affected by the L and memory of the droplet. A strong wave coupling has been observed between the two droplets for a fixed L at smaller memory. It has been observed that the higher memory exhibits chaotic motion, suggesting a weak wave coupling between the two droplets. Several previous studies reported that the walking droplet can mimic the wave particle duality phenomena reminiscent of the quantum-like behaviors [3]. Therefore, we have used this analogy to test the violation of the static Bell's inequality in this hydrodynamic framework.

References

1. Y. Couder, S. Protière, E. Fort & A. Boudaoud, *Nature*, **437**, 208 (2005).
2. C. Borghesi, J. Moukhtar, M. Labousse, A. Eddi, E. Fort & Y. Couder, *Phys. Rev. E*, **90**, 063017 (2014).
3. K. Papatryfonos M. Ruelle, C. Bourdiol, A. Nachbin, J. W. M. Bush & M. Labousse, *Commun. Phys.*, **5**, 142 (2022).

Unveiling the wake of a surface swimming snake

Vincent Stin[1,2], Gatien Polly[1], Alexis Mérigaud[1], Xavier Bonnet[3], Anthony Herrel[2], Ramiro Godoy-Diana[1]

[1] PMMH, CNRS UMR 7636, ESPCI Paris-PSL, Sorbonne Université, Université Paris Cité, Paris, France.
[2] MECADEV, Departement Adaptation du Vivant, MNHN, CNRS UMR 7179, Paris, France.
[3] Centre d'Etudes Biologiques de Chizé, CNRS UMR 7372, Villiers-en-Bois, France.
vincent.stin@espci.fr

Research on animal surface swimming has mainly focused on small insects or on animals that use limb-surface interactions for propulsion, such as ducks or geckos (see [1] for a review). For the case of snakes, apart from the pioneering observations of Hertel [2] (cf. Fig. 1.A), no measurements appear to have been made.

We report here the results from a surface swimming experiment performed with *Natricidae* snakes (cf. Fig. 1.B), where the surface waves produced by the swimming snakes have been quantified by measuring the water surface elevation perturbation (cf. Fig. 1.B). Measurements were performed using a synthetic Schlieren imaging method that gives an instantaneous non-intrusive measurement of the height of the free surface η at every location in space.

Using a filtering technique based on the dispersion relation of capillary-gravity waves on the measured wave field we show that, remarkably, a significant percentage of the waves that compose the wake pattern travel in a direction opposite to the swimming direction . A contribution to the propulsive force of the animal from the waves is thus expected, so the surface wave wake of the snake is not solely a drag wake, despite its similarity with the Kelvin wake of a ship or a duck.

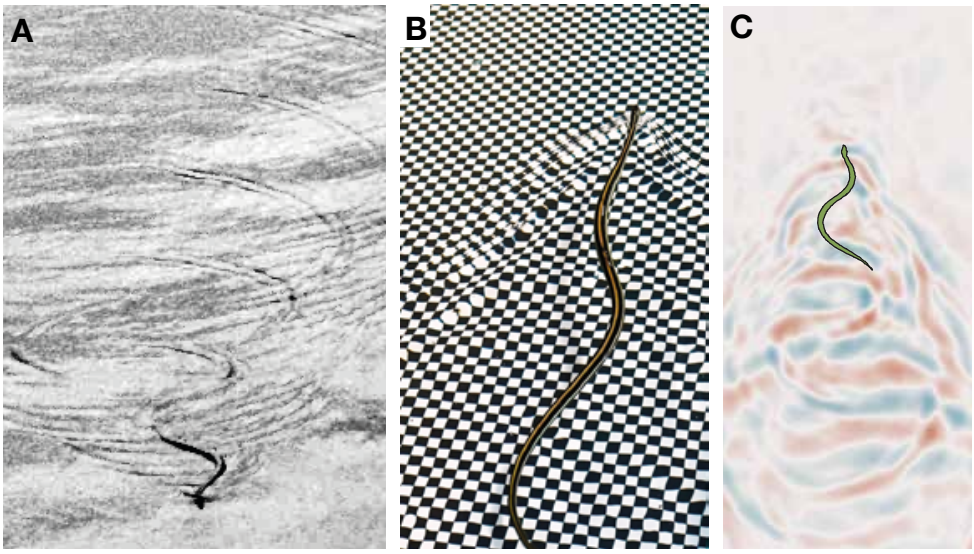

Figure 1. (A) Observation of the surface swimming of Natrix natrix by Hertel [2]. (B) Adult *Natricidae* snake swimming at the surface of the experimental tank at PMMH, ESPCI Paris (Photo: R. Godoy-Diana). The waves produced by the passage of the snake are visible on the checkerboard pattern used to measure the water surface height perturbation. (C) Example of the surface wake measured in the experiment.

References

1. J. W. Bush & D. L. Hu, Walking on water: Biolocomotion at the interface, *Annu. Rev. Fluid Mech.*, **38**, 339 (2006).
2. H. Hertel, *Structure, Form, Movement*, Reinhold Publishing (1966), pp. 178–184.

Small coherent structures in rough turbulent convection

Nathan Carbonneau[1], Julien Salort[2], Anne Sergent[1]

[1] Lab. Interdisciplinaire des Sciences du Numérique, Université Paris-Saclay, CNRS, Orsay, France
[2] Lab. Physique, École Normale Supérieure de Lyon, CNRS, Lyon, France
nathan.carbonneau@lisn.fr

Turbulent convection is a spontaneous physical process present in natural environments as well as in many industrial systems. However, most of these systems are not ideal in terms of underlying surfaces and involve specific topography or small-scale roughness. Interactions between plate roughness and nearby flow can induce changes in turbulence scales [1]. In addition, when the flow is confined by the side walls of a cavity, or when it is enclosed by two large-scale horizontal walls, a large-scale circulation (LSC) is established in the fluid volume [2]. The aim of this work is to reveal how the LSC changes small flow structures by considering either a cavity flow or a fluid layer of reduced size, in particular when a plate is rough.

In this study we consider three types of bottom plates: smooth plate, and two plates with evenly distributed roughness elements (different heights, same aspect ratio and same spatial distribution). Three confined cavities and three periodic fluid domains are modelled by means of direct numerical simulations at constant Rayleigh and Prandtl numbers, considering the different types of plates as indicated above.

We explore the effect of roughness elements on the flow structure at different scales by comparing the rough cases to the smooth ones. Furthermore, the effect of the LSC on the turbulent structures is investigated by comparing closed and periodic configurations for each bottom wall type. For example, in the case of a smooth plate, it appears that the size of the small-scale thermal structures is altered by the LSC. As shown below (figure 1), the presence of the LSC contributes to enlarge the coherent thermal structures.

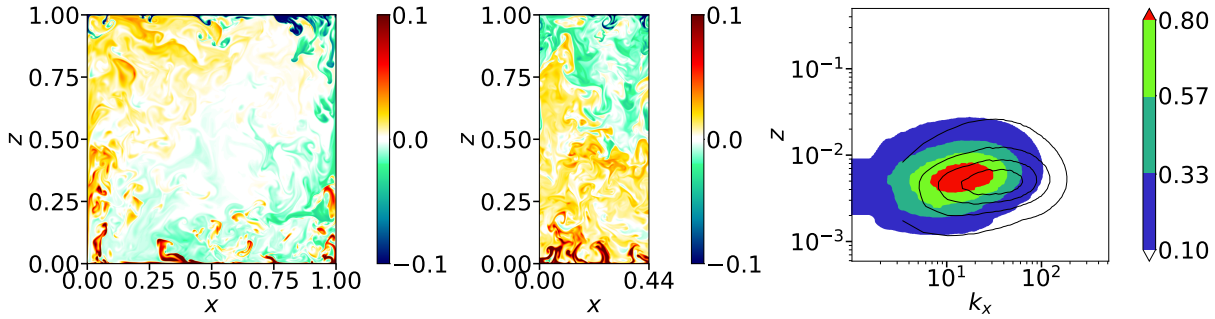

Figure 1. Comparison for the smooth case of two mid-depth temperature snapshots: confined cavity (left) and periodic layer (middle). The colormap is centered on the bulk temperature of the closed cavity $T_{\text{bulk}} = 0.5$. The difference of the thermal structure size is illustrated by the horizontal Fourier transform (in x direction) performed at all altitudes z on the temperature fluctuation field $T' = T - \langle T \rangle_t$ (right). The colors correspond to the complete cavity while the lines correspond to the periodic case.

References

1. O. Liot, Q. Ehlinger, É. Rusaouën, T. Coudarchet, J. Salort & F. Chillà, Velocity fluctuations and boundary layer structure in a rough Rayleigh–Bénard cell filled with water, *Phys. Rev. Fluids*, **2**, 044605 (2017).
2. A. Blass, R. Verzicco, D. Lohse, R. J. A. M. Stevens & D. Krug, Flow organisation in laterally unconfined Rayleigh-Bénard turbulence, *J. Fluid Mech.*, **906**, A26 (2021).

Particules solides et instabilités élasto-inertielles en écoulement de Taylor-Couette

Charles Carré[1], Tom Lacassagne[1], Masoud Moazzen[1], Vincent Thomy[2], S. Amir Bahrani[1]

[1] IMT Nord Europe, Institut Mines Télécom, Univ. Lille, Center for Energy and Environment, F-59000 Lille
[2] IMEN, Institut d'Electronique, de Microélectronique et de Nanotechnologie, F-59650 Villeneuve d'Ascq
charles.carre@imt-nord-europe.fr

Les fluides chargés en particules solides (suspensions) sont fréquemment rencontrés dans les systèmes naturels et industriels (coulées de laves, avalanches, sang, ciment...). Ces particules ont un impact sur l'écoulement, notamment sur le déclenchement des instabilités hydrodynamiques, ce qui constitue un enjeu majeur dans le contrôle ou l'intensification des processus de transferts et de mélange [2, 3]. Par ailleurs, les fluides viscoélastiques, rencontrés dans ces mêmes systèmes, sont connus pour admettre le déclenchement d'instabilités élastiques ou élasto-inertielles à des nombres de Reynolds nuls ou faibles par rapport aux instabilités inertielles dans les fluides Newtoniens [1, 4]. Ce mécanisme repose sur une non linéarité rhéologique du fluide (éventuellement couplée aux non-linéarités inertielles).

Ainsi, ces deux constats amènent à se questionner sur le comportement de fluides où sont présents à la fois des particules et une propriété viscoélastique (rencontrés par exemple dans les procédés pharmaceutiques, cosmétiques, ou d'impression 3D), en termes de stabilité et d'apparition d'écoulements secondaires. La question est ici abordée en utilisant l'écoulement modèle de Taylor-Couette qui consiste en un cylindre intérieur en rotation dans un cylindre extérieur fixe, et pour lequel on caractérise le nombre de Reynolds critique conduisant au déclenchement de l'instabilité élasto-inertielle primaire. En employant des fluides fortement viscoélastiques, une transition directe d'un régime laminaire *Circular Couette Flow* (CCF) à la turbulence Elasto-Inertielle (EIT - *Elasto inertial turbulence*) est observée [4]. Des particules solides iso-denses et non colloïdales sont introduites à des fractions volumiques allant de 0 à 14%. L'influence de l'ajout des particules sur la rhéologie viscoélastique du fluide est caractérisée. L'impact de cette rhéologie sur le déclenchement des instabilités élasto-inertielle est ensuite décrite, en utilisant une approche combinée de visualisation d'écoulement et de mesure du couple exercé sur le cylindre intérieur en rotation.

Il apparaît que l'ajout d'une faible fraction volumique de particules ($\leq 2\%$, régime dilué) ne modifie ni le seuil de déclenchement des instabilités au sens du Reynolds, ni la nature de la transition (CCF-EIT), alors même que l'élasticité apparente des fluides est diminuée. En revanche, à partir de 6% de particules (régime semi-dilué), le régime EIT n'est plus du tout observé dans la gamme de nombre de Reynolds explorée, suggérant *a minima* un retard significatif de la transition causé par les particules, voire une suppression pure et simple de l'instabilité, sans pour autant que l'élasticité apparente des fluides n'ai significativement diminué par rapport aux suspensions diluées. La mesure du couple exercé sur le cylindre intérieur permet de mettre en évidence qu'en régime semi-dilué, à partir d'un nombre de Weissenberg pour lequel une transition vers l'EIT serait attendue, une modification de la dynamique de frottements est bien observée mais ne conduisant à aucun régime d'écoulement secondaire observable avec la méthode de visualisation employée.

Références

1. A. Groisman & V. Steinberg, Couette–Taylor Ffow in a dilute polymer solution, *Phys. Rev. Lett.*, **8**, 1480–1483 (1996).
2. P. Ramesh, S. Bharadwaj & M. Alam, Suspension Taylor–Couette flow : Co-existence of stationary and travelling waves, and the characteristics of Taylor vortices and spirals, *J. Fluid Mech.*, **870**, 901–940 (2019).
3. M. Moazzen, T. Lacassagne, V. Thomy & S. A. Bahrani, Torque scaling at primary and secondary bifurcations in Taylor–Couette flow of suspensions, *J. Fluid Mech.*, **937**, A2 (2022).
4. M. Moazzen, T. Lacassagne, V. Thomy & S. A. Bahrani, Friction dynamics of elasto-inertial turbulence in Taylor–Couette flow of viscoelastic fluids, *Philos. Trans. R. Soc. A*, **381**, 20220300 (2023).

Disambiguation of the different types of crossings in a mycelial branching network through complete identification of its spatio-temporal structure

Thibault Chassereau, Florence Chapeland-Leclerc, Éric Herbert

Laboratoire Interdisciplinaire des Énergies de Demain, Université Paris Cité, 35 rue Hélène-Brion, 75013 Paris
thibault.chassereau@etu.u-paris.fr

From a single spore, fungi can colonize their environment through a very complex interconnected network of hyphae, the mycelium. Yet, the rules governing this growth are simple. Hyphae can only grow from the tip, branch (apically or laterally) [1] creating a new hypha or fuse when meeting another one. However, the local dynamics of growth within the network is not well known such as the inhomogeneity of the density in time and in space. Both types of branching are difficult to analyze spatially and quantitatively, as is the long-distance tracking of apexes. In this work, we characterize the hyphal network expansion and the structure of the model filamentous fungus *Podospora anserina* under controlled culture conditions [2, 3]. To this end, temporal series of pictures of the network dynamics are produced, starting from germinating ascospores and ending when the network reaches thousands of connections approximately 20 hours later. The completely automated image reconstruction steps allow a postprocessing and a quantitative analysis of the spatio-temporal dynamics using gray level information from the entire image series. Taking advantage of the network's properties we can numerically identify each individual hypha and characterize the nature of the branching it emerges from. Building on spatio-temporal information, we can discriminate hyphal fusion from mere overlapping to get a better understanding of the network topology. Thanks to the identification of each hypha, we analyze the growth of the network at both local and global scale.

References

1. M. Riquelme & S. Bartnicki-Garcia, Key differences between lateral and apical branching in hyphae of *Neurospora crassa*, *Fungal Genet. Biol.*, **41**, 842–851 (2004).
2. J. Dikec, A. Olivier, C. Bobée, Y. D'Angelo, R. Catellier, P. David, F. Filaine, S. Herbert, Ch. Lalanne, H. Lalucque, L. Monasse, M. Rieu, G. Ruprich-Robert, A. Véber, F. Chapeland-Leclerc & É. Herbert, Hyphal network whole field imaging allows for accurate estimation of anastomosis rates and branching dynamics of the filamentous fungus *Podospora anserina*, *Sci. Rep.*, **10**, 3131 (2020).
3. C. Ledoux, F. Chapeland-Leclerc, G. Ruprich-Robert, C. Bobée, Ch. Lalanne, É. Herbert & P. David, Prediction and experimental evidence of the optimisation of the angular branching process in the thallus growth of *Podospora anserina*, *Sci. Rep.*, **12**, 12351 (2022).

A very expressive plant: Spathiphyllum shape reactions to water stress

Philippe Marmottant, Benjamin Dollet, Olivier Stephan, Catherine Quilliet, Emmanuel Siéfert

LIPhy, CNRS and Université Grenoble Alpes, 140 rue de la Physique, Saint Martin d'Hères, France
philippe.marmottant@univ-grenoble-alpes.fr

During a period of drought, the content of water in plants diminishes, with a decrease in turgor pressure. If the effects are not easily visible on trees and other lignified plants, it is not the case with Spathiphyllum, a popular interior plant.

After two weeks without watering, the plant seems to desperately cry for help, showing leaves completely falling on the ground (cf. Fig. 1, top). Fortunately, such a state is reversible, and the plant soon recovers its shape after watering. What is so specific about this plant?

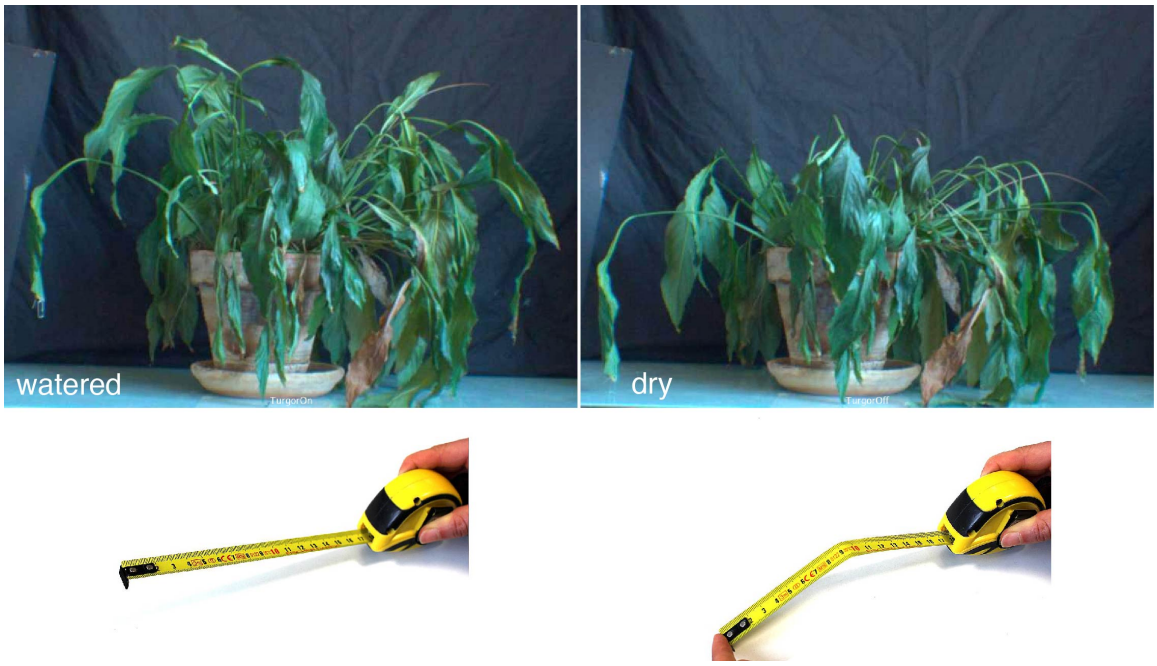

Figure 1. Spathiphyllum plant well watered (top left), and suffering a week without watering (top right). Metallic measuring tape undergoing a buckling instability (bottom line).

First, anatomical sections in thin slices of the stem show that it contains a soft core and a stiff external layer. The soft core shrinks under drought. Second, mechanical tests show that the bending rigidity of the stems decreases by 50%, but not enough to explain this dramatic change in shape.

A good answer can be found at the base of the plant: if the stems are round in cross section, their attachment to the base assumes the shape of a thin U-shaped sheet. This base suddenly bends when the plant is dry: this is analogous to the buckling of the metallic measuring tape submitted to an increasing bending force (Fig. 1, bottom). In the case of the plant, this bifurcation is led by a decrease in stiffness and in the transverse curvature of the U-shaped part of the stem. This bifurcation is reversible and seems super-critical, contrary to the metallic tape bending transition.

Bubble clouds generated by single and multi-plunging jets

Narendra Dev, J.John Soundar Jerome, Hélène Scolan, Jean-Philippe Matas

Univ Claude Bernard Lyon 1, CNRS, Ecole Centrale de Lyon, INSA Lyon, LMFA, UMR5509, 69622 Villeurbanne, France
narendra.dev@univ-lyon1.fr

The impact of a plunging jet with a liquid surface induces air entrainment beneath the surface, resulting in the formation of a bubble cloud (Fig. 1). This phenomenon is widely encountered in nature, such as breaking waves in water bodies, and in industrial techniques aimed at reducing foam formation in chemical processes. The depth (H) of this bubble cloud is an important parameter for modeling in such applications [1]. By employing laboratory-scale experiments and optical probes to carefully measure the local bubble void fraction (ϕ), we demonstrate that a simple momentum balance, including only liquid inertia and the buoyancy force due to the bubble cloud volume, provides a very good estimate for H when ϕ is known. Furthermore, we show that bubble clouds can be classified as inertial or buoyancy-dominated [2] based on a Froude number given by a characteristic bubble terminal speed, cloud depth and the net void fraction of the cloud [3]. Thereby, our findings help unify a large body of data in the literature corresponding to a wide range of injector diameters (250 µm–20 cm) and cloud depths from a few centimetres to a few metres. Finally, we use a simple set-up of closely packed multi-injectors as a model to investigate air entrainment by large scale plunging jets. Our preliminary results confirm that inertia imparted by the plunging liquid jet and the bubble cloud volume are sufficient to determine the cloud depth even in such complex cases, provided the bubble void fraction is given.

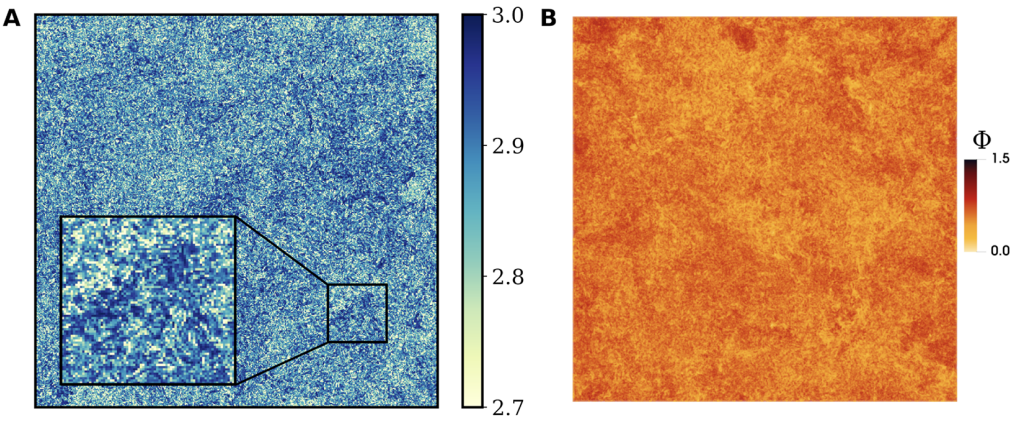

Figure 1. Instantaneous image of conical bubble cloud formed by plunging jet.

References

1. C. Clanet & J. C. Lasheras, Depth of penetration of bubbles entrained by a plunging water jet, *Phys. Fluids*, **9**, 1864–1866 (1997).
2. G. Guyot, A. Cartellier & J.-P. Matas, Penetration depth of a plunging jet: from microjets to cascades, *Phys. Rev. Lett.*, **124**, 194503 (2020).
3. N. Dev, J. John Soundar Jerome, H. Scolan & J.-P. Matas, Liquid inertia versus bubble cloud buoyancy in circular plunging jet experiments, *J. Fluid Mech.*, **978**, A23 (2024).

Numerical computation of a turbulent wind flow over buildings and estimation of its effect on drone's model

Li Chaozhen[1,2], Amine Ammar[4], Alessandro Biancalani[2], Francisco Chinesta[5], Aminallah Rabia[3], Samir Yahiaoui[2]

[1] INSA Toulouse, 31077 Toulouse cedex 4, France
[2] Léonard de Vinci Pôle Universitaire, Research Center, 92916 Paris La Défense, France
[3] É cole supérieure d'ingénieurs Léonard-de-Vinci, 92916 Paris La Défense, France
[4] LAMPA, Arts et Metiers Institute of Technology, 49035 Angers, France
[5] PIMM Lab and ESI Chair, Arts et Metiers Institute of Technology, 75013 Paris, France
aminallah.rabia@devinci.fr

The nonlinear dynamics of turbulence formed by the wind flowing near solid objects can be studied with a variety of different physical models, more or less numerically demanding. An application is the study of the formation of turbulence past buildings, with the goal of determining the no-fly zones for drones in smart cities.

In this paper, we examine the Unsteady Reynolds-averaged Navier-Stokes (URANS, specifically k–Omega Shear Stress Transport) model, which provides accurate prediction of flow separation than other RANS models. We compare the results with those of the Delayed Detached Eddy Simulation (DDES, specifically Spalart–Allmaras DDES) model, more physically comprehensive, but more numerically demanding. Both successfully predicted the average velocity distribution and the average Reynolds stress distribution behind the obstacle [2,3]. However, the predicted loads for simplified geometry for the drone modeled in this study as a cube at certain locations differed by a factor of 4 depending on the turbulence model employed. The analysis of the effect of different turbulence models on a group of simplified drone models with fixed positions close to buildings allows us to check and develop the no-fly zones. In this work, the difference between the DDES and URANS models is investigated for the estimation of the turbulence intensity and the total forces acting on the bluff bodies.

Despite certain limitations in the URANS model, it is still a practical alternative considering the cost advantages and the great demand for meshes in urban simulation. Subsequent studies could develop upon this to correct the results, such as adding a safety factor in predicting the level of turbulence, to ensure the accurate use of drones in urban environments. Additionally, the complexity of urban models could be simplified by using Reduced Order Modelling to allow for the possibility of urban simulation by DDES.

References

1. M. Z. G. Yousif & H. Lim,, On the characteristics of the turbulent wake behind a wall-mounted square cylinder, arXiv:2012.11263 (2020).
2. M. Saeedi, P. P. LePoudre & B.-C. Wang, Direct numerical simulation of turbulent wake behind a surface-mounted square cylinder, *J. Fluids Struct*, **51**, 20–39 (2014).
3. J. A. Bourgeois, P. Sattari & R. J. Martinuzzi, Alternating half-loop shedding in the turbulent wake of a finite surface-mounted square cylinder with a thin boundary layer, *Phys. Fluids*, **23**, 095101 (2011).

Toy-model for the formation of rillenkarren by rainfall

Simeon Djambov, François Gallaire

Laboratory of Fluid Mechanics and Instabilities, EPFL, CH-1015 Lausanne, Suisse
simeon.djambov@epfl.ch

Rillenkarren are dissolution features, adorning the inclined faces of bare soluble rocks, e.g. limestone or gypsum, appearing as an array of regularly-spaced grooves along the incline (fig. 1 (a)). A compelling viewpoint on their formation is that of the raindrop statistics conspiring to carve a coherent structure [1]. We suggest that the transverse pattern would then be owed only to the anisotropy, caused by the incline, of the drops' dissolution "fingerprints" and to a simple steepest-descent-like coupling between raindrop paths and substrate morphology.

We propose a numerical experiment, in which a unique shape is arbitrarily chosen to encode the effect of a drop rolling down the soluble surface. One by one, random impact positions are drawn uniformly and raindrop sizes drawn from Marshall and Palmer's distribution (1948) [2]; the fingerprint shape is rescaled according to the drop's size and remapped along the path of steepest descent from the impact point. These basic ingredients appear as sufficient for the seeked transverse pattern to emerge (fig. 1 (b)).

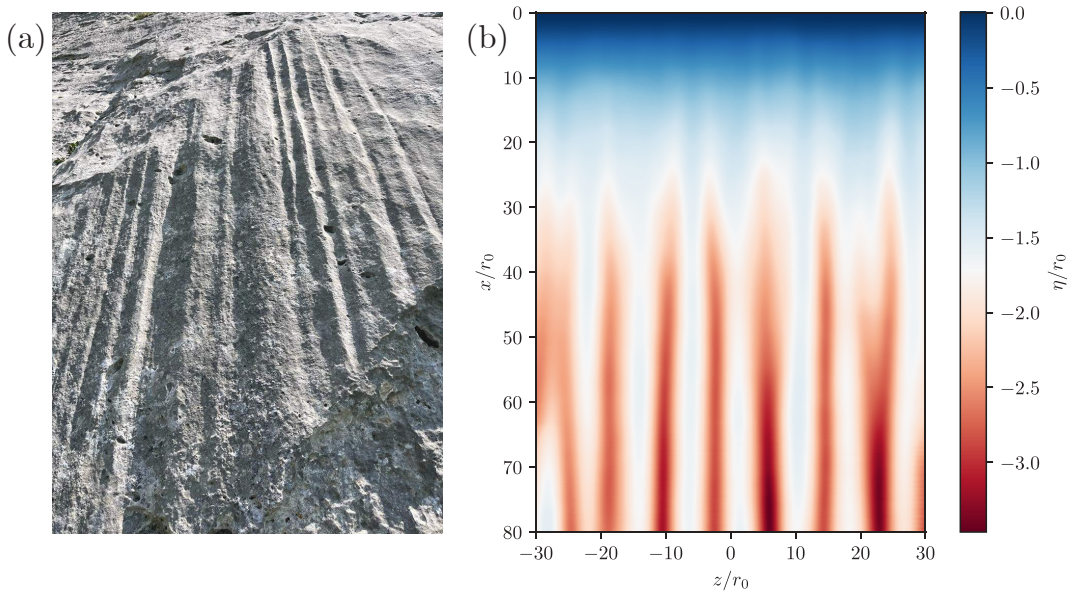

Figure 1. (a) Natural rillenkarren near *La Dent d'Oche* in the Chablais Alps. (b) Surface topography η after 2×10^5 impacts or around 100 h under a rainfall of 3.6 mm/h. Distances are rescaled by the mean raindrop radius $r_0 \approx 0.2$ mm for the same rainfall rate. Here, the solubility is that of gypsum, meaning that each drop can dissolve 10^{-3} of its volume from the solid.

References

1. J. R. Glew & D. C. Ford, A simulation study of the development of rillenkarren, *Earth Surf. Process.*, **5**, 25–36 (1980).
2. J. S. Marshall & W. M. Palmer, The distribution of raindrops with size, *J. Meteorol.*, **5**, 165–166 (1948).

Scaling laws of the plasma velocity in visco-resistive magnetohydrodynamic systems

Anna Krupka, Marie-Christine Firpo

Laboratoire de Physique des Plasmas (LPP), CNRS, Sorbonne Université, École polytechnique, Institut Polytechnique de Paris, 91120 Palaiseau, France
anna.krupka@lpp.polytechnique.fr

We consider a visco-resistive magnetohydrodynamic modeling of a steady-state incompressible tokamak plasma with a prescribed toroidal current drive, featuring constant resistivity η and viscosity ν. We reintroduce in the traditional Grad-Shafranov equation the dissipative viscous term and the non-linear $(\mathbf{v} \cdot \nabla)\mathbf{v}$ term coming from the steady-state Navier–Stokes equation [1–5]. It is shown that the plasma velocity root-mean-square behaves as $\eta f(H)$ as long as the inertial term remains negligible, where H stands for the Hartmann number $H \equiv (\eta\nu)^{-1/2}$, and that $f(H)$ exhibits power-law behaviours in the limits $H \ll 1$ and $H \gg 1$. In the latter limit, we establish that $f(H)$ scales as $H^{1/4}$ (cf. Fig. 1), which is consistent with numerical results [6]. These use the finite element method through the open-source platform FreeFem++ for solving partial differential equations [7].

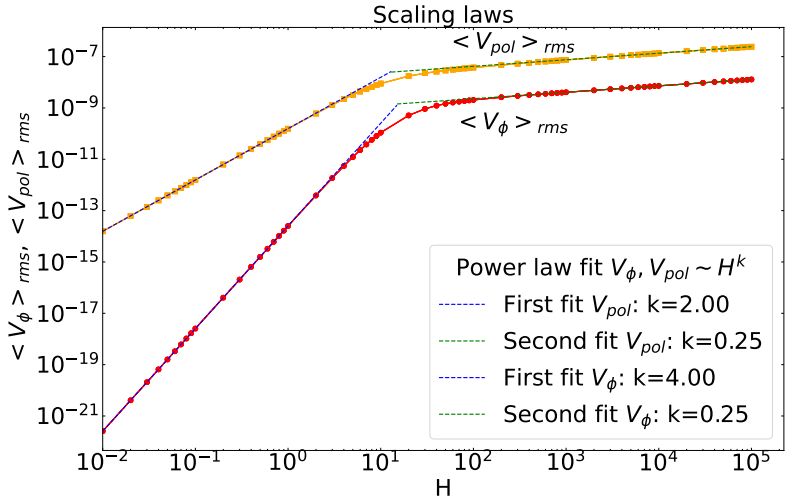

Figure 1. Root-mean square of toroidal and poloidal velocities in Alfvén velocity units as a function of the Hartmann number in log–log scale with power-law fitting curves.

References

1. L. P. Kamp & D. C. Montgomery, Toroidal flows in resistive magnetohydrodynamic steady states, *Phys. Plasmas*, **10**, 157–167 (2003).
2. J. A. Morales, W. J. T. Bos, K. Schneider & D. C. Montgomery, Intrinsic rotation of toroidally confined magnetohydrodynamics, *Phys. Rev. Lett.*, **109**, 175002 (2012).
3. H. Oueslati, T. Bonnet, N. Minesi, M.-C. Firpo & A. Salhi, Numerical derivation of steady flows in visco-resistive magnetohydrodynamics for JET and ITER-like geometries with no symmetry breaking, *AIP Conf. Proc.*, **2179**, 020009 (2019).
4. H. Oueslati & M.-C. Firpo, Breaking up-down symmetry with magnetic perturbations in tokamak plasmas: Increase of axisymmetric steady-state velocities, *Phys. Plasmas*, **27**, 102501 (2020).
5. E. Roverc'h, H. Oueslati, M.-C. Firpo, Steady-state flows in a visco-resistive magnetohydrodynamic model of tokamak plasmas with inhomogeneous heating, *J. Plasma Phys.*, **87**, 905870217 (2021).
6. A. Krupka, M.-C. Firpo, Scaling laws of the plasma velocity in visco-resistive magnetohydrodynamic systems, hal-04459262 (2023).
7. F. Hecht, New development in FreeFem++, *J. Numer. Math.*, **20**, 251–265 (2012).

Noise sustained vs. self-sustained structures in rotor-stator flow

Artur Gesla[1,3], Laurent Martin Witkowski[2], Yohann Duguet[3], Patrick Le Quéré[3]

[1] Sorbonne Université, F-75005 Paris, France
[2] Universite Claude Bernard Lyon 1, CNRS, Ecole Centrale de Lyon, INSA Lyon, LMFA, UMR5509, 69622 Villeurbanne, France
[3] LISN-CNRS, Université Paris-Saclay, F-91400 Orsay, France
artur.gesla@universite-paris-saclay.fr

Rotor–stator flows are known to exhibit instabilities in the form of circular and spiral rolls. While the origin of the latter is known to be a supercritical Hopf bifurcation, the origin of the circular rolls is still unclear. In the present work we propose an explanation for the circular rolls as a linear response of the axisymmetric system to external forcing. Using the singular value decomposition of the resolvent operator [1] the optimal response is computed and takes the form of circular rolls. The optimal energy gain is found to grow exponentially with the Reynolds number (based on the rotation rate and interdisc spacing H), in connection with huge levels of non-normality. The results for both types of forcing are compared with former experimental works [2] and previous numerical studies [3]. The linear response is also compared with the self-sustained states found recently for the unforced problem [4] by the means of Harmonic Balance Method and Self Consistent Model [5]. Additionally the range of forcing amplitudes at which the nonlinearity plays an important role is characterised. Our findings suggest that the circular rolls observed experimentally are the combined effect of the high forcing gain and the roll-like form of the leading response of the linearised operator.

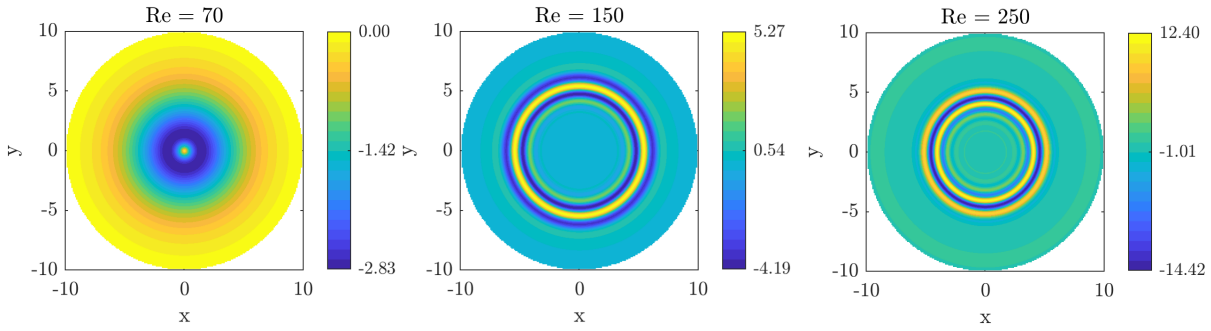

Figure 1. Azimuthal velocity u_θ for the optimal bulk response of the flow for Re = 70, 150, 250 (from left to right) in a plane a quarter gap below the stator.

References

1. S. Cerqueira & D. Sipp, Eigenvalue sensitivity, singular values and discrete frequency selection mechanism in noise amplifiers: The case of flow induced by radial wall injection, *J. Fluid Mech.*, **757**, 770–799 (2014).
2. L. Schouveiler, P. Le Gal & M.-P. Chauve, Instabilities of the flow between a rotating and a stationary disk, *J. Fluid Mech.*, **443**, 329–350 (2001).
3. Y. Do, J. M. Lopez & F. Marques, Optimal harmonic response in a confined Bödewadt boundary layer flow, *Phys. Rev. E*, **82** 036301 (2010).
4. A. Gesla, Y. Duguet, P. Le Quéré & L. Martin-Witkowski, Subcritical axisymmetric solutions in rotor-stator flow, arXiv:2312.09874 (2023).
5. V. Mantič-Lugo, C. Arratia & F. Gallaire, Self-consistent mean flow description of the nonlinear saturation of the vortex shedding in the cylinder wake, *Phys. Rev. Lett.*, **113**, 084501 (2014).

Effet thermoélectrique à l'interface gallium–mercure

Marlone Vernet[1], Stéphan Fauve[2], Christophe Gissinger[2,3]

[1] Université Paris Cité, CNRS, MSC, UMR 7057, F-75013 Paris, France
[2] Laboratoire de Physique de l'Ecole normale supérieure, ENS, Université PSL, CNRS, Sorbonne Université, Université de Paris, Paris, France
[3] Institut Universitaire de France (IUF), Paris, France
marlone.vernet@u-paris.fr

L'effet thermoélectrique consiste en la génération d'une différence de potentiel électrique aux extrémités d'un conducteur lorsque celui-ci est soumis à une différence de température. Si le gradient thermique est appliqué à la jonction conductrice entre deux métaux, un courant électrique est produit. Découvert par Seebeck en 1821, cet effet a été largement utilisé depuis dans nombre d'applications industrielles et scientifiques comme les thermocouples. Principalement étudié dans les conducteurs à l'état solide, son étude expérimentale dans les métaux liquides a fait l'objet de peu de publications.

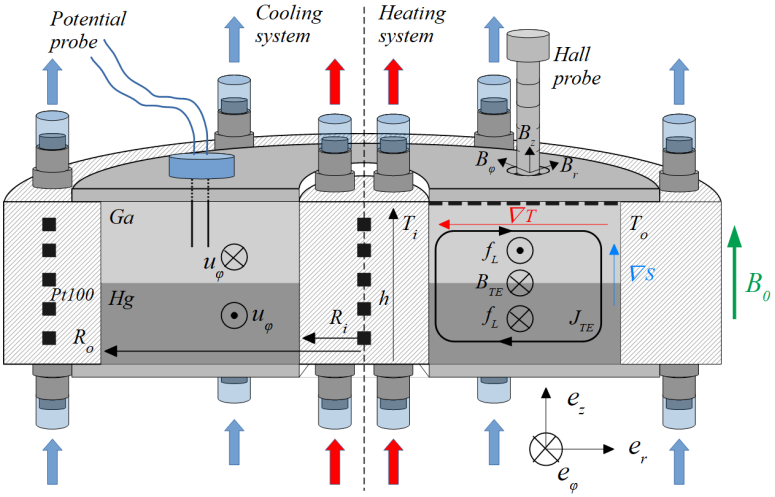

Figure 1. Schéma du dispositif expérimental GALLIMERT.

Le travail présenté ici est la première étude expérimentale de l'effet thermoélectrique à l'interface entre deux métaux liquides. L'expérience GALLIMERT pour GAllium MERcure Thermoelectricité consiste en une cuve cylindrique en cuivre et isolé électriquement (cf. Fig. 1). Une couche de gallium est maintenue à l'état liquide au-dessus d'une couche de mercure, tandis qu'un gradient thermique est imposé entre le cylindre interne et le cylindre externe. Dans cette configuration, la présence d'un gradient thermique horizontal produit une différence de potentiel thermoélectrique mesurable entre les deux métaux liquides. Il est également possible de montrer que la présence de convection naturelle, en prescrivant le profil de température à l'interface, augmente significativement la densité de courant thermoélectrique proche des cylindres. En présence d'un champ magnétique homogène vertical, une force de Laplace engendre dans chaque phase un écoulement azimutal de direction contraire et un cisaillement de l'interface. Plusieurs régimes d'écoulement ont ainsi pu être observés et des lois d'échelles en bon accord avec les mesures ont été obtenues [1]. Ce système permet ainsi d'étudier l'interface liquide–liquide présente dans les batteries à métaux liquides qui, fonctionnant d'ordinaire à des températures élevées (~ 500 °C), sont difficiles à étudier en laboratoire.

Références

1. M. Vernet, S. Fauve & C. Gissinger, Thermoelectricity at a gallium–mercury liquid metal interface, *Proc. Natl. Acad. Sci. USA*, **121**, e2320704121 (2024).

In the search of magnetic reversals in a geodynamo model with a stably-stratified layer

Nicolás P. Müller[1], François Pétrélis[1], Christophe Gissinger[1,2]

[1] Laboratoire de Physique de l'École normale supérieure, ENS, Université PSL, CNRS, Sorbonne Université, Université Paris Cité, F-75005 Paris, France
[2] Institut Universitaire de France (IUF), Paris, France
nicolas.muller@phys.ens.fr

Recent seismic, mineral physics, and geomagnetic investigations have indicated the existence of a stably-stratified layer (SSL) beneath the core-mantle boundary of Earth. This layer, potentially present in other celestial bodies such as Mercury and Saturn, may originate from thermal or compositional influences. In the case of Earth, its depth ranges from 0 to 300 km, exhibiting a stratification strength denoted as $N/\Omega \in (0, 50)$, where N represents the Brunt–Väisälä frequency and Ω the rotation rate [1]. The presence of the SSL on Earth remains a topic of debate, evidenced by the diverse range of parameters yielded by various models. An important aspect of the SSL is its influence on the overall configuration of the magnetic field and on the occurrence of magnetic polarity reversals on a large scale.

In this work, we conduct an extensive study performing numerical simulations of a kinematic geodynamo model within a spherical shell, employing the codensity approximation. The SSL is introduced by assuming a background temperature gradient that undergoes a sign change, being negative near the inner-core boundary and positive in proximity to the core-mantle boundary. Our analysis reveals a transition from dipolar to multipolar dynamo solutions, governed by the magnetic Reynolds number. This transition is found to be influenced not solely by hydrodynamical processes but also by magnetic effects. Furthermore, we explore the modifications imposed by the SSL on this transition.

References

1. T. Gastine, J. Aubert & A. Fournier, Dynamo-based limit to the extent of a stable layer atop Earth's core, *Geophys. J. Int.*, **222**, 1433–1448 (2020).

Comment une singularité en temps fini peut « aveugler » : l'exemple des vortex ponctuels

Perla El Kettani[1], Edgardo Ugalde[2], Xavier Leoncini[1]

[1] Aix Marseille Univ, Université de Toulon, CNRS, CPT, Marseille, France
[2] Instituto de Física, Universidad Autónoma de San Luis Potosí, San Luis Potosí 78295, Mexico
perla.elkettani@cpt.univ-mrs.fr

Dans ce poster, nous illustrons un phénomène de masquage observé numériquement dans le cadre d'un système de vortex ponctuels. La dynamique de vortex ponctuels peut se décrire à l'aide d'un formalisme hamiltonien. Dans le plan infini, il y a quatre constantes du mouvement, mais seules trois sont en involution, ainsi le mouvement de quatre vortex ou plus est génériquement chaotique [1]. Un système de trois vortex ponctuels peut exhiber une singularité en temps fini conduisant à la fusion des trois vortex en un temps fini avec une décroissance au cours du temps linéaire de l'aire du triangle formé par les vortex [2,3]. En inversant le temps, une génération spontanée de vortex peut être envisagée [4]. C'est dans ce cadre qu'un phénomène étrange peut apparaître :

– considérons un vortex ponctuel qui se dissocie en trois en suivant une voie inverse à celle de la fusion ;
– les trois vortex suivent une trajectoire en spirale en s'éloignant du centre de vorticité,

alors dans certaines conditions, si l'un des trois vortex se divise, nous nous retrouvons avec un système de cinq vortex. Mais curieusement alors que du chaos hamiltonien est attendu, on observe que les deux vortex initiaux non divisés, continuent leur course sur la même trajectoire comme si le troisième ne s'était pas cassé i.e. le processus de division est invisible pour les vortex « survivants ».

Références

1. E. A. Novikov, *Sov. Phys. JETP* , **41**, 937 (1975).
2. J. Synge, *Can. J. Math.*, **1**, 257-–270 (1949).
3. X. Leoncini, L. Kuznetsov & G. M. Zaslavsky., *Phys. Fluids*, **12**, 1911-–1927 (2000).
4. X. Leoncini, A. Barrat, C. Josserand & S. Villain-Guillot, *Eur. Phys. J. B*, **82**, 173–178 (2011).

Fluctuations du flux de chaleur en convection thermique à haut nombre de Rayleigh

Martin Caelen, François Pétrélis, Stéphan Fauve

Laboratoire de Physique de l'École Normale Supérieure, CNRS UMR 8023, 24 rue Lhomond, 75005 Paris, France
martin.caelen@phys.ens.fr

Alors que la dépendance en le nombre de Rayleigh (Ra) de la valeur moyenne du flux de chaleur (J) transporté en convection de Rayleigh–Bénard a été largement étudiée, les propriétés statistiques de ses fluctuations sont plus rarement considérées. Il a été montré que, sur la plage $10^6 < \mathrm{Ra} < 10^9$, les fluctuations relatives (écart-type sur valeur moyenne) du flux de chaleur mesuré au niveau des parois horizontales décroissent proportionnellement à l'épaisseur de la couche limite thermique, ce résultat s'interprétant par une corrélation spatiale au niveau des parois qui diminue quand la couche limite s'amincit [1]. Cette observation a été confirmée pour cette plage de nombres de Rayleigh par de récentes simulations numériques [2], mais celles-ci ont mis en évidence une transition à nombre de Rayleigh plus élevé vers un régime où ces fluctuations relatives deviennent indépendantes du nombre de Rayleigh. La compréhension de cette transition est d'autant plus intéressante qu'elle n'est pas observée sur la valeur moyenne du flux de chaleur.

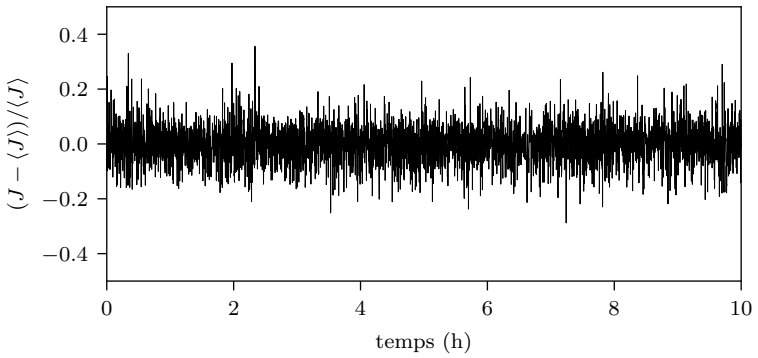

Figure 1. Fluctuations relatives du flux de chaleur mesuré pour $\mathrm{Ra} = 1{,}3 \times 10^{11}$.

Nous réalisons donc l'étude expérimentale des fluctuations du flux de chaleur en convection de Rayleigh–Bénard à des nombres de Rayleigh plus élevés ($10^9 < \mathrm{Ra} < 10^{11}$). Les simulations ayant été réalisées pour un écoulement bidimensionnel, l'expérience permettra de déterminer si la transition prédite à deux dimensions a lieu dans la même gamme de nombres de Rayleigh à trois dimensions. Si celle-ci est observée, l'expérience permettra également d'en étudier les caractéristiques. Cette étude se fait dans une cuve cylindrique de diamètre 60 cm et hauteur 60 cm (rapport d'aspect 1), remplie d'eau, dont les deux parois horizontales (haute et basse) sont thermostatées pour imposer les gradients de température souhaités. La température à chaque paroi est mesurée, ainsi que le flux de chaleur instantané (voir Fig. 1), pour être ensuite comparés aux résultats de S. Aumaître [1] et V. Labarre [2].

Références

1. S. Aumaître & S. Fauve, Statistical properties of the fluctuations of the heat transfer in turbulent convection, *Europhys. Lett.*, **62**, 822–828 (2003).
2. V. Labarre, S.Fauve & S. Chibbaro, Heat-flux fluctuations revealing regime transitions in Rayleigh–Bénard convection, *Phys. Rev. Fluids*, **8**, 053501 (2023).

Spatiotemporal parametric modulation of a soft beam

Éléonore Duval[1,2,3], Johann Asnacios[2], Stéphan Fauve[2], Vincent Tournat[1], François Pétrélis[2], Maxime Lanoy[1]

[1] Laboratoire d'Acoustique de l'Université du Mans (LAUM), UMR 6613, Institut d'Acoustique – Graduate School (IA-GS), CNRS, Le Mans Université
[2] Laboratoire de Physique de l'École normale supérieure, ENS, Université PSL, CNRS, Sorbonne Université, Université Paris Cité, F-75005 Paris, France
[3] Université Paris Cité, CNRS, MSC, UMR 7057, F-75013 Paris, France
eleonore.duval.etu@univ-lemans.fr

A parametric oscillator is a system whose natural frequency is periodically modulated, via the time variation of one of its physical parameters. When this parameter is modulated to about twice the natural frequency, the amplitude of the oscillation increases exponentially: this is known as parametric resonance[1].

Here, we study the behaviour of a pre-stressed beam undergoing longitudinal excitation, which induces a parametric modulation of its tension. At first sight, this system appears similar to a classical parametric oscillator, as described by Melde's experiment [1]. But, when the beam is soft enough, we find that its natural frequency varies both in time and space. This double modulation yields the dynamics of the instability growth to be very different from what is usually observed. We first investigate the beam's linear dynamics by characterising both the compression and bending modes. We then drive the system in the vicinity of the bending natural frequencies, and report the growth of atypical elastic instabilities. To explain our observations, we propose a model taking into account the spatio-temporal modulation and the frequency-dependent dissipation.

Understanding the origin of such unstable behaviours has implications for the domains of soft robotics [2] and energy recovery.

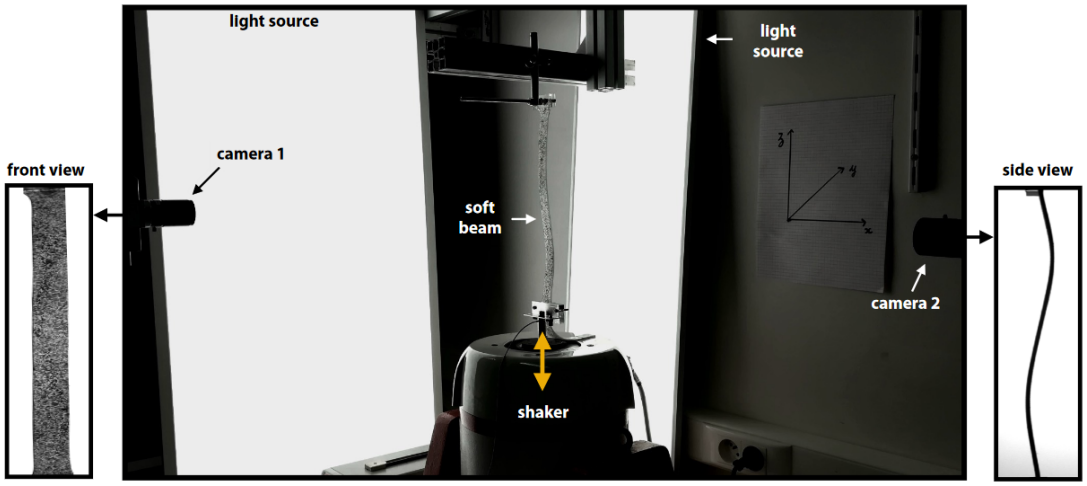

Figure 1. Experiment set-up. A soft beam is fixed at its upper end and parametrically excited at its lower end. Displacements are extracted from the front and side views.

References

1. F. Melde, Ueber die Erregung stehender Wellen eines fadenförmigen Körpers, *Ann. Physik (Leipzig)*, **185**, 193–215 (1860).
2. A. Nagarkar *et al.*, Elastic-instability–enabled locomotion, *Proc. Natl. Acad. Sci. USA*. **118**, e2013801118 (2021).

[1] Other modulation frequencies can also lead to resonance but are usually less efficient.

Fluid response to the inner core's translational oscillations

Paolo Personnettaz[1,2], Nathanaël Schaeffer[2], David Cébron[2], Mioara Mandea[1]

[1] CNES - Centre National d'Etudes Spatiales, 2 Place Maurice Quentin, 75039, Paris, France
[2] Univ. Grenoble Alpes, CNRS, ISTerre, 38000 Grenoble, France
paolo.personnettaz@univ-grenoble-alpes.fr

On the Earth or on other rocky bodies, a sufficiently strong and directional kinetic energy source, such as an asteroid impact or a massive seismic event, can compete with the gravitational energy associated with the internal layers. If liquid shells are present, solid regions are allowed to translate with respect to the planet's centre. These weak motions are known as translation oscillations. Accurately detecting this motion is important to better constrain the physical properties of planetary interiors, such as the densities of solid and liquid phases. In the Earth, the inner core centre is free to weakly oscillate inside the liquid outer core [1]. Due to the planet rotation, the oscillation is split into three modes—the Slichter triplet—two orbital modes in the equatorial plane and one polar mode along the rotation axis [2].

Previous works focused mainly on the linear calculation of mode periods [1, 2]. Our new approach involves the study of the outer core fluid response to these oscillations, in the presence of the planetary magnetic field and rotation. To tackle the non-linear problem numerically, we use XSHELLS, a state-of-the-art magneto-hydrodynamic (MHD) solver for spherical shells [3]. The inner core motion is modelled by parameterized boundary conditions, keeping intact the spectral code's efficiency.

We have conducted a systematic exploration of the parameter space, by varying inner core radius, kinematic viscosity and magnetic diffusivity, forcing amplitude and frequency, as well as magnetic field intensity and distribution. We have obtained robust scaling laws for the viscous and Ohmic dissipation, which are employed to extrapolate the associated damping time to planetary conditions that exceed our numerical capabilities. In addition, we have identified several hydrodynamic and MHD regimes. As an example, inertial waves emerge when the oscillation period exceeds half of the spin one, as observed experimentally for the equatorial modes [4]. Furthermore, we have investigated the presence of boundary layer instabilities, and the role of mean zonal flows produced by nonlinear interactions.

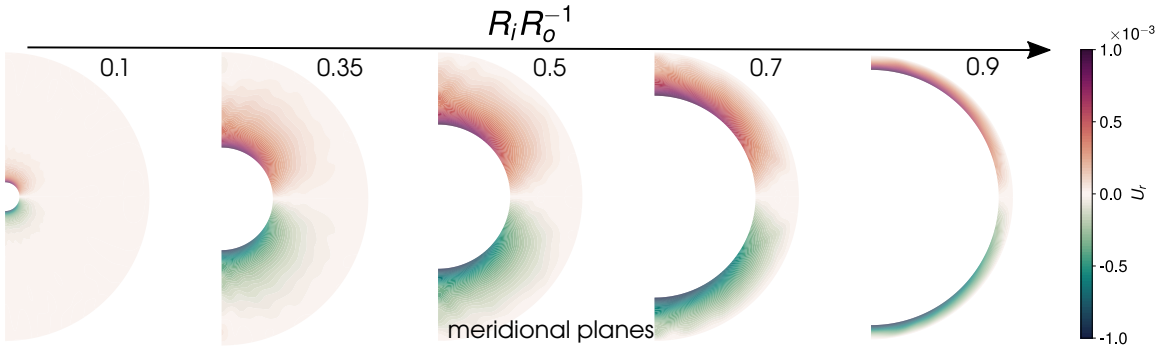

Figure 1. Effect of the inner core radius on the velocity distribution.

References

1. F. H. Busse, On the free oscillation of the Earth's inner core, *J. Geophys. Res.*, **79**, 753–757 (1974).
2. M. Rieutord, Slichter modes of the Earth revisited, *Phys. Earth Planet. Inter.*, **131**, 269–278 (2002).
3. N. Schaeffer, Efficient spherical harmonic transforms aimed at pseudospectral numerical simulations, *Geochem. Geophys. Geosyst.*, **14**, 751–758 (2013).
4. S. Subbotin & M. Shiryaeva, On the linear and non-linear fluid response to the circular forcing in a rotating spherical shell, *Phys. Fluids*, **33**, 066603 (2021).

Dripping flow with solidification: An analogue system for the growth of tubular stalactites

Anne Mongruel, Antonin Eddi, Philippe Claudin

Physique et Mécanique des Milieux Hétérogènes (PMMH), CNRS, ESPCI Paris, PSL Research University, Sorbonne Université, Université Paris Cité, 75005 Paris, France
anne.mongruel@sorbonne-universite.fr

Among the various and beautiful shapes shown by calcite concretions in limestone caves, the soda-straw speleothems exhibit an astonishing regularity in diameter (Fig. 1 (a)). The drop size ($\cong 5$ mm), fixed by gravity and capillary forces, templates the growing structure [1,2]. Tubular stalactites can also grow in open air from concrete exposed to rainwater (Fig. 1(b)). Here, the calcite deposition occurs by absorption of CO_2 from the atmosphere, as opposed to cave growth where deposition relies on the degassing of CO_2 from solution. This difference leads to faster growth rates in open air than in caves : 1 cm/year as compared to 10–100 µm/year [3].

Whereas the chemical processes leading to calcium deposition are well known, the factors determining these growth rates are still far from being understood and difficult to be quantified in field conditions. In order to relate the spatio-temporal scales to the relevant physical parameters, and to elucidate the growth mechanisms, we study in the laboratory an analogue system for the formation of soda-straws. We work with a saturated solution of strontium hydroxide, $Sr(OH)_2$, dripping in an atmosphere containing gaseous CO_2. Precipitation of strontium carbonate, $SrCO_3$, occurs at the drop interface by absorption of CO_2. A hanging tube grows downwards as successive drops leave a ring of solid material, with growth rates of 10 µm/min (Fig. 1(c)). The influence of dripping rate and CO_2 concentration is investigated. Comparisons with field measurements are under progress (Fig. 1 (b)).

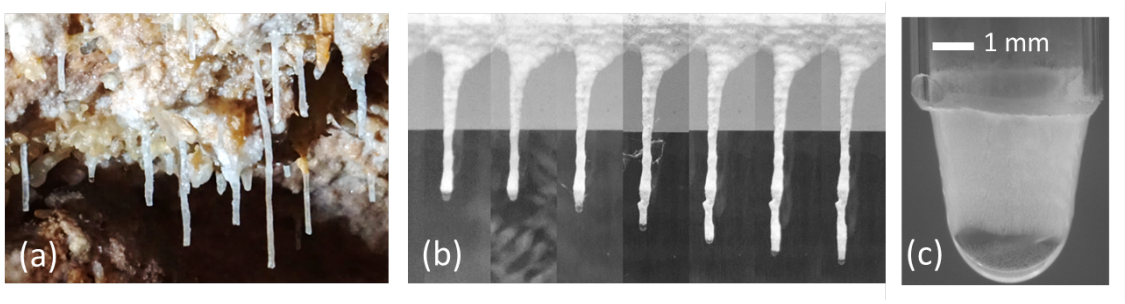

Figure 1. (a) Natural soda-straws (Grotte de la Madeleine, Ardèche). (b) Temporal evolution of a tubular stalactite growing in open air (campus Jussieu, Paris), time between successive images : 2 weeks. (c) Interfacial solidification of a strontium hydroxide solution dripping in an atmosphere containing gaseous CO_2 (scale bar : 2 mm).

References

1. B. Schmidkonz, Geochemistry in action: Watch a dripstone grow!, *J. Chem. Educ.*, **94**, 1492–1497 (2017).
2. D. A. Stone & R. E. Goldstein, Tubular precipitation and redox gradients on a bubbling template, *Proc. Natl. Acad. Sci. USA*, **101**, 11537–11541 (2004).
3. A. Hartland, I. J. Fairchild, J. R. Lead, D. Dominguez-Vilar, A. Baker, J. Gunn, M. Baalousha & Y. Ju-Nam , The dripwaters and speleothems of Poole's Cavern: A review of recent and ongoing research, *Cave and Karst Sci.*, **36**, 37–46 (2009).

Instabilities around a Spheroid Spinning in a Rotating Stratified Fluid

Antoine Chauchat, Michael Le Bars, Patrice Meunier

IRPHE, Aix-Marseille Université, Centrale Méditerranée, CNRS 49 rue Frédérick Joliot-Curie, 13013 Marseille
antoine.chauchat@univ-amu.fr

To better predict Earth's climate evolution, the CO2 and heat fluxes between the oceans and the atmosphere must be taken into account. These fluxes are governed by the vertical mixing in the ocean. But the measured mixing rate is 10 times smaller than necessary to balance the energy budget of the oceans: this calls for new, local mechanisms of mixing. At the edge of meso-scale eddies, an horizontal layering is observed, corresponding to density steps [1]. This is a local signature of an increased vertical mixing. To quantify its influence we need to determine the origin of the underlying instability/ies. To model this geophysical flow, a solid ellipsoid differentially rotates anticyclonically in a rotating stratified medium. We numerically and experimentally study this setup to assess the intensity and the structures of instabilities around the ellipsoid in the different regions of the Rossby, Froude, Ekman, Prandtl and Schmidt numbers space.

The experimental apparatus uses salty water in a large rotating cylindrical tank of 1 m in diameter. Metrology includes Particle Image Velocimetry (PIV) in horizontal planes and Schlieren in the vertical ones. First the base flow is measured and compared to an analytical solution. This solution is derived for any aspect ratio of the rotating ellipsoid thanks to spheroidal coordinates. Then the unstable modes are observed experimentally and compared to a linear stability analysis conducted using the pseudo-spectral eigenvalue problem solver Dedalus [2]. Various types of instabilities are observed, including baroclinic, double diffusive, convective and centrifugal ones, see e.g. Fig. 1. Their efficiency and relevance to explain the observed mixing are systematically assessed.

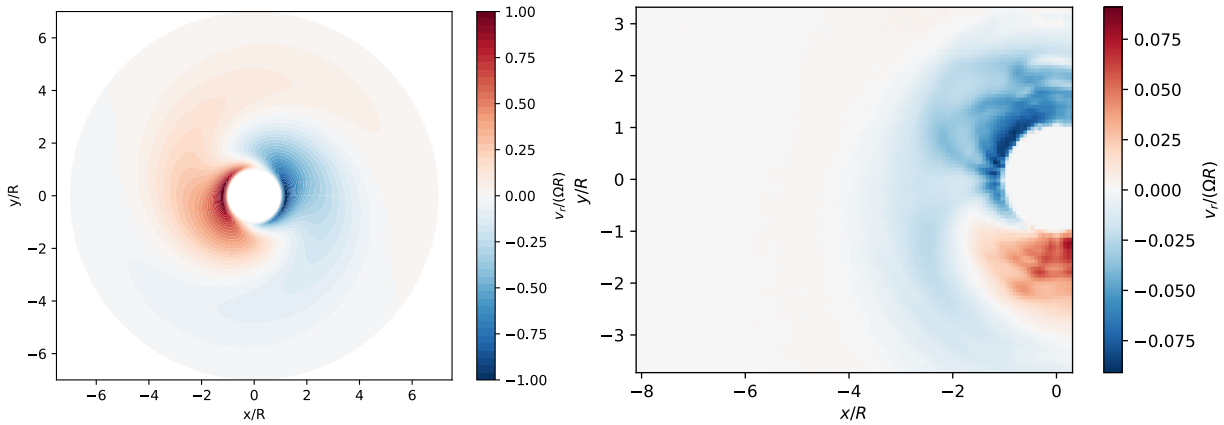

Figure 1. Left: Radial velocity map in the equatorial plane of a numerical eigenmode obtained using Dedalus. Right: Temporally filtered radial velocity map of an equatorial instability obtained by PIV.

References

1. B. L. Hua *et al.*, Layering and turbulence surrounding an anticyclonic oceanic vortex: *In situ* observations and quasi-geostrophic numerical simulations, *J. Fluid Mech.*, **731**, 418–442 (2013).
2. K. J. Burns *et al.*, Dedalus: A flexible framework for numerical simulations with spectral methods, *Phys. Rev. Res.*, **2**, 023068 (2020).

Topographic effects in planetary magneto-hydrodynamic flows

Rémy Monville, David Cébron, Dominique Jault

Univ. Grenoble Alpes, Univ. Savoie Mont Blanc, CNRS, IRD, Univ. Gustave Eiffel, ISTerre, 38000 Grenoble, France

remy.monville@univ-grenoble-alpes.fr

While mechanical couplings between fluid and solid domains have been widely studied, their estimation remains challenging for deep planetary fluid layers with buoyancy, magnetic field, and topographic effects. Results from atmospheric or oceanic sciences are unsuitable for thick layers such as subsurface oceans of icy moons, or liquid cores of planets. Rapid rotation and/or the presence of a magnetic field in these regions may also cause difficulties. Considering a rotating and stratified fluid layer, we have developed an asymptotic local model to investigate the small-scale topographic fluid-solid coupling due to pressure or magnetic stresses. Our code unlocks several previous limitations of planetary coupling studies. Considering three-dimensional bumps, it provides the fluid stress at higher order of perturbation than previous linear studies, on an electrically conducting solid (e.g. the mantle lowermost layer). We explore a wide range of parameters and boundary conditions for arbitrary topography shapes, and account for planetary curvature effects by considering a 'non-traditional β-plane' approximation. Carrying out a detailed study of the wave drag mechanism, we show that the Rossby planetary waves, which are absent from recent asymptotic models, can significantly modify the boundary stress. We also show that the results are drastically different when considering 3D topographies instead of ridges.

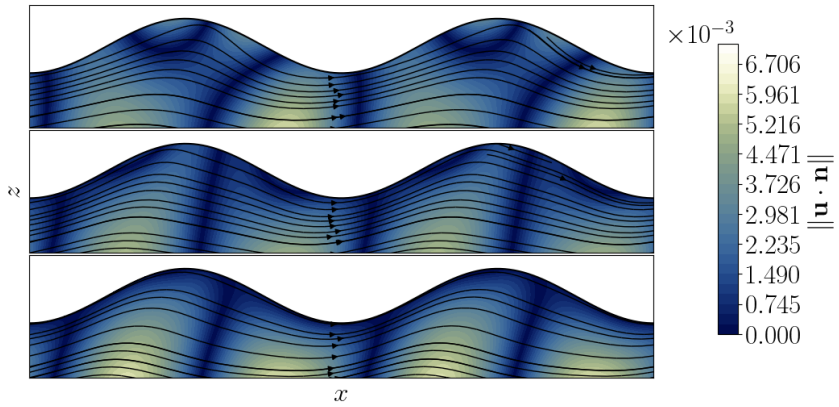

Figure 1. Flow streamlines and $\|\boldsymbol{u}\cdot\boldsymbol{n}\|$ (with an artificial normal vector $\boldsymbol{n}$ defined in the whole volume) field at order 1,2 and 4 (top to bottom).

Low-cost realization of a quantitative chaotic waterwheel

Grégoire Le Lay[1]

Laboratoire MSC, Université Paris Cité, Paris, France
gregoire.le-lay@u-paris.fr

In the 60's, several teams of researchers try to tackle the problem of better understanding thermal convection in fluids. Among them E. N. Lortenz, who was studying atmospheric convection. Using a reduction of the equations obtained while studying the Rayleigh–Bénard system, he obtained the now famous Lorenz system of three equations, which he first discovered to be able to exhibit chaotic behaviour for certain ranges of parameters [1].

Several years later, Keller and Welander, interested in oceanic convection, studied a simplified system consisting in a single rectangular fluid loop heated at its top and cooled from below [2, 3].

Howard and Malkus later modified this idea by using a circular loop [4]. They discovered that its behaviour was ruled by system of equations that Lorenz had found earlier. Malkus then had the idea to build a mechanical analag to the fluid loop, where buckets losing and gaining water rrepsented fluid being heated or cooled.

The waterwheel indeed realises a mechanical equivalent of a single convection loop, and the equation ruling its behaviour are remarkably simple :

$$\begin{aligned} \dot{\omega}/\sigma &= x - \omega \\ \dot{x} &= -x + \omega y \\ \dot{y} &= -y - \omega x + \rho \end{aligned}$$

with ω being the rotational speed of the wheel, and x, y the coordinates of its center of gravity. The behaviour of the whole system depends on only two dimentionless parameters, the Rayleigh number ρ which transcripts the competition between the weight torque and the dissipation, and the Prandtl number σ which compares two modality of dissipation (mechanical friction and leakage).

The wheel is an excellent demonstration tool to discuss with the general public about topics such as atmospheric convection, sensitivity to initial conditions, and the difference between wheater and climate. It can also be used as a tool when teaching students about dynamical systems, nonlinear physics and chaos theory.

We designed a portable, low-cost and easy to use chaotic waterwheel using 3D printing and cheap microcontrollers. A rotary encodr is used to make the wheel quantitative, allowing for real-time observation of the dynamics.

References

1. E. N. Lorenz, Deterministic Nonperiodic Flow, *J. Atmos. Sci.*, **20**, 130–141 (1963).
2. J. B. Keller, Periodic oscillations in a model of thermal convection, *J. Fluid Mech.*, **26**, 599–606 (1966).
3. P. Welander, On the oscillatory instability of a differentially heated fluid loop, *J. Fluid Mech.*, **29**, 17–30 (1967).
4. W. V. R. Malkus, Non-periodic convection at high and low Prandtl number, *Mem. Soc. R. Sci. Liège*, **6**, 125–128 (1972).

Compétition entre convection naturelle et convection forcée en érosion par dissolution

Martin Chaigne, Mathieu Receveur, Sylvain Courrech du Pont, Michael Berhanu

Matière et Systèmes Complexes (MSC), Université Paris Cité, CNRS (UMR 7057), 75013 Paris
martin.chaigne@u-paris.fr

À la surface de la Terre, les paysages sont façonnés par l'érosion : l'eau et le vent sculptent roches, montagnes, vallées et grottes. L'érosion peut être d'origine mécanique mais aussi chimique. On parle alors d'érosion par dissolution : la roche se dissout avant d'être transportée par l'écoulement d'eau sous forme de soluté. C'est le mécanisme principal pour des roches solubles comme le sel, le gypse ou le calcaire. Dans ce cas, le couplage entre la topographie de la roche et l'écoulement peut mener à l'apparition de motifs réguliers, dont la taille et la forme dépendent des conditions hydrodynamiques.

Précédemment, nous avons étudié le cas d'un bloc soluble placé horizontalement dans un aquarium rempli d'eau, aucun écoulement n'étant imposé. Ce sont alors les gradients de densité induits par la dissolution du bloc qui engendrent un écoulement de convection solutale. Celui-ci mène à l'apparition d'un motif constitué de cavités concaves entourées de crêtes acérées, qui évoque les coups de gouge, ou scallops, observées sur les parois des grottes calcaires [1]. Cependant, les scallops naturelles apparaissent lorsque les galeries des grottes sont traversées par des rivières souterraines.

Cela nous motive à étudier la compétition entre convection solutale et convection forcée. Nous plaçons nos blocs solubles dans un canal hydraulique, permettant d'imposer des vitesses d'écoulement jusqu'à 40 cm/s. Nous reconstruisons la surface des blocs en 3D, et observons l'apparition de motifs sous leur face inférieure (Fig. 1), où l'écoulement de convection naturelle est cisaillé par l'écoulement moyen. Nous montrons que l'anisotropie et la taille caractéristique de ces motifs augmentent avec la vitesse de l'écoulement. Ces expériences nous permettent de discuter de la possibilité que la convection solutale puisse jouer un rôle dans la formation des scallops naturelles.

Figure 1. Motifs sur la surface inférieure d'un bloc de sel rose (20 cm × 10 cm), après 20 minutes de dissolution dans un canal hydraulique avec une vitesse d'écoulement de 15 cm/s (de la gauche vers la droite).

Références

1. C. Cohen, M. Berhanu, J. Derr & S. Courrech du Pont, Buoyancy-driven dissolution of inclined blocks: Erosion rate and pattern formation, *Phys. Rev. Fluids*, **5**, 053802 (2020).

Caractérisation par mesure sismique de la banquise soumise à la houle

Baptiste Auvity[1], Sarah Chekir[1], Dany Dumont[2], Ludovic Moreau[3], Laurent Duchemin[1], Antonin Eddi[1], Stéphane Perrard[1]

[1] Laboratoire de Physique et Mécanique des Milieux Hétérogènes, PMMH, ESPCI Paris, 7 Quai Saint-Bernard, 75005, Paris, France
[2] Institut des Sciences de la Mer de Rimouski (ISMER), UQAR, 310 Allée des Ursulines, Rimouski, Canada
[3] Institut des Sciences de la Terre (ISTerre), USMB, 1381 rue de la Piscine, Gières, France
baptiste.auvity@espci.fr

Le pôle nord est recouvert toute l'année d'une couche de glace appelée banquise qui joue un rôle déterminant dans le système climatique terrestre [1]. Pour pouvoir comprendre la dynamique de ce système, il est nécessaire de caractériser la glace à différentes échelles. Les mesures sismiques en particulier permettent de mesurer les propriétés mécaniques comme le module d'Young, le coefficient de Poisson et l'épaisseur de la glace à l'aide de sources actives ou passives de bruit [2]. En revanche il n'existe pas de méthode pour caractériser la banquise à partir d'une source unidirectionnelle et passive de bruit : la houle.

Lors d'une campagne de terrain en mars 2023 dans l'estuaire du Saint-Laurent (Rimouski, Canada), nous avons placé trois sismographes (géophones) en triangle sur une banquise soumise à une légère houle incidente.

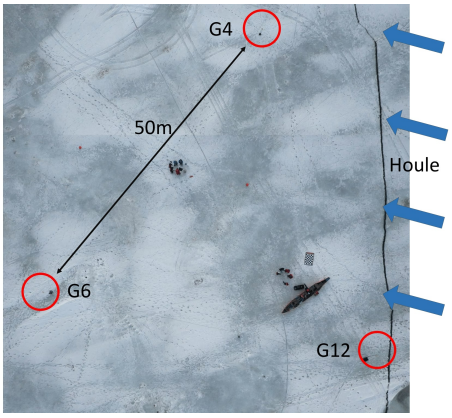

Figure 1. Photographie aérienne du dispositif déployé en baie de Rimouski le 13 mars 2023. La houle se propageait sous la banquise et était enregistrée par les trois sismomètres, placés en triangle équilatéral de 50 mètres de coté.

Pour extraire les caractéristiques physiques de cette glace, nous avons developpé une nouvelle méthode de traitement du signal. Nous avons corrélé les signaux de géophones par paire, filtrés à différentes fréquences. En utilisant les corrélations extraites de deux paires de géophones, nous avons déduit l'angle d'incidence des vagues. A l'aide de cet angle, nous avons mesuré la longueur d'onde des vagues se propageant dans la glace en fonction de la fréquence. Ceci nous a permis d'obtenir la relation de dispersion des ondes hydro-élastiques dans la banquise qui dépend principalement de l'épaisseur et du module d'Young. Les valeurs obtenues coincident quantitativement avec nos mesures de réferences.

Références

1. T. D. Williams, L. G. Bennetts, V. A. Squire, D. Dumont & L. Bertino, Wave-–ice interactions in the marginal ice zone. Part 1: Theoretical foundations, *Ocean Model*, **71**, 81–91 (2013).
2. L. Moreau, J. Weiss & D. Marsan, Accurate estimations of sea–ice thickness and elastic properties from seismic noise recorded with a minimal number of geophones: From thin landfast ice to thick pack ice, *J. Geophys. Res. Oceans*, **125**, 2169–9275 (2020).

Internal wave instabilities and transition to turbulence in large aspect ratio wave attractors

Ilias Sibgatullin, Stepan Elistratov, Thierry Dauxois

Laboratoire de Physique (UMR CNRS 5672) ENS de Lyon 46, allée d'Italie Lyon
ilias.sibgatullin@ens-lyon.fr

Geophysical turbulence exhibits distinct characteristics compared to conventional turbulence flows, primarily due to the effects of stratification and/or rotations which are different at various scales of flows. We will focus on the small-scale effects where the direct action of buoyancy significantly affects momentum equations and cannot be neglected, as opposed to quasi-hydrostatic modeling at large scales.

Continuous stratification itself profoundly impacts the onset of hydrodynamical instabilities due to a unique dispersion relation. According to this relation, wave beams and wave energy propagate perpendicular to the phase lines. It has also been observed that the dynamics of wave beams (webs of rays) in closed domains differ considerably from conventional ray tracing. In a general case, an attracting trajectory exists for the wave beams, referred to as wave attractors. These trajectories evolve due to the focusing/defocusing of wave packets upon reflection from the walls inclined with respect to gravity or rotation axis [1].

Owing to the high concentration of wave energy along these attracting paths, they are particularly susceptible to instabilities and serve as a source for the propagation of secondary waves. In our previous works, we demonstrated that if the aspect ratio of the motion is of the order of one, the transitions to turbulence can be effectively described using a laboratory toy-box model [2, 3]. In such a laboratory model, turbulence originates from cascades of triadic resonances. This model represents an important case of natural flows. Another case involves large aspect ratio motions, where the horizontal scale is much larger than the vertical, yet buoyancy effects cannot be neglected.

Previously, we described the peculiarities of linear regimes of large aspect ratio wave attractors and their instabilities at multiples of half the forcing frequency. Now we complement this scenario with cascades of triadic resonance instabilities in each half-harmonic frequency interval and show the corresponding changes in spatial spectra.

References

1. L. R. M. Maas, D. Benielli, J. Sommeria & F.-P. A. Lam, Observation of an internal wave attractor in a confined, stably stratified fluid, *Nature*, **388**, 557–561 (1997).
2. C. Brouzet, I. Sibgatullin, H. Scolan, E. Ermanyuk & Thierry Dauxois, Internal wave attractors examined using laboratory experiments and 3d numerical simulations, *J. Fluid Mech.*, **793**, 109–131 (2016).
3. C. Brouzet, E. Ermanyuk, S. Joubaud, I. Sibgatullin & T. Dauxois, Energy cascade in internal-wave attractors, *Europhys. Lett.*, **113**, 44001 (2016).

Quantifying the flows in a freezing liquid foam

Krishan Bumma[1], Axel Huerre[2] Juliette Pierre[1] Thomas Séon[1,3]

[1] Institut Jean Le Rond ∂'Alembert, Sorbonne Université - CNRS, Paris, France
[2] Laboratoire Matière et Systèmes Complexes, Université Paris Cité, Paris, France
[3] Institut Franco-Argentin de Dynamique des Fluides pour l'Environnement , CNRS, Buenos Aires, Argentina
k.bumma@gmail.com

The manufacture of a solid foam, widely used for its mechanical, thermal, or acoustic properties, always begins with the solidification of a liquid foam. By placing a model aqueous foam in contact with a cold surface, we observe that, as it freezes, the foam undergoes a drastic change in volume and color revealing important water and air migration in the foam.

Through conductivity measurement, we are able to measure the liquid fraction of the liquid foam; coupled with the the information on the height of the freezing front, we can retrieve the density profile in the frozen foam as shown on Figure 1 (b)). This reveals that a large amount of water flows towards the solidification front, significantly affecting the resulting frozen slab caused. This water flow is partly due to imbibition events during which water penetrates into the porous medium that is the frozen foam. Figure 1 (a) shows one such event, where within in a few seconds the front gets filled with water before freezing starts again.

We can show that the density profile measured is indeed coherent with the observed solidification front dynamics. Next, we present scaling laws for the collapse velocity of the foam and for its final volume, which depend on the size of the liquid films and the substrate temperature. Finally, based on these results and the observation of bubbles behaviour at the solidification front, we discuss mechanisms to explain the gas and liquid flows. These results improve our understanding of the mechanisms involved in foam solidification, in particular the flows generated by the presence of a solidification front.

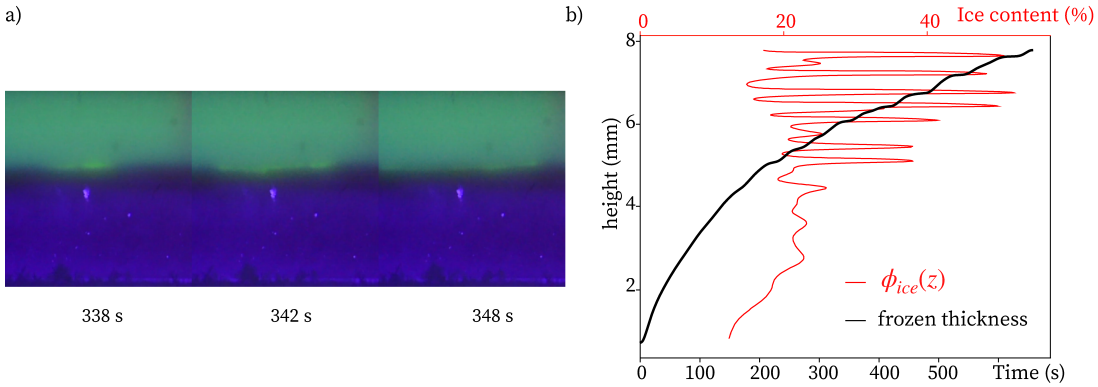

Figure 1. (a) Cascading imbibition event during a 1D foam freezing experiment. The liquid foam appears green and the frozen part purple. A bright green line propagates at the solidification front, due to the presence of a large amount of liquid locally. (b) Experimental measurement of the density of the frozen foam as a function of the height in the frozen slab. the density of the frozen foam increases gradually as the freezing front advances, then is dramatically increased by large imbibition events.

Investigating Tayler instability in a liquid metal experiment

Guillaume Bermudez, Christophe Gissinger

Laboratoire de Physique de l'Ecole Normale Supérieure (LPENS), ENS, Université PSL, CNRS, Sorbonne Université, Université Paris Cité, Paris, France
guillaume.bermudez@ens.fr

The Tayler instability is believed to play a crucial role in a number of astrophysical objects [1], as well as in industrial applications [2]. When an electrically conducting fluid is subjected to a sufficiently strong toroidal magnetic field, this kink-type magnetohydrodynamic (MHD) instability can produce non-axisymmetric flow motions and even turbulence.

This induced turbulence may explain why the cores of many stars rotate more slowly than expected, especially in radiative zones, where heat is transported outwards by radiation rather than convection [3]. It may also influence the efficiency of liquid metal batteries, a very promising technology recently proposed for high-capacity grid energy storage and balancing intermittent renewable energy sources [4].

We present an experimental setup that evidences Tayler instability in the laboratory. It consists of a cylindrical vessel filled with a liquid metal (Gallinstan) into which a high electric current (up to 3000 amperes) is injected axially, generating a toroidal magnetic field. In addition, external coils are used to apply an axial magnetic field (300 G). Measurements using magnetic Hall probes, electric potential velocimetry electrodes and several resistive temperature detectors (RTDs) are performed. By carefully controlling the apparatus temperature, we characterize the bifurcation, geometry and linear growth rate of the unstable mode.

We show how the axial magnetic field modifies the onset of the Tayler instability and the geometry of the unstable modes. Finally, our results are discussed in the context of astrophysical and industrial applications.

References

1. R. J. Tayler, The adiabatic stability of stars containing magnetic fields–I: Toroidal fields, *Mon. Not. Roy. Astron. Soc.*, **161**, 365–380 (1973).
2. W. Herreman, C. Nore, L. Cappanera & J.-L. Guermond, Tayler instability in liquid metal columns and liquid metal batteries, *J. Fluid Mech.*, **771**, 79–114 (2015).
3. L. Petitdemange, F. Marcotte & C. Gissinger, Spin-down by dynamo action in simulated radiative stellar layers, *Science*, **379**, 300–303 (2023).
4. N. Weber, V. Galindo, F. Stefani & T. Weier, Current-driven flow instabilities in large-scale liquid metal batteries, and how to tame them, *J. Power Sources*, **265**, 166–173 (2014).

Index des auteurs

Index des auteurs

Image de couverture : Camille Arracheloff

27e Rencontre du Non-Linéaire
Université de Paris
Paris 2024

Version en ligne, compilée le 10 juillet 2024

ISBN 978-2-9576145-3-0
EAN 9782957614530

Non-Linéaire Publications (NL Pub.)
Campus universitaire, Bâtiment 508
Rue John von Neumann
91400 ORSAY

27e Rencontre du Non-Linéaire

Université Paris Cité
Paris 2024

ISBN 978-2-9576145-3-0
EAN 9782957614530

nonlineaire.univ-lille.fr/SNL